TESIS DE LA UNIVERSIDAD DE ZARAGOZA

2012

25

Sonia Martínez Salvador

# Trifluorometil-derivados de Pt y Au: síntesis, estructura y reactividad

Departamento

Química Inorgánica

Director/es

Forniés Gracia, Juan

Menjón Ruiz, Babil



ISSN 2254-7606

Prensas de la Universidad Universidad Zaragoza

Universidad Zaragoza
1542

Tesis Doctoral

# TRIFLUOROMETIL-DERIVADOS DE PT Y AU: SÍNTESIS, ESTRUCTURA Y REACTIVIDAD


Autor

Sonia Martínez Salvador

Director/es

Forniés Gracia, Juan
Menjón Ruiz, Babil

**UNIVERSIDAD DE ZARAGOZA**

Química Inorgánica


2012

# TRIFLUOROMETIL-DERIVADOS DE Pt Y Au: SÍNTESIS, ESTRUCTURA Y REACTIVIDAD

TESIS DOCTORAL

Sonia Martínez Salvador

Zaragoza, 2011

# TRIFLUOROMETIL-DERIVADOS DE Pt Y Au: SÍNTESIS, ESTRUCTURA Y REACTIVIDAD

Memoria presentada en la Facultad de Ciencias de la Universidad de Zaragoza para optar al grado de Doctor en Ciencias, Sección Químicas por la Licenciada

Sonia Martínez Salvador

JUAN FORNIÉS GRACIA, Profesor Emérito del Departamento de Química Inorgánica de la Facultad de Ciencias de la Universidad de Zaragoza.

BABIL MENJÓN RUIZ, Investigador Científico del C.S.I.C. en el Instituto de Síntesis Química y Catálisis Homogénea (Universidad de Zaragoza-C.S.I.C.)

CERTIFICAN:

Que la presente Memoria titulada “TRIFLUOROMETIL-DERIVADOS DE Pt Y Au: SÍNTESIS, ESTRUCTURA Y REACTIVIDAD” ha sido realizada en el Instituto de Síntesis Química y Catálisis Homogénea (I.S.Q.C.H.) bajo nuestra dirección; que se ajusta en su totalidad al proyecto de tesis aprobado en su momento y autorizamos su presentación para que sea calificada como Tesis Doctoral.

Zaragoza, 16 de Noviembre de 2011.

Fdo: Juan Forniés Gracia

Fdo: Babil Menjón Ruiz

**AUTORIZACIÓN DEL DIRECTOR/DIRECTORES DE TESIS:**

VºBº Director de Tesis

Fdo.: Dr. Juan Forni®s

VºBº Director de Tesis

Fdo.: Dr. Babil Menj· n

**INFORME MOTIVADO DEL ÓRGANO RESPONSABLE:**

El trabajo contenido en la presente Memoria ha sido realizado por la doctoranda **Sonia Martínez Salvador** en el Departamento de Química Inorgánica en su mayor parte, así como en el Laboratorio del Prof. Dr. Konrad Seppelt de la Freie Universität Berlin (Alemania) durante una estancia de tres meses. En la Memoria que se acompaña se recogen los resultados obtenidos en ambos centros, buena parte de los cuales ha sido publicada en revistas especializadas de Química de carácter internacional y con elevados índices de impacto (Impact Factor) tal y como se recoge en la relación adjunta. Así mismo se incluyen copias de las mismas como pare integrante de la Memoria.

Los resultados (y por tanto las publicaciones a las que ha dado lugar) mantienen una unidad temática que, además, se ajusta estrachamente al título propuesto en el Proyecto de Tesis aprobado en su día por este Departamento.

Teniendo en cuenta la unidad temática del trabajo presentado, la validez de los resultados contenidos y su probada relevancia, consideramos favorablemente su presentación como Tesis Doctoral en su modalidad de Compendio de Publicaciones.

Zaragoza, a 18 de Noviembre de 2011

sello

El Director del órgano responsable

Fdo.: Dr. Jos®Antonio L· pez

COMISION DE DOCTORADO

A la vista de las publicaciones incluidas en la tesis y del informe motivado del órgano responsable del programa de doctorado, la Comisión de Doctorado ha acordado en su reunión de.....**AUTORIZAR / NO AUTORIZAR** *(táchese lo que no proceda)* la presentación de la tesis en la modalidad de compendio de pulblicaciones.

Zaragoza, a ____de _____ de 20____

La Presidente de la Comisión de Doctorado

sello

Fdo.: Mª. Pilar Diago Diago

Esta tesis doctoral se presenta mediante un compendio de cinco trabajos previamente publicados en revistas científicas con un índice de impacto incluido en la relación de revistas del *Journal of Citation Reports*. La unidad temática de estos trabajos es la síntesis y el estudio de la reactividad de los trifluorometil-derivados homolépticos de Pt(II) y Au(I).

Las referencias de dichas publicaciones son las siguientes:

Título: Oxidative Addition of Halogens to Homoleptic Perfluoromethyl or Perfluorophenyl Derivatives of Platinum(II): A Comparative Study
Autores: B. Menjón, S. Martínez-Salvador, M. A. Gómez-Saso, J. Forniés, L. R. Falvello, A. Martín, A. Tsipis
Revista: CHEMISTRY-A EUROPEAN JOURNAL Vol.: 15 Fasc.: 26 Págs.: 6371-6382 DOI: 10.1002/chem.200900323 Año: 2009
Impact Factor: 5.48 ISI Journal Citation Reports Ranking 2010: 18/147) (Chemistry Multidisciplinary)

Título: Trapping a Difluorocarbene-Platinum Fragment by Base Coordination
Autores: S. Martínez-Salvador, B. Menjón, J. Forniés, A. Martín, I. Usón
Revista: ANGEWANDTE CHEMIE-INTERNATIONAL EDITION Vol.: 49 Fasc.: 25 Págs.: 4286-4289 DOI: 10.1002/anie.200907031 Año: 2010
Impact Factor: 12.73 ISI Journal Citation Reports Ranking 2010: 5/147) (Chemistry Multidisciplinary)

Título: [Au($CF_3$)(CO)]: A Gold Carbonyl Compound Stabilized by a Trifluoromethyl Group
Autores: S. Martínez-Salvador, J. Forniés, A. Martín, B. Menjón
Revista: ANGEWANDTE CHEMIE-INTERNATIONAL EDITION Vol.: 50 Fasc.: 29 Págs.: 6571-6574 DOI: 10.1002/anie.201101231 Año: 2011
Impact Factor: 12.73 ISI Journal Citation Reports Ranking 2010: 5/147) (Chemistry Multidisciplinary)

Título: Highly Trifluoromethylated Platinum Compounds
Autores: S. Martínez-Salvador, J. Forniés, A. Martín, B. Menjón
Revista: CHEMISTRY-A EUROPEAN JOURNAL Vol.: 17 Fasc.: 29 Págs.: 8085-8097 DOI: 10.1002/chem.201100626 Año: 2011
Impact Factor: 5.48 ISI Journal Citation Reports Ranking 2010: 18/147) (Chemistry Multidisciplinary)

Título: Efficient and stereoselective syntheses of isomeric trifluoromethyl-platinum(IV) chlorides
Autores: S. Martínez-Salvador, P. J. Alonso, J. Forniés, A. Martín, B. Menjón
Revista: DALTON TRANSACTIONS Vol.: 15 Fasc.: 26 Págs.: 6371-6382 DOI: 10.1039/c1dt10557d Año: 2011
Impact Factor: 3.65 ISI Journal Citation Reports Ranking 2010: 7/43) (Chemistry Inorganic & Nuclear )

(1) $[NBu_4]_2[Pt(CF_3)_4]$

(1´) $[PPh_4]_2[Pt(CF_3)_4]$

(2) $[NBu_4]_2[\textit{trans}\text{-}Pt(CF_3)_4Cl_2]$

(3) $[NBu_4]_2[\textit{trans}\text{-}Pt(CF_3)_4Br_2]$

(4) $[NBu_4]_2[\textit{trans}\text{-}Pt(CF_3)_4I_2]$

(5) $[NBu_4]_2[\textit{trans}\text{-}Pt(CF_3)_4FCl]$

(6) $[NBu_4]_2[\textit{trans}\text{-}Pt(CF_3)_4F_2]$

(7) $[NBu_4]_2[\textit{cis}\text{-}Pt(CF_3)_4Cl_2]$

(7´) $[PPh_4]_2[\textit{cis}\text{-}Pt(CF_3)_4Cl_2]$

(8) $[NBu_4]_2[\textit{trans}\text{-}Pt(CF_3)_4Cl(SOCl)]$

(8´) $[PPN]_2[\textit{trans}\text{-}Pt(CF_3)_4Cl(SOCl)]$

(9) $[NBu_4]_2[\textit{fac}\text{-}Pt(CF_3)_3Cl_3]$

(9´) $[PPh_4]_2[\textit{fac}\text{-}Pt(CF_3)_3Cl_3]$

(10) $[NBu_4]_2[\textit{mer}\text{-}Pt(CF_3)_3Cl_3]$

(11) $[NBu_4]_2[Pt(CF_3)_5I]$

(12) $[NBu_4]_2[Pt(CF_3)_4(C_4F_9)I]$

(13) $[NBu_4][Pt(CF_3)_5(H_2O)]$

(14) $[NBu_4][Pt(CF_3)_5(MeCN)]$

(15) $[NBu_4][Pt(CF_3)_5py]$

(16) $[NBu_4][Pt(CF_3)_5(tht)]$

(17) $[NBu_4][Pt(CF_3)_5(CO)]$

(17´) $[PPh_4][Pt(CF_3)_5(CO)]$

(18) $[NBu_4]_2[Pt(CF_3)_5Cl]$

(19) $[NBu_4]_2[Pt(CF_3)_5Br]$

(20) $[NBu_4]_2[Pt(CF_3)_5F]$

(21) $[NBu_4][Pt(CF_3)_3(CO)]$

(21‡) $[NBu_4][Pt(CF_3)_3(=CF_2)]$

(22) $[NBu_4][Pt(CF_3)_3(CN^tBu)]$

(23) $[NBu_4][Pt(CF_3)_3(PPh_3)]$

(24) $[NBu_4][Pt(CF_3)_3(P(2\text{-}MeC_6H_4)_3)]$

(25) $[NBu_4][Pt(CF_3)_3(tht)]$

(26) $[NBu_4]_2[Pt(CF_3)_3Cl]$

(27) $[NBu_4]_2[Pt(CF_3)_3Br]$

(28) $[NBu_4]_2[Pt(CF_3)_3I]$

(29) $[NBu_4][Pt(CF_3)_2(CF_2NC_5H_4S\text{-}\kappa C,\kappa S)]$

(30) $[NBu_4][Pt(CF_3)_3(CNPh)]$

(31) $[NBu_4][Pt(CF_3)_3\{CO(1,2\text{-}C_6H_4)O\text{-}ciclo\}]$

(32) $[NBu_4][Pt(CF_3)_3\{COCH_2CH_2O\text{-}ciclo\}]$

(33) $[cis\text{-}Pt(CF_3)_2(CO)_2]$

(34) $[NBu_4][cis\text{-}Pt(CF_3)_2Cl(CO)]$

(35) $[NBu_4][cis\text{-}Pt(CF_3)Cl_2(CO)]$

(36) $[NBu_4]_2[\{Pt(CF_3)_2\}_2(\mu\text{-}Cl)_2]$

(37) $[cis\text{-}Pt(CF_3)_2(thf)_2]$

(38) $[NBu_4][trans\text{-}Pt(CF_3)_4H(CN^tBu)]$

(39) $[NBu_4][trans\text{-}Pt(CF_3)_4Me(CN^tBu)]$

(40) $[NBu_4][trans\text{-}Pt(CF_3)_4Et(CN^tBu)]$

(41) $[NBu_4][trans\text{-}Pt(CF_3)_4Me(CO)]$

(42) $[NBu_4][trans\text{-}Pt(CF_3)_4Et(CO)]$

(43) $[PPh_4][Au(CF_3)_2]$

(44) $[Au(CF_3)(CO)]$

(44‡) $[Au(CF_3)(=CF_2)]$

(44*) $[Au(CF_3)(^{13}CO)]$

# 1. Introducción

El flúor es un elemento químico fascinante por lo peculiar de sus propiedades. El hecho de que su electronegatividad en la escala de Pauling sea la mayor de todos los elementos químicos ($\chi_F$ = 4.0)[1] condiciona que el flúor actúe con estado de oxidación 0 en el elemento, $F_2$, y -1 en todas sus combinaciones químicas (HF, CsF, $ReF_7$, $PtF_6$, $AuF_5$, $HgF_4$ $PF_5$, $OF_2$, $IF_7$, $KrF_2$, $XeF_6$,…). Esta elevada electronegatividad junto con su pequeño tamaño hacen que el flúor actúe como un substituyente duro, escasamente polarizable. Esto a su vez condiciona el que buena parte de los compuestos de flúor sean iónicos y que, incluso aquellos de carácter covalente tengan una importante componente iónica $E^{\delta+}$–$F^{\delta-}$. Se cree que sea precisamente esta componente iónica la que confiere a los enlaces E–F una especial estabilidad. Así, el enlace C–F, con una energía media de enlace de 489 kJ·mol$^{-1}$, es el más estable de cuantos enlaces sencillos forma el C con el resto de elementos químicos, y el enlace B–F (644 kJ·mol$^{-1}$ de energía media de enlace) es el más estable de los enlaces sencillos entre dos elementos químicos cualesquiera.[2]

La alta estabilidad del enlace C–F junto con su acusada inercia química son los principales responsables del espectacular desarrollo de la química de los derivados organofluorados. De hecho, más del 30% de los productos agroquímicos y más del 10% de los farmacéuticos utilizados en la actualidad contienen flúor.

La fluoración total o parcial de un grupo orgánico altera sustancialmente sus propiedades. Un claro ejemplo de esta transformación se tiene al comparar las propiedades del grupo orgánico más sencillo, el metilo, $CH_3$, con las de su homólogo perfluorado, el trifluorometilo, $CF_3$ (Esquema 1).

La alta electronegatividad del ligando trifluorometilo, similar a la del oxígeno,[3] su pequeño tamaño[4] y su alto carácter hidrófobo[5] (parámetro utilizado para medir la lipofilia) contribuyen también a favorecer el desarrollo de la química de este ligando.[6];[7] De igual forma, la mayor estabilidad tanto química como térmica, junto con la mayor solubilidad y diversas propiedades mecánicas y eléctricas de diferentes moléculas trifluorometiladas (como por ejemplo los polímeros) son algunas de las razones por las que las moléculas que contienen

el sustituyente trifluorometilo resultan de gran interés y son consideradas como fuente importante de nuevos materiales.[8]

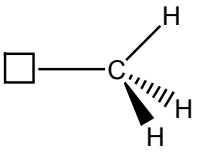


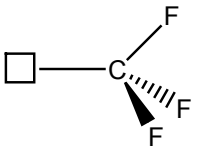


| | |
|---|---|
| $\chi$ = 2.28 | $\chi$ = 3.49 |
| $r_{vdw}$ = 0.27 nm | $r_{vdw}$ = 0.35 nm |
| $V_{vdw}$ = 0.017nm$^3$ | $V_{vdw}$ = 0.042 nm$^3$ |
| Energía media de enlace = 414 kJ.mol$^{-1}$ | Energía media de enlace = 489 kJ.mol$^{-1}$ |

**Esquema 1.** Comparación de las propiedades del grupo metilo, $CH_3$, con las de su homólogo perfluorado trifluorometilo, $CF_3$.

Por otra parte, la influencia del grupo $CF_3$ en moléculas biológicamente activas, generalmente va asociada a un aumento de la lipofilia que hace que las moléculas trifluorometiladas sean capaces de atravesar las membranas de lípidos con más facilidad que sus homólogas no fluoradas.[6] Por este motivo, en diversos programas de química medicinal, el flúor se utiliza para reemplazar al hidrógeno en diferentes moléculas utilizadas dentro de este campo. Estas sustituciones producen cambios electrónicos muy significativos que pueden modificar drásticamente, y generalmente mejorar, las propiedades de una molécula.[9]

Así pues, cuando el grupo $CF_3$ se encuentra unido a un elemento con una electronegatividad entre media y alta, se comporta como un sustituyente monovalente que posee una estabilidad térmica alta y una actividad química prácticamente nula. Sin embargo, cuando el $CF_3$ está unido a un elemento electropositivo se vuelve mucho más reactivo, produciéndose la eliminación de un flúor-$\alpha$ dando lugar a un difluorocarbeno, especie que se resulta extremadamente reactiva. Esta reacción de eliminación de un flúor-$\alpha$ (Esquema 2), se puede producir de forma espontánea o inducida. Un ejemplo del primer tipo es el $LiCF_3$ ($\chi_{Li}$ = 0.97),[10] especie que aún a baja temperatura

se descompone dando lugar a LiF y $CF_2$.[11] En el extremo opuesto estaría el caso del anión $[B(CF_3)_4]^-$ ($\chi_B$ = 2.01),[10] que requiere el tratamiento con $H_2SO_4$ concentrado para dar lugar a $B(CF_3)_3(CO)$ directamente, aunque presumiblemente la reacción transcurre a través de la formación del intermedio $B(CF_3)_3(=CF_2)$. Esta especie, que parece ser muy inestable y no ha podido ser detectada, experimenta hidrólisis inmediata para dar lugar al carbonil derivado final.[12]

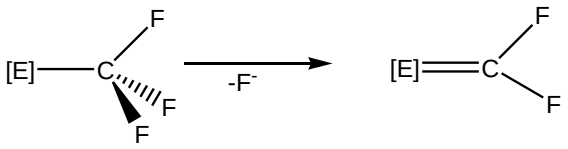


**Esquema 2.** Proceso de eliminación de un flúor-α que tiene lugar en los trifluorometil-derivados de elementos electropositivos.

El caso de los metales de transición, representa una situación intermedia ya que su electronegatividad es moderada ($\chi_{MT}$ = 1.22-1.75).[10] Esta situación junto con la disponibilidad de los orbitales d hace que los trifluorometil derivados de metales de transición con frecuencia den lugar a procesos de activación de enlaces C-F[13] por lo que actualmente son objeto de estudio y están recibiendo una gran atención.[14];[15]

Al igual que ocurre en química orgánica, los grupos alquilo perfluorados dan lugar a derivados organometálicos con una mayor estabilidad química que sus homólogos no fluorados.[16] Sin embargo, la química de los compuestos organometálicos con ligandos alquilo está mucho más desarrollada que la del ligando trifluorometilo. Está diferencia se hace más patente en compuestos que contienen un alto número de ligandos $CF_3$.

Se conocen derivados muy interesantes con hasta ocho ligandos metilo por átomo central, entre los que se cuentan diferentes sales de los aniones $[U(CH_3)_8]^{3-}$,[17] $[W(CH_3)_8]^{2-}$,[18] o $[Re(CH_3)_8]^{2-}$.[19]

Por el contrario, sólo unos pocos derivados organometálicos con un máximo de cuatro grupos trifluorometilo, han sido aislados y caracterizados hasta la fecha. Entre estas especies se encuentra el perfluoroneopentano $C(CF_3)_4$, el cual fue obtenido por primera vez como uno de los muchos componentes de las pirólisis de $CF_3SF_5$ o de $(CF_3)_2SF_4$ con $CF_3CF=CF_2$ llevadas a cabo a 500 ºC.[20]

Esta molécula, así como otras especies homolépticas neutras con fórmula $E(CF_3)_4$ (E = Ge, Sn, Pb, Te) han sido obtenidas mediante al menos uno de los siguientes procedimientos (Esquema 3):[21]

1) fluoración directa del alquil-derivado correspondiente $E(CH_3)_4$ (Esquema 3a).[22]
2) reacción del elemento precursor adecuado con el radical $CF_3$· obtenido por la ruptura homolítica del enlace $CF_3$-$CF_3$ mediante descarga fotolítica en plasma (Esquema 3b).[23]
3) reacción de intercambio un halogenuro neutro $EX_4$ y un agente trifluorometilante nucleófilo como por ejemplo: $[Ag(CF_3)(solv)]$, $[Ag(CF_3)(solv)]$, $[Cd(CF_3)_2]$ o incluso $Sn(CF_3)_4$ (Esquema 3c).[24]

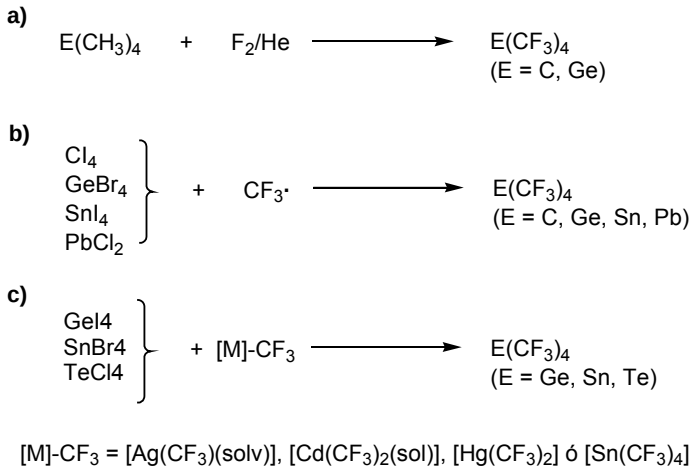


**Esquema 3**: Métodos sintéticos por los cuales se han preparado los trifluorometil-derivados homolépticos neutros $E(CF_3)_4$.

En el caso de especies aniónicas con al menos cuatro ligandos $CF_3$ encontramos la especie $[B(CF_3)_4]^-$, a la que ya se ha hecho referencia anteriormente, y que ha sido preparada recientemente mediante la transformación de un triple enlace C≡N en la especie $[B(CN)_4]^-$ en tres enlaces C-F mediante la reacción con $ClF_3$ en HF(*l*) anhidro (Esquema 4a).[25]

En el caso de los metales de transición en los que se centra nuestro trabajo, Pt y Au, se han obtenido diferentes sales de los aniones homolépticos $[M^{II}(CF_3)_4]^{2-}$ ($M^{II}$ = Pd, Pt)[15] mediante reacción de los sustratos metálicos de partida adecuados con un agente nucleófilo trifluorometilante, generalmente la especie

pentacoordinada de silicio $[Me_3Si(CF_3)F]^-$ que se genera *in situ* por la coordinación de un fluoruro a $Me_3Si(CF_3)$ a baja temperatura (Esquema 4b).[26] La especie isoléptica $[Cd^{II}(CF_3)_4]^-$ parece haber sido detectada como uno de los componentes de disoluciones polares de $Cd(CF_3)_2$ en presencia de CsI.[27] También se ha preparado la serie completa de aniones $[M^{III}(CF_3)_4]^-$ para los tres metales del grupo 11 ($M^{III}$ = Cu[28], Ag[29], Au[30]) .[31]

Algunas especies químicas con más de cuatro ligandos trifluorometilo han sido detectadas pero no aisladas en forma pura. La reacción a baja temperatura de $[Pt(CN)_4]^{2-}$ con ClF implica la transformación de los ligandos CN en ligandos $CF_3$ junto con la oxidación del metal y procesos de intercambio de ligandos.[32] Finalmente, se hace referencia en una patente a los compuestos con alto estado de oxidación $U(CF_3)_6$ y $W(CF_3)_6$ pero sin datos acerca de su caracterización.[33]

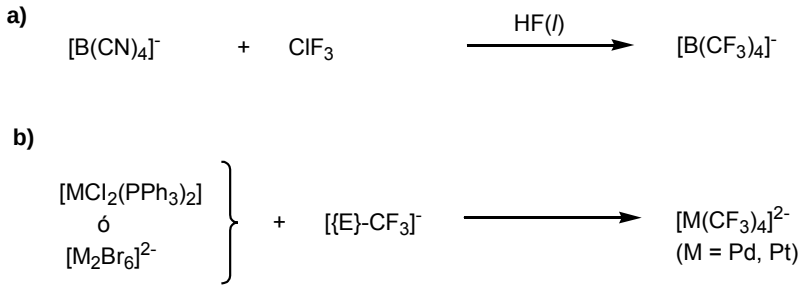


**Esquema 4**: Métodos sintéticos por los cuales se han preparado algunos derivados homolépticos aniónicos que contienen un alto número de ligandos $CF_3$.

En el presente trabajo nos hemos propuesto explorar la química del trifluorometil-derivado homoléptico de $Pt^{II}$ ($d^8$) de fórmula $[NBu_4]_2[Pt(CF_3)_4]$. Se han estudiado por un lado, procesos en los que el centro reactivo es el metal (Secciones 2, 3 y 4) y por otro, procesos en los que el centro reactivo es el ligando $CF_3$ (Sección 5). También se demuestra que, en el sistema objeto de estudio, el centro cinéticamente favorecido es generalmente el metal, aunque sea el grupo $CF_3$ el termodinámicamente favorecido (Sección 5). Finalmente se aplican algunos de los resultados obtenidos con el sustrato de platino al trifluorometil-derivado homoléptico de $Au^{I}$ ($d^{10}$) de fórmula $[PPh_4][Au(CF_3)_2]$ (Sección 6).

## 2. Adición oxidante de halógenos sobre el perfluorometil-derivado homoléptico de Pt(II).

B. Menjón, S. Martínez-Salvador, M. A. Gómez-Saso, J. Forniés, L. R. Falvello, A. Martín, A. Tsipis, *Chem. Eur. J*. **2009**, *15*, 6371.

La sal $[NBu_4]_2[Pt(CF_3)_4]$ (**1**) se ha sintetizado mediante un método similar al utilizado por D. Naumann y sus colaboradores para obtener el derivado $[NMe_4]_2[Pt(CF_3)_4]$.[15] Este procedimiento consiste en el tratamiento a -78ºC del derivado $[NBu_4]_2[(PtBr_2)_2(\mu\text{-}Br)_2]$ con $Me_3Si(CF_3)$, en presencia de CsF y de la cantidad estequiométrica requerida de $[NBu_4]Br$ (Esquema 5). El hecho de utilizar esta sal radica en su mayor solubilidad en disolventes orgánicos lo que la hace mucho más adecuada para realizar el estudio de sus propiedades.

Se han llevado a cabo las reacciones de adición oxidante de la cantidad estequiométrica de halógeno $X_2$ (X = Cl, Br, I) sobre el trifluorometil-derivado homoléptico de Pt(II) **1** a baja temperatura dando lugar a las especies octaédricas de Pt(IV) $[NBu_4]_2[$*trans*-$Pt(CF_3)_4X_2]$ (X = Cl(**2**), Br(**3**), I(**4**)) (Esquema 5) de forma cuantitativa y estereoselectiva según se observa en los espectros de RMN de $^{19}F$. Estos trifluorometil-derivados de Pt(IV) poseen una estabilidad mucho mayor que el derivado de partida de Pt(II) sobre todo frente a procesos de eliminación de flúor-$\alpha$ (ver Sección 5). Esta diferencia de estabilidad puede explicarse por la menor densidad electrónica del centro metálico en el caso de derivados octaédricos de Pt(IV), que hace que sean mucho más inertes frente a procesos de hidrólisis que el derivado de partida de Pt(II) con geometría cuadrada plana.

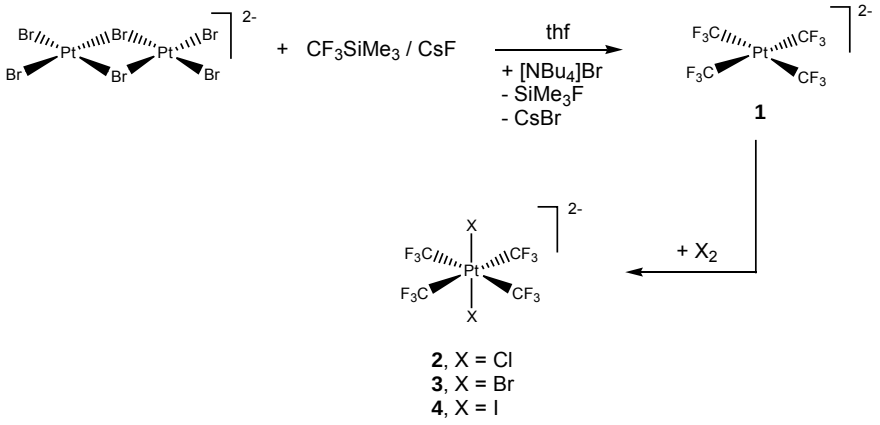


**Esquema 5.** Síntesis de los trifluorometil-derivados de Pt **1**, **2**, **3** y **4**. $[NBu_4]^+$ es el catión en todos los casos.

El hecho de formular los derivados $[NBu_4]_2[trans\text{-}Pt(CF_3)_4X_2]$ como isómeros *trans* se basa en sus espectros de RMN de $^{19}F$ y $^{13}C\{^{19}F\}$ que consisten en singletes flanqueados por satélites de $^{195}Pt$ ($I$ = ½, 33.831557(42)% de abundancia natural relativa).[34] Los desplazamientos químicos a los que aparecen las señales de $^{195}Pt$ y $^{13}C\{^{19}F\}$ aumentan a medida que aumenta la electronegatividad del halógeno (Tabla 1). Sin embargo en los espectros de $^{19}F$ se observa la tendencia inversa (Tabla 1).

Las constantes de acoplamiento de spin internuclear $^1J(^{13}C,^{195}Pt)$ y $^2J(^{19}F,^{195}Pt)$ para los trifluorometil-derivados de Pt(IV) $[NBu_4]_2[trans\text{-}Pt(CF_3)_4X_2]$ experimentan una importante reducción con respecto al trifluorometil-derivado de Pt(II) de partida (**1**) (1284 y 542 Hz respectivamente).[15]

**Tabla 1.** Datos espectroscópicos de RMN para los trifluorometil derivados de Pt(IV) $[NBu_4]_2[trans\text{-}Pt(CF_3)_4X_2]$

| | (X = Cl) | (X = Br) | (X = I) |
|---|---|---|---|
| $\delta_C$ [ppm] | 117.3 | 116.7 | 114.6 |
| $^1J(^{13}C,^{195}Pt)$ [Hz] | 858 | 859 | 888 |
| $\delta_F$ [ppm] | -34.0 | -31.3 | -18.5 |
| $^2J(^{19}F,^{195}Pt)$ [Hz] | 268 | 275 | 308 |
| $\delta_{Pt}$ [ppm] | -1805 | -2105 | -3656 |

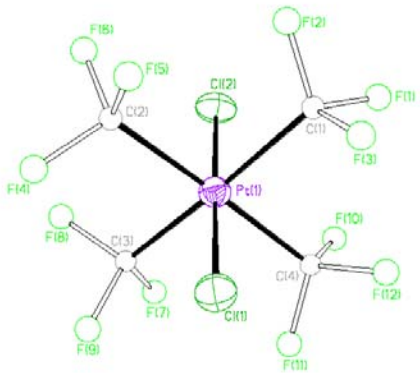


**Figura 1.** Estructura cristalina del anión $[trans\text{-}Pt(CF_3)_4Cl_2]^{2-}$ del complejo **2**

Los espectros de $^{195}Pt$ aparecen como señales con una alta multiplicidad debida al acoplamiento de núcleo de Pt con los 12 núcleos equivalentes de $^{19}F$ ($I$ = ½, 100% de abundancia natural).[34]

La estructura del derivado **2** ha sido determinada mediante difracción de rayos X en un monocristal de la sal $[NBu_4]_2$[*trans*-$Pt(CF_3)_4Cl_2$] (Figura 1) y está de acuerdo con las propiedades espectroscópicas encontradas en disolución.

Se han realizado diferentes cálculos teóricos acerca de la estabilidad relativa de los iones $[Pt(CF_3)_4X_2]^{2-}$ (X = Cl, Br, I). Estos estudios indican que los isómeros *cis* deberían ser ligeramente más estables que sus correspondientes isómeros *trans*. El hecho de que, en nuestro caso, la adición oxidante de halógenos sobre el compuesto **1** dé lugar cuantitativamente a la formación de los isómeros *trans* puede ser atribuida a una serie de factores que se describen a continuación:

1) Las suaves condiciones en las que se llevan a cabo estas reacciones (disolución de $CH_2Cl_2$ y -78ºC) lo que nos llevaría a obtener el isómero favorecido cinéticamente en vez del termodinámicamente más favorecido.
2) El efecto del disolvente, no tenido en cuenta en dichos cálculos y que, como se verá más adelante, desempeña un papel importante a la hora de estabilizar el intermedio **Z** (Esquema 6), y determinar su geometría. Este tipo de interacción **Z**/disolvente dependerá en cada caso de la acidez de Lewis y de la accesibilidad del centro metálico en el intermedio insaturado **Z**, así como de la capacidad coordinante del propio disolvente (basicidad de Lewis del disolvente). Aunque en este caso no se ha detectado ningún intermedio, sí se han podido detectar al estudiar el mismo tipo de reacciones sobre el pentafluorofenil-derivado $[NBu_4]_2[Pt(C_6F_5)_4]$ análogo al compuesto **1**. También se presentan a continuación otros casos en los que se ve claramente cómo el disolvente influye de forma evidente en el mecanismo de este tipo de reacciones.

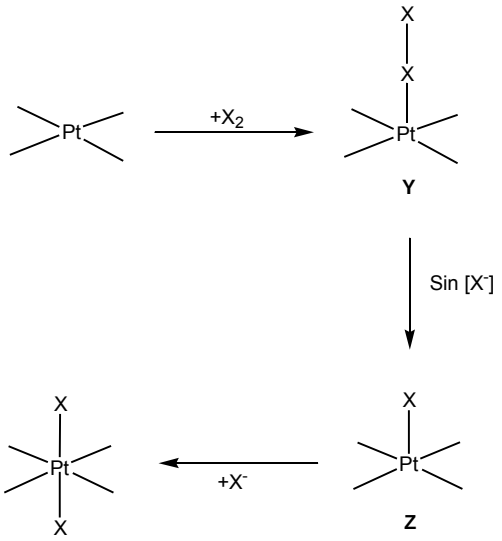


**Esquema 6.** Mecanismo más aceptado par la adición oxidante de halógenos sobre los derivados *SP*-4 de Pt(II)

Desde que en el año 1962 se sintetizara el primer derivado de un gas noble "$XePtF_6$",[35] el interés por estas especies no ha cesado de aumentar como lo reflejan la cantidad de artículos y monografías dedicadas a ellos. El difluoruro de xenón, $XeF_2$, es el más manejable de todos estos derivados, por lo que su química es también la más estudiada. Su síntesis es relativamente simple[36];[37] y no hay peligro de formación de óxidos de xenón explosivos.[38]

El $XeF_2$ tiene un potencial de oxidación considerablemente alto, lo cual es debido a su baja energía de enlace (133.9 kJ $mol^{-1}$) y a que su producto de reducción, Xe, es completamente inerte. Además, el $XeF_2$ es un buen agente fluorante por lo que podría considerarse como una versión "*domesticada*" de la molécula de $F_2$.

El $XeF_2$ se disuelve en una variedad de disolventes como por ejemplo, $BrF_5$, $BrF_3$, $IF_5$, HF(*l*) anhidro, $CH_3CN$, etc. sin experimentar ningún proceso redox. [39] Sin embargo, reacciona con otros disolventes en los cuales debería ser inerte: $CH_2Cl_2$ y $CHCl_3$. Los productos obtenidos en estas reacciones son el resultado de procesos de intercambio flúor-cloro y flúor-hidrógeno (Ecuaciones 1 y 2). Sin embargo, las reacciones con estos disolventes a temperatura ambiente son lentas y se completan sólo al cabo de 2 días.

**Ec. 1** $XeF_2 + CH_2Cl_2 \longrightarrow CH_2FCl\ (24.4\%) + CHFCl_2\ (25.6\%) + HF\ (37\%) + \text{otros}$

**Ec.2** $XeF_2 + CHCl_3 \longrightarrow CH_2FCl\ (24.4\%) + CHFCl_2\ (25.6\%) + HF\ (37\%) + CHF_2Cl\ (1.2\%)$

En vista de las propiedades del $XeF_2$ y las dificultades experimentales asociadas al uso de $F_2$ como reactivo, para lo cual no disponemos de infraestructura adecuada, se ha realizado un estudio acerca de la reactividad del derivado homoléptico **1** frente a $XeF_2$. Estas reacciones se han llevado a cabo en distintos disolventes, lo que ha permitido ver de una forma más directa el papel tan importante que desempeña el disolvente en este tipo de procesos. También se ha llevado a cabo la reacción en ausencia de disolvente, lo cual ha permitido completar la serie de trifluorometil-derivados de Pt(IV) $[NBu_4]_2$[*trans*-$Pt(CF_3)_4X_2$] al incluir también el caso en el que X = F (Esquema 7).

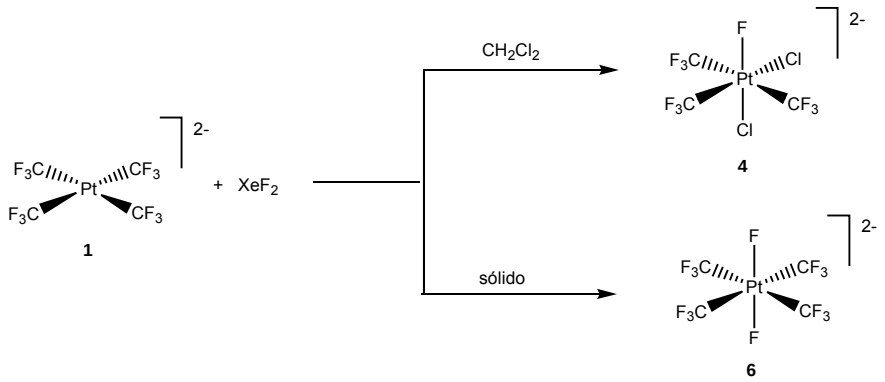


**Esquema 7.** Reactividad del derivado **1** frente a $XeF_2$ en $CH_2Cl_2$ como disolvente y en estado sólido. $[NBu_4]^+$ es el catión en todos los casos.

La reacción a baja temperatura de **1** con la cantidad estequiométrica requerida de $XeF_2$ en $CH_2Cl_2$ ó $CHCl_3$ da lugar a la formación de $[NBu_4]_2$[*trans*-$Pt(CF_3)_4ClF$] (**4**) de forma cuantitativa. La estructura del derivado **4** se ha establecido mediante técnicas espectroscópicas entre las que destaca la espectrometría de RMN multinuclear de $^{19}F$, $^{13}C\{^{19}F\}$ y $^{195}Pt$.

Se observa claramente cómo el disolvente interviene de forma directa en el proceso. El mecanismo propuesto consta de varios pasos:

1) Coordinación del Xe al centro de Pt(II). El $XeF_2$ pierde $F^-$ con mucha facilidad formándose el fragmento $[XeF]^+$ que es el que oxidará al centro metálico.
2) Transferencia electrónica del metal al Xe, produciéndose la oxidación del centro metálico de Pt(II) a Pt(IV), la reducción del $Xe^{2+}$ a Xe que se desprende y la formación de un enlace Pt-F. Este intermedio pentacoordinado de Pt(IV) se estabiliza mediante la coordinación de una molécula de disolvente ($CH_2Cl_2$).
3) Activación del enlace Cl-$CH_2Cl$ para dar lugar al producto final **4** junto con otros subproductos orgánicos no identificados.

En el tercer paso, se plantea la duda de si el Cl coordinado al Pt en el producto final **4** procede realmente de una activación de la molécula de $CH_2Cl_2$ coordinada o simplemente de la substitución de $Cl^-$ por $F^-$ en el disolvente libre. Para comprobarlo se ha llevado a cabo la reacción de fluoración en presencia de $[NBu_4]Br$ en exceso. En estas condiciones, el resultado de la reacción ha sido el mismo, la formación de **4**, por lo que claramente se concluye que la activación se produce sobre la molécula de disolvente una vez coordinada al centro metálico.

Cuando se hace reaccionar la sal $[PPh_4]_2[Pt(CF_3)_4]$ (**1´**) con un exceso de $XeF_2$, a 0ºC y en ausencia de disolvente, se obtiene el producto resultante de la adición oxidante de $F_2$ $[PPh_4]_2[$*trans*-$Pt(CF_3)_4F_2]$ (**6**) como producto mayoritario. Esta reacción es sorprendente por cuanto tiene lugar de forma estereoselectiva y prácticamente cuantitativa, en condiciones muy suaves y sin necesidad de utilizar disolvente alguno.

La formulación *trans* del difluoro-derivado **6** está basada en el análisis de sus espectros de RMN de $^{19}F$ y de $^{13}C\{^{19}F\}$. El espectro de $^{19}F$ consiste en un triplete por acoplamiento con los dos fluoruros flanqueados por satélites de $^{195}Pt$, cuya frecuencia es la más baja de la serie de los halógenos (-39.82 ppm) (Figura 2) y un multiplete a frecuencia muy baja (-414.31 ppm) con una elevada multiplicidad debida al acoplamiento con los 12 átomos de flúor equivalentes de los grupos $CF_3$ y una constante de acoplamiento de spin internuclear $^1J(^{19}F,^{195}Pt)$ = 1449 Hz que corresponde a los dos ligandos fluoruro unidos directamente al átomo de Pt. La constante de acoplamiento de spin

internuclear $^{2}J(^{19}F,^{195}Pt)$ del los grupos $CF_3$ es también la más baja de toda la serie (234 Hz).

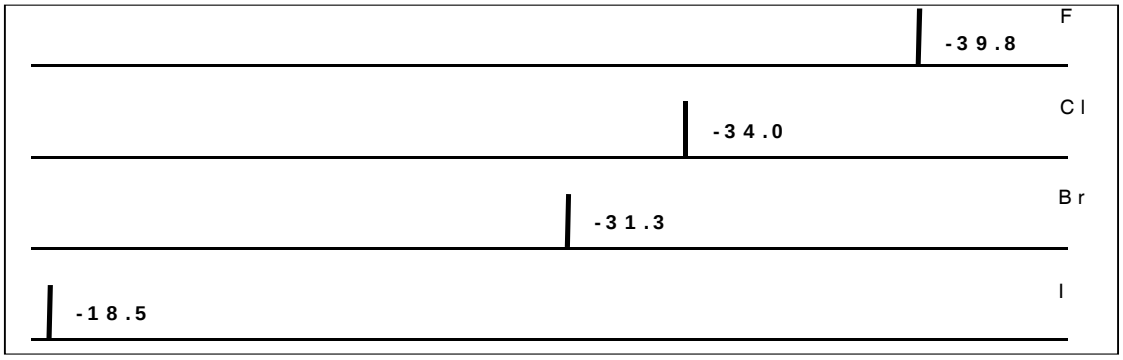


**Figura 2.** Desplazamientos químicos de las especies $[NBu_4]_2[trans\text{-}Pt(CF_3)_4X_2]$ [X = F (**6**), Cl (**2**), Br (**3**) y I (**4**)].

Al igual que sus homólogos con Cl, Br y I, el derivado **6** presenta una alta estabilidad térmica y química, siendo inerte frente a un buen número de reactivos.

### 3. Síntesis eficiente y estereoselectiva de diferentes isómeros de triflurometil-derivados de Pt(IV) que contienen ligandos cloruro.

S. Martínez-Salvador, P. J. Alonso, J. Forniés, A. Martín, B. Menjón, *Dalton Trans*. **2011**, *40*, 10440.

La estereoisomería ha desempeñado un papel fundamental en el desarrollo de la química de la coordinación.[40] Sin embargo, la gran variedad estereoquímica que existe para el Pt(IV) en compuestos de coordinación[41], contrasta con la situación encontrada para los derivados organometálicos de Pt(IV), para los cuales sólo una de las posibles disposiciones estereoquímicas parece estar favorecida. Este hecho ya fue señalado por Tobias[42] y puede ser explicado mediante la gran influencia *trans* que tienen asignada los grupos orgánicos σ-dadores y que tiene como consecuencia una desestabilización del enlace M-L situado en la posición *trans* a dichos grupos.[43];[44] El hecho de que "*dos ligandos blandos en posición mutuamente trans tendrán un efecto desestabilizante el uno sobre el otro cuando estén unidos a un átomo metálico de clase b*" fue denominado como efecto antisimbiótico por Pearson.[45] Ésta, bien podría ser la explicación de por qué todos los derivados organometálicos

octaédricos de Pt(IV) que contienen los fragmentos $PtMe_4$ o $PtMe_3$ presentan geometrías *cis* o *fac* respectivamente. Preferencias estequiométricas similares serían esperadas para los trifluorometil-derivados de Pt(IV) en vista de la considerable influencia *trans* del grupo $CF_3$, casi tan alta como la asignada al grupo $CH_3$.[46]

En esta sección se describe un procedimiento sintético muy eficiente para obtener de forma estereoselectiva diferentes sales de las siguientes parejas de trifluorometil derivados de Pt(IV): *cis/trans*-$[Pt(CF_3)_4Cl_2]^{2-}$ y *fac*/*mer*-$[Pt(CF_3)_3Cl_3]^{2-}$. Estos derivados han sido aislados con buen rendimiento y han sido caracterizados por una combinación de métodos analíticos, espectroscópicos y de difracción de rayos X.

Aunque los derivados $[NBu_4]_2$[*cis*-$Pt(CF_3)_4Cl_2$] (**7**) y $[NBu_4]_2$[*fac*-$Pt(CF_3)_3Cl_3$] (**9**) ya habían sido detectados con anterioridad como algunos de los productos de la reacción entre $[NBu_4]_2[Pt(CN)_4]$ con ClF en disolución de $CH_2Cl_2$[32], no habían podido ser aislados en forma pura.

El trifluorometil-derivado homoléptico de Pt(II) **1**, reacciona con $SOCl_2$ a temperatura ambiente y en disolución de acetona (Esquema 8) para dar el derivado $[NBu_4]_2$[*cis*-$Pt(CF_3)_4Cl_2$] (**7**) de forma cuantitativa y en apenas 15 minutos de reacción.

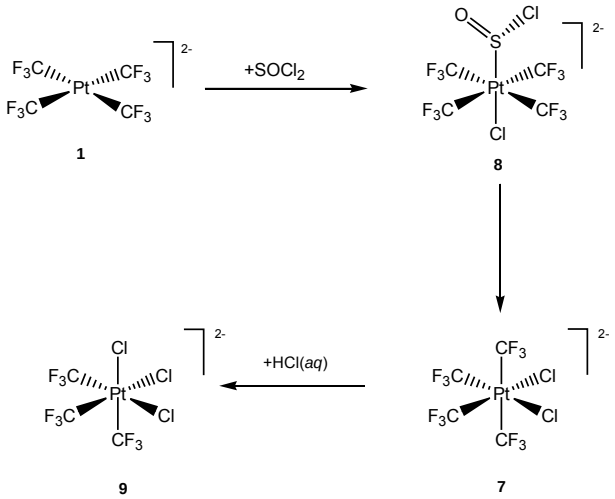


**Esquema 8.** Formación de los isómeros [*cis*-$Pt(CF_3)_4Cl_2]^{2-}$/[*fac*-$Pt(CF_3)_3Cl_3]^{2-}$ mediante la oxidación de **1** con $SOCl_2$. $[NBu_4]^+$ es el catión en todos los casos.

La estereoquímica de este compuesto ha podido ser determinada mediante el análisis de sus propiedades espectroscópicas, las cuales están de acuerdo con las asignadas previamente al anión [*cis*-$Pt(CF_3)_4Cl_2]^{2-}$.[32] Su espectro de RMN de $^{19}F$ ha contribuido en gran medida a esta determinación estructural. Este espectro consta de dos septupletes de igual intensidad correspondientes a las señales de los grupos trifluorometilo sitúados *trans* a Cl y $CF_3$ y que son químicamente inequivalentes (Figura 3). Ambas señales están flanqueadas por satélites de $^{195}Pt$.

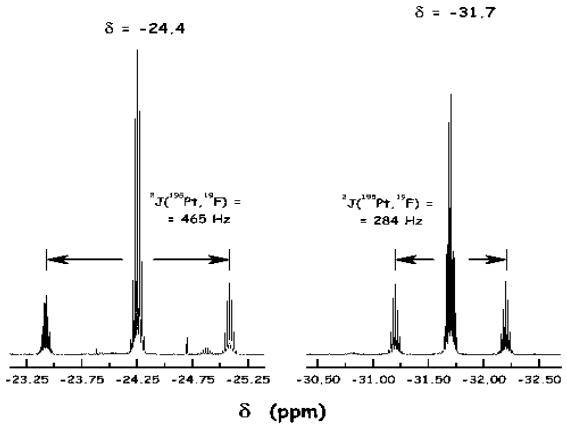


**Figura 3.** Espectro de RMN de $^{19}F$ del derivado **7** en [$^2H$]acetona a temperatura ambiente.

Los diferentes cálculos teóricos que se han realizado acerca de la estabilidad relativa de los iones $[Pt(CF_3)_4X_2]^{2-}$ (X = Cl, Br, I), comentados con anterioridad (véase Sección 2), indican que los isómeros *cis* deberían ser algo más estables que sus correspondientes isómeros *trans*. El isómero [*cis*-$Pt(CF_3)_4Cl_2]^{2-}$, es el producto mayoritario de la reacción de $[NBu_4]_2[Pt(CN)_4]$ con ClF en $CH_2Cl_2$,[32] sin embargo, al realizar la adición oxidante de $Cl_2$ sobre el compuesto **1** a baja temperatura, sólo se obtiene el isómero [*trans*-$Pt(CF_3)_4Cl_2]^{2-}$ (Esquema 9a) cuyas propiedades espectroscópicas ya han sido descritas anteriormente (véase Sección 2). Todos los intentos llevados a cabo para provocar la isomerización al isómero *cis*, en principio más estable, mediante tratamiento térmico fracasaron. La reacción de **1** con $SOCl_2$ a temperatura ambiente (Esquema 8) tiene lugar mediante la reordenación estereoquímica de la unidad "$Pt(CF_3)_4$" que pasa de una disposición inicial con geometría cuadrada plana en el derivado de partida **1** a una disposición final con geometría de silla de montar

en el entorno del Pt en el compuesto **7** (equivalente a dejar dos huecos en *cis*). Esta reorganización no había sido observada hasta el momento, por lo que se ha llevado a cabo la misma reacción a baja temperatura con intención de detectar algún intermedio de reacción y poder así, entender con más detalle el mecanismo del proceso.

Cuando el derivado de partida **1** reacciona con $SOCl_2$ a -78ºC, el medio de reacción, inicialmente de color amarillo claro, adquiere un color verde. El espectro de RMN de $^{19}F$ a baja temperatura muestra un singlete con un desplazamiento químico a menor frecuencia que el derivado de partida (-32.1 ppm) y una constante de acoplamiento de spin internuclear también menor $^{2}J(^{195}Pt,^{19}F)$ = 262 Hz, lo cual es indicativo de que ha habido una oxidación del centro metálico. Aunque estos datos indican que se trata de un trifluorometil-derivado de Pt(IV) con alta simetría en el que no se ha producido una reordenación de la unidad "$Pt(CF_3)_4$" no son concluyentes a la hora de determinar la estructura de este intermedio. Para ello, se aisló un sólido verde del medio de reacción cuyos análisis elementales junto con las propiedades espectroscópicas y la determinación de su estructura mediante difracción de rayos X en un monocristal de la sal $[N(PPh_3)_2]_2$[*trans*-$Pt(CF_3)_4Cl(SOCl)$] (**8´**)(Figura 4), confirmaron la estructura de este intermedio de reacción. Se observa que se ha producido la adición oxidante del enlace S-Cl de la molécula $SOCl_2$ sobre los trifluorometil-derivados de Pt(II) **1** ó **1´** para dar lugar a los trifluorometil-derivados octaédricos de Pt(IV) que contienen el ligando clorosulfinilo, muy poco habitual dentro de la química de la coordinación y organometálica, $[NBu_4]_2$[*trans*-$Pt(CF_3)_4Cl(SOCl)$] (**8**) o $[N(PPh_3)_2]_2$[*trans*-$Pt(CF_3)_4Cl(SOCl)$] (**8´**) .

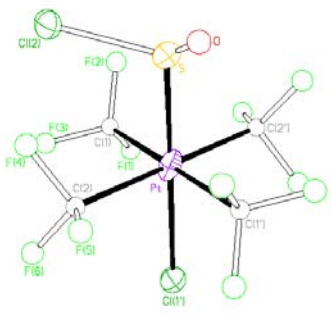


**Figura 4.** Estructura cristalina del anión [*trans*-$Pt(CF_3)_4Cl(SOCl)]^{2-}$ del complejo **8´**

El derivado $[NBu_4]_2[cis\text{-}Pt(CF_3)_4Cl_2]$ (**7**) reacciona con la cantidad equimolar de HCl(aq) para dar lugar a la especie $[NBu_4]_2[fac\text{-}Pt(CF_3)_3Cl_3]$ (**9**) de forma cuantitativa (Esquema 8). Esta reacción implica la pérdida estereoselectiva de un grupo $CF_3$ sitúado *trans* a otro grupo trifluorometilo en el derivado de partida $[NBu_4]_2[cis\text{-}Pt(CF_3)_4Cl_2]$ (**7**). Su espectro de RMN de $^{19}F$ consiste en un singlete flanqueado con satélites de $^{195}Pt$. Los parámetros encontrados están de acuerdo con los asignados previamente al anión $[fac\text{-}Pt(CF_3)_3Cl_3]^{2-}$ en disolución.[SB04] La geometría de este derivado se ha establecido mediante la difracción de rayos X en un monocristal de la sal $[PPh_4]_2[fac\text{-}Pt(CF_3)_3Cl_3]$ (**9´**) (Figura 5).

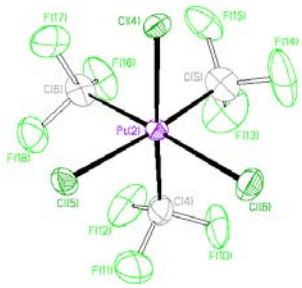


**Figura 5.** Estructura cristalina del anión $[fac\text{-}Pt(CF_3)_3Cl_3]^{2-}$ del complejo **9´**

Ya se ha comentado que no se conocen precedentes de trifluorometil-dertivados de Pt(IV) con geometría *mer* caracterizados estructuralmente. En nuestro caso, hemos conseguido llevar a cabo la síntesis del estereoisómero $[mer\text{-}Pt(CF_3)_3Cl_3]^{2-}$. Para ello se ha hecho reaccionar el trifluorometil-derivado de Pt(II) $[NBu_4]_2[Pt(CF_3)_3Cl]$ en disolución de $CH_2Cl_2$ con $Cl_2$ (disuelto en $CCl_4$) a baja temperatura. De esta forma se obtiene de forma cuantitativa el derivado $[NBu_4]_2[mer\text{-}Pt(CF_3)_3Cl_3]$ (**10**) (Esquema 9b).

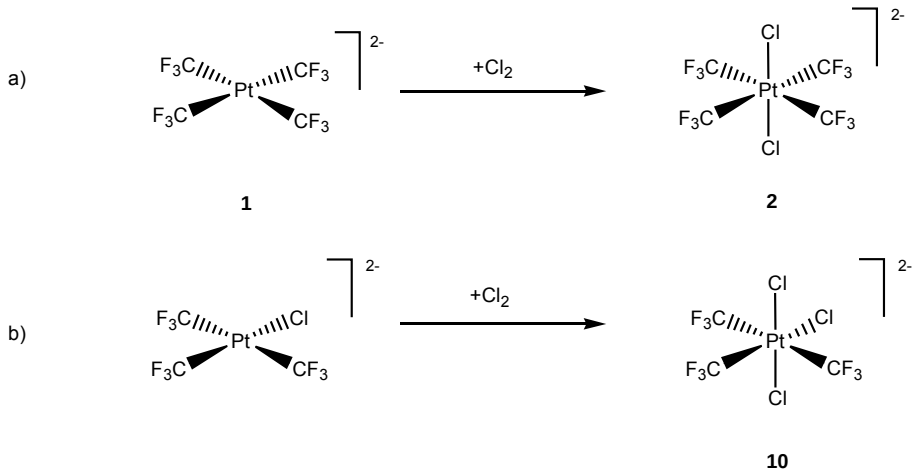


**Esquema 9.** Métodos de síntesis de los isómeros a) [*trans*-$Pt(CF_3)_4Cl_2]^{2-}$ y b) [*mer*-$Pt(CF_3)_3Cl_3]^{2-}$. $[NBu_4]^+$ es el catión en todos los casos.

El espectro de RMN de $^{19}F$ del derivado $[NBu_4]_2$[*mer*-$Pt(CF_3)_3Cl_3$] (**10**) tiene el mismo patrón que el correspondiente al derivado de partida de Pt(II) $[NBu_4]_2[Pt(CF_3)_3Cl]$ aunque los valores de los parámetros asociados son diferentes. El espectro consiste en un septuplete y un cuartete con intensidades 1:2 y flanqueadas por satélites de $^{195}Pt$ (Figura 6). La señal correspondiente al grupo $CF_3$ situado *trans* a Cl aparece a mayor frecuencia y tiene una constante de acoplamiento de spin internuclear $^2J(^{195}Pt,^{19}F)$ mayor que la señal correspondiente a los grupos $CF_3$ situados mutuamente *trans*. Este hecho puede explicarse por la mayor influencia *trans* que tiene el grupo $CF_3$ con respecto al Cl.

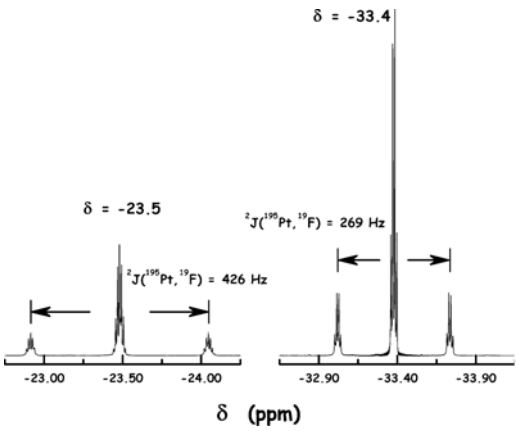


**Figura 6.** Espectro de RMN de $^{19}F$ del derivado **10** en [$^2$H]acetona a temperatura ambiente.

La estructura del derivado **10** ha sido establecida mediante difracción de rayos X en un monocristal del solvato $[NBu_4]_2[$*mer*-$Pt(CF_3)_3Cl_3]\cdot 0.42CH_2Cl_2$ (Figura 7). Sus propiedades espectroscópicas están de acuerdo con su estructura en estado sólido.

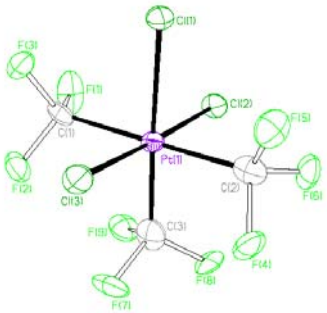


**Figura 7.** Estructura cristalina del anión [*mer*-$Pt(CF_3)_3Cl_3]^{2-}$ del complejo **10**

En esta sección se han descrito métodos sintéticos eficientes para obtener sales de alguna de las siguientes parejas de isómeros *cis*/*trans* y *fac*/*mer* de los iones $[Pt(CF_3)_4Cl_2]^{2-}$ y $[Pt(CF_3)_3Cl_3]^{2-}$ respectivamente. Estas especies han sido aisladas en forma pura y su estructura ha sido determinada mediante el análisis de sus propiedades espectroscópicas (principalmente RMN de $^{19}F$). La pareja de isómeros *fac*/*mer* ha sido caracterizada estructuralmente mediante la difracción de rayos X en un monocristal de alguna de sus sales. Además, el intermedio de reacción, térmicamente inestable, que contiene el ligando poco común clorosulfinilo, $[NBu_4]_2[$*trans*-$Pt(CF_3)_4Cl(SOCl)]$ (**8**), ha sido detectado y caracterizado de forma completa. Esta especie parece ser clave en el mecanismo de isomerización *trans*/*cis*.

## 4. Derivados de platino altamente trifluorometilados

S. Martínez-Salvador, J. Forniés, A. Martín, B. Menjón, *Chem. Eur. J*. **2011**, *17*, 8085.

En vista de los escasos antecedentes de derivados organometálicos con alto contenido en ligandos $CF_3$, en esta sección planteamos la posibilidad de acceder de forma limpia y eficiente a la química de los pentakis(trifluorometil)-derivados de Pt(IV).

Hasta el momento de la publicación de este trabajo, solo algunos trifluorometil-derivados de Pt(IV) con más de cuatro grupos $CF_3$ habían sido detectados en disolución mediante la ya mencionada reacción de diferentes sales de $[Pt(CN)_4]^{2-}$ con ClF a baja temperatura en $CH_2Cl_2$ que llevaron a cabo H. Willner y sus colaboradores.[32] Esta es una reacción compleja en la que tienen lugar procesos de intercambio de ligandos junto con la oxidación del metal, como resultado de lo cual se obtiene una mezcla de productos entre los que se encuentran especies de fórmula $[Pt(CF_3)_5X]^{2-}$ (X = F, Cl, OH). Incluso el derivado homoléptico $[Pt(CF_3)_6]^{2-}$ ha sido detectado en dicho medio de reacción. Sin embargo, ninguno de estos compuestos había podido ser aislado en forma pura.

La sal $[NBu_4]_2[Pt(CF_3)_4]$ (**1**) disuelta en MeCN reacciona con un ligero exceso de $CF_3I$ (disolución de *n*-hexano), para dar lugar a la especie $[NBu_4]_2[Pt(CF_3)_5I]$ (**11**) (Esquema 10). La reacción se completa después de 24 horas a temperatura ambiente. El derivado **11** se obtiene de forma cuantitativa. Las condiciones tan suaves en las que se forma el compuesto $[NBu_4]_2[Pt(CF_3)_5I]$, contrastan con las que se necesitan en la mayoría de los procesos de síntesis de los derivados organometálicos con alto contenido en ligandos $CF_3$ mencionados en la introducción (véase sección 1). Otro aspecto destacable acerca de esta reacción es que cuando el derivado **1** se trata con $CF_3I$ usando acetona o $CH_2Cl_2$ como disolventes en lugar de MeCN, no se observa ningún tipo de reacción.

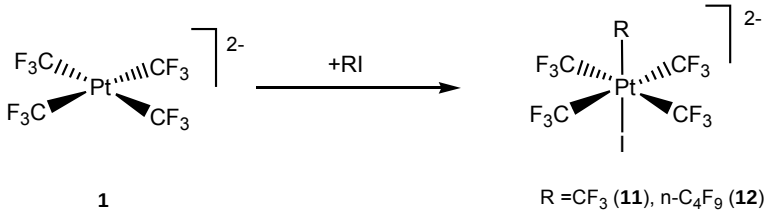


**1** R = $CF_3$ (**11**), n-$C_4F_9$ (**12**)

**Esquema 10.** Adición oxidante de RI sobre el trifluorometil-derivado homoléptico de Pt(II) **1**. $[NBu_4]^+$ es el catión en todos los casos.

La estructura del compuesto **11** ha sido establecida mediante la difracción de rayos X en un monocristal del solvato $[NBu_4]_2[Pt(CF_3)_5I]\cdot CH_2Cl_2$ (Figura 8). Todos los datos espectroscópicos de RMN en disolución están de acuerdo con su estructura en estado sólido.

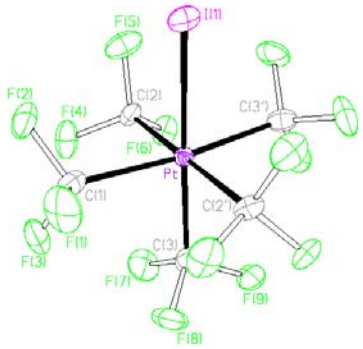


**Figura 8.** Estructura cristalina del anión $[Pt(CF_3)_5I]^{2-}$ del complejo **11**

El espectro de RMN de $^{19}F$ consiste en dos señales con intensidades 4:1 correspondientes a los dos tipos de grupos $CF_3$ presentes en el anión $[Pt(CF_3)_5I]^{2-}$: un cuartete a $\delta_F$ = -24.1 ppm y un multiplete a $\delta_F$ = -26.0 ppm con una constante de acoplamiento mutuo de spin internuclear $^4J(^{19}F,^{19}F)$ = 7 Hz (Figura 9). Cada una de estas señales aparece flanqueada por satélites de $^{195}Pt$ con constantes de acoplamiento de spin internuclear de $^2J(^{195}Pt,^{19}F)$ = 288 y 452 Hz respectivamente. El espectro de RMN de $^{195}Pt$ ($\delta_{Pt}$ = -2446 ppm) es particularmente rico debido al acoplamiento con los átomos de F de los grupos $CF_3$ coordinados (Figura 10).

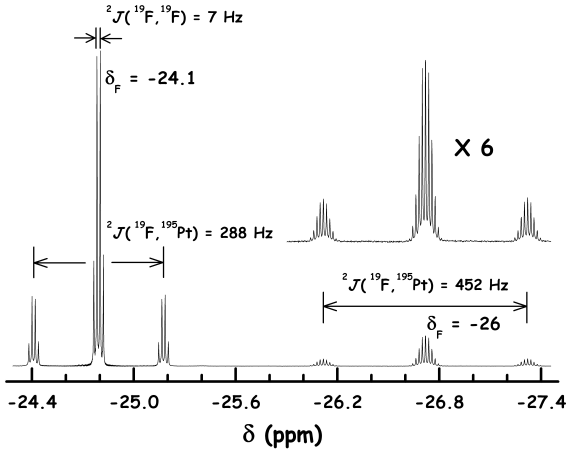


**Figura 9.** Espectro de RMN de $^{19}F$ del derivado **11** en [$^2$H]acetonitrilo a temperatura ambiente.

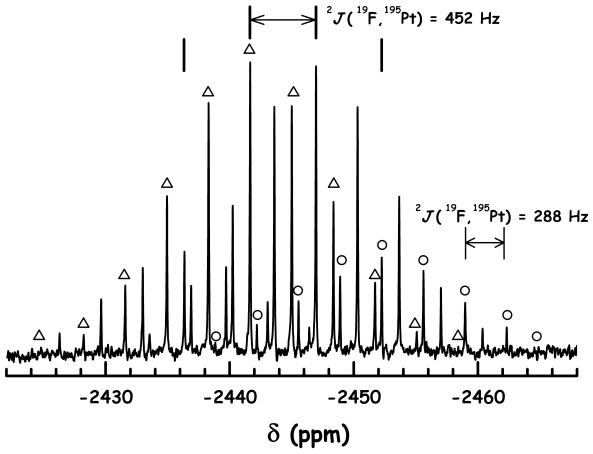


**Figura 10.** Espectro de RMN de $^{195}Pt$ del derivado **11** en [$^2$H]acetonitrilo a temperatura ambiente.

El derivado $[NBu_4]_2[Pt(CF_3)_5I]$ (**11**) resulta de la adición oxidante de $CF_3I$ sobre **1**. Sin embargo, dada la estequiometría del producto final, no está claro si dicha adición tiene lugar en *cis* o en *trans*. Para aclarar esta situación, se ha llevado a cabo la reacción de **1** con *n*-$C_4F_9I$. El grupo perfluoro-*n*-butilo resulta muy adecuado para este propósito, ya que su carbono-$\alpha$ tiene dos sustituyentes F y una cadena corta perfluorada, $CF_2(n\text{-}C_3F_7)$, por lo que, al menos desde el punto de vista electrónico, guarda una gran similitud con el grupo $CF_3$. En ausencia de factores estéricos, los resultados obtenidos con *n*-$C_4F_9I$ podrán ser aplicados a la especie $CF_3I$. La reacción **1** con *n*-$C_4F_9I$ en condiciones similares a las descritas para la reacción con $CF_3I$ (Esquema 10) da lugar a $[NBu_4]_2[trans\text{-}Pt(CF_3)_4(n\text{-}C_4F_9)I]$ (**12**) de forma estereoselectiva como así lo indica el espectro de RMN de $^{19}F$. Por lo tanto, es de esperar que la adición oxidante de $CF_3I$ sobre **1** también tenga lugar en *trans*. Esta observación junto con la marcada dependencia que tiene este proceso con respecto al disolvente utilizado, pueden tomarse como evidencia de que la reacción tiene lugar mediante la formación de un carbanión en vez de la formación de especies radicalarias.

Se ha llevado a cabo un estudio acerca del comportamiento químico del derivado $[NBu_4]_2[Pt(CF_3)_5I]$ (**11**) como precursor de trifluorometil-derivados de Pt(IV) que contienen un elevado número de ligandos $CF_3$.

El derivado **11** disuelto en acetona reacciona en corriente de aire húmedo con diferentes sales de $Ag^+$ de aniones poco coordinantes como $(SO_3CF_3)^-$, $(ClO_4)^-$ o $(CF_3CO_2)^-$, dando lugar a la especie $[NBu_4][Pt(CF_3)_5(OH_2)]$ (**13**) (Esquema 11). Este solvato se ha aislado con buen rendimiento y se ha caracterizado mediante métodos analíticos y espectroscópicos apropiados.

Si se lleva a cabo el tratamiento de la especie **11** con la misma sal de $Ag^+$ en MeCN como disolvente y en atmósfera inerte, se obtiene el solvato $[NBu_4][Pt(CF_3)_5(NCMe)]$ (**14**) (Esquema 11) de forma cuantitativa. Este compuesto se ha aislado con buen rendimiento y se ha caracterizado mediante métodos analíticos y espectroscópicos apropiados.

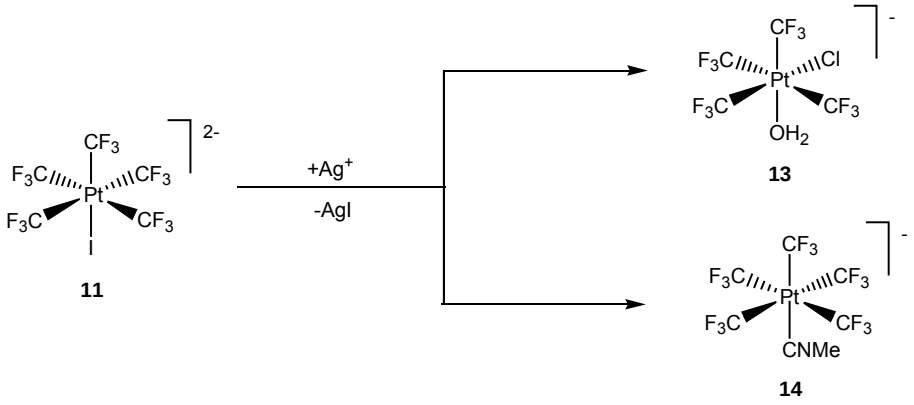


**Esquema 11.** Métodos de síntesis para obtener los solvato-derivados de Pt(IV) **13** y **14**. $[NBu_4]^+$ es el catión en todos los casos.

Tanto el grupo nitrilo en $[NBu_4][Pt(CF_3)_5(NCMe)]$ como el ligando $H_2O$ en $[NBu_4][Pt(CF_3)_5(OH_2)]$ se comportan como ligandos lábiles y pueden ser substituídos por una serie de bases de Lewis. Se han llevado a cabo substituciones de ambos ligandos por otros neutros o aniónicos (Esquema 12), obteniéndose así una serie de pentakis(trifluorometil)-derivados de Pt(IV) con fórmulas $[NBu_4][Pt(CF_3)_5L]$ [L = py (**15**), tht (**16**), CO (**17**)] y $[NBu_4]_2[Pt(CF_3)_5X]$ [X= Cl (**18**), Br (**19**)]. Todos estos derivados han sido aislados con muy buen rendimiento y su estructura ha sido determinada mediante diversas técnicas espectroscópicas entre las que destaca el RMN de $^{19}F$.

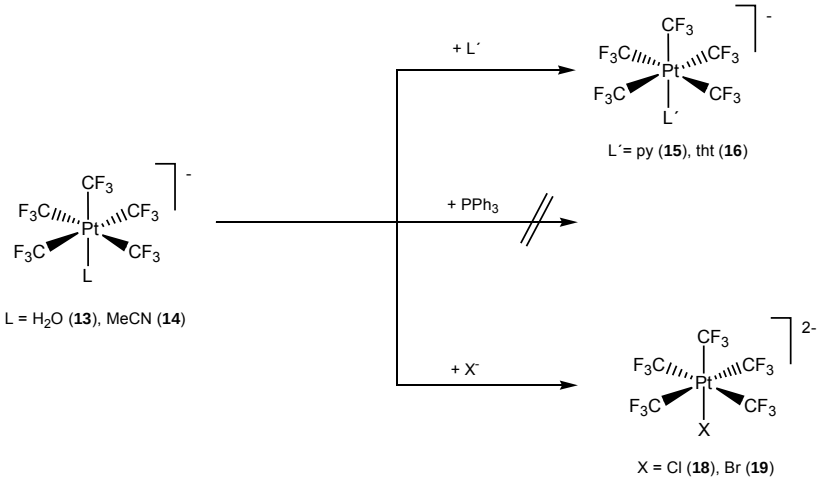


**Esquema 12.** Métodos de síntesis de los pentakis(trifluorometil)-derivados de Pt(IV) **15, 16, 18 y 19**. $[NBu_4]^+$ es el catión en todos los casos.

En el caso de los derivados $[NBu_4][Pt(CF_3)_5(NCMe)]$ (**14**) y $[NBu_4][Pt(CF_3)_5(py)]$ (**15**) su estructura ha sido establecida mediante difracción de rayos X (Figuras 11 y 12).

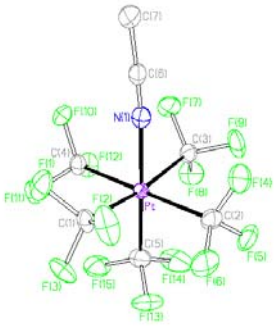

**Figura 11.** Estructura cristalina del anión $[Pt(CF_3)_5(NCMe)]^-$ del complejo **14**

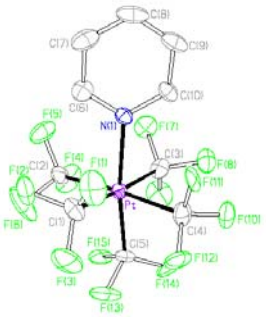

**Figura 12.** Estructura cristalina del anión $[Pt(CF_3)_5py]^-$ del complejo **15**

De entre todos los pentakis(trifluorometil)-derivados de Pt(IV), sintetizados en esta sección, cabe destacar, por su inesperada estabilidad y sorprendentes propiedades el derivado $[NBu_4][Pt(CF_3)_5(CO)]$ (**17**).

Los carbonilos de Pt(IV), debido a la capacidad reductora del CO y al alto estado de oxidación en el que se encuentra el centro metálico son extremadamente raros. De hecho el único carbonil derivado de Pt(IV) cuya estructura había sido establecida hasta el momento era el compuesto $[NBu_4][\textit{trans}\text{-}Pt(C_6F_5)_4Br(CO)]$.[47] En el caso del derivado $[NBu_4][Pt(CF_3)_5(CO)]$ (**17**) el riesgo de reducción del $Pt^{IV}$ por acción del CO sería, en principio, mayor ya que el centro metálico está unido a cinco grupos $CF_3$, que retiran mucha densidad electrónica.

El compuesto $[NBu_4][Pt(CF_3)_5(OH_2)]$ (**13**) disuelto en $CH_2Cl_2$ y bajo presión normal de CO experimenta la substitución del ligando $H_2O$ por CO dando lugar al derivado $[NBu_4][Pt(CF_3)_5(CO)]$ (**17**) de forma cuantitativa después de 12 horas a temperatura ambiente (Esquema 13). El CO, también es capaz de sustituir al grupo MeCN en el derivado $[NBu_4][Pt(CF_3)_5(NCMe)]$ (**14**), aunque este proceso tiene lugar más lentamente (Esquema 13).

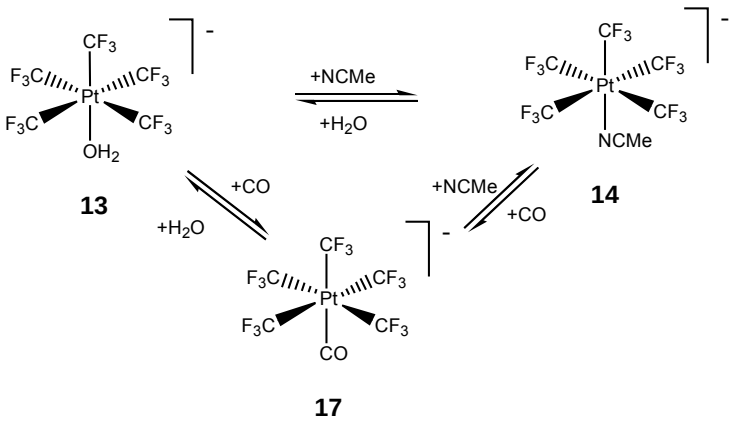


**Esquema 13.** Intercambio entre los derivados organometálicos de Pt(IV) $[NBu_4][Pt(CF_3)_5(OH_2)]$, $[NBu_4][Pt(CF_3)_5(NCMe)]$ y $[NBu_4][Pt(CF_3)_5(CO)]$ mediante procesos de substitución reversibles. $[NBu_4]^+$ es el catión en todos los casos.

La estructura del anión $[Pt(CF_3)_5(CO)]^-$ ha sido establecida mediante difracción de rayos X en un monocristal de la sal $[PPh_4][Pt(CF_3)_5(CO)]$ (**17´**) (Figura 13).

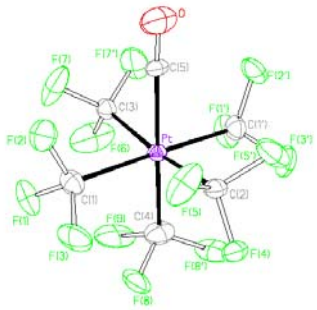

**Figura 13.** Estructura cristalina del anión $[Pt(CF_3)_5(CO)]^-$ del complejo **17´**

Analizando todas las características espectroscópicas y estructurales asociadas a la unidad Pt-CO en **17** ó **17´**, éstas apuntan claramente a una casi nula retrodonación M→CO:

1) Alto valor de la banda asignada a la vibración ν(CO) en su espectro de IR a (2194 $cm^{-1}$ en estado sólido y a 2189 $cm^{-1}$ en disolución de $CH_2Cl_2$).
2) Bajo valor del desplazamiento químico, $\delta_C$, para la señal asignada al $^{13}C$ en su espectro de RMN de $^{13}C$.
3) Bajo valor de la constante de acoplamiento de spin internuclear $^1J(^{195}Pt, ^{13}C)$.
4) Distancia de enlace Pt-CO larga.

5) Distancia internuclear C-O corta.

Por último, aunque todos los intentos para obtener el trifluorometil-derivado homoléptico de Pt(IV) $[Pt(CF_3)_6]^{2-}$ han fracasado, la reacción de $[NBu_4]_2[Pt(CF_3)_5I]$ (**11**) con $XeF_2$ en $CH_2Cl_2$, da lugar a la formación de $[NBu_4]_2[Pt(CF_3)_5F]$ (**20**) de forma cuantitativa. Aunque la determinación de la estructura de **20** mediante difracción de rayos X en este caso no resulta una técnica determinante (por la imposibilidad de distinguir el átomo de F del OH), sus espectros de RMN de $^{19}F$ y $^{195}Pt$ sí resultan determinantes a la hora de establecer la estructura de este derivado de forma inequívoca.

En esta sección, el derivado $[NBu_4]_2[Pt(CF_3)_5I]$ (**11**) se perfila como una vía de acceso eficaz a la química de los derivados organometálicos con alto contenido en ligandos $CF_3$. Los derivados **11**-**20** son los derivados mononucleares con el mayor contenido en ligandos $CF_3$ de todo el Sistema Periódico de los Elementos que hayan aislados y caracterizados adecuadamente hasta la fecha.

## 5. Estabilización mediante coordinación de una base del fragmento platino-difluorocarbeno, $[Pt]=CF_2$

S. Martínez-Salvador, B. Menjón, J. Forniés, A. Martín, I. Usón, *Angew. Chem. Int. Ed*. **2010**, *49*, 4286.

Se ha realizado un estudio exhaustivo acerca de la reactividad del derivado $[NBu_4]_2[Pt(CF_3)_4]$ (**1**) frente a procesos de hidrólisis y de los intermedios que intervienen en este tipo de procesos, así como de los productos que se obtienen.

El derivado **1** experimenta reacciones de hidrólisis para dar el monocarbonil derivado $[NBu_4][Pt(CF_3)_3(CO)]$ (**21**) de forma cuantitativa y con buen rendimiento (Esquema 14). Esta reacción tiene lugar en condiciones muy suaves y por simple acción de la humedad. Esta facilidad con la que un grupo $CF_3$ se transforma en CO contrasta con los precedentes conocidos que requieren el tratamiento del correspondiente trifluorometil-derivado de Pt con $HBF_4/Et_2O$ o $HClO_4/H_2O$.[48]

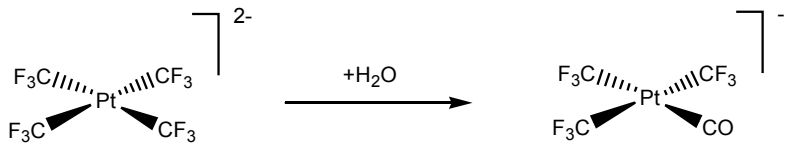


**Esquema 14**. Proceso de hidrólisis que experimenta el tetrakis(trifluorometil)-derivado homoléptico de platino (II) **1**. $[NBu_4]^+$ es el cation en todos los casos.

Aunque se conoce un buen número de compuestos que contienen la unidad $[M]=CF_2$ para los metales de los Grupos 8 y 9,[49] hasta la fecha no se ha aislado ninguno en el que el metal sea Pt. Esto es debido, probablemente, al fuerte carácter electrófilo que sería de esperar para el fragmento $[Pt]=CF_2$.

La estructura del anión (*SP*-4)-$[Pt(CF_3)_3(CO)]^-$ ha sido establecida mediante difracción de rayos X en un monocristal de la sal $[PPh_4][Pt(CF_3)_3(CO)]$ (**21´**) (Figura 14). Las propiedades espectroscópicas del ión $[Pt(CF_3)_3(CO)]^-$ están de acuerdo con la estructura encontrada en estado sólido. Entre las propiedades espectroscópicas destaca la banda $\nu$(CO) (2117 $cm^{-1}$ en disolución de $CH_2Cl_2$ y 2121 $cm^{-1}$ en estado sólido) que aparece en su espectro de IR. Su alto valor denota la baja retrodonación Pt→CO. Este hecho viene motivado por la carencia de densidad electrónica del metal por el hecho de estar unido a tres grupos $CF_3$ que tienen una alta electronegatividad.

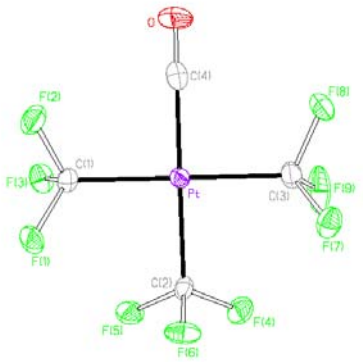


**Figura 14.** Estructura cristalina del anión $[Pt(CF_3)_3(CO)]^-$ del complejo **21´**

El compuesto $[NBu_4][Pt(CF_3)_3(CO)]$ (**21**), reacciona con una serie de ligandos neutros (L) o aniónicos ($X^-$) en presencia de óxido de *N*-trimetilamina ($ONMe_3$)

experimentando procesos de substitución del grupo CO por el ligando entrante L o $X^-$ (Esquema 15).

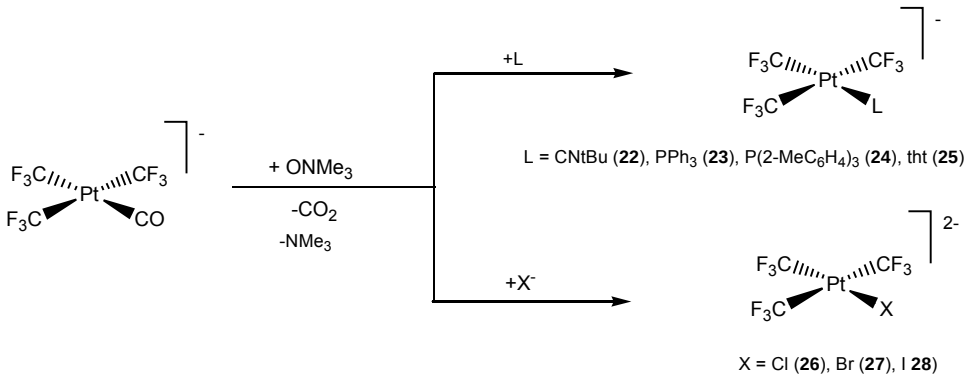


**Esquema 15.** Síntesis de los tris(trifluorometil)-derivados de platino(II) mono- o dianiónicos: $[NBu_4][Pt(CF_3)_3(L)]$ [L = $CN^tBu$ (**22**), $PPh_3$ (**23**), $P(2\text{-}MeC_6H_4)_3$ (**24**), tht (**25**)] y $[NBu_4]_2[Pt(CF_3)_3X]$ [X = Cl (**26**), Br (**27**), I (**28**)].

Siguiendo este procedimiento, se han sintetizado una serie de trifluorometil-derivados de Pt(II) mono- o dianiónicos de fórmula $[NBu_4][Pt(CF_3)_3(L)]$ [L = $CN^tBu$ (**22**), $PPh_3$ (**23**), $P(2\text{-}MeC_6H_4)_3$ (**24**), tht (**25**)] y $[NBu_4]_2[Pt(CF_3)_3X]$ [X = Cl (**26**), Br (**27**), I (**28**)].

El tratamiento de $[NBu_4][Pt(CF_3)_3(CO)]$ (**21**) con piridín-2-tiol ($C_5H_5NS$) en presencia de $ONMe_3$ da lugar al derivado metalacíclico *gem*-difluorado $[NBu_4][Pt(CF_3)_2(CF_2NC_5H_4S\text{-}\kappa C,\kappa S)]$ (**29**) con buen rendimiento (Esquema 16; parte superior). Este proceso no solo implica substitución de CO en $[NBu_4][Pt(CF_3)_3(CO)]$ (**21**), sino también activación del enlace C-F y acoplamiento C-N (Esquema 16; parte inferior).

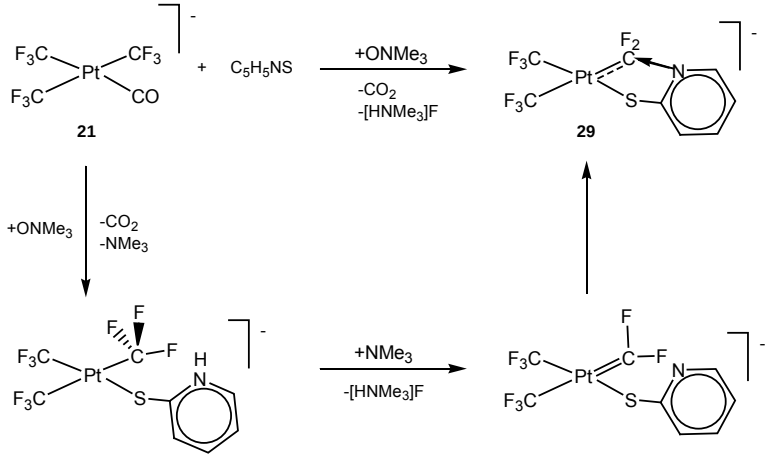


**Esquema 16.** Formación del derivado $[NBu_4][Pt(CF_3)_2(CF_2NC_5H_4S\text{-}\kappa C,\kappa S)]$ observada experimentalmente (parte superior) y mecanismo de reacción propuesto (parte inferior).

La estructura de este derivado ha sido determinada mediante difracción de rayos X (Figura 15), en vista de la cual el derivado $[NBu_4][Pt(CF_3)_2(CF_2NC_5H_4S\text{-}\kappa C,\kappa S)]$ (**29**) puede considerarse como un modelo válido para la etapa inicial de la solvolisis (incluyendo hidrólisis) de los derivados que contienen la unidad $[E]=CF_2$.[50]

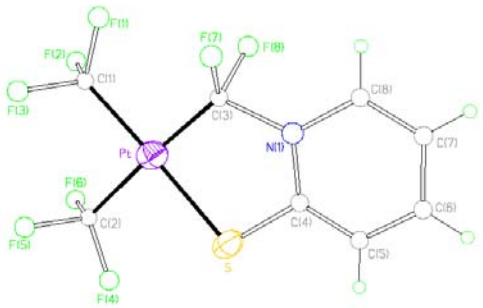


**Figura 15.** Estructura cristalina del anión $[Pt(CF_3)_2(CF_2NC_5H_4S\text{-}\kappa C,\kappa S)]^-$ del complejo **29**

Con las evidencias encontradas acerca de la formación del intermedio de reacción $[Pt]=CF_2$ altamente reactivo, se ha llevado a cabo la reacción de **1** con $BF_3.OEt_2$ a baja temperatura. En esas condiciones ha sido posible mediante espectroscopia de RMN de $^{19}F$ a baja temperatura la detección del intermedio de reacción para estos procesos $[Pt(CF_3)_3(=CF_2)]^-$ (**21**$^‡$).

El tratamiento a baja temperatura de **1** con $BF_3.OEt_2$ da lugar a la abstracción de un flúor-α de uno de los ligandos $CF_3$ equivalentes y la formación de la especie térmicamente inestable $[Pt(CF_3)_3(=CF_2)]^-$ (**21**$^‡$) (Esquema 17) como indica su espectro de RMN de $^{19}F$ registrado a baja temperatura en el que, además de las señales correspondientes a los dos tipos de grupos $CF_3$ presentes en esta especie, aparece otra con un desplazamiento químico a muy alta frecuencia ($\delta_F$ = 152.61 ppm) flanqueada con satélites de $^{195}Pt$ con una constante de acoplamiento de spin internuclear $^2J(^{195}Pt,^{19}F)$ = 638 Hz. Esta señal se asigna al grupo $=CF_2$ unido al centro metálico.

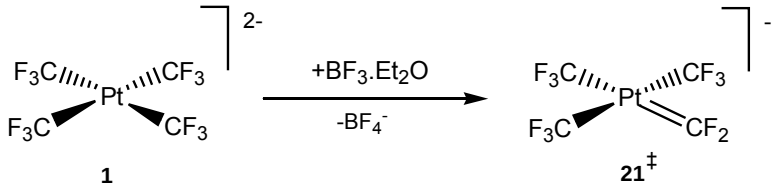


**1** **21**‡

**Esquema 17**. Formación de la especie **21**‡ por tratamiento de **1** con $BF_3.OEt_2$ $[NBu_4]^+$ es el catión en todos los casos.

La especie $[Pt(CF_3)_3(=CF_2)]^-$ (**21**‡) tiene, en efecto, un acusado carácter electrófilo y reacciona fácilmente con $NH_2Ph$ para dar $[NBu_4][Pt(CF_3)_3(CNPh)]$ (**30**) o con $H_2O$ para dar $[NBu_4][Pt(CF_3)_3(CO)]$ (**21**) (Esquema 18).

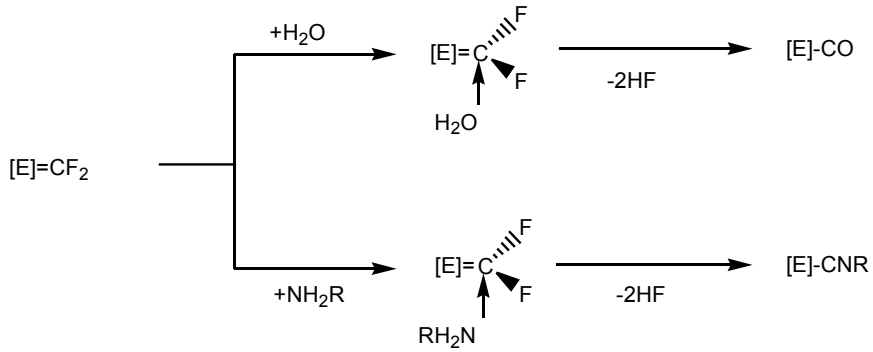


**Esquema 18.** Mecanismo de reacción sugerido para los procesos de solvolisis que experimentan las especies que contienen el fragmento difluorocarbeno.

Esta especie reacciona también con dioles como el 1,2-etanodiol o catecol dando lugar a especies que contienen como ligando un carbeno *O*-heterocíclico (OHC) $[NBu_4][Pt(CF_3)_3(OHC)]$, donde (OHC) = $:CO(1,2\text{-}C_6H_4)O$-*ciclo* (**31**) o $:COCH_2CH_2O$-*ciclo* (**32**) respectivamente (Esquema 19).

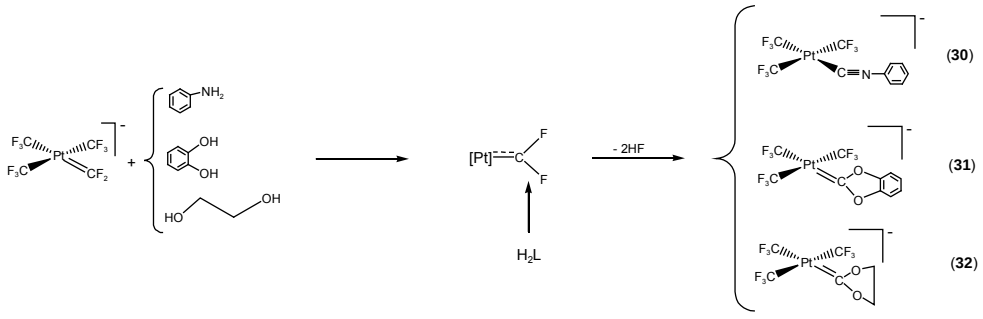


**Esquema 19** Reacciones de solvolisis de **21**‡ con anilina, catecol y 1-2,etanodiol para dar lugar a los derivados **30**, **31** y **32**. $[NBu_4]^+$ es el catión en todos los casos.

El ligando benzodioxolilideno presente en el derivado $[NBu_4][Pt(CF_3)_3\{CO(1,2\text{-}C_6H_4)O\text{-}ciclo\}]$ (**31**) adopta una disposición perpendicular al plano de coordinación del metal en estado sólido como se observa en su estructrura cristalina determinada mediante difracción de rayos X (Figura 16).

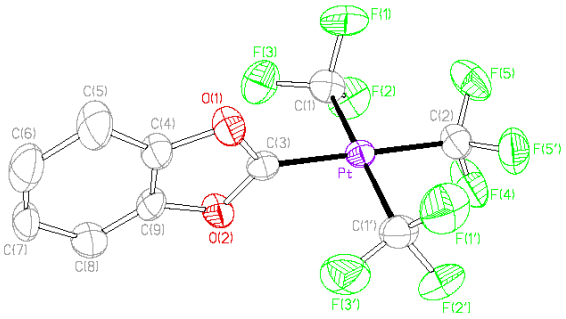


**Figura 16.** Estructura cristalina del anión $[Pt(CF_3)_3\{CO(1,2\text{-}C_6H_4)O\text{-}ciclo\}]^-$ del complejo **31**

Aunque los derivados **31** y **32** son sustancialmente más estables que **21**‡, también experimentan procesos de hidrólisis dando lugar igualmente al derivado $[NBu_4][Pt(CF_3)_3(CO)]$ (**21**).

Cuando se lleva a cabo el tratamiento de **1** con $BF_3.OEt_2$ de forma prolongada se forma el dicarbonil-derivado *cis*-$[Pt(CF_3)_2(CO)_2]$ (**33**), para el que las bandas asignadas a las vibraciones $\nu$(CO) en su espectro de IR tienen valores altos: 2196 y 2171 $cm^{-1}$. La estructura del derivado **33** ha sido establecida mediante difracción de rayos X (Figura 17).

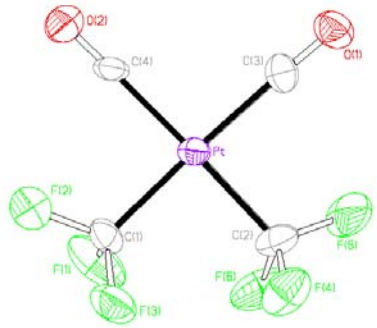


**Figura 17.** Estructura cristalina del complejo *cis*-$[Pt(CF_3)_2(CO)_2]$ (**33**)

Hemos visto que por la simple acción de la humedad, el trifluorometil-derivado de Pt(II) **1** experimenta un proceso de hidrólisis de uno de sus grupos $CF_3$ dando lugar al carbonil-derivado $[NBu_4][Pt(CF_3)_3(CO)]$ (**21**). La transformación de uno de los grupos aniónicos $CF_3$ en la unidad homoléptica (*SP*-4)-$[Pt(CF_3)_4]^{2-}$ en el ligando neutro CO con poco carácter σ-dador tiene como consecuencia la desactivación de la especie resultante $[Pt(CF_3)_3(CO)]^-$ frente a nuevos procesos de hidrólisis por lo que el derivado $[NBu_4][Pt(CF_3)_3(CO)]$ (**21**) resulta ser una especie estable a la humedad. La desactivación que ocasiona el ligando CO en los trifluorometil-derivados de $Pt^{II}$ frente a la hidrólisis resulta especialmente patente en el caso del derivado neutro *cis*-$[Pt(CF_3)_2(CO)_2]$. En este compuesto los grupos $CF_3$ resisten a la acción de los ácidos, siendo estable incluso en HF(*l*) anhidro.

Sin embargo, el tratamiento de $[NBu_4][Pt(CF_3)_3(CO)]$ (**21**) con HCl(*aq*) en exceso (1:15), da lugar al derivado $[NBu_4][$*cis*-$Pt(CF_3)_2Cl(CO)]$ (**34**) el cual, al prolongar el tiempo de reacción con el exceso de HCl da lugar a su vez a $[NBu_4][$*cis*-$Pt(CF_3)Cl_2(CO)]$ (**35**). Esta especie ya no experimenta reacción alguna con HCl (Esquema 20).

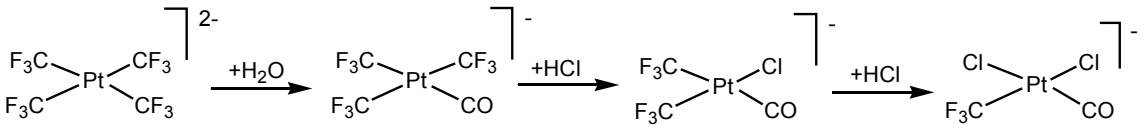


**Esquema 20.** Proceso de degradación gradual de los grupos $CF_3$ en trifluorometil-derivados de Pt(II) empezando por el derivado homoléptico **1**. $[NBu_4]^+$ es el catión en todos los casos.

La especie $[NBu_4][cis\text{-}Pt(CF_3)_2Cl(CO)]$ (**34**), en ausencia de ligando, experimenta un proceso de dimerización por reacción con $ONMe_3$ dando lugar a la especie dinuclear $[NBu_4]_2[\{Pt(CF_3)_2\}_2(\mu\text{-}Cl)_2]$ (**36**) (Esquema 21). La reacción del derivado dinuclear $[NBu_4]_2[\{Pt(CF_3)_2\}_2(\mu\text{-}Cl)_2]$ disuelto en un disolvente coordinante como thf con $AgClO_4$, produce la precipitación de los ligandos cloruro en forma de AgCl, obteniéndose así el solvato *cis*-$[Pt(CF_3)_2(thf)_2]$ (**37**) (Esquema 21). El carácter altamente lábil de los ligandos thf en **37** hace de este derivado un sintón adecuado de la unidad "*cis*-$Pt(CF_3)_2$".

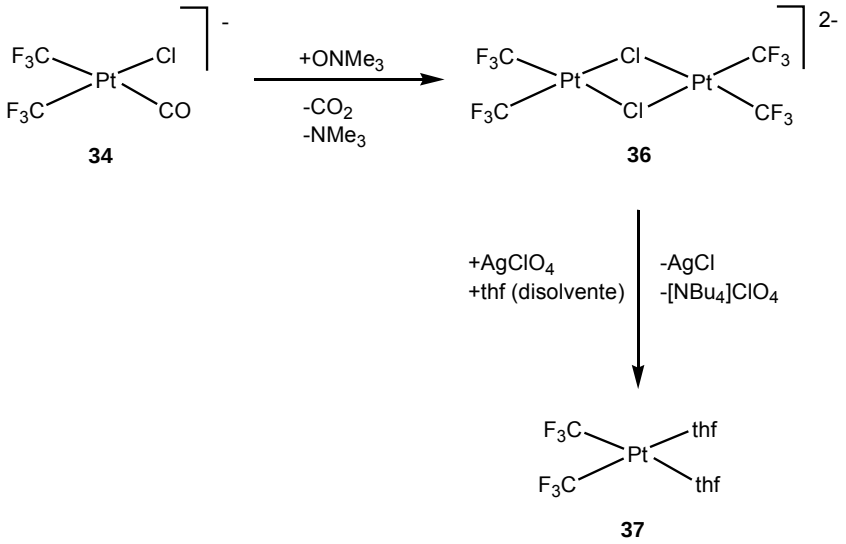


**Esquema 21.** Dimerización llevada a cabo por el compuesto $[NBu_4][cis\text{-}Pt(CF_3)_2Cl(CO)]$ (**34**) bajo abstracción de CO y en ausencia de ligando para dar lugar a la especie **36** (el catión es $[NBu_4]^+$) junto con la síntesis del solvato-derivado neutro *cis*-$[Pt(CF_3)_2(thf)_2]$ (**37**).

La estructura del solvato-derivado **37** ha sido establecida mediante difracción de rayos X (Figura 18).

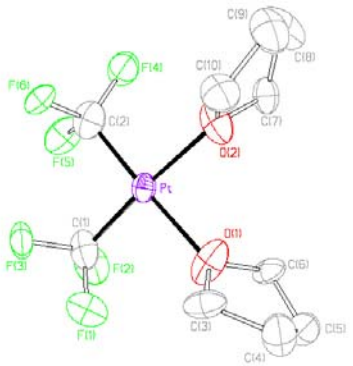


**Figura 18.** Estructura cristalina del complejo *cis*-$[Pt(CF_3)_2(thf)_2]$ (**37**)

Según hemos visto, la acción de sustancias ácidas sobre la unidad (*SP*-4)-$[Pt(CF_3)_4]^{2-}$ tiene como consecuencia la eliminación de un flúor-$\alpha$ y la formación de un intermedio difluorocarbeno, altamente reactivo y susceptible a su vez de experimentar diversos procesos solvolíticos. Este comportamiento contrasta fuertemente con la reactividad de la unidad Pt-$CH_3$ frente a los ácidos, que transcurre preferentemente con ruptura del enlace Pt-C. Se han propuesto diferentes mecanismos para este tipo de reacciones en los que el ataque del protón, $H^+$ (como caso particular de electrólilo $E^+$), se produce bien sobre el centro metálico o sobre el enlace Pt-C (Esquema 22).[51] Sin embargo, se desconocen los detalles del mecanismo mediante el cual tiene lugar la eliminación de flúor-$\alpha$ en los trifluorometil-derivados metálicos.

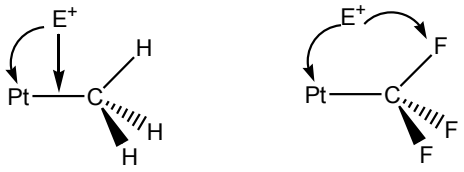


**Esquema 22.** Mecanismos propuestos para la reacción de ataque electrófilo de $E^+$ sobre la unidad Pt-$CH_3$ y Pt-$CF_3$.

Como acabamos de ver, el trifluorometil-derivado homoléptico de Pt(II) $[NBu_4]_2[Pt(CF_3)_4]$ (**1**) experimenta procesos de degradación de uno de los grupos $CF_3$ en presencia de un ácido tan débil como lo es el $H_2O$ (humedad) dando lugar la derivado $[NBu_4][Pt(CF_3)_3(CO)]$ (**21**). Ácidos más fuertes u otro

tipo de electrófilos producen el mismo efecto (Esquema 23). Sin embargo, se ha observado que el derivado **1** reacciona con ácidos fuertes tales como $HClO_4$(*ac*) o HCl(*ac*) a baja temperatura y en presencia de $CN^tBu$ dando lugar a la formación del hidruro derivado de Pt(IV) $[NBu_4][trans\text{-}Pt(CF_3)_4H(CN^tBu)]$ (**38**) con buen rendimiento (Esquema 23).

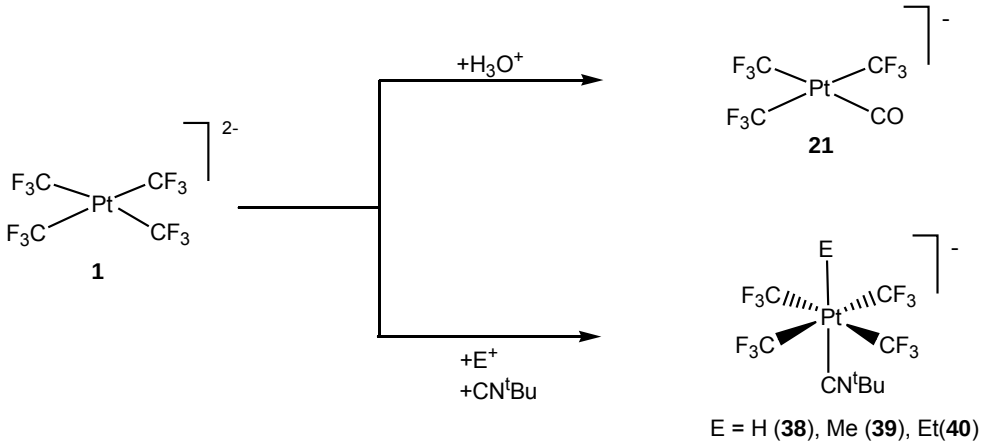


**Esquema 23.** Reactividad de la especie homoléptica $[Pt(CF_3)_4]^{2-}$ frente a electrófilos simples en ausencia y en presencia de $CN^tBu$ como ligando adicional; $[NBu_4]^+$ es el catión en todos los casos.

La estructura de este hidruro derivado ha sido determinada mediante difracción de rayos X (Figura 19) y está de acuerdo con las propiedades espectroscópicas observadas en disolución. La señal observada en el espectro de RMN de $^1H$ de **38** en $CD_2Cl_2$ (Figura 20) que aparece a muy baja frecuencia ($\delta_H$ = -13.77 ppm) con alta multiplicidad debida al acoplamiento con los átomos de F de los cuatro grupos $CF_3$ equivalentes, y tiene un valor alto de la constante de acoplamiento de spin internuclear con el isótopo de $^{195}Pt$, $^1J(^{195}Pt,^1H)$ = 1201 Hz, es indicativa de la existencia de un hidruro unido directamente al Pt.[52]

En las mismas condiciones, el derivado **1** reacciona con triflurometilsulfatos de alquilo, $ROSO_2CF_3$ (R = Me, Et), en presencia de $CN^tBu$ y CO para dar lugar a los trifluorometil-derivados de Pt(IV) $[NBu_4][trans\text{-}Pt(CF_3)_4R(CNtBu)]$ [R = Me (**39**), Et (**40**)] (Esquema 23) y $[NBu_4][trans\text{-}Pt(CF_3)_4R(CO)]$ [R = Me (**41**), Et (**42**)]. A pesar de la marcada electronegatividad de los grupos $CF_3$, parece que el centro metálico en el compuesto de partida **1** todavía posee suficiente densidad electrónica para ser el centro reactivo cinéticamente favorecido en procesos de ataque electrófilo.

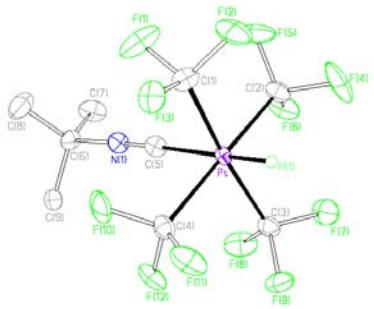

**Figura 19.** Estructura cristalina del anión [*trans*-$Pt(CF_3)_4H(CN^tBu)]^-$ del complejo **38**

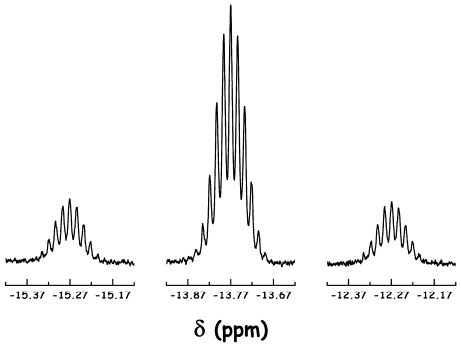


**Figura 20**. Señal correspondiente al hidruro en el espectro de RMN de $^1H$ del derivado **38** registrado a temperatura ambiente en disolución de $CD_2Cl_2$.

Así pues, este tipo de reacciones puede verse como un proceso de neutralización de Lewis en el que el metal es la base y el electrófilo $E^+$ el ácido. La oxidación del centro metálico de Pt(II) ($d^8$) a Pt(IV) ($d^6$) que tiene lugar en estos procesos de neutralización no es puramente formal, sino que también entraña los correspondientes efectos espectroscópicos y estructurales que dicha oxidación trae consigo. El ataque del electrófilo $E^+$ al centro de Pt en **1** supone un aumento en su carácter electrófilo favoreciendo así la coordinación de un ligando adicional en la sexta posición de coordinación.[53] El ligando $CN^tBu$ cuando $E^+ = H^+$, $Me^+$, $Et^+$ e incluso el CO cuando $E^+ = Me^+$, $Et^+$ son capaces de estabilizar el trifluorometil-derivado de Pt(IV) resultante, dando lugar a los derivados **38**, **39**, **40**, **41** y **42**, especies estables a la humedad y térmicamente muy robustas.

## 6. $[Au(CF_3)(CO)]$: Un carbonil derivado de oro estabilizado mediante un grupo trifluorometilo.

S. Martínez-Salvador, J. Forniés, A. Martín, B. Menjón, *Angew. Chem. Int. Ed*. **2011**, *50*, 6571.

En esta sección se presenta la síntesis y caracterización del carbonil-derivado de Au(I) $[Au(CF_3)(CO)]$ (**44**), especie muy inestable y altamente reactiva, que representa uno de los poquísimos casos de carbonil-derivados de Au aislados y caracterizados en fase condensada.[54]

Mediante un método similar al utilizado por S. Mathur y sus colaboradores para sintetizar el derivado $[NMe_4]_2[Au(CF_3)_2]$,[55] se ha sintetizado la sal $[PPh_4][Au(CF_3)_2]$ (**43**)**.** El tratamiento del derivado $[PPh_4][Au(CF_3)_2]$ (**43**) con $BF_3.OEt_2$ en disolución de $CH_2Cl_2$ a baja temperatura da lugar al carbonil-derivado $[Au(CF_3)(CO)]$ (**44**) de forma **cuantitativa** y con un **rendimiento razonable**. En esta reacción, no se observa ningún tipo de proceso de descomposición siempre y cuando se lleve a cabo estrictamente en atmósfera inerte sin trazas de humedad.

El mecanismo para esta reacción (Esquema 24), se propone por analogía con los resultados obtenidos en los trifluorometil-derivados de Pt. La primera etapa consistiría en la abstracción de un flúor-$\alpha$ de uno de los grupos $CF_3$ del producto de partida **43** por reacción con $BF_3.OEt_2$. Esta etapa daría lugar a un intermedio de tipo difluorocarbeno $[Au(CF_3)(=CF_2)]$ (**44**$^{\ddagger}$) que posiblemente podría verse estabilizado mediante la coordinación de una base, en este caso $Et_2O$, antes de dar lugar al producto final. Esta molécula de $Et_2O$ podría actuar también como fuente de oxígeno para el ligando CO porque la extrema sensibilidad de **44** a la humedad hace que la posibilidad de que haya alguna traza de humedad sea poco plausible.

Se han realizado diferentes intentos de detectar el intermedio de reacción $[Au(CF_3)(=CF_2)]$ (**44**$^{\ddagger}$) mediante medidas de RMN a baja temperatura pero no han dado el resultado apetecido.

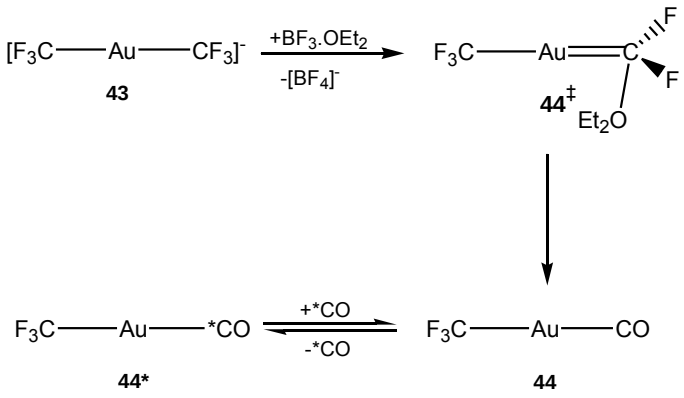


43 44‡ 44* 44

**Esquema 24.** Mecanismo de reacción sugerido para la transformación de **43** (catión $[PPh_4]^+$) en **44** e intercambio de CO observado en **44**.

La estructura del compuesto **44** ha sido establecida mediante difracción de rayos X (Figura 21). Cada uno de los centros de $Au^{I}$ muestra interacciones aurófilas débiles (Au···Au = 345.9(1) pm)[56] con tres átomos de $Au^{I}$ vecinos relacionados por simetría localizados en un plano perpendicular al eje C-Au-CO, dando lugar a una red tridimensional de interacciones aurófilas (Figura 22). La naturaleza débil de estas interacciones aurófilas está de acuerdo con el carácter duro del grupo $CF_3$ y el poco carácter σ-dador del ligando CO que debería tener como consecuencia una disminución en la densidad electrónica del centro de Au.[57]

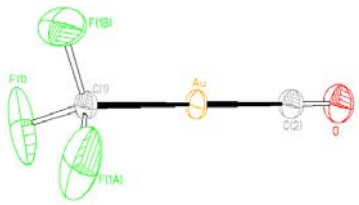

**Figura 21**. Estructura cristalina del complejo $[Au(CF_3)(CO)]$ (**44**)

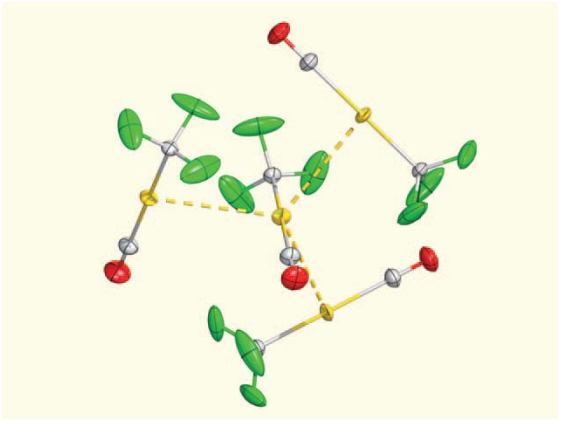

**Figura 22.** Entorno local de cada molécula $[Au(CF_3)(CO)]$ en la red cristalina, incluyendo indicaciones de las interacciones aurófilas con tres moléculas vecinas equidistantes.

En el espectro de IR en disolución de $CH_2Cl_2$ del compuesto **44**, aparece una banda muy intensa a 2180 $cm^{-1}$ que se asigna al modo de vibración ν(CO). Esta absorción, que tiene un valor incluso mayor que la observada para [AuCl(CO)] (2162 $cm^{-1}$ en disolución de $CH_2Cl_2$),[58];[59] es debida a la alta electronegatividad atribuida al grupo trifluorometilo. Esta frecuencia ν(CO) tan alta denota que la molécula de CO en **44** actúa predominantemente como dador-σ.

La especie **44** experimenta un rápido proceso de intercambio con $^{13}CO$ libre a presión atmosférica para dar la especie marcada isotópicamente $[Au(CF_3)(^{13}CO)]$ (**44***) (Esquema 25). Este ligando marcado isotópicamente permite determinar la señal correspondiente al CO unido al Au de forma

inequívoca, así como el acoplamiento con los tres átomos de F del grupo $CF_3$ (Figura 23a). Además, la señal de RMN de $^{19}F$ aparece desdoblada por acoplamiento con el $^{13}C$ con la misma constante de acoplamiento $^3J(^{13}C,^{19}F)$ (Figura 23b).

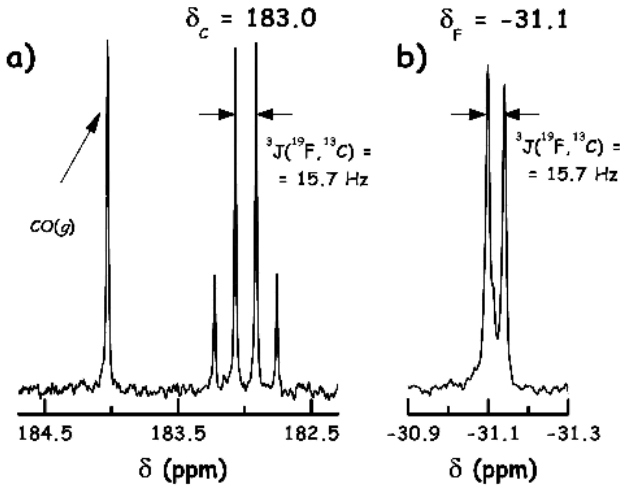


**Figura 23.** Espectros de RMN de **44*** a baja temperatura en disolución de $CD_2Cl_2$. a) $^{13}C$, b) $^{19}F$. La señal correspondiente a $^{13}CO$ disuelto aparece a $\delta_C$ = 184.0 ppm en el espectro de RMN de $^{13}C$ (a).

La combinación de la capacidad reductora del CO y la facilidad con la que el Au se reduce es la principal razón de la escasez de carbonil-derivados de Au aislados y caracterizados de forma adecuada.[54]

El ligando CO puede ser fácilmente reemplazado por otros ligandos, por lo que el compuesto **44** puede considerarse como un valioso sintón del fragmento "$Au(CF_3)$" para el que se puede encontrar un gran uso en la química del oro.

De esta forma, el derivado $[Au(CF_3)(CO)]$ (**44**), reacciona con una serie de ligandos neutros (L) experimentando procesos de substitución del grupo CO por el ligando entrante L (Esquema 25). Mediante este procedimiento, se han sintetizado una serie de trifluorometil-derivados de Au(I) neutros de fórmula $[Au(CF_3)(L)]$ [L = tht (**45**), py (**46**) y CNtBu (**47**)]. Estos derivados han sido aislados y caracterizados de forma inequívoca utilizando para ello una combinación de técnicas espectroscópicas y analíticas adecuadas.

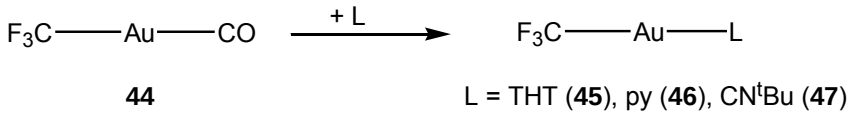


**Esquema 25.** Síntesis de los trifluorometil-derivados de $Au^{I}$ neutros [$Au(CF_3)(L)$] [L = tht (**45**), py (**46**), $CN^tBu$ (**47**)].

## 7. Conclusions

- The $CF_3$ ligand is especially suited to stabilize organometallic derivatives in high oxidation states. This can be attributed to its high group electronegativity together with its reluctance to undergo reductive-elimination processes.

- The homoleptic perfluoromethyl species $[NBu_4]_2[Pt(CF_3)_4]$ (**1**) straightforwardly adds $Cl_2$, $Br_2$, $I_2$ in a stereoseletive way giving rise to the thermally stable organoplatinum(IV) derivatives $[NBu_4]_2[$*trans*-$Pt(CF_3)_4X_2]$ (X = Cl, Br, I).

- An efficient synthetic method to stereoselectively obtain salts of any of the following trifluoromethyl-platinum(IV) isomeric couples: *cis*/*trans*-$[Pt(CF_3)_4Cl_2]^{2-}$ and *fac*/*mer*-$[Pt(CF_3)_3Cl_3]^{2-}$ has been described. The thermally unstable derivative $[NBu_4]_2[$*trans*-$Pt(CF_3)_4Cl(SOCl)]$ containing the unusual chlorosulfinyl ligand has been detected, isolated and thoroughly characterized. This intermediate species has been found to be instrumental in opening the *cis*→*fac* path.

- Compound $[NBu_4]_2[Pt(CF_3)_5I]$ (**11**) has been obtained by oxidative addition of $CF_3I$ to the homoleptic organoplatinum(II) derivative **1** under mild conditions. This compound has shown itself to be a convenient entry to the chemistry of highly trifluoromethylated platinum complexes. The pentakis(trifluoromethyl)platinum(IV) compounds obtained from **11** are, to the best of our knowlekge, the organoelement compounds with the highest $CF_3$-content that have been isolated and adequately characterized to date. Of particular importance is the unexpected thermal stability and chemical behaviour of the $[NBu_4]+$ or $[PPh_4]+$ salts of the $Pt^{IV}$ carbonyl derivative $[Pt(CF_3)_5(CO)]^-$ (**13** or **13´**, respectively), especially considering that all structural and spectroscopic

features associated with the Pt-CO unit point to the near absence of M→CO π back-bonding.

- The homoleptic compound **1** was found to undergo stepwise $CF_3$ degradation under mild conditions. Evidence for the intermediacy of highly reactive [Pt]=$CF_2$ especies was attained by the isolation of the ligand-stabilized adduct $[NBu_4][Pt(CF_3)_2(CF_2NC_5H_4S$-κ*C*,κ*S*)] (**29**) in which the $CF_2$ unit still preserves much of its original carbene nature. Moreover the intermediacy of highly reactive $[Pt(CF_3)_3(=CF_2)]^-$ species was detected by $^{19}F$ NMR spectroscopy at low temperature.

- The compound $[Au(CF_3)(CO)]$ (**44**) has been isolated and fully characterized. Preliminary results reveal that the CO molecule in **44** can be readily replaced by a number of other ligands. Therefore, compound **44** can be considered as a valuable synthon of the "$Au(CF_3)$" fragment that may find wide use in gold chemistry.

## 8. Bibliografía


[1] L. Pauling, *The Nature of the Chemical Bond,* Cornell University Press, Ithaca, NY, **1939**.

[2] T. Moeller, *Inorganic Chemistry*, John Wiley & Sons, New York, **1982**, Tabla 5-8, pg. 238.

[3] J. E. Huheey, *J. Phys. Chem.* **1965**, *69*, 3284.

[4] D. Seebach, *Angew. Chem. Int. Ed. Engl.* **1990**, *29*, 1320.

[5] T. Fujita, *Prog. In Phys. Org. Chem.* **1983**, *14*, 75; N. Muller, *J. Pharm. Sci.* **1986**, *75*, 987.

[6] R. E. Banks, 6ª ed, "*Organofluorine Chemicals and their Industrial Applications*", Ellis Harwood Ltd., **1979**.

[7] J. T. Welch, *Tetrahedron*, **1987**, *43*, 3123; J. Mann, *Chem. Soc. Rev*. **1987**, *16*, 381; C. D. Hewitt, M. J. Silvester, *Aldrichimica Acta* **1988**, *21*, 3; M. J. Silvester, *Aldrichimica Acta* **1991**, *24*, 31.

[8] D. W. Reynolds, P. E. Casidy, C. G. Johnson, M. L. Cameron, *J. Org. Chem*. **1990**, *55*, 4448.

[9] D. O´Hagan, *Chem. Soc. Rev.* **2008**, *37*, 308.

[10] J. E. Huheey, E. A. Keiter, R. L. Keiter, *Inorganic Chemistry*, 4ª Ed., Harper Collins, New York, 1993, pp. 182–199; E. J. Little, Jr., M. M. Jones, *J. Chem. Educ.* **1960**, *37*, 231; A. L. Allred, E. G. Rochow, *J. Inorg. Nucl. Chem.* **1958**, *5*, 264.

[11] D. J. Burton, L. Lu, *Top. Curr. Chem.* **1997**, *193*, 45; D. J. Burton, Z.-Y. Yang, *Tetrahedron* **1992**, *48*, 189.

[12] M. Finze, E. Bernhardt, H. Willner, *Angew. Chem. Int. Ed.* **2007**, *46*, 9180; M. Finze, E. Bernhardt, A. Terheiden, M. Berkei, H. Willner, D. Christen, H. Oberhammer, F. Aubke, *J. Am. Chem. Soc.* **2002**, *124*, 15385; A. Terheiden, E. Bernhardt, H. Willner, F. Aubke, *Angew. Chem. Int. Ed.* **2002**, *41*, 799.

[13] H. Amii, K. Uneyama, *Chem. Rev.* **2009**, *109*, 2119; H. Torrens, *Coord. Chem. Rev.* **2005**, *249*, 1957; T. G. Richmond, *Angew. Chem. Int. Ed.* **2000**, *39*, 3241; T. G. Richmond, *Top. Organomet. Chem.* **1999**, *3*, 243; J. Burdeniuc, B. Jedicka, R. H. Crabtree, *Chem. Ber./Recueil* **1997**, *130*, 145; H. Plenio, *Chem. Rev.* **1997**, *97*, 3363; J. L. Kiplinger, T. G. Richmond, C. E. Osterberg, *Chem.Rev.* **1994**, *94*, 373.

[14] Referencias selectas: J. Vicente, J. Gil-Rubio, J. Guerrero-Leal, D. Bautista, *Dalton Trans.* **2009**, 3854; J. Goodman, V. V. Grushin, R. B.

Larichev, S. A. Macgregor, W. J. Marshall, D. C. Roe, *J. Am. Chem. Soc.* **2009**, *131*, 4236; G. G. Dubinina, J. Ogikubo, D. A. Vicic, *Organometallics* **2008**, *27*, 6233; G. G. Dubinina, W. W. Brennessel, J. L. Miller, D. A. Vicic, *Organometallics* **2008**, *27*, 3933; V. V. Grushin, W. J. Marshall, *J. Am. Chem. Soc.* **2006**, *128*, 12644; J. Vicente, J. Gil-Rubio, J. Guerrero-Leal, D. Bautista, *Organometallics* **2005**, *24*, 5634; S. Balters, E. Bernhardt, H. Willner, T. Berends, *Z. anorg. allg. Chem.* **2004**, *630*, 257; E. Bernhardt, M. Finze, H. Willner, *J. Fluorine Chem.* **2004**, *125*, 967; J. Vicente, J. Gil-Rubio, J. Guerrero-Leal, D. Bautista, *Organometallics* **2004**, *23*, 4871; R. Eujen, B. Hoge, D. J. Brauer, *Inorg. Chem.* **1997**, *36*, 1464; J. A. Schlueter, J. M. Williams, U. Geiser, J. D. Dudek, S. A. Sirchio, M. E. Kelly, J. S. Gregar, W. H. Kwok, J. A. Fendrich, J. E. Schirber, W. R. Bayless, D. Naumann, T. Roy, *J. Chem. Soc., Chem. Commun.* **1995**, 1311; D. Naumann, T. Roy, K.-F. Tebbe, W. Crump, *Angew. Chem., Int. Ed. Engl.* **1993**, *32*, 1482; J. A. Morrison, *Adv. Organomet. Chem.* **1993**, *35*, 211.

[15] D. Naumann, N. V. Kirij, N. Maggiarosa, W. Tyrra, Y. L. Yagupolskii, M. S. Wickleder, *Z. anorg. allg. Chem.* **2004**, *630*, 746.

[16] F. G. A. Stone, *J. Fluorine Chem.* **1999**, *100*, 227; R. P. Hughes, *Adv. Organomet. Chem.* **1990**, *31*, 183; J. C. Tatlow, *J. Fluorine Chem.* **1984**, *25*, 99; R. Nyholm, *Q. Revs. Chem. Soc.* **1970**, *24*, 1; F. G. A. Stone, *Endeavour* **1966**, *25*, 33; R. D. Chambers, T. Chivers, *Organomet. Chem. Rev., Sect. A* **1966**, *1*, 279; P. M. Treichel, F. G. A. Stone, *Adv. Organomet. Chem.* **1964**, *1*, 143; R. E. Banks, R. N. Haszeldine, *Adv. Inorg. Chem. Radiochem.* **1961**, *3*, 337; J. J.Lagowski, *Q. Revs. Chem. Soc.* **1959**, *13*, 233.

[17] E. R. Sigurdson, G. Wilkinson, *J. Chem. Soc., Dalton Trans.* **1977**, 812.

[18] A. L. Galyer, G. Wilkinson, *J. Chem. Soc., Dalton Trans.* **1976**, 2235; L. Galyer, K. Mertis, G. Wilkinson, *J. Organomet. Chem.* **1975**, *85*, C37.

[19] V. Pfennig, N. Robertson, K. Seppelt, *Angew. Chem., Int. Ed. Engl.* **1997**, *36*, 1350; J. F. Gibson, G. M. Lack, K. Mertis, G. Wilkinson, *J. Chem. Soc., Dalton Trans.* **1976**, 1492; K. Mertis, G. Wilkinson, *J. Chem. Soc., Dalton Trans.* **1976**, 1488.

[20] R. D. Dresdner, T. J. Mao, J. A. Young, *J. Am. Chem. Soc.* **1958**, *80*, 3007; R. D. Dresdner, *J. Am. Chem. Soc.* **1956**, *78*, 876; R. Dresdner, *J. Am. Chem. Soc.* **1955**, *77*, 6633.

[21] R. J. Lagow, J. A. Morrison, *Adv. Inorg. Chem. Radiochem.* **1980**, *23*, 177.

[22] R. J. Lagow, J. L. Margrave, *Prog. Inorg. Chem.* **1979**, *26*, 161; E. K. Liu, R. J. Lagow, *J. Chem. Soc., Chem. Commun.* **1977**, 450; N. J. Maraschin, B. D. Catsikis, L. H. Davis, G. Jarvinen, R. J. Lagow, *J. Am. Chem. Soc.* **1975**, *97*, 513; N. J. Maraschin, R. J. Lagow, *Inorg. Chem.* **1973**, *12*, 1458.

[23] T. J. Juhlke, J. I. Glanz, R. J. Lagow, *Inorg. Chem.* **1989**, *28*, 980; R. A. Jacob, L. L. Gerchman, T. J. Juhlke, R. J. Lagow, *J. Chem. Soc., Chem. Commun.* **1979**, 128; R. J. Lagow, L. L. Gerchman, R. A. Jacob, J. A. Morrison, *J. Am. Chem. Soc.* **1975**, *97*, 518.

[24] D. Naumann, H. Butler, J. Fisher, J. Hanke, J. Mogias, B. Wilkes, *Z. anorg. allg. Chem.* **1992**, *608*, 69; L. J. Krause, J. A. Morrison, *J. Am. Chem. Soc.* **1981**, *103*, 2995; R. J. Lagow, R. Eujen, L. L. Gerchman, J. A. Morrison, *J. Am. Chem. Soc.* **1978**, *100*, 1722.

[25] E. Bernhardt, M. Finze, H. Willner, *Inorg. Chem*. **2011**, *50*, 10273; E. Bernhardt, G. Henkel, H. Willner, G. Pawelke, H. Bürger, *Chem. Eur. J.* **2001**, *7*, 4696.

[26] N. Maggiarosa, W. Tyrra, D. Naumann, N. V. Kirij, Y. L. Yagupolskii, *Angew. Chem. Int. Ed.* **1999**, *38*, 2252.

[27] D. Naumann, W. Tyrra, *J. Organomet. Chem.* **1989**, *368*, 131.

[28] D. Naumann, T. Roy, K.-F. Tebbe, W. Crump, *Angew. Chem., Int. Ed. Engl.* **1993**, *32*, 1482.

[29] W. Dukat, D. Naumann, *Rev. Chim. Miner.* **1986**, *23*, 589.

[30] E. Bernhardt, M. Finze, H. Willner, *J. Fluorine Chem.* **2004**, *125*, 967; J. A. Schlueter, J. M. Williams, U. Geiser, J. D. Dudek, S. A. Sirchio, M. E. Kelly, J. S. Gregar, W. H. Kwok, J. A. Fendrich, J. E. Schirber, W. R. Bayless, D. Naumann, T. Roy, *J. Chem. Soc., Chem. Commun.* **1995**, 1311.

[31] U. Preiss, I. Krossing, *Z. anorg. allg. Chem.* **2007**, *633*, 1639; J. A. Schlueter, U. Geiser, A. M. Kini, H. H. Wang, J. M. Williams, D. Naumann, T. Roy, B. Hoge, R. Eujen, *Coord. Chem. Rev.* **1999**, *190–192*, 781.

[32] S. Balters, E. Bernhardt, H. Willner, T. Berends, *Z. anorg. allg. Chem.* **2004**, *630*, 257;S. Balters, Ph.D. Thesis, University of Wuppertal **2005** [urn:nbn:de:hbz:468-20050702].

[33] Massachusetts Institute of Technology (R. J. Lagow, L. L. Gerchman, R. A. Jacob), US 3992424 (November 16, 1976), p. 7 [*Chem. Abstr.* **1977**, *86*, 72887]; Massachusetts Institute of Technology (R. J. Lagow, L. L. Gerchman, R. A. Jacob), US 3954585 (May 4, 1976), p. 8 [*Chem. Abstr.* **1976**, *85*, 160324].

[34] K. J. R. Rosman, P. D. P. Taylor, *Pure Appl. Chem.* **1998**, *70*, 217.

[35] N. Barlett, *Proc. Chem. Soc.* **1962**, *218*.

[36] R. Hoppe, W. Dähne, H. Mattauch, K. M. Rödder, *Angew. Chem*. *Int. Ed. Engl*. **1962**, *1*, 599.

[37] C. L. Chernick, H. H. Claassen, P. R. Fields, H. H. Hyman, J. G. Malm, W. M. Manning, M. S. Matheson, L. A. Quarterman, F. Schreiner, H. H. Selig, I. Sheft, S. Siegel, E. N. Sloth, L. Stein, M. H. Studier, J. L. Weeks, M. H. Zirin, *Science* **1962**, *138*, 136.

[38] B. Žemva, *Croat. Chim. Acta* **1988**, *61*, 163.

[39] K. Seppelt, D. Lentz, *Prog. Inorg. Chem*. **1982**, *29*, 167.

[40] L. H. Gade, *Chem. unserer Zeit* **2002**, *36*, 168; G. B. Kauffman, en *Coordination Chemistry – A Century of Progress*, ed. G. B. Kauffman, ACS Symposium Series 565, American Chemical Society,Washington, DC 1994, ch. 1, pp. 2‑33; G. B. Kauffman, *Inorganic Coordination Compounds*, Heyden & Son Ltd, London, UK 1981, ch. 6, pp. 86‑136; G. B. Kauffman, *Coord. Chem. Rev.* **1975**, *15*, 1.

[41] *Gmelins Handbuch der Anorganischen Chemie Platin Teil D*, Verlag Chemie GmbH, Weinheim, Germany, 8ª ed, **1957**, pp. 554-557.

[42] R. S. Tobias, *Inorg. Chem.* **1970**, *9*, 1296.

[43] A. Pidcock, R. E. Richards, L. M. Venanzi, *J. Chem. Soc. A* **1966**, 1707.

[44] T. G. Appleton, H. C. Clark,L. E. Manzer, *Coord. Chem. Rev.* **1973**, *10*, 335.

[45] R. G. Pearson, *Inorg. Chem.* **1973**, *12*, 712.

[46] T. G. Appleton, M. H. Chisholm, H. C. Clark, L. E. Manzer, *Inorg. Chem.* **1972**, *11*, 1786.

[47] J. Forniés, M. A. Gómez-Saso, A. Martín, F. Martínez, B. Menjón, J. Navarrete, *Organometallics* **1997**, *16*, 6024.

[48] R. A. Michelin, R. Ros, G. Guadalupi, G. Bombieri, F. Benetollo, G. Chapuis, *Inorg. Chem.* **1989**, *28*, 840; T. G. Appleton, R. D. Berry, J. R. Hall, D. W. Neale, *J. Organomet. Chem.* **1989**, *364*, 249; R. A. Michelin, G. Facchin, R. Ros, *J. Organomet. Chem.* **1985**, *279*, C25.

[49] D. Huang, P. R. Koren, K. Folting, E. R. Davidson, K. G. Caulton, *J. Am. Chem. Soc.* **2000**, *122*, 8916; P. J. Brothers, W. R. Roper, *Chem. Rev.* **1988**, *88*, 1293; M. A. Gallop, W. R. Roper, *Adv. Organomet. Chem.* **1986**, *25*, 121; W. R. Roper, *J. Organomet. Chem.* **1986**, *300*, 167.

[50] Se ha propuesto que este tipo de aductos intervengan como estados de transición en reacciones de ataque nucleófilo sobre el átomo de C de carbenos metálicos de carácter electrófilo: M. A. Sierra, I. Fernández, F. P. Cossío, *Chem. Commun.* **2008**, 4671.

[51] J. E. Bercaw, G. S. Chen, J. A. Labinger, B.-L. Lin, *J. Am. Chem. Soc.* **2008**, *130*, 17654; R. Romeo, G. D'Amico, *Organometallics* **2006**, *25*, 3435; B. J. Wik, M. Lersch, M. 75 Tilset, *J. Am. Chem. Soc.* **2002**, *124*, 12116; J. G. Hinman, C. R. Baar, M. C. Jennings, R. J. Puddephatt, *Organometallics* **2000**, *19*, 563; R. Romeo, M. R. Plutino, L. I. Elding, *Inorg. Chem.* **1997**, *36*, 5909; G. S. Hill, L. M. Rendina, R. J. Puddephatt, *Organometallics* **1995**, *14*, 4966; U. Belluco, R. A. Michelin, P. 80 Uguagliati, B. Crociani, *J. Organomet. Chem.* **1983**, *250*, 565; M. D. Johnson, *Acc. Chem. Res.* **1978**, *11*, 57; U. Belluco, M. Giustiniani, M. Graziani, *J. Am. Chem. Soc.* **1967**, *89*, 6494.

[52] R. J. Puddephatt, *Coord. Chem. Rev.* **2001**, *157***,** 219.

[53] G. Aullón and S. Alvarez, *Inorg. Chem.*, **1996**, *35*, 3137.

[54] H. Schmidbaur, A. Schier in *Comprehensive Organometallic Chemistry III, Vol.* 2 (Eds.:D. M. P. Mingos, R. H. Crabtree, K. Meyer), Elsevier, Amsterdam, **2007**, sect. 2.05.9, pp. 296-298; D. B. dell´Amico, F. Calderazzo, *Gold Bull*. **1997**, *30*, 21.

[55] D. Zopes, S. Kremer, H. Scherer, L. Belkoura, I. Pantenburg, W. Tyrra, S. Mathur, *Eur. J. Inorg. Chem*. **2011**, 273.

[56] H. Schmidbaur, A. Schier, *Chem. Soc. Rev*. **2008**, *37*, 1931; P. Pyykk, *Chem. Soc. Rev*. **2008**, *37*, 1967; J. Muiz, E. Sansores, Mater. Avanzados **2007**, 15; P. Pyykk, *Angew. Chem. Int. Ed*. **2004**, 43, 4412.

[57] P. Pyykk, N. Runeberg, F. Mendiz_bal, *Chem. Eur. J*. **1997**, *3*, 1451; D. V. Toronto, B.Weissbart, D. S. Tinti, A. L. Balch, I*norg. Chem*. **1996**, *35*, 2484.

[58] J. Browning, P. L. Goggin, R. J. Goodfellow, M. G. Norton, A. J. M. Rattray, B. F. Taylor, J. Mink, *J. Chem, Soc. Dalton Trans*. **1977**, 2061.

[59] D. B. Dell´Amico, F. Calderazzo, P. Robino, A. Segre, *J. Chem. Soc. Dalton Trans.* **1991**, 3017.

DOI: 10.1002/chem.200900323

# Oxidative Addition of Halogens to Homoleptic Perfluoromethyl or Perfluorophenyl Derivatives of Platinum(II): A Comparative Study

**Babil Menjón,[a] Sonia Martínez-Salvador,[a] Miguel A. Gómez-Saso,[a] Juan Forniés,*[a] Larry R. Falvello,[a] Antonio Martín,[a] and Athanassios Tsipis*[b]**

*Dedicated to Prof. Dr. José Vicente on the occasion of his 65th birthday.*

**Abstract:** The equilibrium geometries of the homoleptic perfluorinated organoplatinate(II) anions $[Pt(CF_3)_4]^{2-}$ and $[Pt(C_6F_5)_4]^{2-}$ have been computed at the B3P86/LANL2DZ level of theory. Remarkably good agreement with the experimentally determined structures has been obtained by X-ray diffraction methods. The reactivity of $[NBu_4]_2[Pt(CF_3)_4]$ (**1**) towards halogens ($Cl_2$, $Br_2$, and $I_2$) has been investigated by using a combined experimental and theoretical approach. The perfluoromethyl derivative **1** has been found to undergo clean oxidative addition of the three halogens under investigation, giving rise to $[NBu_4]_2[trans\text{-}Pt(CF_3)_4X_2]$ (X = Cl (**7**), Br (**10**), I (**13**)) in a quantitative and stereoselective way. In the low-temperature reaction of the perfluorophenyl derivative $[NBu_4]_2[Pt(C_6F_5)_4]$ (**3**) with $Cl_2$ or $Br_2$, the corresponding oxidative-addition products $[NBu_4]_2[trans\text{-}Pt(C_6F_5)_4X_2]$ (X = Cl (**14**), Br (**15**)) can also be obtained. In the case in which X = Br and working in $CHCl_3$ at −55 °C, it has been possible to detect the formation of an intermediate species to which we assign the formula $[trans\text{-}Pt(C_6F_5)_4Br(ClCHCl_2)]^-$ (**16**). The solvento complex **16** is thermally unstable and prone to undergo reductive elimination of $C_6F_5{-}C_6F_5$. In the presence of PhCN, complex $[NBu_4][trans\text{-}Pt(C_6F_5)_4Br(NCPh)]$ (**17**) was isolated and structurally characterized. The reaction of **3** with $I_2$ gave no organoplatinum(IV) compound. Our comparative study reveals that the $CF_3$ group is especially suited to stabilize organometallic compounds in high oxidation states. This ability can be attributed to a combination of factors: its hardness, its high group electronegativity, its small size, and its reluctance to undergo reductive elimination processes.

**Keywords:** density functional calculations · halogens · homoleptic compounds · oxidation · platinum

## Introduction

Perfluorinated organyl groups ($R^F$) have played an important role in the development of organo–transition-metal chemistry containing M−C σ bonds.[1] As a rule, these $R^F$ ligands endow the resulting organo–transition-metal compound with a higher thermal stability than the corresponding non-fluorinated R groups. Moreover, the small size of the C donor atom, together with the high electronegativity of the F substituent, makes these $R^F$ groups useful "hard" ligands with a marked electron-withdrawing ability. They are therefore especially suited to help to create highly acidic organometallic fragments "$M(R^F)_n$". In particular, there is much current interest in obtaining highly acidic "$Pt(L)_n$" fragments because of their potential involvement in C−H bond activation and functionalization processes.[2] One of the possible mechanisms for that kind of process seems to entail oxidative addition of a C−H bond to a $Pt^{II}$ center, giving a transient organoplatinum(IV) species. $Pt^{II}/Pt^{IV}$ couples connected by oxidative addition/reductive elimination processes are also frequently encountered in many areas of transition-metal chemistry and have received much attention.[3]

[a] Dr. B. Menjón, Dipl.-Chem. S. Martínez-Salvador, Dr. M. A. Gómez-Saso, Prof. Dr. J. Forniés, Prof. Dr. L. R. Falvello, Dr. A. Martín
Instituto de Ciencia de Materiales de Aragón (I.C.M. A.)
Universidad de Zaragoza-C.S.I.C., C/Pedro Cerbuna 12
50009 Zaragoza (Spain)
Fax: (+34) 976-761-187
E-mail: juan.fornies@unizar.es

[b] Dr. A. Tsipis
Laboratory of Inorganic and General Chemistry
Department of Chemistry, University of Ioannina
Ioannina 451 10 (Greece)
Fax: (+30) 26510-44831
E-mail: attsipis@uoi.gr

Supporting information for this article is available on the WWW under http://dx.doi.org/10.1002/chem.200900323.

   

We were interested in studying the $Pt^{II}/Pt^{IV}$ system using $R^F$ ligands. For this purpose, we chose the homoleptic species $[Pt(R^F)_4]^{2-}$ with $R^F$ being the prototypical perfluoromethyl and -phenyl groups, $CF_3$ and $C_6F_5$, respectively. Whereas the perfluorophenyl derivative $[NBu_4]_2[Pt(C_6F_5)_4]$ has been known for many years[4] and its chemistry has been thoroughly developed, the analogous perfluoromethyl compound $[NMe_4]_2[Pt(CF_3)_4]$ was only recently prepared by D. Naumann and co-workers.[5] The advantage of using homoleptic derivatives in a comparative study lies mainly in the fact that the number of variables affecting the system is restricted to a minimum. Herewith, we report on the reactivity of $[NBu_4]_2[Pt(CF_3)_4]$ (**1**) and $[NBu_4]_2[Pt(C_6F_5)_4]$ (**3**) towards halogens ($Cl_2$, $Br_2$, and $I_2$).[1] Any difference in behavior between them will to be attributed solely to the nature of the corresponding $R^F$ ligand.

## Results and Discussion

**Synthesis and characterization of $[NBu_4]_2[Pt(CF_3)_4]$ (1)**: The salt $[NBu_4]_2[Pt(CF_3)_4]$ (**1**) has been prepared by a similar method to that used by D. Naumann and co-workers to synthesize $[NMe_4]_2[Pt(CF_3)_4]$ (**1′**).[5] The procedure consists of low-temperature (−78 °C) treatment of $[NBu_4]_2[(PtBr_2)_2(\mu\text{-}Br)_2]$ with $CF_3SiMe_3$ in the presence of both CsF and the stoichiometrically required amount of solid $[NBu_4]Br$ (Scheme 1). As a result, compound **1** was obtained and isolated as a white solid in 70% yield, and exhibited spectroscopic properties in keeping with those reported for the $[NMe_4]^+$ salt **1′**. Complex **1** is, however, much more soluble in organic solvents, which makes it more amenable for studying its structural and chemical properties. The cyclic voltammogram of **1** in $CH_2Cl_2$ showed no redox process taking place between 1.6 and −1.6 V.

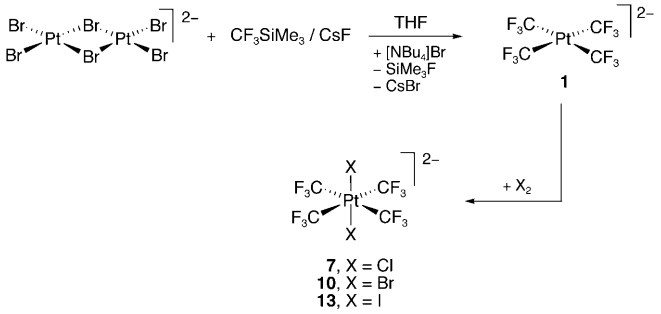


Scheme 1. Synthesis of trifluoromethylplatinate compounds as their corresponding $[NBu_4]^+$ salts.

[1] Explanation of the compound numbering system used in this manuscript: Anions **A1**–**A13** were investigated by density functional calculations. The anions **A1**, **A3**, **A7**, **A10**, and **A13**, were isolated as salts and are then given the numbers **1**, **3**, **7**, **10** and **13**, respectively. Compounds **14**–**17** are the products of the reaction of **3** with different halogens.

The crystal and molecular structures were established by single-crystal X-ray diffraction methods. Crystals of **1** constitute a case of pseudo-symmetry, arising from the fact that the Pt-containing anions form a pattern with *Pnab* symmetry, with the cations forming a pattern with the lower symmetry $Pna2_1$. The geometry of the homoleptic anion $[Pt(CF_3)_4]^{2-}$ (Figure 1) in **1** can be described as essentially

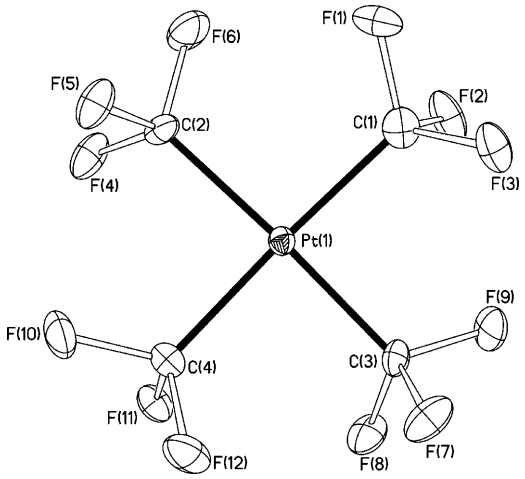


Figure 1. Thermal ellipsoid diagram (50% probability) of the $[Pt(CF_3)_4]^{2-}$ anion in **1**. Selected bond lengths [Å] and angles [°] with estimated standard deviations: Pt–C(1) 2.045(5), Pt–C(2) 2.051(4), Pt–C(3) 2.052(4), Pt–C(4) 2.051(4), C(1)-Pt-C(2) 93.53(13), C(1)-Pt-C(3) 89.53(18), C(1)-Pt-C(4) 174.30(18), C(2)-Pt-C(3) 175.38(18), C(2)-Pt-C(4) 89.39(18), C(3)-Pt-C(4) 87.87(12).

square-planar (*SP*-4) given the small value of continuous shape measure (CShM)[6] obtained for that geometry: $S(SP\text{-}4) = 0.18$.[7] The mutually *trans*-standing $CF_3$ groups are eclipsed. The Pt–C distance (2.050(4) Å average) is significantly shorter than that found in the non-fluorinated homoleptic methyl derivative $[PtMe_4]^{2-}$ (2.117(6) Å average).[8] The observation that M–$CF_3$ bond lengths are generally shorter than the corresponding M–$CH_3$ ones had been explained in terms of a larger s component at the C atom in forming the M–C bond.[9] In fact, the Pt–C distance in **1** is similar to that found in the perfluorophenyl derivative $[CoCp_2]_2[Pt(C_6F_5)_4]$ (Pt–C 2.059(5) Å average).[10]

Having confirmed the structural relationship between the perfluorinated ions $[Pt(CF_3)_4]^{2-}$ and $[Pt(C_6F_5)_4]^{2-}$, we sought to become acquainted with the factors influencing their chemical behavior. To do this, we carried out a theoretical study of the electronic structure of both $[Pt(R^F)_4]^{2-}$ perfluorinated anions, as well as an experimental comparative study of their behavior towards halogens ($Cl_2$, $Br_2$, and $I_2$).

### Theoretical Study

*Structures*: The equilibrium geometries of the $[Pt(CF_3)_4]^{2-}$ (**A1**) and $[Pt(C_6F_5)_4]^{2-}$ (**A3**) dianions and their dissociated $[Pt(CF_3)_3]^-$ (**A2**) and $[Pt(C_6F_5)_3]^-$ (**A4**) ionic species were computed at the B3P86/LANL2DZ level of theory and are shown in Figure S1 of the Supporting Information.

  

Comparing and contrasting the structures of the respective pairs of species some key structural differences emerged. At first the structure of the $[Pt(CF_3)_4]^{2-}$ ion deviates slightly from the perfect *SP*-4 configuration; the root-mean-square (RMS) deviation from the coordination plane is predicted to be 0.054 Å at the B3P86/LANL2DZ level. The RMS deviation from the coordination plane in the experimentally determined structure of the $[Pt(CF_3)_4]^{2-}$ ion was found to be 0.024 Å, which was in accordance with the calculated value. In contrast, the geometry of the $[Pt(C_6F_5)_4]^{2-}$ ion corresponds to a perfect *SP*-4 configuration with Pt–C bonds shorter by 0.011 Å compared to those of the $[Pt(CF_3)_4]^{2-}$ ion. It should be noted that the computed equilibrium geometries of the $[Pt(CF_3)_4]^{2-}$ and $[Pt(C_6F_5)_4]^{2-}$ ions closely resemble those determined by X-ray structural analysis.

The structures of the three-coordinate species that resulted from dissociation of the first perfluoro ligands are similar, corresponding to an almost T-shaped structure with C-Pt-C bond angles of 168.1 and 171.8° for the $[Pt(CF_3)_3]^-$ and $[Pt(C_6F_5)_3]^-$ ions, respectively (Figure S1, Supporting Information). It is worth noting that in poorly coordinating solvents and in the absence of better ligands, the unsaturated $[Pt(C_6F_5)_3]^-$ fragment is unstable and dimerizes. As a result, the dinuclear species $[\{Pt(C_6F_5)_2\}_2(\mu\text{-}C_6F_5)_2]^{2-}$ is obtained, which contains an electron-deficient double bridging system.[11] Although it is suggested to appear in highly reactive transition states,[12] to the best of our knowledge no similar E-$R^F$-E[2e,3c] bond has been experimentally identified so far with $R^F = CF_3$ and E = any chemical element.

*Energetic, electronic, and bonding properties*: We begin with the discussion of the electronic structure and the bonding mode of the parent $[Pt(CF_3)_4]^{2-}$ ion, comparing and contrasting them with those of the $[Pt(C_6F_5)_4]^{2-}$ ion. The orbital interaction diagrams for the Pt–C bond formation of the $[Pt(CF_3)_4]^{2-}$ and $[Pt(C_6F_5)_4]^{2-}$ ions computed at the B3P86/LANL2DZ level of theory are given in the Supporting Information (Figures S2 and S3). Selected electronic parameters of the parent $[Pt(CF_3)_4]^{2-}$ and $[Pt(C_6F_5)_4]^{2-}$ ions and their dissociated $[Pt(CF_3)_3]^-$ and $[Pt(C_6F_5)_3]^-$ ionic species are indicated in Table 1.

The highest occupied molecular orbital (HOMO) of the $[Pt(CF_3)_4]^{2-}$ and $[Pt(C_6F_5)_4]^{2-}$ ions (Figure 2) corresponds to about 96% of the highest occupied fragment orbital (HOFO) of the three-coordinate species for the $[Pt(CF_3)_4]^{2-}$ and $[Pt(C_6F_5)_4]^{2-}$ ions, and, as expected, they have been moved to higher energies upon interaction with the perfluoro fragment. The lowest unoccupied molecular orbital (LUMO) of the $[Pt(CF_3)_4]^{2-}$ ion corresponds to about 90% of the lowest unoccupied fragment orbital (LUFO) LUFO+

Table 1. Selected electronic parameters of the anions **A1** to **A4** computed at the B3P86/LANL2DZ level.

| | $E_{tot}$ [Hartree] | $\varepsilon_{HOMO}$ [eV] | $\varepsilon_{LUMO}$ [eV] | $\eta$[a] [eV] | $\omega$[b] [eV] | *nec*(Pt)[c] 5d/6s | $q_{Pt}$[d] | $q_C$[e] |
|---|---|---|---|---|---|---|---|---|
| $[Pt(CF_3)_4]^{2-}$ (**A1**) | −1472.584341 | −0.221 | 6.171 | 3.196 | 2.77 | 9.00/0.64 | 0.34 | 0.73 |
| $[Pt(CF_3)_3]^-$ (**A2**) | −1134.348048 | −4.493 | 0.143 | 2.316 | 2.04 | 8.93/0.64 | 0.42 | |
| $[Pt(C_6F_5)_4]^{2-}$ (**A3**) | −3036.469412 | −1.253 | 3.581 | 2.417 | 0.05 | 8.93/0.52 | 0.52 | −0.36 |
| $[Pt(C_6F_5)_3]^-$ (**A4**) | −2307.230996 | −4.731 | −0.652 | 2.040 | 3.55 | 8.87/0.54 | 0.58 | |
| $C_6F_5^-$ | −729.202956 | −2.123 | 2.902 | 2.513 | 0.06 | | | −0.36 |

[a] Hardness $\eta = (\varepsilon_{LUMO} - \varepsilon_{HOMO})/2$. [b] Electrophilicity index $\omega = \mu^2/2\eta$, in which $\mu$ is the chemical potential given by $\mu = (\varepsilon_{LUMO} + \varepsilon_{HOMO})/2$. [c] Natural electron configuration (*nec*). [d] Natural atomic charge on Pt. [e] Natural atomic charge on the C donor atom.

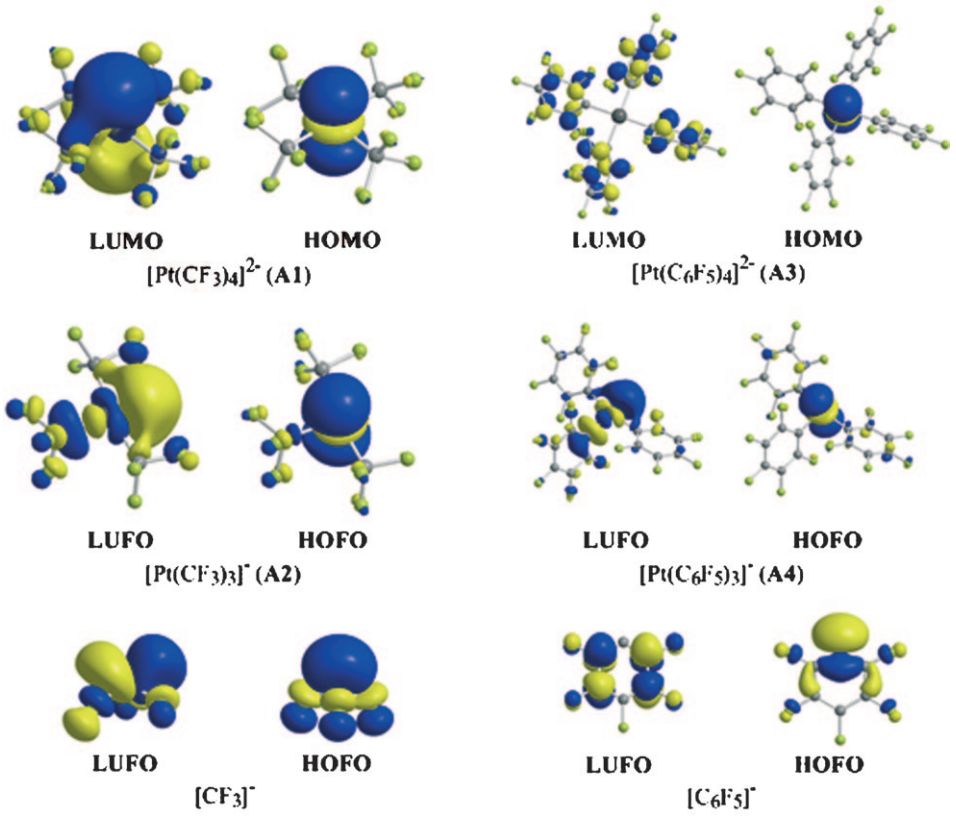


Figure 2. Frontier molecular orbitals (MOs) of the $[Pt(CF_3)_4]^{2-}$ and $[Pt(C_6F_5)_4]^{2-}$ ions, their dissociated $[Pt(CF_3)_3]^-$ and $[Pt(C_6F_5)_3]^-$ ionic species, and the "free" $[CF_3]^-$ and $[C_6F_5]^-$ ligands.

1 of the three-coordinate species, whereas the LUMO of the $[Pt(C_6F_5)_4]^{2-}$ ion corresponds to the antibonding interaction of the LUFO+2 of the three-coordinate fragment and the LUFO of the perfluoro-ligand with a composition of 46.0% and 25.7%, respectively. The $\sigma$(Pt–C) natural bonding orbital in the $[Pt(CF_3)_4]^{2-}$ ion is constructed from an $sd^{1.11}$ (52.67% d character) natural hybrid orbital (NHO) on the Pt atom interacting in-phase with an $sp^{1.49}$ (59.90% p character) NHO on the bonded C atom, thus having the form $\sigma$-(Pt–C) = 0.539 $h_{Pt}$ + 0.842 $h_C$.

On the other hand, the $\sigma$(Pt–C) natural bonding orbital in the $[Pt(C_6F_5)_4]^{2-}$ ion is constructed from an $sd^{1.09}$ (52.05% d character) NHO on the Pt atom interacting in-phase with an $sp^{2.44}$ (70.90% p character) NHO on the bonded C atom, thus having the form $\sigma$(Pt–C) = 0.526 $h_{Pt}$ + 0.851 $h_C$. The higher percentage contribution of the carbon p orbital in the lone pair NHO of the $C_6F_5^-$ than the $CF_3^-$ ligand forming the Pt–C bonds is noteworthy. This is due to the fact that the carbon p orbital in the $CF_3^-$ ligand is primarily involved in an $sp^{9.40}$ (90.40% p character) NHO participating in the formation of the C–F bonds, whereas in the $C_6F_5^-$ ligand the carbon p orbital is involved in an $sp^{1.97}$ (66.30% p character) NHO participating in the formation of the adjacent C=C double bonds. According to the NBO analysis of the "free" $C_6F_5^-$ and $CF_3^-$ ligands, the carbon lone pair resides on an $sp^{2.04}$ ($sp^{1.69}$) and $sp^{0.37}$ ($sp^{0.53}$) NHO, respectively, at the B3P86/LANL2DZ (B3P86/6-31+G*) levels. It is worth noting that at the B3P86/6-31+G** level of theory the carbon lone pair of the $CH_3^-$ ligand resides on an $sp^{7.11}$ (87.65% p character) NHO.

The computed interaction energies (without basis set superposition error corrections) of −25.4 and −30.2 kcal mol$^{-1}$ between the two fragments in the $[Pt(CF_3)_4]^{2-}$ and $[Pt(C_6F_5)_4]^{2-}$ ions, respectively, illustrate that the Pt–$C_6F_5$ bond is slightly stronger than the Pt–$CF_3$ bond. Thus, the $[Pt(CF_3)_4]^{2-}$ ion would be expected to undergo ligand substitution reactions more easily through a dissociative mechanism.

According to the charge decomposition analysis (CDA) there is a charge transfer of about 0.289 |e| and 0.145 |e| from the $CF_3^-$ and $C_6F_5^-$ perfluoro ligands, respectively, to the Pt central metal atom, with a concomitant charge transfer of about 0.035 |e| and 0.070 |e| from the Pt to $CF_3^-$ and $C_6F_5^-$ ligands, respectively. The electron density is transferred to Pt 5d and 6s AOs, thus acquiring a natural electron configuration of $5d^{9.00}6s^{0.64}$ and $5d^{8.93}6s^{0.52}$, respectively (Table 1).

Finally, the calculated proton affinities of 400.2 and 371.8 kcal mol$^{-1}$ for the $CF_3^-$ and $C_6F_5^-$ ligands, respectively, at the B3LYP/6-31G(d) level of theory illustrates that the $CF_3^-$ ligand exhibits slightly higher $\sigma$-donor capacity (basicity) than the $C_6F_5^-$ one, in line with the computed values of the net charge donation of the ligands.

**Oxidative addition reactions of the $[Pt(CF_3)_4]^{2-}$ ion**: The equilibrium geometries of the products resulting from oxidative addition of halogens ($Cl_2$, $Br_2$, and $I_2$) to **A1** computed at the B3P86/LANL2DZ level are shown in Figure S4, and selected electronic parameters are compiled in Table 2.

Table 2. Selected electronic parameters of the oxidative-addition products of the $[Pt(CF_3)_4]^{2<M->}$ (**A1**) dianion computed at the B3P86/LANL2DZ level.

| | $E_{tot}$ [Hartree] | $\varepsilon_{HOMO}$ [eV] | $\varepsilon_{LUMO}$ [eV] | $\eta$[a] [eV] | *nec*(Pt)[b] 5d/6s | $q_{Pt}$[c] | $\Delta_R H$[d] [kcal mol$^{-1}$] |
|---|---|---|---|---|---|---|---|
| $[Pt(CF_3)_4Cl]^-$ (**A5**) | −1487.659669 | −5.149 | −1.640 | 1.754 | 8.65/0.50 | 0.81 | −62.0 |
| *cis*-$[Pt(CF_3)_4Cl_2]^{2-}$ (**A6**) | −1502.833269 | −0.680 | 3.833 | 2.256 | 8.67/0.51 | 0.78 | −60.4 |
| *trans*-$[Pt(CF_3)_4Cl_2]^{2-}$ (**A7**) | −1502.824294 | −1.161 | 3.00 | 2.081 | 8.67/0.50 | 0.79 | −54.6 |
| $[Pt(CF_3)_4Br]^-$ (**A8**) | −1485.879561 | −4.790 | −1.673 | 1.559 | 8.68/0.52 | 0.76 | −56.6 |
| *cis*-$[Pt(CF_3)_4Br_2]^{2-}$ (**A9**) | −1499.272696 | −0.307 | 3.520 | 1.913 | 8.73/0.53 | 0.69 | −43.5 |
| *trans*-$[Pt(CF_3)_4Br_2]^{2-}$ (**A10**) | −1499.266815 | −0.864 | 2.670 | 1.767 | 8.75/0.53 | 0.68 | −39.8 |
| $[Pt(CF_3)_4I]^-$ (**A11**) | −1484.100789 | −4.410 | −1.702 | 1.354 | 8.70/0.54 | 0.71 | −53.3 |
| *cis*-$[Pt(CF_3)_4I_2]^{2-}$ (**A12**) | −1495.715683 | −0.046 | 3.223 | 1.635 | 8.77/0.56 | 0.61 | −32.2 |
| *trans*-$[Pt(CF_3)_4I_2]^{2-}$ (**A13**) | −1495.713148 | −0.594 | 2.388 | 1.491 | 8.81/0.57 | 0.56 | −30.5 |

[a] Hardness $\eta = (\varepsilon_{LUMO} - \varepsilon_{HOMO})/2$. [b] Natural electron configuration (*nec*). [c] Natural atomic charge on Pt. [d] Enthalpy change for the reactions: $[Pt(CF_3)_4]^{2-} + X_2 \rightarrow [Pt(CF_3)_4X]^- + X^-$ or $[Pt(CF_3)_4]^{2-} + X_2 \rightarrow [Pt(CF_3)_4X_2]^{2-}$, where appropriate.

The most widely accepted mechanism for the oxidative addition of halogens to $d^8$ *SP*-4 transition metal complexes giving rise to $d^6$ *OC*-6 compounds is depicted in Scheme 2.[13] The first step would involve donor–acceptor interaction (**Y**) between the electrophilic $X_2$ molecule (a "class B" reagent in Puddephatt's classification)[3a] and the metal atom. This type of adduct (Lewis neutralization product) is favored by the basicity of the metal center.[14] Efficient transfer of electron density from the metal fragment to the antibonding orbitals of the $X_2$ molecule should cause its heterolytic cleavage under release of $X^-$. This means the formal two-electron oxidation of the metal center (from $d^8$ to $d^6$) caused by the $X^+$ fragment giving rise to a transient five-coordinate species **Z**. Coordination of the $X^-$ ligand to

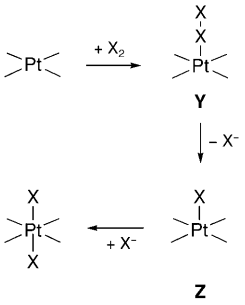


Scheme 2. The most accepted mechanism for the oxidative addition of halogens to *SP*-4 platinum(II) compounds.

the unsaturated intermediate **Z** eventually gives the oxidative addition product. Along this reaction path, the most versatile species is **Z**, because it can also undergo isomerization[15] and/or reductive elimination of R–R or R–X depending on the nature of R and X.

In isolated, gas-phase molecules unperturbed by the solvent's action, all the reactions depicted in Scheme 2 are predicted to be exothermic. The most exothermic reaction is the oxidative addition of $Cl_2$, followed by the oxidative addition of $Br_2$ and $I_2$. From a mechanistic point of view, these oxidative addition reactions proceed via a polar five-coordinate transition state, formed upon HOMO–LUMO interactions involving transformation of a nonbonding electron pair of the $Pt^{II}$ central atom to a bonding electron pair; thereby the $Pt^{II}$ metal center is oxidized to $Pt^{IV}$. We were able to locate on the potential-energy surface (PES) the five-coordinate intermediates **A5**, **A8**, and **A11** (Figure S4 in the Supporting Information). The geometry of these intermediate species can be described as square pyramidal (*SPY*-5) according to their CShM values.[6] An increasing degree of distortion is observed with the size of the halo ligand located in the basal plane. Anions **A5**, **A8**, and **A11**, upon interaction with the $X^-$ ligand, would lead to the formation of the respective oxidative addition products. According to our calculations, for the $[Pt(CF_3)_4X_2]^{2-}$ (X = Cl, Br, I) anions the *cis* isomers are predicted to be slightly more stable than the *trans* isomers by 5.6, 3.7, and 1.6 kcal mol$^{-1}$, respectively. Therefore, both isomers could be the products of the oxidative addition reactions with halogens. It is interesting to note that the relative stabilities of all species is reflected in the hardness values ($\eta$) given in Table 2.[16]

**Oxidative addition of halogens to the perfluoromethyl compound $[NBu_4]_2[Pt(CF_3)_4]$ (1)**: Compound **1** reacts with the stoichiometrically required amount of halogen, giving rise to the organoplatinum(IV) derivatives $[NBu_4]_2$[*trans*-$Pt(CF_3)_4X_2$] (X = Cl (**7**), Br (**10**), I (**13**)) according to Scheme 1. The oxidative addition reactions proceed in a quantitative and stereoselective way, as shown by $^{19}F$ NMR spectroscopy. From the reaction media, compounds **7**, **10**, and **13** can be isolated as air-stable, thermally robust solids in good yields.

The formulation of compounds **7**, **10**, and **13** as the *trans* isomers relies on their $^{13}C\{^{19}F\}$ and $^{19}F$ NMR spectra, which consist of singlets flanked by $^{195}Pt$-satellites ($^{195}Pt$: $I = 1/2$, 33.831557(42) % relative natural abundance).[17] The chemical shifts of the $^{13}C$ and $^{195}Pt$ NMR signals in **7**, **10**, and **13** appear at an increasing frequency with the electronegativity of the halide (Table 3). In contrast, the $^{19}F$ NMR signals follow the opposite trend. The $^{195}Pt$ NMR spectra appear as high-multiplicity signals due to coupling with 12 equivalent $^{19}F$ nuclei ($^{19}F$: $I = 1/2$, 100 % natural abundance).[17] In these multiplets, however, the less intense signals located at the extreme sides of the central resonance are too weak to emerge from the background and are therefore not observed. The internuclear spin coupling constants $^1J(^{13}C,^{195}Pt)$ and $^2J(^{19}F,^{195}Pt)$ in **7**, **10**, and **13** show an important decrease with respect to the values observed in the parent species **1** (1284 and 542 Hz, respectively).[5] This kind of decrease has been mainly attributed to the change in the s-orbital character of metal bonding orbitals on going from (*SP*-4)-$Pt^{II}$ to (*OC*-6)-$Pt^{IV}$.[18]

Table 3. Spectroscopic NMR data for the organoplatinum(IV) compounds $[NBu_4]_2$[*trans*-$Pt(CF_3)_4X_2$].

| | **7** (X = Cl) | **10** (X = Br) | **13** (X = I) |
|---|---|---|---|
| $\delta_C$ [ppm] | 117.3 | 116.7 | 114.6 |
| $^1J(^{13}C,^{195}Pt)$ [Hz] | 858 | 859 | 888 |
| $\delta_F$ [ppm] | −34.0 | −31.3 | −18.5 |
| $^2J(^{19}F,^{195}Pt)$ [Hz] | 268 | 275 | 308 |
| $\delta_{Pt}$ [ppm] | −1805 | −2105 | −3656 |

The crystal structure of **7** was determined by X-ray diffraction methods. The structure was solved in space group *I*2/*a* and can be considered an interesting case of the crystal packing of fairly small chemical units exhibiting different degrees of disorder for the constituent residues, depending on their location within the asymmetric unit. A detailed account on the satisfactory modeling of the different kinds of disorder can be found in the Supporting Information. The [*trans*-$Pt(CF_3)_4Cl_2]^{2-}$ ion in the crystal (Figure 3) shows a nearly *OC*-6 structure as calculated for the gas-phase anion **A7** (Figure S4 in the Supporting Information). The equatorial Pt–C distance (2.092(5) Å average) is slightly longer than that found in the $Pt^{II}$ parent compound **1** (2.050(4) Å average). The observed elongation is at variance with the contraction expected for the metal center on oxidation and can be attributed to the concomitant increase in coordination number. It must be noted, however, that a substantially

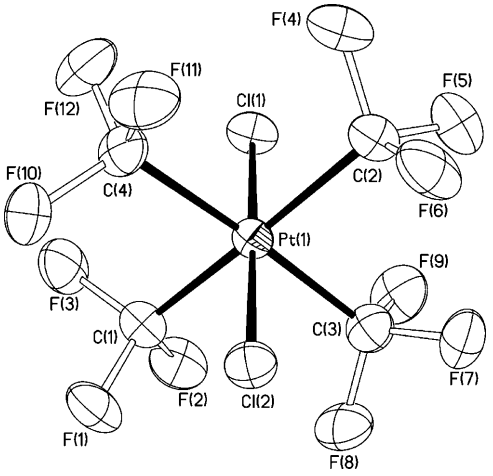


Figure 3. Thermal ellipsoid diagram (50 % probability) of one of the two crystallographically independent [*trans*-$Pt(CF_3)_4Cl_2]^{2-}$ anions in **7**. Selected bond lengths [Å] and angles [°] with estimated standard deviations: Pt(1)–Cl(1) 2.3319(13), Pt(1)–Cl(2) 2.3265(13), Pt(1)–C(1) 2.097(5), Pt(1)–C(2) 2.086(5), Pt(1)–C(3) 2.094(5), Pt(1)–C(4) 2.092(5), Cl(1)-Pt(1)-Cl(2) 179.24(4), Cl(1)-Pt(1)-C(1) 87.44(14), Cl(1)-Pt(1)-C(2) 88.37(16), Cl(1)-Pt(1)-C(3) 92.48(17), Cl(1)-Pt(1)-C(4) 92.15(16), Cl(2)-Pt(1)-C(1) 91.87(14), Cl(2)-Pt(1)-C(2) 92.33(16), Cl(2)-Pt(1)-C(3) 87.84(17), Cl(2)-Pt(1)-C(4) 87.51(16), C(1)-Pt(1)-C(2) 175.8(2), C(1)-Pt(1)-C(3) 90.7(2), C(1)-Pt(1)-C(4) 88.5(2), C(2)-Pt(1)-C(3) 88.9(2), C(2)-Pt(1)-C(4) 92.3(2), C(3)-Pt(1)-C(4) 175.3(2).

  

shorter Pt–C distance (2.000(8) Å average) has been found in the similar *OC*-6 compound $K_2[\{Pt(CF_3)_2F_2\}_2(\mu\text{-}OH)_2]\cdot 2H_2O$.[19] The key difference between the latter dinuclear compound and complex **7** might be the nature of the *trans*-standing ligand: OH versus $CF_3$. Although excellent agreement is observed between the calculated and experimentally observed Pt–C distance in **7**, the calculated Pt–Cl distance in the gas-phase anion **A7** (2.426 Å) is much longer than that found for the same anion in the crystal (2.3292(13) Å average). This difference (≈4% elongation) might mean that the π component in the Pt–Cl bond has been underestimated in the calculations due to the limited LANL2DZ basis set used.

Our theoretical calculations on the relative stability of the $[Pt(CF_3)_4X_2]^{2-}$ ions (X = Cl, Br, I), indicate that the *cis* isomers should be slightly more stable than their corresponding *trans* isomers. However, we have observed experimentally that the oxidative addition of halogens to **1** in solution results in the quantitative formation of the *trans* isomer. This difference can be ascribed mainly to the following factors: 1) the mild conditions under which the reactions are carried out, and 2) the effect of the solvent, which was not taken into account in the gas-phase calculations. Under the mild experimental conditions used ($CH_2Cl_2$ solution, −78 °C), the kinetically more accessible compound could be favored over the thermodynamically more stable one. Moreover, the solvent molecules (solv) may play an important role in stabilizing the intermediate **Z** (Scheme 2), as well as in deciding its geometry. The particular type of **Z**/solv interaction—ranging from loose solvation to strong coordination—will depend in each case on the Lewis acidity and accessibility of the metal center at the unsaturated intermediate **Z**, as well as the coordination ability of the solvent itself (solv Lewis basicity). However, we have not been able to detect any intermediate species in any of these reactions.

It is interesting to note that the stereoisomer $[NBu_4]_2[cis\text{-}Pt(CF_3)_4Cl_2]$ had been observed to form as the main reaction product between $[NBu_4]_2[Pt(CN)_4]$ and ClF in $CH_2Cl_2$.[19] It is apparent that the reaction path determines the stereochemistry of the final product in each case. Once formed, the *trans* isomer **7** is kinetically rather robust. Attempts to thermally promote *trans*/*cis* isomerization failed. After one week of heating under reflux, solutions of **7** in acetone or acetonitrile showed no sign of isomerization or decomposition ($^{19}$F NMR spectroscopy). The spectroscopic properties of the two $[NBu_4]_2[Pt(CF_3)_4Cl_2]$ isomers are in general different, according to their different stereochemistry. However, the $^{195}$Pt chemical shift, which should not depend upon the specific stereochemical arrangement of the coordinated ligands, is virtually identical in both cases: $\delta_{Pt} \approx -1800$ ppm.

**Oxidative addition of halogens to the perfluorophenyl compound $[NBu_4]_2[Pt(C_6F_5)_4]$ (3)**: In contrast to the straightforward behavior of **1** towards halogens, the perfluorophenyl homologous species $[NBu_4]_2[Pt(C_6F_5)_4]$ (**3**) had been found to react with $Cl_2$ or $I_2$ in $CH_2Cl_2$ at room temperature, producing no organoplatinum(IV) compound but just elimination products.[20] Thus, the room temperature reaction of **3** with $Cl_2$ gave a complex mixture of perfluorophenyl platinum(II) derivatives with variable amounts of Pt-bound Cl content. With $I_2$ as the oxidant, the reaction takes place more cleanly, giving rise to compounds $[NBu_4]_2[Pt(C_6F_5)_3I]$ or $[NBu_4]_2[\{Pt(C_6F_5)_2\}_2(\mu\text{-}I)_2]$ depending on the **3**:$I_2$ ratio.[20]

In view of the markedly different behavior shown by the homoleptic perfluoromethyl and perfluorophenyl platinum(II) derivatives **1** and **3** against halogens, we found it interesting to explore the reaction progress of **3** + $X_2$ with the aid of low-temperature $^{19}$F NMR spectroscopy. As commented above, compounds **1** and **3** both have overall *SP*-4 geometry and virtually identical Pt–C distances. However, the perpendicular arrangement of the much bulkier $C_6F_5$ rings with respect to the metal coordination plane, together with their restricted rotation about the Pt–C bond, enable this perfluoroaryl group to act as a fine stereochemical probe throughout the process under study.[21]

We monitored the reaction of **3** with halogens in $CH_2Cl_2$ at low temperature by $^{19}$F NMR spectroscopy. The reaction of **3** with $Cl_2$ or $Br_2$ at −80 °C gives the corresponding oxidative-addition compounds $[NBu_4]_2[trans\text{-}Pt(C_6F_5)_4X_2]$ (X = Cl (**14**), Br (**15**)) in nearly quantitative yield (based on $^{19}$F NMR spectroscopy). In contrast, the reaction of **3** with $I_2$ even at −80 °C produces $[NBu_4]_2[Pt(C_6F_5)_3I]$ as the only organometallic species[22] with concomitant formation of $C_6F_5$–I.[23] No intermediate species were detected in any of these processes.

Using $CHCl_3$ instead of $CH_2Cl_2$ as the solvent results in an unexpected change of behavior. Thus, by reacting **3** with $Cl_2$ in $CHCl_3$ at −55 °C, complex mixtures are observed that contain massive amounts of decomposition products including $C_6F_5$–$C_6F_5$. The low-temperature reaction of **3** with $Br_2$ gives, in turn, a single species (Figure 4), which we ascribe to the solvated intermediate $[trans\text{-}Pt(C_6F_5)_4Br(solv)]^-$ (solv = $CHCl_3$/$CDCl_3$ (**16**); Scheme 3). Although largely considered as "non-coordinating" molecules, halocarbons are now well documented to be able to act as ligands towards

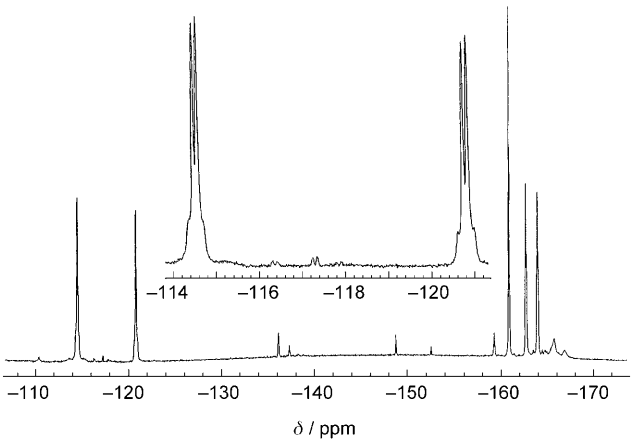


Figure 4. $^{19}$F NMR spectrum of **16** in $CHCl_3$/$CDCl_3$ (3:1) at −55 °C with inset showing the *o*-F signals in more detail. Values of $\delta_F$ and $^3J(^{195}Pt,^{19}F)$ are given in Table 4.

  

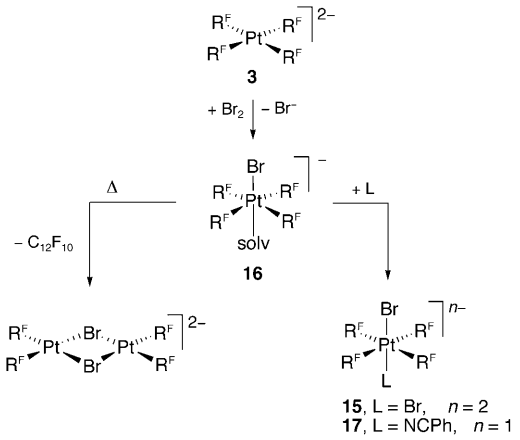


Scheme 3. Reactivity of compound **3** ($R^F = C_6F_5$) with $Br_2$ in $CHCl_3$. Intermediate species **16** (solv = $CHCl_3$/$CDCl_3$) was only detected by low-temperature $^{19}F$ NMR spectroscopy. The remaining species were isolated as their corresponding $[NBu_4]^+$ salts.

metal centers.[24,25] The presence of only one *para*-F signal in the $^{19}F$ NMR spectrum of **16** denotes that the $C_6F_5$ groups are chemically equivalent, while the two equally intense *ortho*-F and two *meta*-F signals are evidence of significantly different magnetic and chemical environments for those substituents (Table 4). These spectroscopic features would, in principle, be in keeping with species of both type **Y** and **Z** (Scheme 2), conveniently stabilized by solvent coordination. Since the addition of $AgClO_4$ to the reaction medium causes the precipitation of AgBr, but no significant change in the $^{19}F$ NMR spectrum, the assignment of **16** as a donor–acceptor adduct of type **Y** can be ruled out. The overall spectroscopic pattern of **16** is very similar to that observed for the *OC*-6 compound $[NBu_4][trans\text{-}Pt(C_6F_5)_4Br(CO)]$[26] as well as for the related *SPY*-5 species $[N(PPh_3)_2][Pt(C_6F_5)_4(NO)]$ at low temperature (Table 4).[27] All our efforts to detect a signal corresponding to coordinated $CHCl_3$ by low-temperature $^{13}C$ NMR spectroscopy[25] failed, probably due to exchange with free solvent molecules.

The fact that the oxidative addition of $Br_2$ to **3** is arrested at −55 °C at stage **Z**·(solv) can be attributed to the fortunate conjunction of electronic and steric factors. Firstly, pentafluorophenyl groups are quite space-demanding ligands, in spite of which it is apparent that they allow the Pt atom to be approached by the $Br_2$ molecule (atomic radius: 1.14 Å).[28,29] Secondly, the basic character of the anionic Pt center seems to be strong enough to promote a very rapid heterolytic cleavage of the $Br_2$ molecule so that the transient species **Y** is not even detectable in this case. According to previous theoretical calculations,[14] the nature of the metal center upon oxidation would turn from basic to acidic, thus favoring axial coordination of a solvent molecule. Thirdly, the failure of the $Br^-$ ion (ionic radius: 1.82 Å)[28a] to reach the metal center at **16** at −55 °C can be ascribed to the shielding effect of the *ortho*-F atoms of the $C_6F_5$ groups on the coordinated solvent molecules. As we will see later, this shielding effect can be overcome by sterically more favorable incoming ligands.

The chemical behavior of **16** is also in keeping with that expected for an (*OC*-6)-$Pt^{IV}$ species of type **Z**·(solv) in which the solvent molecule is loosely coordinated to the metal center. Thus, when the reaction mixture **16** + $Br^-$ is allowed to warm to above −40 °C, two competing processes are observed (Scheme 3). One of the paths entails replacement of coordinated solvent by $Br^-$ to yield **15** (Table 4), thereby fulfilling the oxidative-addition process. The other path involves reductive elimination of $C_6F_5$–$C_6F_5$ and formation of the dinuclear species $[NBu_4]_2[\{Pt(C_6F_5)_2\}_2(\mu\text{-}Br)_2]$. Formation of **15** is favored by the presence of excess $Br^-$. Hence, the best experimental conditions found to obtain **15** in reasonable yields involve working at low temperature (between −40 and −30 °C) to avoid decomposition of **16** and in the presence of a threefold excess of $Br^-$. In contrast to the thermal instability of intermediate species **16**, the final product **15** needs two days of heating at 60 °C to undergo a similar reductive elimination process.

Table 4. $^{19}F$ NMR data for the perfluorophenylplatinum(IV) compounds **14**–**17** and other related species.[a]

| | *ortho*-F[b] | *meta*-F[b] | *para*-F |
|---|---|---|---|
| $[NBu_4]_2[Pt(C_6F_5)_4]$ (**3**) | −113.3 (451) | −168.6 (140) | −170.5 |
| $[NBu_4]_2[trans\text{-}Pt(C_6F_5)_4Cl_2]$ (**14**) | −116.0 (85) | −168.1 | −166.9 |
| $[NBu_4]_2[trans\text{-}Pt(C_6F_5)_4Br_2]$ (**15**) | −108.8 (92) | −169.0 | −168.4 |
| $[NBu_4][Pt(C_6F_5)_4Br(ClCH_2Cl)]$ (**16**)[c] | −114.5 (80), −120.8 (95) | −162.4, −164.0 | −160.9 |
| $[N(PPh_3)_2][Pt(C_6F_5)_4(NO)]$[d] | −114.5, −128.3 | −164.6 | −162.2 |
| $[NBu_4][trans\text{-}Pt(C_6F_5)_4Br(CO)]$[e] | −110.0 (130), −115.3 (77) | −163.1, −164.2 | −160.2 |
| $[NBu_4][trans\text{-}Pt(C_6F_5)_4Br(NCPh)]$ (**17**) | −115.6 (80), −119.4 (89) | −165.8, −166.3 | −163.5 |

[a] $\delta_F$ values in ppm referred to $CFCl_3$; unless otherwise stated, measurements were carried out at room temperature. [b] Where observed and sufficiently resolved, $^nJ(^{19}F,^{195}Pt)$ values ($n = 3$ or 4) are given in Hz in parenthesis. [c] In $CDCl_3$ at −55 °C. [d] Registered at −60 °C; Reference [27]; [e] Reference [26].

It must be admitted that the spectroscopic features (Table 4) and most aspects of the chemical behavior of **16** would, in principle, also be in keeping with the solvent-free, five-coordinate species $[Pt(C_6F_5)_4Br]^-$. Although they have often been suggested as key intermediates in reductive-elimination processes,[30] unsaturated (16-electron) five-coordinate $Pt^{IV}$ derivatives have only recently been isolated and structurally characterized.[31] The assumption of a five-coordinate structure for intermediate **16** does not explain why the $Br^-$ ion manages to enter the Pt coordination sphere in $CH_2Cl_2$ at −80 °C, but fails in $CHCl_3$ at −55 °C. This observation would suggest a substitution reaction rather than the coordination of an additional ligand at a vacant site.

Solvent molecules sterically more suitable than $Br^-$ and with better coordination ability than chloroalkanes give rise

  

to more stable compounds, which do not undergo further substitution. Thus, by reaction of **3** with $Br_2$ in $CHCl_3$ containing benzonitrile—a linear, small-sized, hard ligand—the thermally stable complex $[NBu_4][trans\text{-}Pt(C_6F_5)_4Br(NCPh)]$ (**17**) was isolated in high yield. It is interesting to note that replacement of the coordinated solvent molecules in intermediate **16** by NCPh occurs more efficiently than by the $Br^-$ ion, which is equally present in the reaction medium.

The IR spectrum of **17** shows a band at 2315 $cm^{-1}$ assignable to the $\nu$(C≡N) vibration. The $\nu$(C–F) vibration in **17** (961 $cm^{-1}$) appears at a slightly higher value than in the parent $Pt^{II}$ compound **3** (952 $cm^{-1}$), as is commonly observed in other pentafluorophenyl metal compounds on oxidation of the metal center.[32] In contrast, the IR-active X-sensitive vibration mode of the $C_6F_5$ group[32] appears in **17** at exactly the same frequency as in **3**: 765 $cm^{-1}$. Similar frequency values are also observed in the six-coordinate $Pt^{IV}$ compounds **14** and **15** (see Experimental Section). The $^{19}F$ NMR spectra of compounds **14**, **15**, and **17** show only one *para*-F signal according to the axial character of the corresponding anions (Table 4). The presence of the same $X^-$ ligand in the axial positions of **14** (X = Cl) and **15** (X = Br) renders a symmetric environment for the *ortho*-F atoms (the same applies for the *meta*-F atoms). In the case of **17**, however, the dissymmetry in the axial direction produces two different chemical environments for the *ortho*-F substituents within each ring. The fact that the *ortho*-F and the *meta*-F atoms give rise to two signals each means that compound **17** has a static stereochemical configuration in the NMR timescale.

The crystal and molecular structures of the solvate **17**·0.45*n*-hexane was established by single-crystal X-ray diffraction methods. The molecular geometry of the $[trans\text{-}Pt(C_6F_5)_4Br(NCPh)]^-$ ion (Figure 5) can be described as approximately octahedral (*OC*-6). The *trans*-standing $Br^-$ and NCPh ligands define the axial direction around which the equatorial $C_6F_5$ groups are helicoidally arranged. This propeller-like arrangement of the heavily tilted $C_6F_5$ groups (tilt angles: 42.5–47.8°) makes the whole anion chiral. Both enantiomers derived from the two possible orientations of the rings (clockwise and anticlockwise) are present in the crystal. In fact, this structure possesses the unusual and somewhat suggestive combination of a chiral space group ($P2_1$) with $Z' = 2$ and a racemic asymmetric unit containing both *C* and *A* enantiomers (see Supporting Information for details). The overall structure is very similar to that found[26] for the carbonyl derivative $[NBu_4][trans\text{-}Pt(C_6F_5)_4Br(CO)]$ with similar Pt–Br distances (2.474(4) vs. 2.4360(8) Å) despite the different *trans* influence of the CO and NCPh ligands. The $Pt–C_6F_5$ distances are also comparable in both cases.

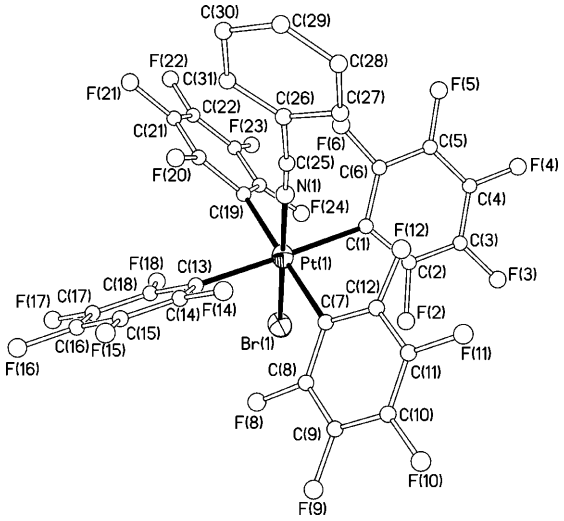


Figure 5. Thermal ellipsoid diagram (50% probability) of one of the enantiomers (*C* isomer) of the $[trans\text{-}Pt(C_6F_5)_4Br(NCPh)]^-$ anion in **17**·0.45$C_6H_{14}$. Selected bond lengths [Å] and angles [°] with estimated standard deviations: Pt(1)–Br(1) 2.4360(8), Pt(1)–N(1) 2.038(6), Pt(1)–C(1) 2.127(7), Pt(1)–C(7) 2.129(9), Pt(1)–C(13) 2.126(6), Pt(1)–C(19) 2.106(8), Br(1)-Pt(1)-N(1) 179.0(2), Br(1)-Pt(1)-C(1) 90.67(19), Br(1)-Pt(1)-C(7) 90.6(2), Br(1)-Pt(1)-C(13) 90.03(18), Br(1)-Pt(1)-C(19) 90.3(2), N(1)-Pt(1)-C(1) 89.9(3), N(1)-Pt(1)-C(7) 88.6(3), N(1)-Pt(1)-C(13) 89.4(3), N(1)-Pt(1)-C(19) 90.5(3), C(1)-Pt(1)-C(7) 90.4(3), C(1)-Pt(1)-C(13) 178.7(5), C(1)-Pt(1)-C(19) 89.0(3), C(7)-Pt(1)-C(13) 90.7(4), C(7)-Pt(1)-C(19) 179.0(3), C(13)-Pt(1)-C(19) 89.9(4).

## Conclusions

The reactivity of the *SP*-4 $d^8$ complexes $[NBu_4]_2[Pt(CF_3)_4]$ (**1**) and $[NBu_4]_2[Pt(C_6F_5)_4]$ (**3**) against halogens is presented and compared. The fine structural and electronic features of the $[Pt(CF_3)_4]^{2-}$ and $[Pt(C_6F_5)_4]^{2-}$ ions are the crucial regulators of their chemical reactivity. The homoleptic perfluoromethyl species **1** straightforwardly adds $Cl_2$, $Br_2$, or $I_2$ in a stereoselective way, giving rise to the thermally stable organoplatinum(IV) derivatives $[NBu_4]_2[trans\text{-}Pt(CF_3)_4X_2]$ [X = Cl (**7**), Br (**10**), I (**13**)]. All these oxidative additions are calculated to be exothermic processes.

By treating the analogous perfluorophenyl compound $[NBu_4]_2[Pt(C_6F_5)_4]$ (**3**) with $Br_2$ under suitable conditions, it has been possible to detect the intermediacy of the solvento-species $[trans\text{-}Pt(C_6F_5)_4Br(solv)]^-$ (**16**), in which the solvent molecule (solv) is the poorly coordinating chlorocarbon $CHCl_3$. This intermediate species is thermally unstable and prone to undergo reductive elimination of $C_6F_5–C_6F_5$ unless the solvent molecules are successfully replaced by more suitable ligands. This is the case of the $Br^-$ ion, which yields the corresponding oxidative addition compound $[NBu_4]_2[trans\text{-}Pt(C_6F_5)_4Br_2]$ (**15**) in a stereoselective way. In a similar way, the use of PhCN as the incoming ligand allows the isolation of the organoplatinum(IV) compound $[NBu_4][trans\text{-}Pt(C_6F_5)_4Br(NCPh)]$ (**17**), which was characterized by X-ray diffraction techniques.

Although detected only in one instance ($R^F = C_6F_5$, X = Br, solv = $CHCl_3$), we suggest that all the oxidative-addition reactions presented in this work proceed through the intermediacy of unstable solvento-complexes of type $[trans\text{-}Pt(R^F)_4X(solv)]^-$. Wherever the stability of these solvento complexes does not enable effective replacement of the weakly coordinated solvent molecules, extensive decomposition occurs.

  

From this comparative study, it emerges that the $CF_3$ ligand is especially suited to stabilizing organometallic derivatives in high oxidation states. This can be attributed to its high group electronegativity together with its reluctance to undergo reductive–elimination processes. Following the results obtained, it would appear that the $CF_3$ groups should also be appropriate for creating highly acidic neutral "Pt-$(CF_3)_2$" or cationic "Pt$(CF_3)^+$" metal fragments.

## Experimental Section

**General procedures and materials**: Unless otherwise stated, the reactions and manipulations were carried out under purified argon using Schlenk techniques. Solvents were dried using an MBraun SPS-800 System. Compound $[NBu_4]_2[Pt(C_6F_5)_4]$ (**3**)[33] was obtained as described elsewhere and the halo-complex $[NBu_4]_2[(PtBr_2)_2(\mu\text{-}Br)_2]$ was prepared in a similar way to that reported for $[NEt_4]_2[(PtBr_2)_2(\mu\text{-}Br)_2]$.[34] Solutions of $Cl_2$ or $Br_2$ in $CCl_4$ were prepared by passing a slow stream of dry $Cl_2(g)$ through cold $CCl_4$ or by diluting a measured volume of $Br_2$ in $CCl_4$; the solutions were titrated before use. CsF (Acros) and $CF_3SiMe_3$ (Apollo Scientific Ltd.) were purchased and used as received. Elemental analyses were carried out with a Perkin–Elmer 2400-Series II microanalyzer. IR spectra of KBr discs were recorded on the following Perkin–Elmer spectrophotometers: 883 (4000–200 $cm^{-1}$) or Spectrum One (4000–350 $cm^{-1}$). NMR spectra were recorded on any of the following spectrometers: Varian Unity-300, Bruker ARX 300, or Bruker ARX 400. Unless otherwise stated, the spectroscopic measurements were carried out at room temperature.

**Synthesis of $[NBu_4]_2[Pt(CF_3)_4]$ (1)**: $CF_3SiMe_3$ (2.10 $cm^3$, 13.8 mmol) was added to a suspension of CsF (2.00 g, 13.2 mmol) in THF (20 $cm^3$) at −78 °C and the mixture was stirred for 1 h. After the subsequent addition of $[NBu_4]_2[(PtBr_2)_2(\mu\text{-}Br)_2]$ (2.02 g, 1.50 mmol) and $[NBu_4]Br$ (0.96 g, 2.99 mmol), the reaction medium was allowed to reach room temperature overnight while stirring. The resulting light brown suspension was filtered and the white solid was extracted with acetone ($3\times10$ $cm^3$). The extract was concentrated to dryness affording a residue, which by treatment with *i*PrOH ($2\times3$ $cm^3$) gave a light yellow solid identified as **1** (1.94 g, 2.03 mmol, 68% yield). Elemental analysis calcd (%) for $C_{36}H_{72}F_{12}N_2Pt$: C 45.2, H 7.5, N 2.9; found: C 45.2, H 7.2, N 2.9; IR (KBr): $\tilde{\nu}=2964$ (s), 2877 (s), 1482 (s), 1382 (s), 1069 (vs), 983 (vs), 963 (vs), 798 (w), 748 $cm^{-1}$ (w; $[NBu_4]^+$). Single crystals suitable for X-ray diffraction purposes were obtained by slow diffusion of an *n*-hexane (10 $cm^3$) layer into a solution of **1** (10 mg) in $Me_2CO$ (3 $cm^3$) at 4 °C.

**Synthesis of $[NBu_4]_2[trans\text{-}Pt(CF_3)_4Cl_2]$ (7)**: $Cl_2$ dissolved in $CCl_4$ (1.24 $cm^3$, 0.42 mmol) was added to a solution of **1** (0.20 g, 0.21 mmol) in $CH_2Cl_2$ (15 $cm^3$) at −78 °C. The resulting mixture was stirred, while allowing it to slowly reach room temperature. The solution was concentrated to dryness. Treatment of the resulting residue with *i*PrOH (3 $cm^3$) at 0 °C rendered a light yellow solid, which was identified as **7** (0.16 g, 0.15 mmol, 71% yield). Elemental analysis calcd (%) for $C_{36}H_{72}Cl_2F_{12}N_2Pt$: C 42.1, H 7.0, N 2.7; found: C 42.5, H 6.9, N 2.75; IR (KBr): $\tilde{\nu}=2964$ (s), 2877 (s), 1484 (s), 1473 (s), 1382 (m), 1095 (vs), 1055 (vs), 1031 (vs), 882 (m; $[NBu_4]^+$), 801 (w), 741 (w; $[NBu_4]^+$), 367 (m; $\nu$(Pt−Cl)), 316 (w), 289 $cm^{-1}$ (w). Single crystals suitable for X-ray diffraction purposes were obtained by slow diffusion of an *n*-hexane (10 $cm^3$) layer into a solution of **7** (12 mg) in $CH_2Cl_2$ (3 $cm^3$) at 4 °C.

**Synthesis of $[NBu_4]_2[trans\text{-}Pt(CF_3)_4Br_2]$ (10)**: By using the procedure described above for the synthesis of **7**, **10** was prepared starting from **1** (0.21 g, 0.22 mmol) and a solution of $Br_2$ in $CCl_4$ (1.32 $cm^3$, 0.33 mmol). Complex **10** was obtained as a yellow solid (0.19 g, 0.17 mmol, 77% yield). Elemental analysis calcd (%) for $C_{36}H_{72}Br_2F_{12}N_2Pt$: C 38.75, H 6.5, N 2.5; found: C 38.9, H 6.2, N 2.5; IR (KBr): $\tilde{\nu}=2962$ (s), 2876 (s), 1483 (s), 1474 (s), 1382 (m), 1092 (vs), 1054 (vs), 1027 (vs), 882 (m; $[NBu_4]^+$), 801 (w), 741 (w; $[NBu_4]^+$), 483 (w), 356 (w; $\nu$(Pt−Br)), 316 $cm^{-1}$ (w).

**Synthesis of $[NBu_4]_2[trans\text{-}Pt(CF_3)_4I_2]$ (13)**: By using the procedure described above for the synthesis of **7**, **13** was prepared starting from **1** (0.22 g, 0.23 mmol) and solid $I_2$ (0.06 g, 0.23 mmol). Complex **13** was obtained as a light orange solid (0.22 g, 0.18 mmol, 79% yield). Elemental analysis calcd (%) for $C_{36}H_{72}F_{12}I_2N_2Pt$: C 35.7, H 5.95, N 2.3; found: C 35.9, H 6.2, N 2.3; IR (KBr): $\tilde{\nu}=2962$ (s), 2875 (s), 1484 (s), 1474 (s), 1381 (m), 1085 (vs), 1049 (vs), 1024 (vs), 882 (m; $[NBu_4]^+$), 801 (w), 740 (w; $[NBu_4]^+$), 317 $cm^{-1}$ (w).

**Synthesis of $[NBu_4]_2[trans\text{-}Pt(C_6F_5)_4Cl_2]$ (14)**: $Cl_2$ dissolved in $CCl_4$ (0.45 mmol) was added to a solution of **3** (0.60 g, 0.45 mmol) and $[NBu_4]Cl\cdot H_2O$ (0.13 g, 0.45 mmol) in $CH_2Cl_2$ (15 $cm^3$) at −78 °C. The temperature of the solution was allowed to rise slowly. By −30 °C, the solution was concentrated to dryness. The residue obtained was treated with cold *i*PrOH ($3\times2$ $cm^3$) and *n*-hexane ($3\times2$ $cm^3$). Recrystallization of the solid in $CH_2Cl_2$/*n*-hexane at −30 °C gave analytically pure **14** as yellow crystals (0.10 g, 0.07 mmol, 15% yield). Elemental analysis calcd (%) for $C_{56}H_{72}Cl_2F_{20}N_2Pt$: C 47.4, H 5.1, N 2.0; found: C 47.7, H 4.9, N 1.8; IR (Nujol): $\tilde{\nu}=1502$ (vs; $C_6F_5$: $\nu$(C−C)), 959 (vs; $\nu$(C−F)), 758 (s; $C_6F_5$: X-sensitive),[32] 347 $cm^{-1}$ (m; $\nu$(Pt−Cl)). $^{195}$Pt NMR ([D$_6$]acetone): $\delta=-1731$ ppm.

**Synthesis of $[NBu_4]_2[trans\text{-}Pt(C_6F_5)_4Br_2]$ (15)**: $Br_2$ dissolved in $CCl_4$ (0.74 mmol) was added to a solution of **3** (1 g, 0.74 mmol) and $[NBu_4]Br$ (0.47 g, 1.48 mmol) in $CH_2Cl_2$ (10 $cm^3$) at −60 °C. The temperature of the solution was allowed to rise slowly. By −30 °C the solution was concentrated and cold *i*PrOH was added (10 $cm^3$). The mixture was concentrated again and a new portion of cold *i*PrOH was added (10 $cm^3$). A yellow solid formed, which was filtered and washed with cold *i*PrOH ($3\times2$ $cm^3$) and *n*-hexane ($3\times2$ $cm^3$) (**15**: 0.45 g, 0.30 mmol, 40% yield). Elemental analysis calcd (%) for $C_{56}H_{72}Br_2F_{20}N_2Pt$: C 44.6, H 4.8, N 1.9; found: C 44.6, H 4.8, N 2.0; IR (Nujol): $\tilde{\nu}=1502$ (vs; $C_6F_5$: $\nu$(C−C)), 959 (vs; $\nu$(C−F)), 758 $cm^{-1}$ (s; $C_6F_5$: X-sensitive);[32] $^{195}$Pt NMR ([D$_6$]acetone): $\delta=-2448$ ppm.

**Spectroscopic detection of $[NBu_4][trans\text{-}Pt(C_6F_5)_4Br(ClCHCl_2)]$ (16)**: $Br_2$ dissolved in $CCl_4$ (0.03 mmol) was added to a solution of **3** (40 mg, 0.03 mmol) in $CHCl_3/CDCl_3$ (3:1, 2 $cm^3$) at −55 °C. After 15 mins of stirring the solution was transferred to a pre-cooled NMR tube. The $^{19}$F NMR spectrum registered at −55 °C (Figure 4) showed the presence of **16** as the only perfluorophenyl platinum species.

**Synthesis of $[NBu_4][trans\text{-}Pt(C_6F_5)_4Br(NCPh)]$ (17)**: $Br_2$ dissolved in $CCl_4$ (0.74 $cm^3$, 0.18 mmol) was added to a solution of **3** (0.25 g, 0.18 mmol) in $CHCl_3$ (15 $cm^3$) containing PhCN (0.06 $cm^3$, 0.56 mmol) at −50 °C . After 1 h of stirring at that temperature, the solution was allowed to slowly reach 0 °C; then it was concentrated to dryness. The residue obtained was treated with *i*PrOH at 0 °C, rendering a light yellow solid, which was filtered, washed with *i*PrOH ($2\times2$ $cm^3$) and *n*-hexane (3 $cm^3$) at 0 °C, and vacuum dried (**17**: 0.21 g, 0.16 mmol, 88% yield). Elemental analysis calcd (%) for $C_{47}H_{41}BrF_{20}N_2Pt$: 43.8 C, 3.2 H, 2.2 N; found: 43.65 C, 3.3 H, 2.0 N; IR (KBr): $\tilde{\nu}=2968$ (s), 2880 (m), 2315 (m; $\nu$(C≡N)), 1634 (m), 1597 (w), 1506 (vs), 1453 (vs), 1439 (vs), 1374 (m), 1349 (s), 1257 (m), 1180 (w), 1113 (w), 1067 (vs), 1005 (w), 961 (vs; $\nu$(C−F)), 878 (w; $[NBu_4]^+$), 765 (s; $C_6F_5$: X-sensitive),[32] 684 (m), 547 (m), 396 $cm^{-1}$ (w; $\nu$(Pt−Br)); $^{195}$Pt NMR ($CDCl_3$): $\delta=-2275$ ppm. Single crystals suitable for X-ray diffraction purposes with formula $[NBu_4][trans\text{-}Pt(C_6F_5)_4Br(NCPh)]\cdot0.45\,n\text{-}C_6H_{14}$ were obtained by slow diffusion of an *n*-hexane (15 $cm^3$) layer into a solution of **17** (15 mg) in $CH_2Cl_2$ (5 $cm^3$) at −35 °C.

**X-ray structure determinations**: Crystal data and other details of the structure analyses are presented in Table 5. Single crystals were mounted on quartz fibers in random orientation and held in place with fluorinated oil. For **1** and **17**$\cdot0.45\,n\text{-}C_6H_{14}$, data collections were performed at 100 K on a Bruker Smart CCD diffractometer, and the diffraction frames were integrated using the SAINT package[35] and corrected for absorption with SADABS.[36] For **7**, data collection was performed at 100 K on an Oxford Diffraction Xcalibur diffractometer, and the diffraction frames were integrated and corrected for absorption using the CrysAlis RED program.[37]

For **1**, the structure was solved and refined to completion in the polar space group *Pna*2$_1$, to which the systematic absences in the data corresponded without exception. The centric group with the same systematic

  

Table 5. Crystal data and structure refinement for complexes **1**, **7** and **17**·0.45*n*-$C_6H_{14}$.

| | **1** | **7** | **17**·0.45*n*-$C_6H_{14}$ |
|---|---|---|---|
| formula | $C_{36}H_{72}F_{12}N_2Pt$ | $C_{36}H_{72}Cl_2F_{12}N_2Pt$ | $C_{47}H_{41}BrN_2F_{20}Pt$·0.45*n*-$C_6H_{14}$ |
| $M_t$ [g mol$^{-1}$] | 956.05 | 1026.95 | 1327.60 |
| $T$ [K] | 100(1) | 100(1) | 100(1) |
| $\lambda$ [Å] | 0.71073 | 0.71073 | 0.71073 |
| crystal system | orthorhombic | monoclinic | monoclinic |
| space group | $Pna2_1$ | $I2/a$ | $P2_1$ |
| $a$ [Å] | 14.0831(18) | 45.6145(11) | 12.786(2) |
| $b$ [Å] | 20.268(3) | 15.4696(4) | 26.481(4) |
| $c$ [Å] | 14.5351(18) | 19.4916(4) | 15.749(2) |
| $\beta$ [°] | 90 | 90.164(2) | 101.393(3) |
| $V$ [Å$^3$] | 4148.8(10) | 13753.9(4) | 5227.3(14) |
| $Z$ | 4 | 12 | 4 |
| $\rho$ [g cm$^{-3}$] | 1.531 | 1.488 | 1.687 |
| $\mu$ [mm$^{-1}$] | 3.463 | 3.252 | 3.556 |
| $F$(000) | 1952 | 6264 | 2610 |
| 2$\theta$ range [°] | 3.4–50.0 | 7.5–55.0 | 2.6–50.0 |
| final $R$ indices [$I>2\sigma(I)$][a] | | | |
| $R_1$ | 0.0191 | 0.0397 | 0.0313 |
| $wR_2$ | 0.0403 | 0.1053 | 0.0835 |
| $R$ indices (all data) | | | |
| $R_1$ | 0.0251 | 0.0579 | 0.0329 |
| $wR_2$ | 0.0429 | 0.1100 | 0.0845 |
| GOF on $F^2$[b] | 1.071 | 0.992 | 1.071 |
| Abs. str. par. | 0.509(7) | – | 0.481(6) |

[a] $R_1=\Sigma(|F_o|-|F_c|)/\Sigma|F_o|$; $wR_2=[\Sigma w(F_o^2-F_c^2)^2/\Sigma w(F_o^2)^2]^{1/2}$. [b] GOF$=[\Sigma w(F_o^2-F_c^2)^2/(n_{obs}-n_{param})]^{1/2}$.

absences was ruled out by visual inspection of the packing, which is polar for the $[NBu_4]^+$ ion containing N(2), and by use of the missed-symmetry algorithm in PLATON.[38] Nevertheless, as indicated by PLATON, a substantial fraction of the atoms in the asymmetric unit, combined with the symmetry operations of $Pna2_1$, form a pattern with *Pnab* symmetry, for which the diffraction data presented 319 exceptions to the extinction condition for the *b* glide perpendicular to the *c* axis. The entire set of 607 reflections (*hk*0) with *k* odd had an average $I/\sigma(I)$ of 5.9. All of this evidence indicates that the correct space group is $Pna2_1$, and that the structure presents pseudo-*Pnab* symmetry. We nevertheless conducted a complete refinement in space group *Pbcn* (the standard setting of *Pnab*), for which the Pt atom lies on a twofold axis and the $[NBu_4]^+$ ion suffers whole-body disorder; that is, two complete congeners, each with one-half occupancy. This refinement produced residuals of $R_1=0.0627$, $wR_2=0.1578$, and quality-of-fit = 1.508, with seven non-positive definite atoms and a number of unreasonable bond lengths, although strong similarity restraints had been imposed on the congeners of the cation in order to obviate instability in the refinement. A difference Fourier map following this refinement had maximum and minimum densities of 7.19 and −7.31 e A$^{-3}$. The results of the refinement using space group *Pbcn* are available from the authors upon request. Here we report the results of the stable refinement using space group $Pna2_1$, for which the Flack parameter[39] refined to a value of almost exactly one-half, indicating polar-axis twinning (note that the twinning operation, if it were present as a symmetry operation rather than a twin law, would produce space group *Pnam* and not *Pnab*). No restraints were imposed for the refinement using space group $Pna2_1$, other than that used to set the origin of the polar axis. Constraints were applied to the hydrogen atoms; those of the methylene groups were placed at calculated positions and refined as riders with $U_{iso}$ set to 1.2 times the equivalent isotropic $U$ of their respective parent atoms. Those of the methyl groups were located in local slant Fourier calculations and refined as riding atoms with variable torsion angles about the local C−C bonds. The methyl hydrogen atoms had $U_{iso}$ constrained to 1.5 times $U_{eq}$ of their parent carbon atoms.

For **7**, the unit cell was chosen so that the *a* and *c* axes would be the shortest axes in the *ac* plane, in line with the recommendations of the Commission on Crystallographic Data of the International Union of Crystallography (IUCr).[40] This gives a space group setting of *I2/a*. The overall stoichiometry is $[NBu_4]_2[Pt(CF_3)_4Cl_2]$, with $Z=12$. The asymmetric unit in space group *I2/a*, $Z'=1.5$, for the formula as given, comprises five independent chemical residues: three $[NBu_4]^+$ ions occupying general positions, and two [*trans*-$Pt(CF_3)_4Cl_2]^{2-}$ ions, of which one lies on a twofold axis. One of the cations suffers minor disorder, and one of the anions, the one in a general position, has no disorder. The three other residues suffer disorder severe enough to merit a detailed description of their refinement (see Supporting Information). Throughout the solution and development of the structure, all non-hydrogen atomic sites were located either by direct methods or in difference Fourier maps. For both the cation and the anion, the disordered sites were restrained loosely to geometrical similarity to the ordered units. In addition, and only for the disordered cations, restraints were applied to the distances and angles (but not the torsion angles) of all of the Bu groups within each cation. Since the disorder is accompanied by close approach of some atomic sites from different disorder groups within a given disorder assembly, restraints were added to the anisotropic displacement parameters where needed. All non-hydrogen atoms were refined with anisotropic displacement parameters. Hydrogen atoms were placed at calculated positions and assigned isotropic displacement parameters equal to 1.2 times the equivalent isotropic displacement parameters of their respective parent atoms. The refinement was convergent, although correlation was present where expected in the parameters of the various disorder assemblies. The data showed some of the characteristics of twinned data sets, and in light of the disorder observed in the structural model we attempted to develop several twin models based on the metrics of the lattice. For example, the monoclinic angle $\beta$ is nearly 90°, which prompted an attempt to test for pseudomerohedral twinning. Other twin models were probed, all resulting in second-component populations that approached zero. The fact that the three major disorder assemblies have distinct, nearly rational occupancy ratios for their disorder groups —two identical and one different from those two— is a strong sign that disorder, rather than twinning, is present. A blind application of the TwinRotMat algorithm in PLATON[41] was also tried—even though the only reason at this point to suspect twinning was that there was such extended disorder—but no plausible twin model was derived.

For **17**·0.45*n*-$C_6H_{14}$, the structure was solved by direct methods and refined using the SHELXL-97 program.[42] All non-hydrogen atoms of the complex were assigned anisotropic displacement parameters. The hydrogen atoms were constrained as indicated for **1**. Two methyl groups of the $[NBu_4]^+$ ion were disordered over two positions and refined with partial occupancy 0.55/0.45 for C(66) and 0.50/0.50 for C(82). A common set of anisotropic thermal parameters was used for each pair of disordered atoms. The C−C distances involving these methyl carbon atoms were constrained to sensible values. No hydrogen atoms for the methylene C atoms bonded to the disordered C atoms were included in the model. Two diffuse *n*-hexane solvent molecules were found and refined with partial occupancies 0.5 and 0.4 and a common set of anisotropic thermal parameters for all the carbon atoms of the same molecule. The interatomic distances in these solvent molecules were constrained to sensible values.

Full-matrix least-squares refinement of these models against $F^2$ converged to the final residual indices given in Table 5. CCDC-717095 (**1**), 717096 (**7**), and 717097 (**17**·0.45*n*-$C_6H_{14}$) contain the supplementary crystallographic data for this paper. These data can be obtained free of charge from the Cambridge Crystallographic Data Centre via www.ccdc.cam.ac.uk/data request/cif.

**Theoretical methods**: All theoretical calculations were carried out using the Gaussian 03 program suite.[43] The geometry optimization of the investigated structures was performed in the gas phase at the B3P86 level[44] of density functional theory, using the LANL2DZ basis set. Full geometry optimization was performed for each structure using Schlegel's analytical gradient method,[45] and the attainment of the energy minimum was verified by calculating the vibrational frequencies that result in the absence of imaginary eigenvalues. The stationary points found on the PES as a result of the geometry optimizations of the homotops were tested to represent energy minima rather than saddle points by using fre-

  

quency analysis. The vibrational modes and the corresponding frequencies are based on a harmonic force field. This was achieved with the SCF convergence on the density matrix of at least $10^{-9}$ and the RMS force less than $10^{-4}$ a.u. All bond lengths and bond angles were optimized to better than 0.001 Å and 0.1°, respectively. The computed electronic energies, the enthalpies of reactions, $\Delta_R H_{298}$, and the free energies, $\Delta G_{298}$, were corrected to constant pressure and 298 K, for zero-point energy (ZPE) differences, and for the contributions of the translational, rotational, and vibrational partition functions. The wavefunctions of all homotops were analyzed by natural bond orbital analyses, involving natural atomic orbital (NAO) populations and natural bond orbitals (NBO).[46] Percentage compositions of molecular orbitals and the orbital interaction diagrams were calculated using the AOMix program.[47]

## Acknowledgements

This work was supported by the Spanish MICINN (DGPTC)/FEDER (Projects CTQ2008-06669-C02-01/BQU and MAT2008-04350/NAN) and the Gobierno de Aragón (Grupo de Excelencia: *Química Inorgánica y de los Compuestos Organometálicos*). We are indebted to Prof. Dr. S. Alvarez (Universitat de Barcelona) for kindly providing values of CShM.

[1] M. A. García-Monforte, P. J. Alonso, J. Forniés, B. Menjón, *Dalton Trans.* **2007**, 3347; F. G. A. Stone, *J. Fluorine Chem.* **1999**, *100*, 227; A. Haas, *J. Fluorine Chem.* **1999**, *100*, 21; J. A. Morrison, *Adv. Organomet. Chem.* **1993**, *35*, 211; R. Nyholm, *Q. Rev. Chem. Soc.* **1970**, *24*, 1; F. G. A. Stone, *Endeavour* **1966**, *25*, 33; R. D. Chambers, T. Chivers, *Organomet. Chem. Rev. Sect. A* **1966**, *1*, 279; P. M. Treichel, F. G. A. Stone, *Adv. Organomet. Chem.* **1964**, *1*, 143.

[2] Selected reviews on the subject: a) M. Lersch, M. Tilset, *Chem. Rev.* **2005**, *105*, 2471; b) U. Fekl, K. I. Goldberg, *Adv. Inorg. Chem.* **2003**, *54*, 259; c) J. A. Labinger, J. E. Bercaw, *Nature* **2002**, *417*, 507; d) S. S. Stahl, J. A. Labinger, J. E. Bercaw, *Angew. Chem.* **1998**, *110*, 2298; *Angew. Chem. Int. Ed.* **1998**, *37*, 2180; e) A. E. Shilov, G. B. Shul′pin, *Chem. Rev.* **1997**, *97*, 2879.

[3] a) L. M. Rendina, R. J. Puddephatt, *Chem. Rev.* **1997**, *97*, 1735; b) J. P. Collman, W. R. Roper, *Adv. Organomet. Chem.* **1969**, *7*, 53.

[4] R. Usón, J. Forniés, F. Martínez, M. Tomás, *J. Chem. Soc. Dalton Trans.* **1980**, 888.

[5] D. Naumann, N. V. Kirij, N. Maggiarosa, W. Tyrra, Y. L. Yagupolskii, M. S. Wickleder, *Z. Anorg. Allg. Chem.* **2004**, *630*, 746.

[6] M. Pinsky, D. Avnir, *Inorg. Chem.* **1998**, *37*, 5575; M. Llunell, D. Casanova, J. Cirera, J. M. Bofill, P. Alemany, S. Alvarez, M. Pinsky, D. Avnir, SHAPE, Version 1.1b 02t, Universitat de Barcelona and The Hebrew University of Jerusalem.

[7] J. Cirera, P. Alemany, S. Alvarez, *Chem. Eur. J.* **2004**, *10*, 190.

[8] R. Wyrwa, H. Görls, *Z. Anorg. Allg. Chem.* **1999**, *625*, 1904.

[9] D. S. Yang, G. M. Bancroft, R. J. Puddephatt, J. S. Tse, *Inorg. Chem.* **1990**, *29*, 2496; M. A. Bennett, H.-K. Chee, J. C. Jeffery, G. B. Robertson, *Inorg. Chem.* **1979**, *18*, 1071; M. A. Bennett, H.-K. Chee, G. B. Robertson, *Inorg. Chem.* **1979**, *18*, 1061; see, however: T. G. Appleton, J. R. Hall, C. H. L. Kennard, M. T. Mathieson, D. W. Neale, G. Smith, T. C. W. Mak, *J. Organomet. Chem.* **1993**, *453*, 299.

[10] D. Bellamy, N. G. Connelly, G. R. Lewis, A. G. Orpen, *CrystEngComm* **2002**, *4*, 68.

[11] R. Usón, J. Forniés, M. Tomás, J. M. Casas, F. A. Cotton, L. R. Falvello, R. Llusar, *Organometallics* **1988**, *7*, 2279.

[12] M. Finze, E. Bernhardt, H. Willner, *Angew. Chem.* **2007**, *119*, 9340; *Angew. Chem. Int. Ed.* **2007**, *46*, 9180; M. Finze, E. Bernhardt, M. Zähres, H. Willner, *Inorg. Chem.* **2004**, *43*, 490.

[13] M. M. Jones, K. A. Morgan, *J. Inorg. Nucl. Chem.* **1972**, *34*, 259; C. E. Skinner, M. M. Jones, *J. Am. Chem. Soc.* **1969**, *91*, 4405.

[14] Donor–acceptor adducts formed by neutralization of a basic *SP*-4 $d^8$ metal complex with a Lewis acid have been the object of careful theoretical calculations. Particular emphasis has been made on the molecular geometry of the resulting adduct as well as on the modified coordination ability of the metal center: G. Aullón, S. Alvarez, *Inorg. Chem.* **1996**, *35*, 3137.

[15] J. Forniés, C. Fortuño, M. A. Gómez, B. Menjón, E. Herdtweck, *Organometallics* **1993**, *12*, 4368.

[16] R. G. Pearson, *J. Chem. Educ.* **1999**, *76*, 267; R. G. Pearson, *Acc. Chem. Res.* **1993**, *26*, 250.

[17] K. J. R. Rosman, P. D. P. Taylor, *Pure Appl. Chem.* **1998**, *70*, 217.

[18] P. S. Pregosin, *Annu. Rep. NMR Spectrosc.* **1986**, *24*, 285; P. S. Pregosin, *Coord. Chem. Rev.* **1982**, *17*, 247.

[19] S. Balters, E. Bernhardt, H. Willner, T. Berends, *Z. Anorg. Allg. Chem.* **2004**, *630*, 257.

[20] R. Usón, J. Forniés, M. Tomás, B. Menjón, R. Bau, K. Sünkel, E. Kuwabara, *Organometallics* **1986**, *5*, 1576.

[21] P. Espinet, A. C. Albéniz, J. A. Casares, J. M. Martínez-Ilarduya, *Coord. Chem. Rev.* **2008**, *252*, 2180.

[22] R. Usón, J. Forniés, M. Tomás, R. Fandos, *J. Organomet. Chem.* **1984**, *263*, 253.

[23] I. J. Lawrenson, *J. Chem. Soc.* **1965**, 1117.

[24] E. S. Chernyshova, R. Goddard, K.-R. Porschke, *Organometallics* **2007**, *26*, 3236; E. Piras, F. Lang, H. Ruegger, D. Stein, M. Worle, H. Grutzmacher, *Chem. Eur. J.* **2006**, *12*, 5849; M. Gonsior, S. Antonijevic, I. Krossing, *Chem. Eur. J.* **2006**, *12*, 1997; J. Zhang, K. A. Barakat, T. R. Cundari, T. B. Gunnoe, P. D. Boyle, J. L. Petersen, C. S. Day, *Inorg. Chem.* **2005**, *44*, 8379; F. A. Cotton, C. A. Murillo, S.-E. Stiriba, X. Wang, R. Yu, *Inorg. Chem.* **2005**, *44*, 8223; A. Bihlmeier, M. Gonsior, I. Raabe, N. Trapp, I. Krossing, *Chem. Eur. J.* **2004**, *10*, 5041; B. K. Corkey, F. L. Taw, R. G. Bergman, M. Brookhart, *Polyhedron* **2004**, *23*, 2943; J. R. Krumper, M. Gerisch, J. M. Suh, R. G. Bergman, T. D. Tilley, *J. Org. Chem.* **2003**, *68*, 9705; F. L. Taw, H. Mellows, P. S. White, F. J. Hollander, R. G. Bergman, M. Brookhart, D. M. Heinekey, *J. Am. Chem. Soc.* **2002**, *124*, 5100; I. Krossing, *Chem. Eur. J.* **2001**, *7*, 490; D. Huang, J. C. Bollinger, W. E. Streib, K. Folting, V. Young, Jr., O. Eisenstein, K. G. Caulton, *Organometallics* **2000**, *19*, 2281; X. Fang, J. Huhmann-Vincent, B. L. Scott, G. J. Kubas, *J. Organomet. Chem.* **2000**, *609*, 95; J. Huhmann-Vincent, B. L. Scott, G. J. Kubas, *Inorg. Chem.* **1999**, *38*, 115; J. Huhmann-Vincent, B. L. Scott, G. J. Kubas, *J. Am. Chem. Soc.* **1998**, *120*, 6808; D. Huang, J. C. Huffman, J. C. Bollinger, O. Eisenstein, K. G. Caulton, *J. Am. Chem. Soc.* **1997**, *119*, 7398; M. D. Butts, B. L. Scott, G. J. Kubas, *J. Am. Chem. Soc.* **1996**, *118*, 11831; J. Forniés, F. Martínez, R. Navarro, E. P. Urriolabeitia, *Organometallics* **1996**, *15*, 1813; B. A. Arndtsen, R. G. Bergman, *Science* **1995**, *270*, 1970; D. M. van Seggen, P. K. Hurlburt, O. P. Anderson, S. H. Strauss, *Inorg. Chem.* **1995**, *34*, 3453; D. M. van Seggen, P. K. Hurlburt, O. P. Anderson, S. H. Strauss, *J. Am. Chem. Soc.* **1992**, *114*, 10995; M. Bown, J. M. Waters, *J. Am. Chem. Soc.* **1990**, *112*, 2442; M. R. Colsman, T. D. Newbound, L. J. Marshall, M. D. Noirot, M. M. Miller, G. P. Wulfsberg, J. S. Frye, O. P. Anderson, S. H. Strauss, *J. Am. Chem. Soc.* **1990**, *112*, 2349; T. D. Newbound, M. R. Colsman, M. M. Miller, G. P. Wulfsberg, O. P. Anderson, S. H. Strauss, *J. Am. Chem. Soc.* **1989**, *111*, 3762; M. R. Colsman, M. D. Noirot, M. M. Miller, O. P. Anderson, S. H. Strauss, *J. Am. Chem. Soc.* **1988**, *110*, 6886.

[25] J. Huhmann-Vincent, B. L. Scott, G. J. Kubas, *Inorg. Chim. Acta* **1999**, *294*, 240; J. M. Fernández, J. A. Gladysz, *Organometallics* **1989**, *8*, 207.

[26] J. Forniés, M. A. Gómez-Saso, A. Martín, F. Martínez, B. Menjón, J. Navarrete, *Organometallics* **1997**, *16*, 6024.

[27] I. Ara, J. Forniés, M. A. García-Monforte, B. Menjón, R. M. Sanz-Carrillo, M. Tomás, A. C. Tsipis, C. A. Tsipis, *Chem. Eur. J.* **2003**, *9*, 4094.

[28] a) J. E. Huheey, E. A. Keiter, R. L. Keiter, *Inorganic Chemistry*, 4th ed., Harper Collins, New York, **1993**, pp. 290–296; b) P. Pyykkö, M. Atsumi, *Chem. Eur. J.* **2009**, *15*, 186.

[29] A slightly higher value (1.20 Å) has been proposed to be taken as the covalent radius of bromine in: B. Cordero, V. Gómez, A. E. Platero-Prats, M. Revés, J. Echeverría, E. Cremades, F. Barragán, S. Alvarez, *Dalton Trans.* **2008**, 2832.

[30] R. J. Puddephatt, *Angew. Chem.* **2002**, *114*, 271; *Angew. Chem. Int. Ed.* **2002**, *41*, 261; K. L. Bartlett, K. I. Goldberg, W. T. Borden, *J.*

  

*Am. Chem. Soc.* **2000**, *122*, 1456; M. P. Brown, R. J. Puddephatt, C. E. E. Upton, *J. Chem. Soc. Dalton Trans.* **1974**, 2457.
[31] S.-B. Zhao, G. Wu, S. Wang, *Organometallics* **2008**, *27*, 1030; A. T. Luedtke, K. I. Goldberg, *Inorg. Chem.* **2007**, *46*, 8496; S. M. Kloek, K. I. Goldberg, *J. Am. Chem. Soc.* **2007**, *129*, 3460; S. Reinartz, P. S. White, M. Brookhart, J. L. Templeton, *J. Am. Chem. Soc.* **2001**, *123*, 6425; U. Fekl, W. Kaminsky, K. I. Goldberg, *J. Am. Chem. Soc.* **2001**, *123*, 6423.
[32] R. Usón, J. Forniés, *Adv. Organomet. Chem.* **1988**, *28*, 219; E. Maslowsky, Jr., *Vibrational Spectra of Organometallic Compounds*, Wiley, New York, **1977**, pp. 437–442.
[33] R. Usón, J. Forniés, *Organometallics* **1986**, *3*, 161; see also Ref. [4].
[34] C. M. Harris, S. E. Livingstone, N. C. Stephenson, *J. Chem. Soc.* **1958**, 3697.
[35] SAINT, Version 6.02, Bruker Analytical X-ray Systems, Madison WI, **1999**.
[36] G. M. Sheldrick, SADABS empirical absorption program, Version 2.03, University of Göttingen, Göttingen, **1996**.
[37] CrysAlis RED, CCD camera reduction program, Oxford Diffraction, Oxford, **2004**.
[38] A. L. Spek, *Acta Crystallogr. Sect. A* **1990**, *46*, c34.
[39] H. D. Flack, *Acta Crystallogr. Sect. A* **1983**, *39*, 876.
[40] O. Kennard, J. C. Speakman, J. D. H. Donnay, *Acta Crystallogr.* **1967**, *22*, 445.
[41] A. L. Spek, *J. Appl. Crystallogr.* **2003**, *36*, 7.
[42] G. M. Sheldrick, SHELXL-97, Program for the refinement of crystal structures from diffraction data, University of Göttingen, Göttingen, **1997**.
[43] Gaussian 03, Revision B.02, M. J. Frisch, H. B. Schlegel, G. E. Scuseria, M. A. Robb, J. R. Cheeseman, V. G. Zakrzewski, J. A. Montgomery, Jr., T. Vreven, K. N. Kudin, J. C. Burant, J. M. Millan, S. S. Iyengar, J. Tomasi, V. Barone, B. Mennucci, M. Cossi, G. Scalmani, N. Rega, G. A. Petersson, H. Nakatsuji, M. Hada, M. Ehara, K. Toyota, R. Fukuda. J. Hasegawa, M. Ishida, T. Nakajima, Y. Honda, O. Kitao, H. Nakai, M. Klene, X. Li, J. E. Knox, M. P. Hratchian, J. B. Cross, C. Adamo, J. Jaramillo, R. Gomperts, R. E. Stratmann, O. Yazyev, A. J. Austin, R. Cammi, C. Pomelli, J. W. Ochterski, P. Y. Ayala, K. Morokuma, G. A. Voth, P. Salvador, J. J. Dannenberg, V. G. Zakrzewski, S. Dapprich, A. D. Daniels, M. C. Strain, O. Farkas, D. K. Malick, A. D. Rabuck, K. Raghavachari, J. B. Foresman, J. V. Ortiz, Q. Cui, A. G. Baboul, S. Clifford, J. Cioslowski, B. B. Stefanov, G. Liu, A. Liashenko, P. Piskorz, I. Komaromi, R. L. Martin, D. J. Fox, T. Keith, M. A. Al-Laham, C. Y. Peng, A. Nanayakkara, M. Challacombe, P. M. W. Gill, B. Johnson, W. Chen, M. W. Wong, C. Gonzalez, J. A. Pople, Gaussian, Inc., Pittsburgh PA, **2003**.
[44] A. D. Becke, *J. Chem. Phys.* **1993**, *98*, 5648; J. P. Perdew, *Phys. Rev. B* **1986**, *33*, 8822.
[45] H. B. Schlegel, *J. Comput. Chem.* **1982**, *3*, 214.
[46] E. D. Glendening, J. K. Badenhoop, A. E. Reed, J. E. Carpenter, J. A. Bohmann, C. M. Morales, F. Weinhold, NBO 5.0, Theoretical Chemistry Institute, University of Wisconsin, Madison, **2001**; A. E. Reed, L. A. Curtiss, F. Weinhold, *Chem. Rev.* **1988**, *88*, 899.
[47] S. I. Gorelsky, AOMix: Program for Molecular Orbital Analysis, http://www.sg-chem.net, University of Ottawa, Ottawa, Canada **2007**; S. I. Gorelsky, A. B. P. Lever, *J. Organomet. Chem.* **2001**, *635*, 187.

Received: February 5, 2009
Published online: May 15, 2009

  

Carbenes

DOI: 10.1002/anie.200907031

# Trapping a Difluorocarbene–Platinum Fragment by Base Coordination**

*Sonia Martínez-Salvador, Babil Menjón, Juan Forniés,* Antonio Martín, and Isabel Usón*

*Dedicated to Prof. Dr. H. W. Roesky on the occasion of his 75th birthday*

The trifluoromethyl group ($CF_3$) when bound to an element E of medium to high electronegativity behaves as a monovalent substituent with a high thermal stability and a marked chemical inertness. This low-reactivity profile together with its unique combination of electronic and steric properties have definitely encouraged the increasing use of $CF_3$ as a robust terminal group in modern organic chemistry.[1] When bound to an electropositive atom, however, $CF_3$ becomes more reactive: α-fluoride elimination and the formation of a difluorocarbene unit (Scheme 1) is a general reaction pathway for such [E]–$CF_3$ species. This kind of reaction may occur spontaneously or require the action of an acid. The failure of preparations of $LiCF_3$ ($\chi_{Li} = 0.97$)[2] has been attributed to the ready decomposition into LiF and $:CF_2$ even at very low temperatures.[3] At the other extreme is the case of the highly stable tetrahedral anion $[B(CF_3)_4]^-$, which required treatment with concentrated $H_2SO_4$ (Scheme 2 A)[4] to be brought into reaction ($\chi_B = 2.01$).[2] The process presumably goes through the unstable difluorocarbene intermediate $B(CF_3)_3(CF_2)$, which undergoes subsequent hydrolysis to give eventually the unusual carbonyl derivative $B(CF_3)_3(CO)$.

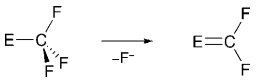


***Scheme 1.*** α-Fluoride elimination process operating in trifluoromethyl derivatives of electropositive elements E.

Transition metals (TMs) belong to the class of moderately electropositive elements ($\chi_{TM} = 1.22$–$1.75$)[2] and are therefore intermediate cases. This feature, together with the richness in reactivity made possible by the availability of d orbitals, makes them attractive as potential agents leading to C–F bond activation,[5] which is the reason why the chemistry of trifluoromethyl–transition-metal derivatives is receiving much current attention.[6,7]

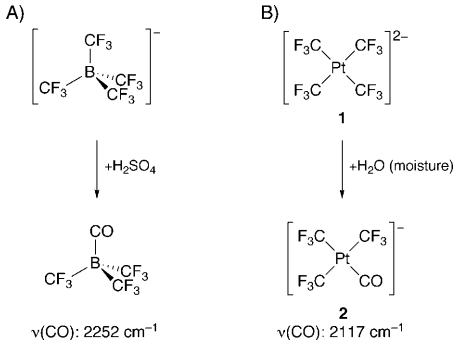


***Scheme 2.*** Hydrolytic processes undergone by homoleptic tetrakis(trifluoromethyl) derivatives of A) main-group element boron (with $K^+$ as counterion) or B) transition-metal element platinum (with $[NBu_4]^+$ as counterion).

We have now observed that $[NBu_4]_2[Pt(CF_3)_4]$ (**1**)[8] undergoes a hydrolytic process to give the monocarbonyl derivative $[NBu_4][Pt(CF_3)_3(CO)]$ (**2**) in high yield (Scheme 2 B; for experimental details, see the Supporting Information). The reaction takes place under mild conditions and is effected simply by moisture. The ease with which one of the Pt-bound $CF_3$ groups in **1** is transformed into CO contrasts with other known precedents that require treatment of the appropriate trifluoromethylplatinum complex with acids as strong as $HBF_4/Et_2O$ or $HClO_4/H_2O$.[9] In this context, it is also interesting to note that, although a number of compounds containing the [TM]=$CF_2$ unit are known for Group 8 and 9 metals,[10] none have been isolated for Pt, probably because of the high electrophilic character of the [Pt]=$CF_2$ moiety. The transformation of one of the anionic $CF_3$ groups within the square-planar (*SP*-4), homoleptic unit $[Pt(CF_3)_4]^{2-}$ into the neutral, poorly σ-donating CO ligand deactivates the resulting $[Pt(CF_3)_3(CO)]^-$ ion towards further hydrolysis. Compound **2** is, in fact, a fairly stable white solid, which can be handled in the air without alteration.

The structure of the (*SP*-4)-$[Pt(CF_3)_3(CO)]^-$ ion (Figure 1) was established by X-ray diffraction methods[11] on single crystals of the salt $[PPh_4][Pt(CF_3)_3(CO)]$ (**2′**), which was obtained by following a simple metathetical process. The Pt–C($CF_3$) bond lengths in **2′** are insensitive to the *trans*-standing ligand (CO vs. $CF_3$)[12] and do not appreciably differ

[*] Dipl.-Chem. S. Martínez-Salvador, Dr. B. Menjón, Prof. Dr. J. Forniés, Dr. A. Martín
Instituto de Ciencia de Materiales de Aragón (I.C.M.A.)
Universidad de Zaragoza—C.S.I.C.
C/Pedro Cerbuna 12, 50009 Zaragoza (Spain)
Fax: (+34) 976-761-187
E-mail: juan.fornies@unizar.es
Dr. I. Usón
Institut de Biologia Molecular de Barcelona—C.S.I.C.
C/Jordi Girona 18–26, 08034 Barcelona (Spain)

[**] This work was supported by the Spanish MICINN (DGPTC)/FEDER (Project CTQ2008-06669-C02-01/BQU) and the Gobierno de Aragón (Grupo de Excelencia: *Química Inorgánica y de los Compuestos Organometálicos*).

Supporting information for this article is available on the WWW under http://dx.doi.org/10.1002/anie.200907031.

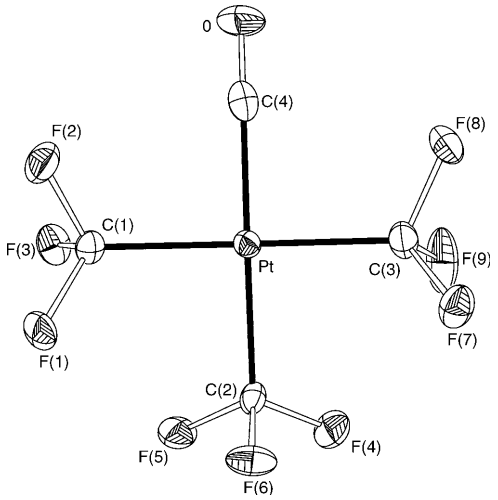


***Figure 1.*** Thermal ellipsoid diagram (50% probability) of the $[Pt(CF_3)_3(CO)]^-$ ion in **2′**. Selected bond lengths [pm] and angles [°] with estimated standard deviations: Pt–C(1) 207.5(4), Pt–C(2) 206.3(3), Pt–C(3) 206.5(3), Pt–C(4) 191.3(4), C(4)–O 113.4(4), average C–F 136.8(4), C(1)-Pt-C(2) 91.1(1), C(1)-Pt-C(3) 175.9(1), C(1)-Pt-C(4) 89.7(1), C(2)-Pt-C(3) 89.5(1), C(2)-Pt-C(4) 171.9(1), C(3)-Pt-C(4) 90.3(1), Pt-C(4)-O 172.3(3), average Pt-C-F 115.1(2), average F-C-F' 103.3(3).

from those observed in the precursor species **1** (average Pt–$C(CF_3)$ bond length 205.0(4) pm).[8] The ν(CO) frequency in **2′** is the highest within the $[PtR_3(CO)]^-$ series: 2117 ($R = CF_3$) > 2084 ($R = C_6F_5$) > 2073 $cm^{-1}$ ($R = C_6Cl_5$),[13] thus denoting the lower electron density on the metal center where $R = CF_3$. This lack of electron density on the metal appears to be the main reason for the enhanced stability against hydrolysis of **2** (or **2′**) with respect to its parent species **1**.

Compound **2** reacts with a number of neutral (L) or anionic ($X^-$) ligands in the presence of trimethylamine *N*-oxide ($ONMe_3$), undergoing efficient replacement of CO by the incoming ligand L or $X^-$ (Scheme 3). Following this procedure, a series of mono- or dianionic complexes of formula $[NBu_4][Pt(CF_3)_3(L)]$ ($L = CNCMe_3$ (**3a**), $PPh_3$ (**3b**),[14] $P(2\text{-}MeC_6H_4)_3$ (**3c**)) and $[NBu_4]_2[Pt(CF_3)_3X]$ ($X = Cl$ (**4a**), Br (**4b**), I (**4c**)) can be easily obtained. Treatment of **2** with pyridin-2-thiol ($C_5H_5NS$) in the presence of $ONMe_3$ unexpectedly gave the *gem*-difluorinated metallacyclic compound $[NBu_4][Pt(CF_3)_2(CF_2NC_5H_4S\text{-}\kappa C,\kappa S)]$ (**5**) in good yield (Scheme 4; upper path). The reaction involves not only replacement of the CO ligand at **2** as observed in the

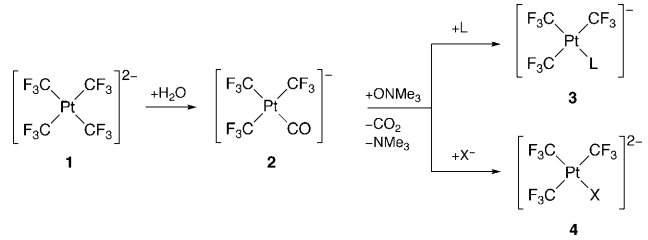


***Scheme 3.*** Synthesis of the mono- or dianionic tris(trifluoromethyl)platinate(II) derivatives: $[NBu_4][Pt(CF_3)_3(L)]$ ($L = CNCMe_3$ (**3a**), $PPh_3$ (**3b**), $P(C_6H_4Me\text{-}2)_3$ (**3c**)) and $[NBu_4]_2[Pt(CF_3)_3X]$ ($X = Cl$ (**4a**), Br (**4b**), I (**4c**)). See the Supporting Information for experimental details.

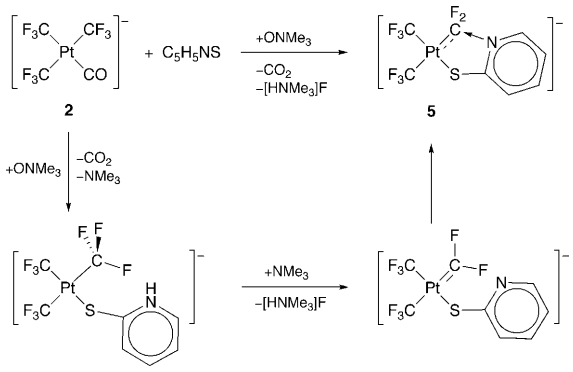


***Scheme 4.*** Experimentally observed (upper path) formation of compound **5** (see the Supporting Information for details) together with the suggested reaction mechanism (lower path).

preceding cases, but also entails C–F bond activation and C–N coupling. This complex reaction can be rationalized by means of the following simple steps (Scheme 4; lower path): 1) $ONMe_3$-assisted replacement of the CO ligand at **2** by the thione tautomer of $C_5H_5NS$; 2) α-fluoride elimination in one of the $CF_3$ groups *cis* to the S-donor atom promoted by the neighboring and moderately acidic pyridinium moiety,[15,16] and 3) attack at the highly electrophilic C atom of the resulting difluorocarbene fragment by the *N*-donor atom of the anchored pyridine ligand.

The crystal and molecular structures of **5** have been established by single-crystal X-ray diffraction methods.[11] The Pt center is in an approximate *SP*-4 environment (Figure 2) formed by two terminal $CF_3$ groups and the *S*- and *C*-donor atoms of the metallacycle. The Pt–$C(CF_3)$ bond lengths are

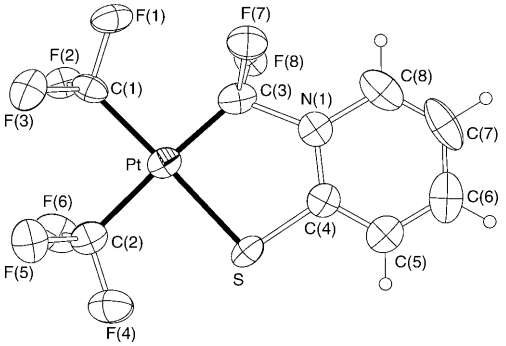


***Figure 2.*** Thermal ellipsoid diagram (50% probability) of one of the two disordered $[Pt(CF_3)_2(CF_2NC_5H_4S\text{-}\kappa C,\kappa S)]^-$ ions in **5**. Selected bond lengths [pm] and angles [°] with estimated standard deviations: Pt–C(1) 200.1(9), Pt–C(2) 202.9(9), Pt–C(3) 185(2), Pt–S 231.0(5), average C–F($CF_3$) 137.8(14), C(3)–N(1) 160(3), C(3)–F(7) 142.2(15), C(3)–F(8) 141.3(16), S–C(4) 174(4), C(1)-Pt-C(2) 89.7(3), C(1)-Pt-C(3) 93.5(7), C(1)-Pt-S 178.2(3), C(2)-Pt-C(3) 176.1(6), C(2)-Pt-S 88.6(3), C(3)-Pt-S 88.2(6), Pt-C(3)-F(7) 122.5(12), Pt-C(3)-F(8) 122.9(12), F(7)-C(3)-F(8) 98.0(13).

  

virtually identical and slightly shorter than those found in the related species **1** and **2′**. The 5-membered metallacycle has a bite angle that is large enough not to induce heavy angular distortions in the overall *SP*-4 geometry around the Pt atom. The Pt–S bond length [231.0(5) pm] is typical of a terminal thiolatoplatinum(II) complex (ca. 232 pm).[17] At first sight, this metallacycle could appear as a Pt derivative of a fluorinated *N*-ylide ligand. However, a closer look reveals geometric parameters associated with the $CF_2$ unit that are inconsistent with this bonding scheme. Thus, the N–C($CF_2$) bond [160(3) pm] is much longer than that previously observed for an N($sp^2$)–C($CF_2$) single bond (ca. 145 pm).[18] The Pt-C(3)-F(7) and Pt-C(3)-F(8) bond angles are approximately 120° and significantly wider than the Pt-C-F angles associated with a terminal $CF_3$ group (ca. 115°). Moreover, the Pt–C($CF_2$) bond length [185(2) pm] is much shorter than the usual Pt–C($CF_3$) bonds (ca. 205 pm) and is comparable to the Pt–C(CO) bond length found in **2′** [191.3(4) pm]. In fact, the Pt–C($CF_2$) bond length is quite similar to the Ir–C($CF_2$) ones found in structurally characterized difluorocarbene–iridium compounds, such as [Ir($CF_3$)(=$CF_2$)(CO)($PPh_3$)$_2$] [187.4(7) pm],[19] [Ir($\eta^5$-$C_5Me_5$)(=$CF_2$)(CO)] [185.5(13) pm],[20] and [Ir($\eta^5$-$C_5Me_5$)(=$CF_2$)($PMe_3$)] [185.4(11) pm].[16] All these structural features suggest that compound **5** can be more appropriately described as a pyridine-stabilized difluorocarbene–platinum derivative. Related structural patterns had been observed in pyridine-stabilized silylene–metal derivatives[21] in which the longer Si–N bond (ca. 195 pm vs. 170–176 pm for a normal Si–N single bond) was taken as evidence of a dative bond.[22,23] In view of its structural properties, compound **5** can be considered a valid model for the initial step operating in the solvolysis (including hydrolysis) of difluorocarbene–element derivatives (Scheme 5).[24] Of particular relevance to the present case is

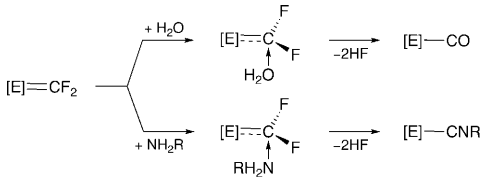


***Scheme 5.*** Suggested reaction path for solvolytic processes undergone by difluorocarbene element species.

the transformation of the [E]=$CF_2$ unit into a coordinated isocyanide ([E]–CNR), which is effected by reaction with a primary amine ($NH_2R$; Scheme 5).[19] The reasonable stability of **5** can be attributed to the lack of H atoms bound to the N-donor atom as well as to the chelate effect.

In short, the homoleptic compound [$NBu_4$]$_2$[Pt($CF_3$)$_4$] (**1**) was found to undergo stepwise $CF_3$ degradation under mild conditions. Evidence for the intermediacy of highly reactive [Pt]=$CF_2$ species was attained by the isolation of the ligand-stabilized adduct **5**, in which the $CF_2$ unit still preserves much of its original carbene nature.

Received: December 14, 2009
Revised: March 8, 2010
Published online: May 6, 2010

**Keywords:** carbene ligands · C–N coupling · fluorinated ligands · metallacycles · platinum

[1] I. Kieltsch, P. Eisenberger, K. Stanek, A. Togni, *Chimia* **2008**, *62*, 260; N. Shibata, S. Mizuta, H. Kawai, *Tetrahedron: Asymmetry* **2008**, *19*, 2633; T. Billard, B. R. Langlois, *Eur. J. Org. Chem.* **2007**, 891; J.-A. Ma, D. Cahard, *J. Fluorine Chem.* **2007**, *128*, 975; M. Schlosser, *Angew. Chem.* **2006**, *118*, 5558; *Angew. Chem. Int. Ed.* **2006**, *45*, 5432; B. R. Langlois, T. Billard, *Synthesis* **2003**, 185; G. K. S. Prakash, M. Mandal, *J. Fluorine Chem.* **2001**, *112*, 123; R. P. Singh, J. M. Shreeve, *Tetrahedron* **2000**, *56*, 7613; G. K. S. Prakash, A. K. Yudin, *Chem. Rev.* **1997**, *97*, 757; T. Umemoto, *Chem. Rev.* **1996**, *96*, 1757; M. A. McClinton, D. A. McClinton, *Tetrahedron* **1992**, *48*, 6555.

[2] J. E. Huheey, E. A. Keiter, R. L. Keiter, *Inorganic Chemistry*, 4th ed., Harper Collins, New York, **1993**, pp. 182–199; E. J. Little, Jr., M. M. Jones, *J. Chem. Educ.* **1960**, *37*, 231; A. L. Allred, E. G. Rochow, *J. Inorg. Nucl. Chem.* **1958**, *5*, 264.

[3] D. J. Burton, L. Lu, *Top. Curr. Chem.* **1997**, *193*, 45; D. J. Burton, Z.-Y. Yang, *Tetrahedron* **1992**, *48*, 189.

[4] M. Finze, E. Bernhardt, H. Willner, *Angew. Chem.* **2007**, *119*, 9340; *Angew. Chem. Int. Ed.* **2007**, *46*, 9180; M. Finze, E. Bernhardt, A. Terheiden, M. Berkei, H. Willner, D. Christen, H. Oberhammer, F. Aubke, *J. Am. Chem. Soc.* **2002**, *124*, 15385; A. Terheiden, E. Bernhardt, H. Willner, F. Aubke, *Angew. Chem.* **2002**, *114*, 823; *Angew. Chem. Int. Ed.* **2002**, *41*, 799.

[5] H. Amii, K. Uneyama, *Chem. Rev.* **2009**, *109*, 2119; H. Torrens, *Coord. Chem. Rev.* **2005**, *249*, 1957; T. G. Richmond, *Angew. Chem.* **2000**, *112*, 3378; *Angew. Chem. Int. Ed.* **2000**, *39*, 3241; T. G. Richmond, *Top. Organomet. Chem.* **1999**, *3*, 243; J. Burdeniuc, B. Jedicka, R. H. Crabtree, *Chem. Ber.* **1997**, *130*, 145; H. Plenio, *Chem. Rev.* **1997**, *97*, 3363; J. L. Kiplinger, T. G. Richmond, C. E. Osterberg, *Chem. Rev.* **1994**, *94*, 373.

[6] Selected references: J. Vicente, J. Gil-Rubio, J. Guerrero-Leal, D. Bautista, *Dalton Trans.* **2009**, 3854; J. Goodman, V. V. Grushin, R. B. Larichev, S. A. Macgregor, W. J. Marshall, D. C. Roe, *J. Am. Chem. Soc.* **2009**, *131*, 4236; G. G. Dubinina, J. Ogikubo, D. A. Vicic, *Organometallics* **2008**, *27*, 6233; G. G. Dubinina, W. W. Brennessel, J. L. Miller, D. A. Vicic, *Organometallics* **2008**, *27*, 3933; V. V. Grushin, W. J. Marshall, *J. Am. Chem. Soc.* **2006**, *128*, 12644; J. Vicente, J. Gil-Rubio, J. Guerrero-Leal, D. Bautista, *Organometallics* **2005**, *24*, 5634; S. Balters, E. Bernhardt, H. Willner, T. Berends, *Z. Anorg. Allg. Chem.* **2004**, *630*, 257; E. Bernhardt, M. Finze, H. Willner, *J. Fluorine Chem.* **2004**, *125*, 967; J. Vicente, J. Gil-Rubio, J. Guerrero-Leal, D. Bautista, *Organometallics* **2004**, *23*, 4871; R. Eujen, B. Hoge, D. J. Brauer, *Inorg. Chem.* **1997**, *36*, 1464; J. A. Schlueter, J. M. Williams, U. Geiser, J. D. Dudek, S. A. Sirchio, M. E. Kelly, J. S. Gregar, W. H. Kwok, J. A. Fendrich, J. E. Schirber, W. R. Bayless, D. Naumann, T. Roy, *J. Chem. Soc. Chem. Commun.* **1995**, 1311; D. Naumann, T. Roy, K.-F. Tebbe, W. Crump, *Angew. Chem.* **1993**, *105*, 1555; *Angew. Chem. Int. Ed. Engl.* **1993**, *32*, 1482; J. A. Morrison, *Adv. Organomet. Chem.* **1993**, *35*, 211.

[7] D. Naumann, N. V. Kirij, N. Maggiarosa, W. Tyrra, Y. L. Yagupolskii, M. S. Wickleder, *Z. Anorg. Allg. Chem.* **2004**, *630*, 746.

[8] B. Menjón, S. Martínez-Salvador, M. A. Gómez-Saso, J. Forniés, L. R. Falvello, A. Martín, A. Tsipis, *Chem. Eur. J.* **2009**, *15*, 6371.

[9] R. A. Michelin, R. Ros, G. Guadalupi, G. Bombieri, F. Benetollo, G. Chapuis, *Inorg. Chem.* **1989**, *28*, 840; T. G. Appleton, R. D. Berry, J. R. Hall, D. W. Neale, *J. Organomet. Chem.* **1989**,

  

*364*, 249; R. A. Michelin, G. Facchin, R. Ros, *J. Organomet. Chem.* **1985**, *279*, c25.

[10] D. Huang, P. R. Koren, K. Folting, E. R. Davidson, K. G. Caulton, *J. Am. Chem. Soc.* **2000**, *122*, 8916; P. J. Brothers, W. R. Roper, *Chem. Rev.* **1988**, *88*, 1293; M. A. Gallop, W. R. Roper, *Adv. Organomet. Chem.* **1986**, *25*, 121; W. R. Roper, *J. Organomet. Chem.* **1986**, *300*, 167.

[11] CCDC 749438 (**2′**) and 749437 (**5**) contains the supplementary crystallographic data for this paper. These data can be obtained free of charge from The Cambridge Crystallographic Data Centre via www.ccdc.cam.ac.uk/data_request/cif.

[12] On the basis of NMR data, the $CF_3$ group was assigned a markedly higher *trans* influence than the CO ligand: T. G. Appleton, M. A. Bennett, *Inorg. Chem.* **1978**, *17*, 738.

[13] R. Usón, J. Forniés, M. Tomás, I. Ara, B. Menjón, *J. Organomet. Chem.* **1987**, *336*, 129.

[14] The molecular structure of the $[Pt(CF_3)_3(PPh_3)]^-$ ion in **3b** would be expected to be quite similar to that observed in its tetramethylammonium salt: see Ref. [7].

[15] α-Fluoride elimination at a $CF_3$ group promoted by moderately acidic pyridinium salts has been documented in the Ir chemistry: see Ref. [16].

[16] R. P. Hughes, R. B. Laritchev, J. Yuan, J. A. Golen, A. N. Rucker, A. L. Rheingold, *J. Am. Chem. Soc.* **2005**, *127*, 15020.

[17] A. G. Orpen, L. Brammer, F. H. Allen, O. Kennard, D. G. Watson, R. Taylor, *J. Chem. Soc. Dalton Trans.* **1989**, S1.

[18] G. Bissky, G.-V. Röschenthaler, E. Lork, J. Barten, M. Médebielle, V. Staninets, A. A. Kolomeitsev, *J. Fluorine Chem.* **2001**, *109*, 173; R. M. Schoth, E. Lork, A. A. Kolomeitsev, G.-V. Röschenthaler, *J. Fluorine Chem.* **1997**, *84*, 41; A. Kolomeitsev, R.-M. Schoth, E. Lork, G.-V. Röschenthaler, *Chem. Commun.* **1996**, 335.

[19] P. J. Brothers, A. K. Burrell, G. R. Clark, C. E. F. Rickard, W. R. Roper, *J. Organomet. Chem.* **1990**, *394*, 615.

[20] C. J. Bourgeois, R. P. Hughes, J. Yuan, A. G. di Pasquale, A. L. Rheingold, *Organometallics* **2006**, *25*, 2908.

[21] H. Sakaba, M. Tsukamoto, T. Hirata, C. Kabuto, H. Horino, *J. Am. Chem. Soc.* **2000**, *122*, 11511; H. Tobita, T. Sato, M. Okazaki, H. Ogino, *J. Organomet. Chem.* **2000**, *611*, 314.

[22] A. Haaland, *Angew. Chem.* **1989**, *101*, 1017; *Angew. Chem. Int. Ed. Engl.* **1989**, *28*, 992.

[23] The presence of the referred dative bond can be taken as the main reason to explain the upfield shift of the $CF_2$ signal in the $^{13}C\{^{19}F\}$ NMR spectrum of **5** ($\delta = 145.69$ ppm) with respect to the CO signal in **2** ($\delta = 174.21$ ppm). This difference notwithstanding, similar values of $^1J(^{195}Pt,^{13}C)$ are observed in both cases: 1067 Hz for the $CF_2$ unit in **5** vs. 1103 Hz for the CO ligand in **2**.

[24] In a broader sense, this kind of adduct has been suggested to be involved as a transition state (saddle point in the calculations) in the reaction of a nucleophile with an electrophilic carbene carbon atom: M. A. Sierra, I. Fernández, F. P. Cossío, *Chem. Commun.* **2008**, 4671.

  

Organogold Compounds

DOI: 10.1002/anie.201101231

# [Au(CF$_3$)(CO)]: A Gold Carbonyl Compound Stabilized by a Trifluoromethyl Group**

*Sonia Martínez-Salvador, Juan Forniés,* Antonio Martín, and Babil Menjón*

*Dedicated to José M. Casas on the occasion of his 50th birthday*

Gold nanoparticles (Au NPs)[1] are attracting increasing interest in the scientific community as new and fascinating properties are being discovered with potential applications in the fields of technology,[2] chemistry,[3] and biomedicine.[4] Within the realm of chemistry, Au NPs have been found to act as efficient catalysts in an ever-growing number of chemical processes.[5] The performances achieved, however, seem to be highly dependent on the size, shape, and morphology of these Au NPs,[6] and thus new efficient and reliable methods to prepare them are being eagerly sought.[7] A recently reported procedure[8] to obtain monodisperse Au NPs with circa 28.7 nm average size consists of hydrolysis of the homoleptic trifluoromethyl derivative $[Au(CF_3)_2]^-$; this synthesis was suggested to proceed through "an intermediately formed, short-lived species $AuCF_3{\cdot}CO$." Herein we present the synthesis, isolation, and characterization of this unstable and highly reactive intermediate species, which is one of the very few gold carbonyl derivatives isolated in the condensed phase.[9]

Low-temperature treatment of $[PPh_4][Au(CF_3)_2]$ (**1**)[10] with $BF_3{\cdot}OEt_2$ in $CH_2Cl_2$ cleanly affords the carbonyl derivative $[Au(CF_3)(CO)]$ (**2**).[11] No decomposition is observed throughout the process, provided that moisture is carefully excluded from the reaction medium. The reaction path depicted in Scheme 1 is proposed in analogy with results obtained in platinum chemistry.[12] The first step would involve α-fluoride abstraction from the starting material **1** by the etherate $BF_3{\cdot}OEt_2$, thus giving rise to a transient difluorocarbene species that could possibly be stabilized by base coordination before further evolving into the final product **2**.[13] Transformation of **1** into **2** is evidenced by the shift of the $CF_3$ signal in the $^{19}F$ NMR spectrum from $\delta = -28.6$ to $-31.1$ ppm and the appearance of a sharp, strong band at 2180 $cm^{-1}$ in the IR spectrum that can be assigned to the ν(CO) vibration mode. The frequency of this absorption is even higher than that observed for [AuCl(CO)] (2162 $cm^{-1}$ in $CH_2Cl_2$ solution),[14,15] and is similar to that reported for the mixed-valence compound $[Cl_3Au(\mu\text{-}Cl)Au(CO)]$ (2180 $cm^{-1}$ in $SOCl_2$ solution).[15,16] The high ν(CO) frequency denotes that the CO molecule in **2** is acting predominantly as a σ-donor ligand;[17] it also confirms the electron-withdrawing character of the $CF_3$ group, which has been recently questioned.[18] Compound **2** readily undergoes CO exchange with free $^{13}CO$ at atmospheric pressure to give the labeled species $[Au(CF_3)(^{13}CO)]$ (**2***). This labeling experiment enables the CO signal to be unambiguously located in the $^{13}C$ NMR spectrum ($\delta_C = 183.0$ ppm), as coupling with the F nuclei is clearly observed (Figure 1a). Furthermore, the $^{19}F$ NMR signal of **2*** appears to be split into a doublet with the same coupling constant: $^3J(^{13}C,^{19}F) = 15.7$ Hz (Figure 1b).

Compound **2** is extremely water-sensitive and suffers massive decomposition to $Au^0$ under the action of moisture.

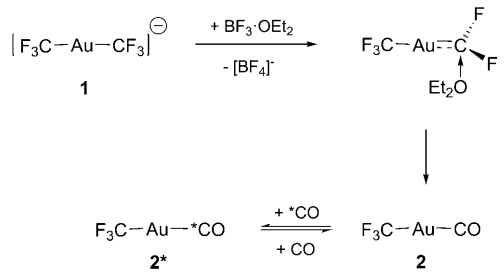


***Scheme 1.*** Suggested reaction path for the transformation of **1** (cation: $[PPh_4]^+$) into **2**, and the observed CO exchange in **2**.

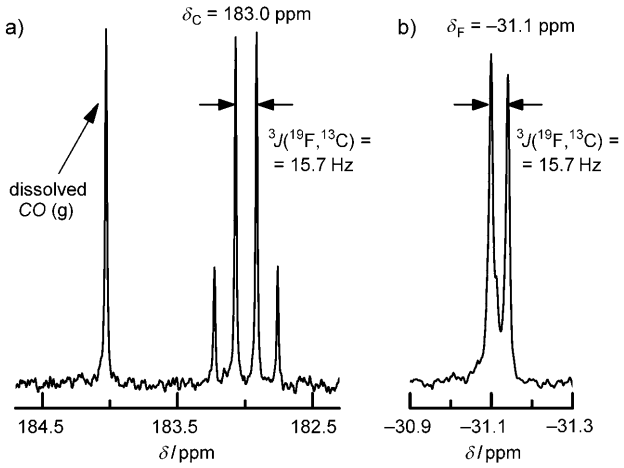


***Figure 1.*** Low-temperature NMR spectra and selected parameters for compound **2*** in $CD_2Cl_2$ solution: a) $^{13}C$, b) $^{19}F$. The signal corresponding to dissolved $^{13}CO(g)$ appears at $\delta = 184.0$ ppm in the $^{13}C$ NMR spectrum (a).

[*] S. Martínez-Salvador, Prof. Dr. J. Forniés, Dr. A. Martín, Dr. B. Menjón
Instituto de Síntesis Química y Catálisis Homogénea (ISQCH)
Universidad de Zaragoza-C.S.I.C.
C/Pedro Cerbuna 12, E-50009 Zaragoza (Spain)
Fax: (+34) 976-761-187
E-mail: juan.fornies@unizar.es

[**] This work was supported by the Spanish MICINN (DGPTC)/FEDER (Project CTQ2008-06669-C02-01/BQU) and the Gobierno de Aragón (Grupo Consolidado 21: Química Inorgánica y de los Compuestos Organometálicos).

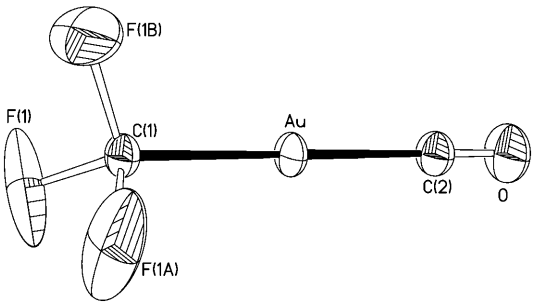


***Figure 2.*** Thermal ellipsoid diagram (50% probability) of the [Au(CF$_3$)(CO)] molecule. Selected bond lengths [pm] and angles [°]: Au–C(1) 204.7(14), Au–C(2) 197.7(16), C(2)–O 108(2), C(1)–F 132.6(10), C(1)-Au-C(2) 180.0(3), Au-C(2)-O 180.0(18), F-C(1)-Au 114.3(7), F-C(1)-F′ 104.2(8).

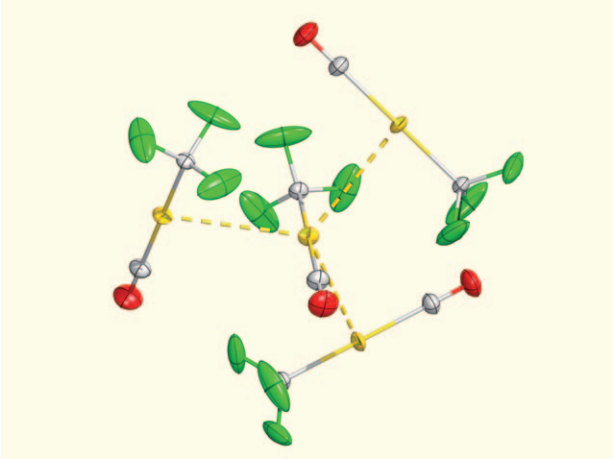

***Figure 3.*** Local environment of each [Au(CF$_3$)(CO)] molecule in the crystal lattice, including indications of the aurophilic interactions with three equidistant neighbor molecules. Au yellow, C gray, F green, O red. Au···Au = 345.9(1) pm.

This extreme water sensitivity is the reason why compound **2** is indeed a short-lived intermediate under the wet conditions required to produce the hydrolysis of $[Au(CF_3)_2]^-$.[8] Under strictly anhydrous conditions, however, compound **2** can be isolated as light yellow crystals.[11] The ν(CO) frequency observed in the solid state (2194 cm$^{-1}$) is similar to that found in [Au(OSO$_2$F)(CO)] (2195 cm$^{-1}$),[19] but is still significantly lower than that reported for the cationic species $[Au(CO)_2][Sb_2F_{11}]$ (2254 cm$^{-1}$).[20]

The crystal and molecular structures of **2** have been established by single-crystal X-ray diffraction methods.[21–23] The only crystallographically independent F$_3$C–Au–CO molecule (Figure 2) longitudinally coincides with a $C_3$ axis and therefore has a symmetry-imposed linear C–Au–C≡O arrangement. The Au–CO bond length (197.7(16) pm) is virtually identical to that found in the cationic species $[Au(CO)_2]^+$ (197.1(8) pm)[24] and is comparable to that reported for [AuCl(CO)] (193(2) pm);[25] it is, however, significantly longer than that found in the tetrahedrally coordinated compound [Au{BH(pz*)$_3$}(CO)] (186.2(9) pm; pz* = 3,5-bis(trifluoromethyl)pyrazolyl).[26] The long Au–CO bond in **2** is a further indication of the mainly σ-donor character of the CO ligand.[17] Each of the Au$^{\text{I}}$ centers (closed d$^{10}$ shell) shows weak aurophilic interactions (Au···Au = 345.9(1) pm)[27] with three symmetry-related Au$^{\text{I}}$ neighbors located in a plane perpendicular to the C–Au–CO axis (Figure 3), yielding an extended three-dimensional network of aurophilic interactions. The weak nature of these aurophilic interactions is also in keeping with the hard character or the CF$_3$ group and the poor σ-donating ability of the CO ligand that should result in a diminished electron density on the Au center.[28]

The interplay between gold and CO has been a fascinating subject for over a century. As early as 1905, J. Donau reported that action of CO on aqueous $[AuCl_4]^-$ solutions produced red colloidal gold.[29] The procedure has been conveniently modified and newly exploited to efficiently produce sub-10 nm Au NPs,[30] ultrathin gold nanowires (Au NWs),[31] and also plasmonic nanoparticles with highly regular Au shell layers.[32] Moreover, one of the most characteristic and thoroughly studied reactions catalyzed by Au NPs is the low-temperature oxidation of CO.[33] It is precisely the combination of the reducing ability of CO and the readiness with which gold is reduced that can be considered the main reason for the paucity of well-defined isolated carbonyl derivatives.[9] In fact, to our knowledge, compound **2** is the only gold carbonyl derivative stabilized by an organyl group.[34] Lower stabilities would be anticipated for the lighter isoleptic species [M(CF$_3$)(CO)] (M = Cu, Ag) considering the behavior of the [MCl(CO)] series: Au > Cu > Ag.[35] The methyl derivative [Au(CH$_3$)(CO)] would also be expected to be substantially less stable than **2**, given the lower stability of the related species [Au(CH$_3$)(CNMe)] with respect to its fluorinated homologue [Au(CF$_3$)(CNMe)].[36]

The isolation of [Au(CF$_3$)(CO)] (**2**) underlines the importance of gold carbonyl derivatives as intermediate species in the preparation of Au NPs. Preliminary results reveal that the CO molecule in **2** can be readily replaced by a number of other ligands. Therefore, compound **2** can be considered as a valuable synthon of the "Au(CF$_3$)" fragment that may find wide use in gold chemistry.[37]

Received: February 18, 2011

**Keywords:** aurophilic interactions · carbonyl ligands · fluorinated compounds · gold · reactive intermediates

[1] O. Vaughan, *Nat. Nanotechnol.* **2010**, *5*, 5; P. P. Edwards, J. M. Thomas, *Angew. Chem.* **2007**, *119*, 5576; *Angew. Chem. Int. Ed.* **2007**, *46*, 5480; M.-C. Daniel, D. Astruc, *Chem. Rev.* **2004**, *104*, 293.

[2] X. Liu, J. Zhang, X. Guo, S. Wu, S. Wang, *Nanotechnology* **2010**, *21*, 095501; T. Keel, *Chem. Ind.* **2010**, *24*; M. Ando, T. Kobayashi, M. Haruta, *Sens. Actuators B* **1995**, *25*, 851; N. Funazaki, A. Hemmi, S. Ito, Y. Asano, S. Yamashita, T. Kobayashi, M. Haruta, *Sens. Actuators B* **1993**, *14*, 536.

[3] D. W. Goodman, *Nature* **2008**, *454*, 948; M. Haruta, *Nature* **2005**, *437*, 1098.

[4] C. M. Cobley, J. Chen, E. C. Cho, L. V. Wang, Y. Xia, *Chem. Soc. Rev.* **2011**, *40*, 44; Y. Li, H. J. Schlüsener, S. Xu, *Gold Bull.* **2010**, *43*, 29; C. M. Cobley, Y. Xia, *Elements* **2009**, *5*, 309; R. Wilson,

  

*Chem. Soc. Rev.* **2008**, *37*, 2028; R. A. Sperling, P. Rivera-Gil, F. Zhang, M. Zanella, W. J. Parak, *Chem. Soc. Rev.* **2008**, *37*, 1896; C. J. Murphy, A. M. Gole, J. W. Stone, P. N. Sisco, A. M. Alkilany, E. C. Goldsmith, S. C. Baxter, *Acc. Chem. Res.* **2008**, *41*, 1721; Y. Xia, *Nat. Mater.* **2008**, *7*, 758; S. E. Skrabalak, J. Chen, L. Au, X. Lu, X. Li, Y. Xia, *Adv. Mater.* **2007**, *19*, 3177; M. Hu, J. Chen, Z.-Y. Li, L. Au, G. V. Hartland, X. Li, M. Márquez, Y. Xia, *Chem. Soc. Rev.* **2006**, *35*, 1084.

[5] A. Corma, H. García, *Chem. Soc. Rev.* **2008**, *37*, 2096; G. J. Hutchings, *Chem. Commun.* **2008**, 1148; T. Ishida, M. Haruta, *Angew. Chem.* **2007**, *119*, 7288; *Angew. Chem. Int. Ed.* **2007**, *46*, 7154; A. S. K. Hashmi, G. J. Hutchings, *Angew. Chem.* **2006**, *118*, 8064; *Angew. Chem. Int. Ed.* **2006**, *45*, 7896; M. Haruta, *Chem. Rec.* **2003**, *3*, 75; T. V. Choudhary, D. W. Goodman, *Top. Catal.* **2002**, *21*, 25; G. C. Bond, D. T. Thompson, *Catal. Rev. Sci. Eng.* **1999**, *41*, 319.

[6] M. Boronat, A. Corma, *Dalton Trans.* **2010**, *39*, 8538; T. V. W. Janssens, B. S. Clausen, B. Hvolbæk, H. Falsig, C. H. Christensen, T. Bligaard, J. K. Nørskov, *Top. Catal.* **2007**, *44*, 15; M. Comotti, C. della Pina, R. Matarrese, M. Rossi, *Angew. Chem.* **2004**, *116*, 5936; *Angew. Chem. Int. Ed.* **2004**, *43*, 5812; M. Haruta, *Catal. Today* **1997**, *36*, 153; M. Valden, X. Lai, D. W. Goodman, *Science* **1998**, *281*, 1647.

[7] J. Zeng, Y. Ma, U. Jeong, Y. Xia, *J. Mater. Chem.* **2010**, *20*, 2290; Y. Xia, Y. Xiong, B. Lim, S. E. Skrabalak, *Angew. Chem.* **2009**, *121*, 62; *Angew. Chem. Int. Ed.* **2009**, *48*, 60; M. Grzelczak, J. Pérez-Juste, P. Mulvaney, L. M. Liz-Marzín, *Chem. Soc. Rev.* **2008**, *37*, 1783.

[8] D. Zopes, S. Kremer, H. Scherer, L. Belkoura, I. Pantenburg, W. Tyrra, S. Mathur, *Eur. J. Inorg. Chem.* **2011**, 273.

[9] H. Schmidbaur, A. Schier in *Comprehensive Organometallic Chemistry III*, *Vol. 2* (Eds.: D. M. P. Mingos, R. H. Crabtree, K. Meyer), Elsevier, Amsterdam, **2007**, sect. 2.05.9, pp. 296–298; D. B. dell′Amico, F. Calderazzo, *Gold Bull.* **1997**, *30*, 21.

[10] The phosphonium salt **1** has been obtained by a similar procedure to that reported to prepare other salts of the $[Au(CF_3)_2]^-$ ion; see Ref. [8].

[11] Synthetic procedure: $BF_3{\cdot}OEt_2$ (38 μL, 0.30 mmol) was added to a solution of **1** (0.20 g, 0.30 mmol) in $CH_2Cl_2$ (10 mL) at −78 °C and under exclusion of light. The mixture was allowed to react for 4 h while the temperature rose to 0 °C, and the initially yellow solution gradually faded. Addition of pre-cooled *n*-hexane (20 mL) to the now colorless solution caused the precipitation of a white solid, which was filtered off. By allowing the filtrate to stand at −60 °C, light yellow crystals of **2** were obtained, which were filtered, washed with cold *n*-pentane (3 mL), and vacuum dried, while maintaining the temperature at −78 °C to avoid decomposition (0.03 g, 0.10 mmol, 34 % yield). Crystals of **2** quickly darken at room temperature and/or when exposed to moist air. No satisfactory elemental analyses were obtained owing to the instability of the substance.

[12] S. Martínez-Salvador, B. Menjón, J. Forniés, A. Martín, I. Usón, *Angew. Chem.* **2010**, *122*, 4382; *Angew. Chem. Int. Ed.* **2010**, *49*, 4286.

[13] The $Et_2O$ molecule (Scheme 1) might also act as the oxygen source for the CO ligand. Although the presence of small amounts of adventitious water as a possible oxygen source cannot be categorically excluded, the extreme sensitivity of **2** towards moisture makes such a possibility less plausible.

[14] J. Browning, P. L. Goggin, R. J. Goodfellow, M. G. Norton, A. J. M. Rattray, B. F. Taylor, J. Mink, *J. Chem. Soc. Dalton Trans.* **1977**, 2061.

[15] D. B. dell'Amico, F. Calderazzo, P. Robino, A. Segre, *J. Chem. Soc. Dalton Trans.* **1991**, 3017.

[16] D. B. dell'Amico, F. Calderazzo, F. Marchetti, *J. Chem. Soc. Dalton Trans.* **1976**, 1829.

[17] H. Willner, F. Aubke, *Chem. Eur. J.* **2003**, *9*, 1668; H. Willner, F. Aubke, *Organometallics* **2003**, *22*, 3612; H. Willner, F. Aubke in *Inorganic Chemistry Highlights* (Eds.: G. Meyer, L. Wesemann, D. Naumann), Wiley-VCH, Weinheim, **2002**, chap. 11, pp. 195–212; H. Willner, F. Aubke, *Angew. Chem.* **1997**, *109*, 2506; *Angew. Chem. Int. Ed. Engl.* **1997**, *36*, 2402.

[18] J. Goodman, V. V. Grushin, R. B. Larichev, S. A. Macgregor, W. J. Marshall, D. C. Roe, *J. Am. Chem. Soc.* **2010**, *132*, 12013.

[19] H. Willner, F. Aubke, *Inorg. Chem.* **1990**, *29*, 2195.

[20] H. Willner, J. Schaebs, G. Hwang, F. Mistry, R. Jones, J. Trotter, F. Aubke, *J. Am. Chem. Soc.* **1992**, *114*, 8972.

[21] Crystal data for **2**: $C_2AuF_3O$, $M_r = 293.99$; crystal size: $0.41 \times 0.37 \times 0.13$ mm$^3$; space group $I2_13$; $a = b = c = 968.170(10)$ pm, $V = 0.907517(16)$ nm$^3$; $Z = 8$; $\rho_{calcd} = 4.303$ g cm$^{-3}$; $\mu = 32.361$ mm$^{-1}$; graphite-monochromated $Mo_{K\alpha}$ radiation ($\lambda = 71.073$ pm); $T = 100(2)$ K; range for data collection: $4.21 \le \theta \le 28.59°$; reflections collected/unique: 2912/376 ($R_{int} = 0.0760$); Oxford Diffraction Xcalibur CCD diffractometer. The diffraction frames were integrated and corrected for absorption using the CrysAlis RED package.[22] Lorentz and polarization corrections were applied. The structure was solved by direct methods, and refinement against $F^2$ with SHELXL-97[23] converged to final residual indices of $R_1 = 0.0252$, $wR_2 = 0.0645$ [$I > 2\sigma(I)$] and $R_1 = 0.0253$, $wR_2 = 0.0645$ (all data). GoF = 1.056. CCDC 813000 contains the supplementary crystallographic data for this paper. These data can be obtained free of charge from The Cambridge Crystallographic Data Centre via www.ccdc.cam.ac.uk/data_request/cif.

[22] CrysAlis RED, Program for X-ray CCD camera data reduction, Version 1.171.32.19, Oxford Diffraction Ltd., Oxford, UK, **2008**.

[23] G. M. Sheldrick, SHELXL-97, Program for the refinement of crystal structures from diffraction data, University of Göttingen, Germany, **1997**.

[24] R. Küster, K. Seppelt, *Z. Anorg. Allg. Chem.* **2000**, *626*, 236.

[25] P. G. Jones, *Z. Naturforsch. B* **1982**, *37*, 823.

[26] H. V. R. Dias, W. Jin, *Inorg. Chem.* **1996**, *35*, 3687.

[27] H. Schmidbaur, A. Schier, *Chem. Soc. Rev.* **2008**, *37*, 1931; P. Pyykkö, *Chem. Soc. Rev.* **2008**, *37*, 1967; J. Muñiz, E. Sansores, *Mater. Avanzados* **2007**, *15*; P. Pyykkö, *Angew. Chem.* **2004**, *116*, 4512; *Angew. Chem. Int. Ed.* **2004**, *43*, 4412.

[28] P. Pyykkö, N. Runeberg, F. Mendizábal, *Chem. Eur. J.* **1997**, *3*, 1451; D. V. Toronto, B. Weissbart, D. S. Tinti, A. L. Balch, *Inorg. Chem.* **1996**, *35*, 2484.

[29] J. Donau, *Monatsh. Chem.* **1905**, *26*, 525.

[30] L. A. Pretzer, Q. X. Nguyen, M. S. Wong, *J. Phys. Chem. C* **2010**, *114*, 21226.

[31] Y. Kang, X. Ye, C. B. Murray, *Angew. Chem.* **2010**, *122*, 6292; *Angew. Chem. Int. Ed.* **2010**, *49*, 6156.

[32] B. E. Brinson, J. B. Lassiter, C. S. Levin, R. Bardhan, N. Mirin, N. J. Halas, *Langmuir* **2008**, *24*, 14166.

[33] H. Falsig, B. Hvolbœk, I. S. Kristensen, T. Jiang, T. Bligaard, C. H. Christensen, J. K. Nørskov, *Angew. Chem.* **2008**, *120*, 4913; *Angew. Chem. Int. Ed.* **2008**, *47*, 4835; B. K. Min, C. M. Friend, *Chem. Rev.* **2007**, *107*, 2709; M. Haruta, N. Yamada, T. Kobayashi, S. Iijima, *J. Catal.* **1989**, *115*, 301; M. Haruta, T. Kobayashi, H. Sano, N. Yamada, *Chem. Lett.* **1987**, 405; see also Ref. [5].

[34] The term organyl is used for any kind of alkyl, aryl, acyl, alkenyl, or alkynyl group, be it normal or cyclic and with any degree of substitution.

[35] I. Antes, S. Dapprich, G. Frenking, P. Schwerdtfeger, *Inorg. Chem.* **1996**, *35*, 2089.

[36] N. H. Dryden, J. G. Shapter, L. L. Coatsworth, P. R. Norton, R. J. Puddephatt, *Chem. Mater.* **1992**, *4*, 979.

[37] **Note added in proof (20.5.2011)**: After submission of this article, two reports have appeared on the synthesis and characterization of cationic gold(I) carbonyl compounds with the formula

  

$[Au(L)(CO)][SbF_6]$, where L is trimesitylphosphine[37a] or an *N*-heterocyclic carbene ligand.[37b] Their high ν(CO) values (ca. 2195 $cm^{-1}$) and their long Au–CO distances have been attributed mainly to the electrostatic effect of the cationic $[Au(L)]^+$ fragment on the polarization of the C≡O bond. Such an explanation, although appealing, cannot be invoked in the case of our neutral compound $[Au(CF_3)(CO)]$, for which similar ν(CO) values are observed. No aurophilic interactions were observed in these newly reported cationic compounds.

a) H. V. R. Dias, C. Dash, M. Yousufuddin, M. A. Celik, G. Frenking, *Inorg. Chem.* **2011**, *50*, 4253; b) C. Dash, P. Kroll, M. Yousufuddin, H. V. R. Dias, *Chem. Commun.* **2011**, *47*, 4478.

  

DOI: 10.1002/chem.201100626

# Highly Trifluoromethylated Platinum Compounds

**Sonia Martínez-Salvador, Juan Forniés,* Antonio Martín, and Babil Menjón[a]**

**Abstract:** The homoleptic, square-planar organoplatinum(II) compound $[NBu_4]_2[Pt(CF_3)_4]$ (**1**) undergoes oxidative addition of $CF_3I$ under mild conditions to give rise to the octahedral organoplatinum(IV) complex $[NBu_4]_2[Pt(CF_3)_5I]$ (**2**). This highly trifluoromethylated species reacts with $Ag^+$ salts of weakly coordinating anions in $Me_2CO$ under a wet-air stream to afford the aquo derivative $[NBu_4][Pt(CF_3)_5(OH_2)]$ (**4**) in around 75% yield. When the reaction of **2** with the same $Ag^+$ salts is carried out in MeCN, the solvento compound $[NBu_4][Pt(CF_3)_5(NCMe)]$ (**5**) is obtained in around 80% yield. The aquo ligand in **4** as well as the MeCN ligand in **5** are labile and can be cleanly replaced by neutral and anionic ligands to furnish a series of pentakis(trifluoromethyl)platinate(IV) compounds with formulae $[NBu_4][Pt(CF_3)_5(L)]$ (L = CO (**6**), pyridine (py; **7**), tetrahydrothiophene (tht; **8**)) and $[NBu_4]_2[Pt(CF_3)_5X]$ (X = Cl (**9**), Br (**10**)). The unusual carbonyl–platinum(IV) derivative $[NBu_4][Pt(CF_3)_5(CO)]$ (**6**) is thermally stable and has a $\nu_{CO}$ of 2194 $cm^{-1}$. The crystal structures of $\mathbf{2}\cdot CH_2Cl_2$, **5**, $[PPh_4][Pt(CF_3)_5(CO)]$ (**6′**), and **7** have been established by X-ray diffraction methods. Compound **2** has shown itself to be a convenient entry to the chemistry of highly trifluoromethylated platinum compounds. To the best of our knowledge, compounds **2** and **4**–**10** are the organoelement compounds with the highest $CF_3$ content to have been isolated and adequately characterized to date.

**Keywords:** fluorinated ligands · NMR spectroscopy · octahedral compounds · platinum · trifluoromethylation

## Introduction

For a very long time perfluoroalkyl groups have been known to endow organoelement derivatives with enhanced stability compared with their nonfluorinated counterparts.[1] This well-established idea notwithstanding, the chemistry of organoelements that contain the methyl group $CH_3$ is by far better understood and more thoroughly developed than that of the trifluoromethyl group $CF_3$. This difference is especially patent in compounds with a high alkyl-group content. Thus, interesting derivatives with up to eight methyl groups per central atom are known, such as different salts of the octamethyluranate(V)[2] $[U(CH_3)_8]^{3-}$, octamethyltungstate(VI)[3] $[W(CH_3)_8]^{2-}$, or the octamethylrhenate(VI)[4] $[Re(CH_3)_8]^{2-}$ anions. In contrast, organoelement derivatives with up to just four $CF_3$ groups have been isolated and characterized. This type of compounds includes perfluoroneopentane $C(CF_3)_4$, which was first obtained as one of the many components in the pyrolysis at around 500 °C of $CF_3SF_5$ or $(CF_3)_2SF_4$ with $CF_3CF{=}CF_2$.[5] This fluorocarbon molecule as well as other homoleptic neutral species of formula $E(CF_3)_4$ (E = Ge, Sn, Pb, and Te) have been subsequently obtained by at least one of the following procedures (Scheme 1):[6] 1) direct fluorination of the corresponding $E(CH_3)_4$ derivatives (Scheme 1a);[7] 2) reaction of the suitable element precursor with plasma-generated $CF_3^{\bullet}$ radicals obtained from homolytic cleavage of the $CF_3{-}CF_3$ bond by glow discharge (Scheme 1b);[8] and 3) by exchange reaction between a neutral halide $EX_4$ and a nucleophilic trifluoromethylating agent such as $[Ag(CF_3)(solv)]$, $[Cd(CF_3)_2(solv)]$, $[Hg(CF_3)_2]$, or even $Sn(CF_3)_4$ (Scheme 1c).[9]

The anionic species $[B(CF_3)_4]^-$ was only recently prepared by transformation of the C≡N triple bond in the cyano de-

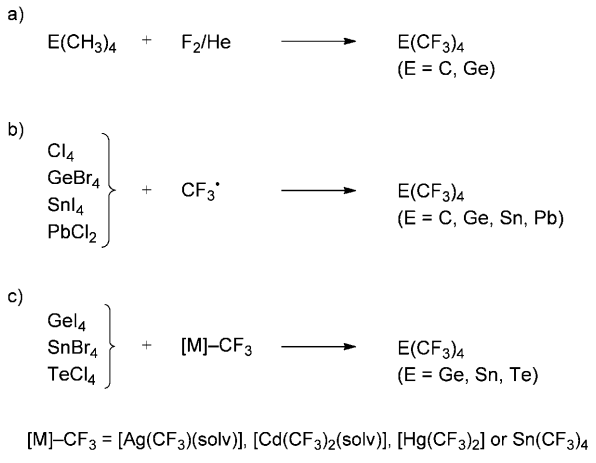


Scheme 1. Synthetic methods by which the known homoleptic neutral organoelement derivatives $E(CF_3)_4$ have been prepared.

[a] Dipl.-Chem. S. Martínez-Salvador, Prof. Dr. J. Forniés, Dr. A. Martín, Dr. B. Menjón
Instituto de Síntesis Química y Catálisis Homogénea (ISQCH)
Universidad de Zaragoza-C.S.I.C.
c/ Pedro Cerbuna 12, 50009 Zaragoza (Spain)
Fax: (+34) 976-761-187
E-mail: juan.fornies@unizar.es

  

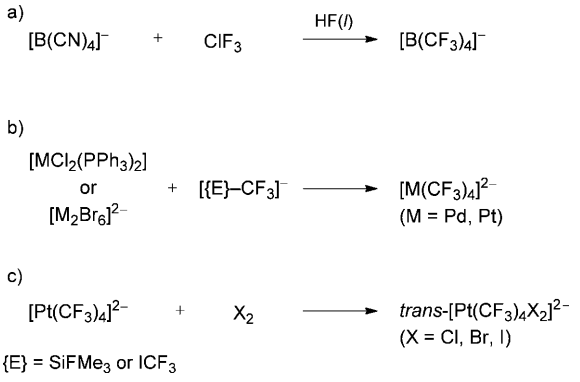


Scheme 2. Synthetic methods by which some anionic organoelement derivatives with a high $CF_3$ content have been prepared.

rivative $[B(CN)_4]^-$ into three C–F bonds brought about by reaction with $ClF_3$ in anhydrous $HF_{(l)}$ solution (Scheme 2a).[10] Different salts of the homoleptic anions $[M^{II}(CF_3)_4]^{2-}$ ($M^{II}$ = Pd, Pt)[11,12] have been obtained by reaction of the suitable metal substrate with a nucleophilic trifluoromethylating agent—typically the five-coordinate organosilicate species $[Me_3Si(CF_3)F]^-$ generated in situ by fluoride coordination to $Me_3SiCF_3$ at low temperature (Scheme 2b).[13] The isoleptic species $[Cd^{II}(CF_3)_4]^{2-}$ seems to have been detected as one of the components in polar solutions of $Cd(CF_3)_2$·dme (dme = 1,2-dimethoxyethane) in the presence of CsI.[14] The complete series of $[M^{III}(CF_3)_4]^-$ anions for all three Group 11 metals ($M^{III}$ = Cu,[15] Ag,[16] Au[17]) has also been prepared.[18] We have recently reported[12] that oxidative addition of halogens to $[NBu_4]_2[Pt(CF_3)_4]$ takes place stereoselectively to afford the heteroleptic compounds $[NBu_4]_2$*trans*-$[Pt(CF_3)_4X_2]$ (X = Cl, Br, I) in high yield (Scheme 2c). Isomer *cis*-$[Pt(CF_3)_4Cl_2]^{2-}$ has also been detected as a solution species by other authors.[19]

A few chemical species with higher $CF_3$ content have been detected but not isolated in pure form. Thus, the low-temperature reaction of $[Pt(CN)_6]^{2-}$ salts with ClF involves the transformation of CN into $CF_3$ ligands, together with ligand-exchange processes.[19] As a result, complex mixtures of compounds are obtained that contain species with formula $[Pt(CF_3)_5X]^{2-}$ (X = F, Cl, OH) among various other reaction products. Even the homoleptic $[Pt(CF_3)_6]^{2-}$ derivative was detected to be present in those reaction media. H. Willner and his co-workers revealed a great deal of skill in the hard task of assigning the multinuclear NMR spectroscopic properties of such complex reaction mixtures to each of the referred $Pt^{IV}$ species. Finally, a vague reference to poorly characterized, high-valent compounds $[U(CF_3)_6]$ and $[W(CF_3)_6]$ has been made in patent literature[20] but, to the best of our knowledge, further details have never ensued. Possible formation of the latter compound by low-temperature reaction between $WBr_6$ and $Cd(CF_3)_2$·dme was also presumed. However, the formulation of this apparently unstable derivative relied merely on the nature of its decomposition products.[21]

We now report on efficient synthetic procedures to selectively obtain a number of pentakis(trifluoromethyl)platinum(IV) derivatives in high yields. These are, to the best of our knowledge, the organoelement compounds with the highest $CF_3$ content that have been isolated and adequately characterized to date.

## Results and Discussion

**The parent species**: The salt $[NBu_4]_2[Pt(CF_3)_4]$ (**1**) dissolved in MeCN reacts with a slight excess amount of $CF_3I$ under mild conditions to give rise to $[NBu_4]_2[Pt(CF_3)_5I]$ (**2**). The reaction (Scheme 3) proceeds in a quantitative way over

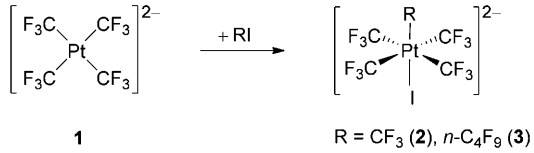


**1** R = $CF_3$ (**2**), *n*-$C_4F_9$ (**3**)

Scheme 3. Oxidative addition of perfluoroalkyl iodide molecules, RI, to the homoleptic platinum(II) compound **1** ($[NBu_4]^+$ is the counterion in all cases).

24 h at room temperature, as monitored by $^{19}F$ NMR spectroscopy. After the appropriate workup, compound **2** can be isolated as a white solid in 76% yield. The mild conditions under which compound **2** is formed contrast with the harsh conditions needed in many of the synthetic procedures used to prepare highly trifluoromethylated organoelement derivatives as mentioned in the Introduction. It is worth noting that compound **1** treated with $CF_3I$ does not undergo any reaction at all ($^{19}F$ NMR spectroscopy) if $CH_2Cl_2$ or $Me_2CO$ are used as solvents instead of MeCN.

The crystal and molecular structures of **2** have been established by X-ray diffraction methods on single crystals of the solvate **2**·$CH_2Cl_2$. The Pt atom has been found to be in an approximately octahedral (*OC*-6) environment (Figure 1)

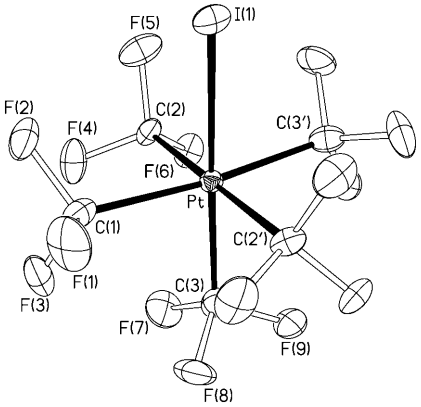


Figure 1. Thermal ellipsoid diagram (50% probability) of the $[Pt(CF_3)_5I]^-$ anion as found in single crystals of **2**·$CH_2Cl_2$.

  

with the iodo ligand heavily disordered over several coordination sites (see the Experimental Section). All NMR spectroscopic data of **2** in solution are in agreement with its solid-state structure. Thus, the room-temperature $^{19}F$ NMR spectrum of **2** (Figure 2, Table 1) consists of two signals with 4:1 integrated areas that correspond to the two chemically

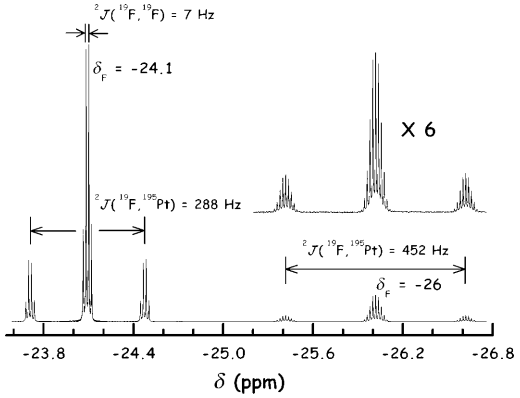


Figure 2. Room-temperature $^{19}F$ NMR spectrum of compound **2** in [$D_3$]acetonitrile solution with spectral parameters indicated.

inequivalent $CF_3$ groups present in the $[Pt(CF_3)_5I]^{2-}$ anion: a quartet at $\delta_F = -24.1$ ppm and a multiplet[22] at $\delta_F = -26.0$ ppm with a mutual coupling constant of $^4J(^{19}F,^{19}F) = 7$ Hz. Each signal is flanked by $^{195}Pt$ satellites with $^2J(^{195}Pt,^{19}F)$ values of 288 and 452 Hz, respectively. The $^{195}Pt$ NMR spectrum of **2** ($\delta_{Pt} = -2446$ ppm) is particularly rich due to extensive coupling with the F atoms of the coordinated $CF_3$ groups (Figure 3).

Compound **2** results from the oxidative addition of $CF_3I$ to **1**. However, given the stoichiometry of the final product, it is not clear whether such addition takes place in a *cis* or in a *trans* fashion. To shed some light on this point, we also carried out the reaction of **1** with $nC_4F_9I$. The perfluoro-*n*-butyl group is particularly suited for this purpose as the α-C atom has two F substituents plus a short perfluoroalkyl chain, $CF_2(nC_3F_7)$, thus bearing a close relationship with the $CF_3$ group—at least from the electronic point of view. In the

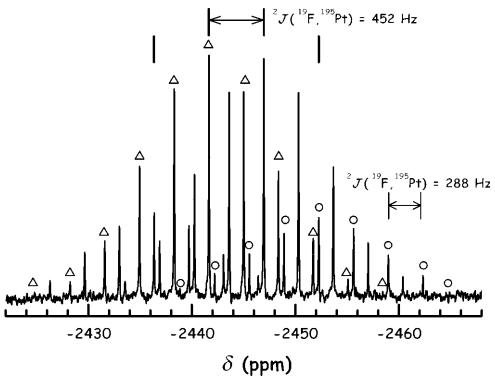


Figure 3. Room-temperature $^{195}Pt$ NMR spectrum of compound **2** in [$D_3$]acetonitrile solution with spectral parameters indicated. Only the left strong and right weak branches of the quartet of multiplets are labeled for clarity; their corresponding counterparts are clearly observed by symmetry.

absence of important steric effects, the results obtained with $nC_4F_9I$ will be applicable to the $CF_3I$ case. Compound **1** reacts with $nC_4F_9I$ under conditions similar to those given above (Scheme 3), thereby affording $[NBu_4]_2$*trans*-$[Pt(CF_3)_4(nC_4F_9)I]$ (**3**) in a stereoselective way ($^{19}F$ NMR spectroscopy). The chemical shift of the equatorial $CF_3$ groups in **3**, $\delta_F(eq) = -21.2$ ppm, is close to that observed for compound **2** (Table 1). This signal appears as a triplet of triplets due to coupling to the α- and β-F atoms of the $nC_4F_9$ chain: $^4J(^{19}F,^{19}F) = 10.7$ Hz and $^5J(^{19}F,^{19}F) = 8.25$ Hz, which shows additional coupling to the $^{195}Pt$ isotope: $^2J(^{195}Pt,^{19}F) = 287$ Hz. Compound **3** slowly undergoes spontaneous dissociation of the iodo ligand in MeCN at room temperature to give rise to a further species, to which we assign the formula $[NBu_4]$*trans*-$[Pt(CF_3)_4(nC_4F_9)(NCMe)]$ (*post*-**3**).[23] Our assignment relies on the invariability of the $^{19}F$ NMR spectrum of the latter species upon addition of the equimolar amount of $AgSO_3CF_3$. Moreover, this spectrum shows a close relationship with that observed for the isolated derivative $[NBu_4][Pt(CF_3)_5(NCMe)]$ (see below).

Given the *trans* stereochemistry observed for the reaction product **3**, the possibility of a concerted addition of the per-

Table 1. Multinuclear NMR spectroscopic parameters of the $Pt(CF_3)_5$ core[a] in compounds **2** and **4**–**10**.[b]

| Compound | $\delta_F$(eq)[c] [ppm] | $\delta_F$(ax)[c] [ppm] | $^4J(^{19}F,^{19}F)$ [Hz] | $\delta_C$(eq)[c] [ppm] | $\delta_C$(ax)[c] [ppm] | $\delta_{Pt}$ [ppm] |
|---|---|---|---|---|---|---|
| $[NBu_4]_2[Pt(CF_3)_4]$ (**1**)[d] | −23.6 (548) | – | – | 141.2 (1284) | – | −4232 |
| $[NBu_4]_2[Pt(CF_3)_5I]$ (**2**)[e] | −24.1 (288) | −26.0 (452) | 7.0 | 117.0 (940) | 94.8[f] | −2446 |
| $[NBu_4][Pt(CF_3)_5(OH_2)]$ (**4**) | −35.2 (269) | −22.8 (578) | 5.1 | 122.2 (943) | 86.7[f] | −1785 |
| $[NBu_4][Pt(CF_3)_5(NCMe)]$ (**5**) | −32.2 (270) | −25.5 (542) | 5.7 | 119.2 (925) | 92.2 (1590) | −2070 |
| $[NBu_4][Pt(CF_3)_5(CO)]$ (**6**)[g] | −24.0 (269) | −29.2 (490) | 5.9 | 116.2 (888) | 103.0 (1408) | −2650 |
| $[NBu_4][Pt(CF_3)_5(py)]$ (**7**) | −32.8 (263) | −24.2 (484) | 7.0 | 119.5 (941) | 92.6 (1462) | −1872 |
| $[NBu_4][Pt(CF_3)_5(tht)]$ (**8**)[g] | −28.9 (265) | −24.2 (487) | 6.1 | 118.3 (929) | 100.9[f] | −2283 |
| $[NBu_4]_2[Pt(CF_3)_5Cl]$ (**9**)[h] | −31.4 (281) | −25.1 (470) | 6.4 | 119.0 (940) | 101.6 (1491) | −2128 |
| $[NBu_4]_2[Pt(CF_3)_5Br]$ (**10**) | −27.8 (284) | −24.1 (471) | 6.7 | 118.2 (940) | 99.8 (1489) | −2219 |

[a] The parameters associated with the sixth ligand are listed in the Experimental Section. [b] Unless otherwise stated, all measurements were carried out in [$D_6$]acetone at room temperature. [c] Axial and equatorial positions are labeled ax and eq, respectively; $^1J(^{195}Pt,^{13}C)$ and $^2J(^{195}Pt,^{19}F)$ values [Hz] are given in parentheses where appropriate. [d] NMR spectroscopic parameters of **1** (see Ref. [11]) are also included for comparison. [e] In [$D_3$]acetonitrile. [f] $^{195}Pt$ satellites not clearly observed. [g] In [$D_2$]dichloromethane. [h] See values given in Ref. [19].

  

fluoroalkyl iodide $nC_4F_9I$ to compound **1** can be ruled out and seems rather unlikely in the case of $CF_3I$ by analogy. Furthermore, a polar $S_N2$ attack by the metal at the α-C atom would seem improbable because of the unfavorable polarity of the $C^{\delta-}$–$I^{\delta+}$ bond in perfluoroalkyl iodides, as already noted by Hughes and his co-workers.[24] It would, therefore, be expected that the nucleophilic attack would take place at the positively charged iodine atom (Scheme 4a), much in analogy with our previous observations with halogen molecules (Scheme 4b).[12] Indeed, $CF_3I$ is known to form thermally labile adducts of the type $[CF_3I(Nu)]^-$ with a range of anionic nucleophiles, $Nu^-$, such as $Cl^-$, $Br^-$, $OCF_3^-$,[25] or even $CF_3^-$[26] (Scheme 4c). The fact that, once formed, compound **3** slowly dissociates the iodo ligand can be taken as evidence for Pt–I being the primary stable bond formed between the Pt center and the $nC_4F_9I$ molecule. The suggested initial step (Scheme 4a) could, in principle, evolve in two different ways depending on the kind of electron transfer taking place between the Pt center and the I atom.[27] A single-electron transfer should result in the homolytic cleavage of the I–$CF_3$ bond and formation of a $CF_3^{\bullet}$ radical.[28] On the other hand, a two-electron donation should result in the heterolytic cleavage of the I–$CF_3$ bond and formation of a solvent-stabilized $(CF_3)^-$ carbanion.[29] In both cases, the generated fluorocarbon moiety would be expected to be highly reactive and to rapidly recombine with the corresponding metal fragment. We have no experimental proof to decide between these two possible mechanisms. However, we have already noted (see above) that the reaction proceeds quantitatively in MeCN—an organic solvent with a fairly high relative permitivity ($\varepsilon_r = 35.94$) and sizable permanent dipole moment ($\mu = 13.0 \times 10^{30}\ C^{-1}\,m^{-1}$), thus enabling efficient charge separation—but in no perceptible way in $CH_2Cl_2$ ($\varepsilon_r = 8.93$, $\mu = 3.8 \times 10^{30}\ C^{-1}\,m^{-1}$) or $Me_2CO$ ($\varepsilon_r = 20.56$, $\mu = 9.0 \times 10^{30}\ C^{-1}\,m^{-1}$) under similar conditions.[30] This marked solvent dependence can be taken as indirect evidence that favors the intermediacy of the carbanion versus that of the radical species. The carbanion $(CF_3)^-$ could also be stabilized by adduct formation with unreacted $CF_3I$ to give rise to $[CF_3ICF_3]^-$ (Scheme 4c),[26] which is known to act as a nucleophilic trifluoromethylating agent.[11] Entry of the $CF_3$ ligand into the sixth coordination site (most probably first occupied by a solvent molecule) would render the final product $[NBu_4]_2[Pt(CF_3)_5I]$ (**2**).

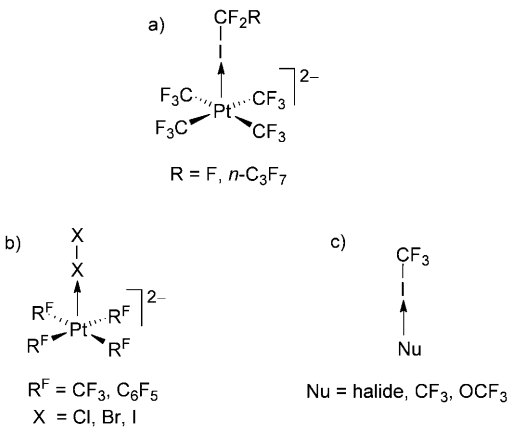


Scheme 4. a) Suggested initial step for the reaction of **1** with perfluoroalkyl iodides together with the known precedents for b) the behavior of the homoleptic organoplatinum(II) anions $[Pt(R^F)_4]^{2-}$ as nucleophiles towards halogens, and c) the reactivity of the $CF_3I$ molecule towards nucleophiles (Nu).

Having devised a convenient and high-yield procedure to prepare compound **2**, we sought to explore its chemical behavior as a potential entry to the chemistry of highly trifluoromethylated platinum compounds.

**Some solvento complexes**: Octahedral metal complexes with $d^6$ electron configuration are 18-electron species that behave as electronically and coordinatively saturated ones. This saturation implies a certain degree of chemical inertness, especially for 6d metals. For instance, ligand-exchange processes are usually slow, with the limiting step being, in most cases, the initial dissociation of one of the ligands (dissociative mechanism).[31] The empty coordination site thus generated can be rapidly occupied by the incoming ligand. To favor this kind of ligand replacement processes, it is highly desirable that at least one of the ligands in the metal coordination sphere has a reasonable lability.[32] Water and organonitrile ligands[33] are class *a* ligands that usually exhibit labile behavior when bound to $Pt^{II}$ or $Pt^{IV}$ centers—both considered to be class *b* metals.[32]

Compound **2** dissolved in $Me_2CO$ reacts with $Ag^+$ salts of weakly coordinating anions, such as $(SO_3CF_3)^-$, $(ClO_4)^-$, or $(CF_3CO_2)^-$, to give $[NBu_4][Pt(CF_3)_5(OH_2)]$ (**4**) under a wet-air stream (Scheme 5). The aqua derivative **4** can be isolated as a white solid in around 75% yield and it has been characterized by analytic and spectroscopic methods. Its IR spectrum shows broad bands in the 3500 $cm^{-1}$ region, which correspond to ν(O–H) vibration modes. The $^{19}F$ NMR spectrum consists of a multiplet at $\delta_F = -22.8$ ppm and a quartet at $\delta_F = -35.2$ ppm with a mutual coupling constant of $^4J(^{19}F,^{19}F) = 5.1$ Hz (Table 1). The overall pattern is similar to that observed for compound **2** with the quartet now appear-

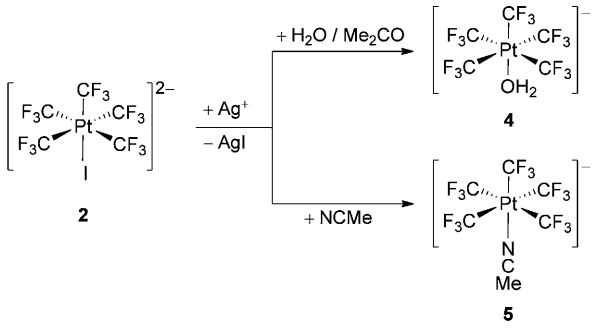


Scheme 5. Synthetic procedures that lead to the platinum(IV) solvento derivatives **4** and **5** ($[NBu_4]^+$ is the counterion in all cases).

  

ing at lower frequency than the multiplet. In fact, the signal that corresponds to the equatorial $CF_3$ groups appears upfield-shifted by more than 10 ppm with respect to the parent species **2**. The axial and equatorial $CF_3$ groups also appear to be in rather dissimilar chemical environments in view of the large separation ($\approx$12.5 ppm) observed between their corresponding signals.

Room-temperature treatment of compound **2** with the same $Ag^+$ salts in MeCN as the solvent under an inert atmosphere (Scheme 5) gives rise to the solvento complex $[NBu_4][Pt(CF_3)_5(NCMe)]$ (**5**) in a quantitative way ($^{19}$F NMR spectroscopy). Compound **5** can eventually be isolated as a white solid in around 80% yield. Its $^1$H NMR spectrum shows a singlet at $\delta_H = 2.61$ ppm with long-range $^{195}$Pt satellites, $^4J(^{195}Pt,^1H) = 5.6$ Hz, which correspond to the Me group of the nitrile ligand. The $^{19}$F NMR spectrum shows a pattern similar to that of the aquo compound **4** (Table 1), with the difference between the chemical shifts corresponding to the axial ($\delta_F = -25.5$ ppm) and equatorial ($\delta_F = -32.2$ ppm) $CF_3$ groups being now of just approximately 6.6 ppm. Since the spectroscopic properties of the $[Pt(CF_3)_5(NCMe)]^-$ anion (including internuclear spin–spin coupling constants) roughly coincide with those formerly assigned to the hydroxo species $[Pt(CF_3)_5(OH)]^{2-}$,[34] we found it appropriate to undertake the structural characterization of compound **5** in the solid state.

The crystal and molecular structures of **5** have been established by single-crystal X-ray diffraction methods. A drawing of the $[Pt(CF_3)_5(NCMe)]^-$ anion is given in Figure 4, in which an *OC*-6 environment for the Pt center can be clearly observed. The mutually *trans*-standing $CF_3$ groups define the equatorial plane with the sum of angles between adjacent groups amounting to 360.2(1)°. The axial $CF_3$ is disordered over two close positions, only one of which is depicted in Figure 4. The Pt–C(eq) distances (average value = 210.8(4) pm) are similar to those found in the organoplatinum(IV) anion *trans*-$[Pt(CF_3)_4Cl_2]^{2-}$ (average value = 209.2(5) pm) and slightly longer than in the organoplatinum(II) precursor species $[Pt(CF_3)_4]^{2-}$ (average value = 205.0(4) pm),[12] whereas the Pt–C(ax) distance (202.6(4) pm) is shorter than any of them. The terminal MeCN ligand is almost linear, with Pt-N(1)-C(6) = 174.8(3)° and N(1)-C(6)-C(7) = 177.7(4)°. The Pt–N(1) distance (208.0(3) pm) is in keeping with that observed in the *OC*-6 organoplatinum(IV) compound [PtIMePh(bpy)(NCMe)]-[$BF_4$] (Pt–N 208(3) pm; bpy = 2,2′-bipyridyl),[35] in which the nitrile ligand is also located *trans* to an organyl group (Ph). The Pt–N(1) distance in **5** is, however, significantly longer than those found in the related species $[NBu_4]$*trans*-$[Pt(C_6F_5)_4Br(NCPh)]$ (Pt–N 203.8(6) pm)[12] or in the cationic derivatives $[PtClMe_2(N\&N)(NCMe)]_2[PtCl_6]$ (Pt–N 198.2(7) pm with N&N = $(C_6H_3Me_2$-2,6)N=CMe–CMe=N$(C_6H_3Me_2$-2,6); Pt–N 197.6(5) pm with N&N = CyN=CH–CH=NCy),[36] in which the nitrile ligands are located *trans* to a halo ligand (Cl or Br) with lower *trans* influence than organyl groups.[37] An even longer Pt–N(nitrile) distance was found in the cationic diimine compound *fac*-$[PtMe_3(NR{=}CH{-}CH{=}NR)(NCMe)][SO_3CF_3]$ (Pt–N = 216.0(6) pm; R = $C_6H_4$(OMe)-4),[38] again with the nitrile ligand *trans* to an organyl group (Me).

The nitrile group in **5** and especially the aquo ligand in **4** behave as labile ligands, being readily replaced by a number of Lewis bases as we will see next.

**A thermally stable $Pt^{IV}$ carbonyl derivative**: Compound **4** dissolved in $CH_2Cl_2$ and under a normal-pressure CO atmosphere undergoes substitution of the $H_2O$ ligand by CO to give rise to $[NBu_4][Pt(CF_3)_5(CO)]$ (**6**) in a quantitative way ($^{19}$F NMR spectroscopy) after 12 h at room temperature (Scheme 6). Carbon monoxide is equally able to replace the nitrile ligand in compound **5** also to afford **6** (Scheme 6); in this case, however, the reaction proceeds rather more slowly, as more than 1 week is now required for completion.

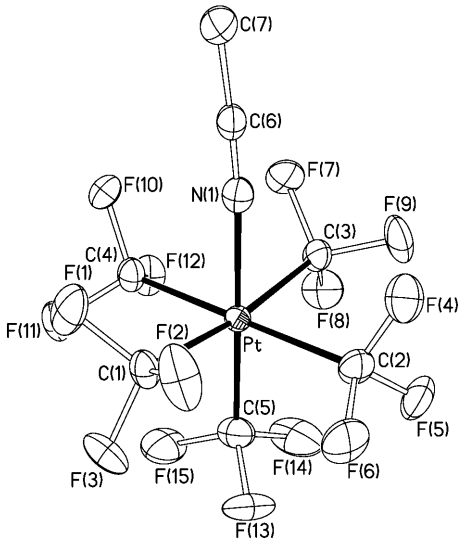


Figure 4. Thermal ellipsoid diagram (50% probability) of the $[Pt(CF_3)_5(NCMe)]^-$ anion as found in single crystals of **5**. Selected bond lengths [pm] and angles [°] with estimated standard deviations: Pt–N(1) 208.0(3), Pt–C(ax) 202.6(4), average Pt–C(eq) 210.8(4), average C(eq)–F 135.8(5), average C(ax)–F 135.0(5); C(5)-Pt-N(1) 178.1(1), Pt-N(1)-C(6) 174.8(3), N(1)-C(6)-C(7) 177.7(4).

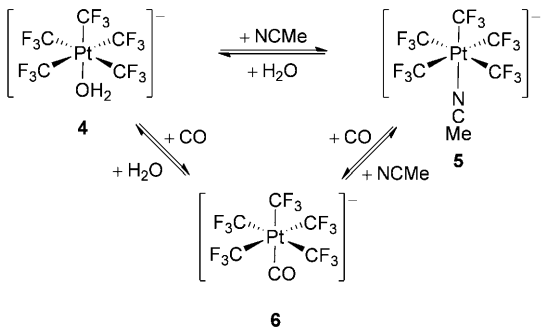


Scheme 6. Interrelationship between the organoplatinum(IV) compounds **4**, **5**, and **6** through reversible ligand substitution processes ($[NBu_4]^+$ is the counterion in all cases).

  

From any of these solutions, compound **6** can be isolated as a white solid in around 65% yield.

Carbon monoxide is a ubiquitous ligand in organometallic chemistry and particularly in the platinum group metals. The starting point of this fruitful and enormously developed area was marked precisely by the synthesis of a number of $Pt^{II}$ carbonyl derivatives by P. Schützenberger in the second half of the nineteenth century.[39] In addition to being a poor σ-donor and a good π-acceptor ligand, CO is a well-known reducing agent. For instance, the action of CO on $PtX'_4$ in nonaqueous media, $SOCl_2$ (X′=Cl)[40] or $HSO_3F$ (X′=$SO_3F$),[41] causes the reduction of high-valent $Pt^{IV}$ to $Pt^{II}$ [Eq. (1)].

$$Pt^{IV}X'_4 + 3\,CO \rightarrow \textit{cis}\text{-}[Pt^{II}X'_2(CO)_2] + COX'_2 \quad (X' = Cl,\ SO_3F) \qquad (1)$$

Considering the reducing ability of CO, it is not surprising that carbonyl derivatives of $Pt^{IV}$ remain rare species even today. Complexes $[PtX_5(CO)]^-$ (X=Cl, Br) were first detected in solution,[42] and then the salt $[NH_2iPr_2][PtCl_5(CO)]$ was isolated in the solid state.[43] To the best of our knowledge, the only $Pt^{IV}$ carbonyl compound for which the molecular structure has been established to date is [$NBu_4$]*trans*-$[Pt(C_6F_5)_4Br(CO)]$.[44] A characteristic feature of this kind of compound is a high ν(CO) value—well above that which corresponds to the free ligand: ν(CO)=2143 $cm^{-1}$.[45]

The IR spectrum of compound **6** shows a single, sharp absorption at 2194 $cm^{-1}$ in the solid state (KBr) and at 2189 $cm^{-1}$ in $CH_2Cl_2$ solution, assignable to the IR-active ν(CO) vibration mode ($A_1$). From a formal point of view, compound **6** can be considered to result from the oxidative addition of $F_3C{-}CF_3$ to the known organoplatinum(II) derivative [$NBu_4$][$Pt(CF_3)_3(CO)$].[46] This formal relationship is in line with the real process that relates the halo-carbonyl $Pt^{IV}$ compounds $[PtX_5(CO)]^-$ (X=Cl, Br) to their parent species $[PtX_3(CO)]^-$. The parallelism also applies to the spectroscopic effects observed upon oxidative addition of the X–X molecule (X=Cl, Br, $CF_3$) to the corresponding organoplatinum(II) precursor (Table 2), namely: 1) a substantial increase in the ν(CO) value (not reported in the case in which X=Br), and 2) a significant reduction in the $^1J(^{195}Pt,^{13}CO)$ value. Both effects are most prominent in the case of the $[Pt(CF_3)_5(CO)]^-/[Pt(CF_3)_3(CO)]^-$ couple, since: 1) the ν(CO) value of **6** is the highest described for any $Pt^{IV}$ carbonyl compound, and 2) an approximately 40% reduction in the $^1J(^{195}Pt,^{13}CO)$ value is observed upon going from $Pt^{II}$ to $Pt^{IV}$. The ν(CO) value of compound **6** in $CH_2Cl_2$ solution, ν(CO)=2189 $cm^{-1}$, is even higher than that reported for the isoleptic halo-carbonyl derivative $[PtCl_5(CO)]^-$ in the same medium: ν(CO)=2184 $cm^{-1}$ (Table 2). This experimental observation is in keeping with the slightly higher electronegativity assigned to the $CF_3$ group in the Pauling scale ($\chi$=3.49) in comparison with that ascribed to Cl ($\chi_{Cl}$=3.16).[47] This fact is at odds with the recently suggested classification of the $CF_3$ group as an excellent σ-donor ligand in organometallic chemistry (but not in organic chemistry!), with its σ-donor ability presumably exceeding those of hydrido or methyl ligands.[48] The electron-withdrawing effect of the $CF_3$ group is a well-established point both in organic and in organoelement chemistry.[49–51] The results of the aforementioned studies are obviously conflicting, and it can be concluded that additional factors other than those taken into account by those authors in their calculations might be operative.

The chemical shift of the carbonyl C atom suffers a considerable upfield shift upon going from the $Pt^{II}$ carbonyl derivative [$NBu_4$][$Pt(CF_3)_3(CO)$] ($\delta_C$=174.2 ppm) to the $Pt^{IV}$ one [$NBu_4$][$Pt(CF_3)_5(CO)$] ($\delta_C$=158.1 ppm) with a concomitant and important reduction in the $^1J(^{195}Pt,^{13}CO)$ value, which drops from 1103 ($Pt^{II}$) to 677 Hz ($Pt^{IV}$) (Table 2). The $^{19}F$ NMR spectrum of **6** shows the typical pattern associated with the (*OC*-6)-$[Pt(CF_3)_5(L)]^-$ unit already discussed (see above). The signal that corresponds to the equatorial $CF_3$ groups ($\delta_F$=−24.0 ppm) undergoes a sizable downfield shift with respect to the parent compounds **4** (L=$H_2O$) or **5** (L=NCMe), whereas the resonance that corresponds to the axial $CF_3$ group now appears upfield-shifted ($\delta_F$=−29.2 ppm). Thus, the overall spectrum resembles that of the iodo-derivative **1** more than those that correspond to the referred parent compounds.

Repeated attempts to obtain single crystals of **6** that could be suitable for X-ray diffraction purposes failed. Nevertheless, we were able to establish the molecular structure of the $[Pt(CF_3)_5(CO)]^-$ anion by an X-ray diffraction study on single crystals of the tetraarylphosphonium salt [$PPh_4$][$Pt(CF_3)_5(CO)$] (**6′**). The anion has an *OC*-6 structure

Table 2. Spectroscopic and structural data of the monocarbonyl $Pt^{II}/Pt^{IV}$ couples $[PtX'_3(CO)]^-/[PtX'_5(CO)]^-$ (X′=Cl, Br, $CF_3$).

| Compound | *d*(Pt–CO) [pm] | *d*(C–O) [pm] | ν(CO)[a] [$cm^{-1}$] | $\delta_C$(CO) [ppm] | $^1J(^{195}Pt,^{13}CO)$ [Hz] | Ref. |
|---|---|---|---|---|---|---|
| $[PtCl_3(CO)]^-$ | 182(1)[b] | 112(2)[b] | 2098 | 152.0 | 1732 | [60] |
| $[PtCl_5(CO)]^-$ | – | – | 2184 | 161.4 | 1267 | [42,61] |
| $[PtBr_3(CO)]^-$ | 186(1)[c] | 111(1)[c] | 2089 | 153.0 | 1720 | [60] |
| $[PtBr_5(CO)]^-$ | – | – | – | – | 1225 | [42] |
| $[Pt(CF_3)_3(CO)]^-$ | 191.3(4)[d] | 113.4(4)[d] | 2117 | 174.2 | 1103 | [46] |
| $[Pt(CF_3)_5(CO)]^-$ | 203.0(3)[e] | 107.2(4)[e] | 2189 | 158.1 | 677 | this work |

[a] All ν(CO) values are given in $CH_2Cl_2$ solution for comparison. [b] Structural parameters corresponding to the [$NBu_4$][$PtCl_3(CO)$] salt; see Ref. [62]. [c] Structural parameters corresponding to the [$NBu_4$][$PtBr_3(CO)$] salt; see Ref. [63]. [d] Structural parameters corresponding to the [$PPh_4$][$Pt(CF_3)_3(CO)$] salt. [e] Structural parameters corresponding to the [$PPh_4$][$Pt(CF_3)_5(CO)$] salt (**6′**) for which a ν(CO)=2200 $cm^{-1}$ is observed in the solid state.

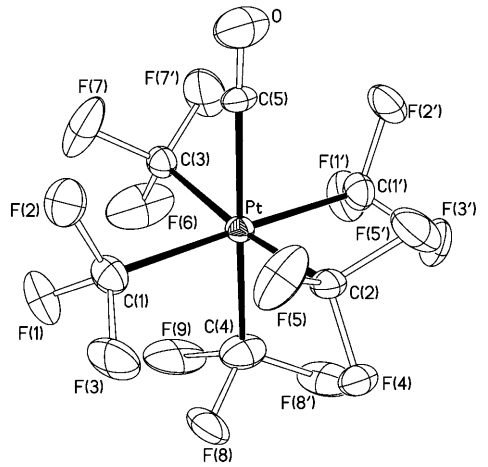


Figure 5. Thermal ellipsoid diagram (50% probability) of the $[Pt(CF_3)_5(CO)]^-$ anion as found in single crystals of **6′**. Selected bond lengths [pm] and angles [°] with estimated standard deviations: Pt–C(5) 203.0(3), Pt–C(ax) 206.0(4), average Pt–C(eq) 212.0(3), C(5)–O 107.2(4), average C(eq)–F 134.8(4), average C(ax)–F 135.3(5); C(4)-Pt-C(5) 178.3(1), Pt-C(5)-O 176.5(3).

(Figure 5) similar to that found in **5** (see above). The equatorial $CF_3$ groups also adopt a nearly planar arrangement (sum of angles between adjacent groups = 360.34(6)°) with an average value of Pt–C(eq) = 212.0(3) pm. Again the axial $CF_3$ group shows a significantly shorter bond to the metal: Pt–C(ax) = 206.0(4) pm. The terminal CO group is almost linearly coordinated: Pt-C(5)-O = 176.5(3)°. The Pt–CO distance, Pt–C(5) = 203.0(3) pm, is substantially longer than that found in the related square-planar $Pt^{II}$ carbonyl compound $[NBu_4][Pt(CF_3)_3(CO)]$ (Pt–CO = 191.3(4) pm).[46] It is also significantly longer than that observed in the only structurally characterized precedent of a $Pt^{IV}$ carbonyl derivative, namely, $[NBu_4]$*trans*-$[Pt(C_6F_5)_4Br(CO)]$, for which Pt–CO = 191(3) pm.[44] The long Pt–CO bond length found in **6′** is, in our opinion, the most salient feature of this molecular structure and is in keeping with the electrophilic character suggested by the high ν(CO) value (which appears shifted to 2200 $cm^{-1}$ in solid samples of **6′**; see Table 2) as well as with the known high *trans* influence exerted by the $CF_3$ ligand.[50] To the best of our knowledge, this is the longest Pt–CO bond length observed for any terminal carbonyl derivative of Pt reported so far[52,53]—including the highly electrophilic $Pt^{II}$ homoleptic species $[Pt(CO)_4][Sb_2F_{11}]_2$, for which an average value of Pt–CO = 198.2(9) pm had been observed.[54] Unusually long M–C bonds in metal carbonyl derivatives have been taken as evidence for the absence of M→CO π backbonding.[55] In line with this bonding scheme, the C–O distance (C(5)–O = 107.2(4) pm) is near the lower end recorded for the same kind of compound.[52,53] Finally, it is interesting to note that two of the F atoms belonging to two symmetry-related, *trans*-standing $CF_3$ groups are located close to the carbonyl C atom: C(5)···F(2) = 278.2 pm. Although this distance is considerably smaller than the sum of the corresponding van der Waals radii, $r_{vdW}(C)+r_{vdW}(F)$ = 319 pm,[56] it is not clear whether this can be taken as enough evidence to invoke the existence of a C···F secondary bonding interaction. In our opinion, it is not advisable to use intermolecular criteria (such as van der Waals radii) to decide on the existence of intramolecular phenomena.

In view of the long Pt–CO bond and the small $^1J(^{195}Pt,^{13}CO)$ value, it can be inferred that the CO ligand in **6**/**6′** is weakly bound to the Pt center. In contrast to these spectroscopic and structural properties, compound **6** is a thermally robust species that is stable up to 110°C in the solid state as revealed by thermogravimetric analysis. The CO molecule in **6** can be cleanly replaced by a number of ligands including $H_2O$ and MeCN. Thus, the reaction that leads to the synthesis of **6** (Scheme 6) can be reverted under suitable conditions, thereby regenerating the parent species **4** and **5** in each case. The oxidation state IV is preserved along these forward- and back-reaction processes. The reversible exchange of CO and $H_2O$ ligands seems particularly remarkable to us, since electrophilic carbonyl derivatives are highly water-sensitive species and usually undergo massive reductive processes when exposed to moisture. Thus, in the case of compound $[PtCl_5(CO)]^-$ "a prompt reaction with water was observed, with carbon dioxide being readily evolved."[43] The good behavior of compound **6** is to be attributed to the presence of the $CF_3$ groups that are especially suited to stabilizing high oxidation states.[12]

**Other related species**: The labile character of the $H_2O$ and MeCN ligands in compounds **4** and **5** has been further checked against a number of neutral (L′ = py, $PPh_3$, tht) and anionic (X = Cl, Br) ligands. Aside from $PPh_3$, which gave no sign of reaction at all (at least under the conditions essayed), all other ligands readily entered the Pt coordination sphere to afford (Scheme 7) singly or doubly charged com-

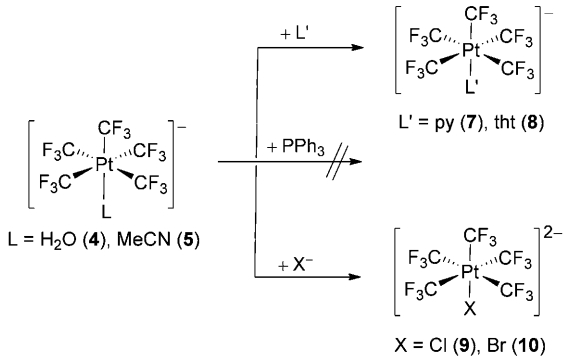


Scheme 7. Synthetic procedures to prepare compounds **7**–**10** ($[NBu_4]^+$ is the counterion in all cases).

pounds with formulae $[NBu_4][Pt(CF_3)_5(L')]$ [L′ = py (**7**), tht (**8**)] and $[NBu_4]_2[Pt(CF_3)_5X]$ [X = Cl (**9**), Br (**10**)]. All these compounds were isolated as fairly stable solids in reasonable yields.

The crystal and molecular structures of $[NBu_4][Pt(CF_3)_5(py)]$ (**7**) as a representative species of these series, were established by single-crystal X-ray diffraction methods.

  

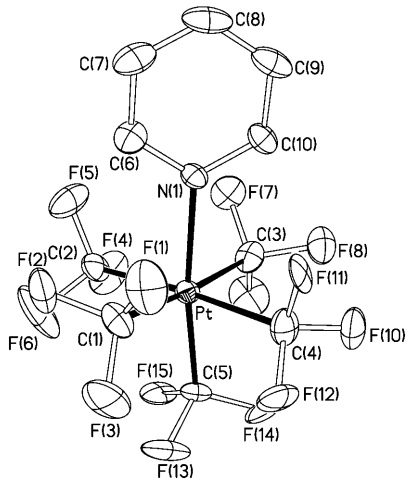


Figure 6. Thermal ellipsoid diagram (50% probability) of the [Pt-$(CF_3)_5$(py)]$^-$ anion as found in single crystals of **7**. Selected bond lengths [pm] and angles [°] with estimated standard deviations: Pt–N(1) 216.9(2), Pt–C(ax) 205.2(6), average Pt–C(eq) 210.7(3), average C(ax)–F 135.4(7), average C(eq)–F 135.7(4); C(5)-Pt-N(1) 171.3(2), Pt-N(1)-C(6) 121.5(2), Pt-N(1)-C(10) 120.6(2).

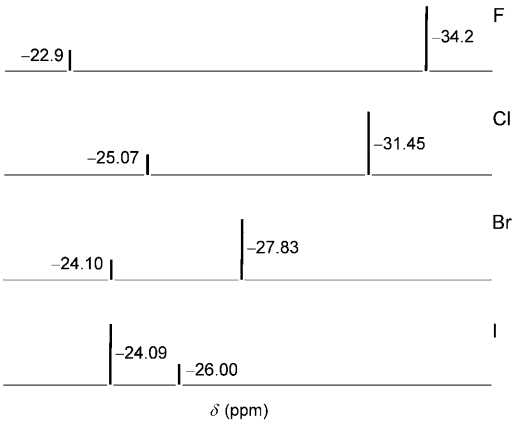


Figure 7. $^{19}$F NMR chemical shifts of the doubly charged species (*OC*-6)-$[Pt(CF_3)_5X]^{2-}$ (X = F, Cl, Br, I): $\delta_F$(ax) and $\delta_F$(eq) appear as short and long bars, respectively.

A drawing of the (*OC*-6)-$[Pt(CF_3)_5(py)]^-$ anion is given in Figure 6. The structural parameters associated with the "Pt-$(CF_3)_5$" unit are similar to those discussed above. The axial $CF_3$ group is once again closer to the Pt center than the equatorial ones by 5.5 pm on average. The py ring is almost perpendicular to the equatorial plane (interplanar angle = 86°) and adopts a staggered arrangement with respect to the equatorial $CF_3$ groups, nearly bisecting two of the nonadjacent *cis*-$[Pt(CF_3)_2]$ angles. It is reasonable to assume that this staggered arrangement adopted in the solid state is favored by steric factors. The overall structure of the [Pt-$(CF_3)_5$(py)]$^-$ anion bears much in common with that reported for the isoleptic species $[PtCl_5(py)]^-$,[57] the most noticeable difference between them being the considerably longer Pt–N distance found in **7** (216.9(2) pm) than in the chloro-derivative (206.2(4) pm). This difference is to be attributed to the higher *trans* influence of the $CF_3$ group with respect to the Cl ligand.[50]

We have at our disposal a rather homogeneous set of compounds with formula $[Pt(CF_3)_5(L)]^{q-}$ ($q = 1$, 2) and nearly axial symmetry, the spectroscopic properties of which will depend upon the variation of just a single ligand, L. Given the stoichiometry and stereochemistry of these compounds, their equatorial and axial $CF_3$ groups can act as sensitive probes for the *trans* and *cis* influences of the differentiating L ligand. We will try to rationalize the observed differences in terms of fundamental parameters in use in coordination chemistry; the careful work of H. C. Clark is taken as a basis on the subject.[50] The data of our halo-compounds $[Pt(CF_3)_5X]^{2-}$ (X = Cl, Br, I) can be supplemented with those attributed to the nonisolated fluoro-derivative [Pt-$(CF_3)_5F]^{2-}$.[19] The $^{19}$F chemical shifts for the whole series of halo-compounds is depicted in Figure 7. It can be clearly seen that the $\delta_F$(eq) values show a qualitative correlation with the halide electronegativity. The $\delta_F$(ax) values, however, show no straightforward trend. The large downfield shift experienced by α-F atoms in perfluoroalkyl-metal derivatives, [M]–$CF_2R$, has been assigned mainly to paramagnetic screening from overlap between filled F(p) and M(d) orbitals.[58] Increasing the electronegativity of the X ligand in $[Pt(CF_3)_5X]^{2-}$ should result in less electron density on the Pt atom, a contraction of d orbitals and diminished F(p)–M(d) overlap, hence a less shifted $\delta_F$ value as is, in fact, observed for the $CF_3$(eq) groups. This postulation is in keeping with the Pt center being more shielded in the order: $\delta_{Pt} = -1667$ (F) > −2128 (Cl) > −2219 (Br) > −2446 (I) ppm. The apparently erratic placement of $CF_3$(ax) signals is to be attributed to additional factors that relate to the σ- and π-donor abilities of the *trans*-standing X ligand. The dependence of $^2J(^{195}Pt,^{19}F)$ values for the $CF_3$(ax) groups is not clear either: virtually the same values (470 Hz) are observed for F, Cl, and Br, whereas for I it drops to 452 Hz. Again the $CF_3$(eq) groups show a more coherent tendency with the following $^2J(^{195}Pt,^{19}F)$ values: 270 (F) < 281 (Cl) < 284 (Br) < 288 Hz (I). The much lower $^2J(^{195}Pt,^{19}F)$ values observed for the equatorial than for the axial $CF_3$ groups can be attributed to the significantly shorter Pt–C bond lengths found for the latter within the same chemical species.

The series of singly charged species $[Pt(CF_3)_5(L)]^-$ (L = $H_2O$, MeCN, CO, py, tht) show a similar spectroscopic behavior (Table 1, Figure 8). Again, the $^2J(^{195}Pt,^{19}F)$ values that correspond to the $CF_3$(eq) groups are rather insensitive to the nature of the L ligand (263–270 Hz), whereas those that correspond to $CF_3$(ax) have a wider range of variation (484–578 Hz). If our explanation of the spectroscopic features of the halo-derivatives given above is correct, the electron density at the Pt center should be in the following order of donor ligand: $OH_2$ < py < NCMe < tht < CO in attendance to the corresponding $\delta_F$(eq) values (Figure 8). This inference is in line with the chemical shifts of the $^{195}$Pt nuclei: $\delta_{Pt} = -1785$ ($OH_2$) > −1872 (py) > −2070 (NCMe) > −2283 (tht) > −2650 ppm (CO). The qualitative correlation ob-

  

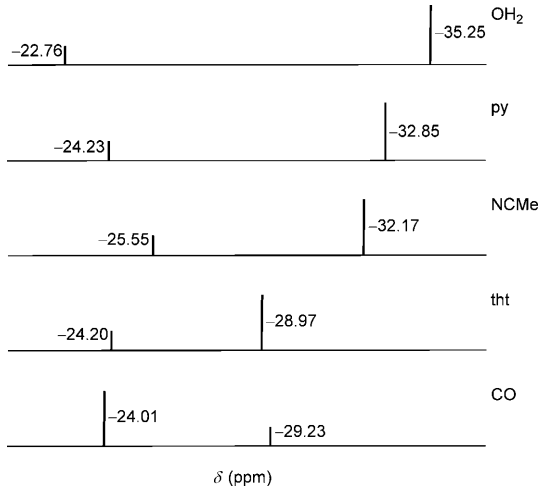


Figure 8. $^{19}F$ NMR chemical shifts of the singly-charged species (*OC*-6)-$[Pt(CF_3)_5(L)]^-$ (L = $H_2O$, py, MeCN, tht, CO): $\delta_F$(ax) and $\delta_F$(eq) appear as short and long bars, respectively.

served between the $\delta_F$(eq) and $\delta_{Pt}$ values is quite apparent. In spite of that, we consider the position of CO within this series to be anomalous, since this ligand is known as a poor σ donor and good π acceptor. It is not uncommon that π-acceptor ligands do not fit the general trend.

All our attempts to replace one of the heteroligands **L** or X by an additional $CF_3$ group with an aim to prepare the anionic species $[Pt(CF_3)_6]^{2-}$ have failed so far. Thus, treatment of compound **2** or **7** with a slight excess amount of the nucleophilic trifluoromethylating agent $[Me_3Si(CF_3)F]^-$ generated in situ by fluoride coordination to $Me_3SiCF_3$ at low temperature produced no reaction at all. The reaction of **2** with $Ag(CF_3)$[59] in MeCN carried out between −40 °C and room temperature just gave rise to a mixture of compounds **2** and **5**. The homoleptic organoplatinum(IV) derivative $[Pt(CF_3)_6]^{2-}$ appears to have been detected in solution[19] and it would be expected to exhibit a high chemical stability and an extremely low coordination ability. The possibility of isolating this fascinating species seems to await the design of a suitable synthetic strategy that would enable its efficient preparation.

## Conclusion

Compound $[NBu_4]_2[Pt(CF_3)_5I]$ (**2**) has been obtained by oxidative addition of $CF_3I$ to the homoleptic organoplatinum(II) derivative $[NBu_4]_2[Pt(CF_3)_4]$ (**1**) under mild conditions. This oxidative-addition process is suggested to occur in a *trans* fashion given that a similar reaction using $nC_4F_9I$ as the organic substrate afforded $[NBu_4]_2$*trans*-$[Pt(CF_3)_4(nC_4F_9)I]$ (**3**).

The solvento derivatives $[NBu_4][Pt(CF_3)_5(OH_2)]$ (**4**) and $[NBu_4][Pt(CF_3)_5(NCMe)]$ (**5**) are readily obtained by reaction of **2** with $Ag^+$ salts of weakly coordinating anions in the presence of $H_2O$ or MeCN, respectively. The aquo and nitrile ligands in compounds **4** and **5** are labile and can be replaced by a number of neutral or anionic ligands, thereby affording a series of singly or doubly charged compounds with formulae $[NBu_4][Pt(CF_3)_5(L)]$ (L = CO (**6**), py (**7**), tht (**8**)) and $[NBu_4]_2[Pt(CF_3)_5X]$ (X = Cl (**9**), Br (**10**)). All our attempts to replace one of the heteroligands L or X by an additional $CF_3$ group have failed so far. Nevertheless, we continue to strive to devise a synthetic procedure to prepare the homoleptic organoplatinum(IV) derivative $[Pt(CF_3)_6]^{2-}$, for which a high chemical stability and a low coordination ability would be anticipated. All the pentakis(trifluoromethyl)platinate(IV) compounds $[Pt(CF_3)_5(L)]^{q-}$ ($q = 1, 2$) reported here have been isolated as fairly stable solids in high yields and have been characterized by analytic and spectroscopic methods—$^{19}F$ NMR spectroscopy being an especially convenient one. Characterization includes the crystal and molecular structures of compounds **2**, **5**, $[PPh_4][Pt(CF_3)_5(CO)]$ (**6′**) and **7**.

Of particular importance is the unexpected thermal stability and chemical behavior of the $Pt^{IV}$ carbonyl derivative **6**/**6′**, especially considering that all structural and spectroscopic features associated with the Pt−CO unit point to the near absence of M→CO π backbonding: 1) a high ν(CO) value in IR spectroscopy; 2) a low chemical shift, $\delta_C$, for the carbonyl C atom in $^{13}C$ NMR spectroscopy; 3) a small $^1J(^{195}Pt,^{13}C)$ coupling constant; 4) a long Pt−CO bond length; and 5) a short C−O internuclear distance.

Compound **2** has shown itself to be a convenient entry into the chemistry of highly trifluoromethylated platinum complexes. To the best of our knowledge, compounds **2** and **4**–**10** reported in this paper are the mononuclear derivatives with the highest $CF_3$ content across the periodic table to have been isolated and adequately characterized to date.

## Experimental Section

**General procedures and materials**: Unless otherwise stated, the reactions and manipulations were carried out under purified argon using Schlenk techniques. Solvents were dried using an MBraun SPS-800 System. Compound $[NBu_4]_2[Pt(CF_3)_4]$ (**1**) was obtained as described elsewhere.[12] Perfluoroalkyl iodides $CF_3I$ (Aldrich) and $nC_4F_9I$ (Acros Organics) were purchased and used as received. Elemental analyses were carried out using a Perkin–Elmer 2400 CHNS/O Series II microanalyzer. IR spectra of KBr discs were recorded using the following Perkin–Elmer spectrophotometers: 883 (4000–200 $cm^{-1}$) or Spectrum One (4000–350 $cm^{-1}$). Mass spectra were registered by MALDI-TOF techniques using Bruker MicroFlex or AutoFlex spectrometers. NMR spectra were recorded using any of the following spectrometers: Varian Gemini-300, Bruker ARX 300, or Bruker ARX 400. Unless otherwise stated, the spectroscopic measurements were carried out at room temperature. Chemical shifts of the measured nuclei ($\delta$ in ppm) are given with respect to the standard references in use: $SiMe_4$ ($^1H$ and $^{13}C$), $CFCl_3$ ($^{19}F$), and 2 M aqueous $Na_2[PtCl_6]$ solution ($^{195}Pt$). NMR spectroscopic parameters associated with the cations are unexceptional and are therefore omitted. The NMR spectroscopic parameters associated with the "$Pt(CF_3)_5$" core in compounds **2** and **4**–**10** are to be found in Table 1 and are therefore omitted in the corresponding synthetic entry.

*Safety note*: Although we have not encountered any problems working under the conditions detailed below, perchlorate salts are potentially explosive when in contact with organic solvents and ligands. For this

  

reason, only small amounts of these materials should be prepared and they should always be handled with great caution.[64]

**Synthesis of $[NBu_4]_2[Pt(CF_3)_5I]$ (2)**: $CF_3I$ dissolved in *n*-hexane (0.78 mmol) was added to a solution of **1** (0.25 g, 0.26 mmol) in MeCN (15 mL) at room temperature. After 24 h of stirring, the solution was concentrated to dryness. Treatment of the resulting residue with *i*PrOH (3 mL) at 0 °C rendered a light yellow solid, which was filtered, washed with *n*-hexane (3×3 mL), dried in vacuo, and identified as **2** (0.23 g, 0.20 mmol, 77 % yield). IR (KBr): $\tilde{\nu}$ = 2964 (s), 2877 (m), 1486 (m), 1476 (m), 1382 (w), 1261 (w), 1168 (s), 1151 (w), 1092 (vs), 1069 (vs), 1031 (s), 882 (w; $[NBu_4]^+$), 802 (w), 741 (w; $[NBu_4]^+$), 326 $cm^{-1}$ (w); MS (MALDI−): *m/z*: 598 $[Pt(CF_3)_4I]^-$, 540 $[Pt(CF_3)_5]^-$, 490 $[Pt(CF_3)_4F]^-$, 452 $[Pt(CF_3)_3(CF_2)]^-$, 440 $[Pt(CF_3)_3F_2]^-$, 402 $[Pt(CF_3)_3]^-$; elemental analysis calcd (%) for $C_{37}H_{72}F_{15}IN_2Pt$: C 38.6, H 6.3, N 2.4; found: C 38.8, H 6.1, N 2.5.

Crystals suitable for X-ray diffraction analysis with formula $[NBu_4]_2[Pt(CF_3)_5I]\cdot CH_2Cl_2$ were obtained by slow diffusion of a layer of *n*-hexane (15 $cm^3$) into a solution of **2** (15 mg) in $CH_2Cl_2$ (5 mL) at 4 °C.

**Synthesis of $[PPh_4]_2[Pt(CF_3)_5I]$ (2′)**: Addition of a solution of $[PPh_4]Br$ (0.11 g, 0.26 mmol) in *i*PrOH (3 mL) to a solution of **2** (0.15 g, 0.13 mmol) in $Me_2CO$ (5 mL) caused the immediate precipitation of a white solid, which was filtered, washed with *n*-hexane (3×3 mL), dried in vacuo, and identified as **2′** (0.15 g, 0.11 mmol, 85 % yield). Multinuclear NMR spectroscopic data associated with the $[Pt(CF_3)_5I]^{2-}$ ion are in keeping with those found for the $[NBu_4]^+$ salt (**2**). IR (KBr): $\tilde{\nu}$ = 1586 (w), 1484 (w), 1441 (m), 1339 (w), 1191 (w), 1167 (m), 1106 (sh), 1091 (vs), 1069 (vs), 1061 (vs), 1032 (s), 997 (m), 762 (w), 756 (w), 723 (s), 688 (m), 528 $cm^{-1}$ (s); elemental analysis calcd (%) for $C_{53}H_{40}F_{15}IP_2Pt$: C 47.3, H 3.0; found: C 47.0, H 2.8.

**Reaction of 1 with $nC_4F_9I$**: $nC_4F_9I$ (55 $mm^3$, 0.31 mmol) was added to a solution of **1** (0.25 g, 0.26 mmol) in MeCN (15 mL) at room temperature, and the reaction progress was monitored by $^{19}F$ NMR spectroscopy. After 24 h, compound **1** had been totally consumed and had been transformed into a mixture of species **3** and *post*-**3** in a 2:1 integrated ratio. Compound **3** completely evolved into *post*-**3** in a 36 h lapse. Addition of $AgSO_3CF_3$ to the latter solutions caused immediate precipitation of a yellow solid (AgI) with no effect on the $^{19}F$ NMR spectroscopic signals that corresponded to the "$Pt(CF_3)_4(nC_4F_9)$" unit. $^{19}F$ NMR of **3** ([$D_3$] acetonitrile): $\delta$ = −21.2 (tt, $^4J(^{19}F,^{19}F)$ = 10.7 Hz, $^5J(^{19}F,^{19}F)$ = 8.25 Hz, $^2J(^{195}Pt,^{19}F)$ = 287 Hz, 12F; Pt−$CF_3$), −76.4 (m, $^2J(^{195}Pt,^{19}F)$ = 273 Hz, 2F; α-$CF_2$), −81.4 (tt, $^3J(^{19}F,^{19}F)$ = 10.3 Hz, $^4J(^{19}F,^{19}F)$ = 4.8 Hz, 3F; $CF_2CF_3$), −118.1 (br, 2F; γ-$CF_2$), −124.7 ppm (m, $^3J(^{19}F^{\beta},^{19}F^{\gamma})$ = 19.8 Hz, 2F; β-$CF_2$); $^{19}F$ NMR of *post*-**3** ([$D_3$]acetonitrile): $\delta$ = −30.5 (tt, $^4J(^{19}F,^{19}F)$ = 8.2 Hz, $^5J(^{19}F,^{19}F)$ = 7.1 Hz, $^2J(^{195}Pt,^{19}F)$ = 265 Hz, 12F; Pt−$CF_3$), −77.2 (m, $^3J(^{19}F,^{19}F)\approx$ 18 Hz, $^2J(^{195}Pt,^{19}F)$ = 326 Hz, 2F; α-$CF_2$), −81.6 (tt, $^3J(^{19}F,^{19}F)$ = 10.1 Hz, $^4J(^{19}F,^{19}F)$ = 4.8 Hz, 3F; $CF_2CF_3$), −119.4 (br, 2F; γ-$CF_2$), −125.2 ppm (m, $^3J(^{19}F^{\beta},^{19}F^{\gamma})$ = 19.3 Hz, 2F; β-$CF_2$).

**Synthesis of $[NBu_4][Pt(CF_3)_5(OH_2)]$ (4)**: The addition of $AgSO_3CF_3$ (56 mg, 0.22 mmol) to a solution of **2** (0.25 g, 0.22 mmol) in $Me_2CO$ (15 mL) at room temperature and under light exclusion resulted in the abundant precipitation of a yellow solid (AgI). After 2 h of stirring, the precipitate was filtered off and the filtrate was concentrated under an air stream. Treatment of the resulting residue with *i*PrOH (3 mL) at 0 °C rendered a white solid, which was filtered, washed with *n*-hexane (3× 3 mL), dried in vacuo, and identified as **4** (0.13 g, 0.16 mmol, 73 % yield). IR (KBr): $\tilde{\nu}$ = 3613 (w), 3540 (w), 2970 (m), 2881 (w), 1610 (w), 1476 (m), 1384 (w), 1198 (s), 1125 (vs), 1106 (vs), 1068 (vs), 895 (w), 886 (w; $[NBu_4]^+$), 802 (w), 739 (m; $[NBu_4]^+$), 711 (w), 335 $cm^{-1}$ (w); MS (MALDI−): *m/z*: 540 $[Pt(CF_3)_5]^-$; elemental analysis calcd (%) for $C_{21}H_{38}F_{15}NOPt$: C 31.5, H 4.8, N 1.75; found: C 31.8, H 4.9, N 1.8.

**Synthesis of $[PPh_4][Pt(CF_3)_5(OH_2)]$ (4′)**: Using the procedure just described for synthesizing **4**, compound **4′** was prepared starting from **2′** (0.15 g, 0.11 mmol) and $AgSO_3CF_3$ (29 mg, 0.11 mmol). Complex **4′** was obtained by precipitation with an *i*PrOH/$H_2O$ mixture (4+2 mL) as a white solid (0.08 g, 0.09 mmol, 82 % yield). Multinuclear NMR spectroscopic data associated with the $[Pt(CF_3)_5(OH_2)]^-$ ion are in keeping with those found for the $[NBu_4]^+$ salt (**4**). IR (KBr): $\tilde{\nu}$ = 3602 (w), 3530 (w), 1587 (w), 1485 (w), 1439 (m), 1227 (w), 1196 (m), 1114 (vs), 1095 (vs), 1058 (vs), 1032 (s), 996 (m), 760 (w), 725 (s), 689 (s), 527 $cm^{-1}$ (vs); elemental analysis calcd (%) for $C_{29}H_{22}F_{15}OPPt$: C 38.8, H 2.5; found: C 39.0, H 2.5.

**Synthesis of $[NBu_4][Pt(CF_3)_5(NCMe)]$ (5)**: The addition of $AgClO_4$ (45 mg, 0.22 mmol) to a solution of **2** (0.25 g, 0.22 mmol) in MeCN (15 mL) at room temperature and under light exclusion resulted in the abundant precipitation of a yellow solid (AgI). After 20 min of stirring, the precipitate was filtered off and the filtrate was concentrated to dryness under vacuum. Treatment of the resulting residue with *i*PrOH (3 mL) at 0 °C rendered a light yellow solid, which was filtered, washed with *n*-hexane (3×3 mL), dried in vacuo, and identified as **5** (0.14 g, 0.17 mmol, 77 % yield). $^1H$ NMR ([$D_6$] < acetone): $\delta$ = 2.61 ppm (s, $^4J(^{195}Pt,^1H)$ = 6 Hz, 3H; Me); $^{13}C\{^1H\}$ NMR ([$D_6$]acetone): $\delta$ = 2.0 ppm (s; Me);[65] IR (KBr): $\tilde{\nu}$ = 2968 (m), 2881 (w), 2347 (w; ν(N≡C)), 1474 (m), 1384 (w), 1189 (s), 1164 (m), 1102 (vs), 1084 (sh), 1048 (vs), 881 (w; $[NBu_4]^+$), 800 (w), 738 (m; $[NBu_4]^+$), 712 (w), 666 (w), 623 (w), 334 $cm^{-1}$ (w); MS (MALDI): *m/z*: 540 $[Pt(CF_3)_5]^-$, 490 $[Pt(CF_3)_4F]^-$, 440 $[Pt(CF_3)_3F_2]^-$; elemental analysis calcd (%) for $C_{23}H_{39}F_{15}N_2Pt$: C 33.5, H 4.8, N 3.4; found: C 33.45, H 4.6, N 3.2.

Crystals suitable for X-ray diffraction analysis were obtained by slow diffusion of a layer of *n*-hexane (15 $cm^3$) into a solution of **5** (15 mg) in $CH_2Cl_2$ (5 $cm^3$) at 4 °C.

**Synthesis of $[NBu_4][Pt(CF_3)_5(CO)]$ (6)**: A solution of **4** (0.25 g, 0.31 mmol) in $CH_2Cl_2$ (15 $cm^3$) at room temperature was allowed to react with CO at atmospheric pressure. After 48 h, the reaction medium was concentrated to dryness under vacuum. Treatment of the resulting residue with *n*-hexane (3 $cm^3$) rendered a white solid, which was filtered, washed with further portions of *n*-hexane (3×3 $cm^3$), dried in vacuo, and identified as **6** (0.16 g, 0.20 mmol, 64 % yield). $^{13}C\{^{19}F\}$ NMR ([$D_2$]dichloromethane): $\delta$ = 158.1 ppm ($^1J(^{195}Pt,^{13}C)$ = 677 Hz; CO); IR (KBr): $\tilde{\nu}$ = 2970 (m), 2881 (w), 2194 (s; ν(C≡O)), 1476 (m), 1384 (w), 1190 (s), 1120 (vs), 1098 (vs), 1075 (vs), 884 (w; $[NBu_4]^+$), 799 (w), 738 (w; $[NBu_4]^+$), 713 (w), 638 (w), 452 (w), 322 $cm^{-1}$ (w); MS (MALDI−): *m/z*: 540 $[Pt(CF_3)_5]^-$, 490 $[Pt(CF_3)_4F]^-$, 440 $[Pt(CF_3)_3F_2]^-$, 402 $[Pt(CF_3)_3]^-$, 352 $[Pt(CF_3)_2F]^-$; elemental analysis calcd (%) for $C_{22}H_{36}F_{15}NOPt$: C 32.6, H 4.5, N 1.7; found: C 32.5, H 4.5, N 1.7.

**Synthesis of $[PPh_4][Pt(CF_3)_5(CO)]$ (6′)**: Using the procedure just described for synthesizing **6**, compound **6′** was prepared starting from **4′** (0.15 g, 0.17 mmol). Compound **6′** was obtained as a white solid (0.11 g, 0.12 mmol, 71 % yield). Multinuclear NMR spectroscopic data associated with the $[Pt(CF_3)_5(CO)]^-$ anion are in keeping with those found for the $[NBu_4]^+$ salt (**6**). IR (KBr): $\tilde{\nu}$ = 2200 (s; ν(C≡O)), 1587 (w), 1484 (w), 1439 (m), 1187 (s), 1121 (vs), 1100 (vs), 1070 (vs), 1032 (s), 995 (m), 759 (w), 725 (s), 689 (s), 527 (vs), 450 (w), 322 $cm^{-1}$ (w); elemental analysis calcd (%) for $C_{30}H_{20}F_{15}OPPt$: C 39.7, H 2.2; found: C 39.9, H 2.3.

Crystals suitable for X-ray diffraction analysis were obtained by slow diffusion of a layer of *n*-hexane (15 $cm^3$) into a solution of **6′** (15 mg) in $CH_2Cl_2$ (5 $cm^3$) at 4 °C.

**Synthesis of $[NBu_4][Pt(CF_3)_5(py)]$ (7)**

*Method A*: $AgSO_3CF_3$ (56 mg, 0.22 mmol) was added to a solution of **2** (0.25 g, 0.22 mmol) in $Me_2CO$ (15 mL) at room temperature and under light exclusion and, after 30 min of stirring, the yellow precipitate (AgI) was filtered off. Following this, py (52 $mm^3$, 0.65 mmol) was added to the colorless filtrate and, after 24 h of stirring, the reaction medium was concentrated to dryness. Treatment of the resulting residue with *i*PrOH (3 mL) at 0 °C rendered a white solid, which was filtered, washed with *n*-hexane (3×3 mL), dried in vacuo, and identified as **7** (0.15 g, 0.17 mmol, 77 % yield). $^1H$ NMR ([$D_6$]acetone): $\delta$ = 9.06 (dd, $^3J(^1H,^1H)$ = 5.9 Hz, $^4J(^1H,^1H)$ = 1.3 Hz, $^3J(^{195}Pt,^1H)$ = 14 Hz, 2H; $H^{ortho}$), 8.08 (tt, $^3J(^1H,^1H)$ = 7.6 Hz, 1H; $H^{para}$), 7.54 ppm (td, 2H; $H^{meta}$); $^{13}C\{^1H\}$ NMR ([$D_6$]acetone): $\delta$ = 155.2 (s; $C^{meta}$), 140.2 (s; $C^{para}$), 124.7 ppm (s, $^2J(^{195}Pt,^{13}C)$ = 13 Hz; $C^{ortho}$); IR (KBr): $\tilde{\nu}$ = 2968 (m), 2880 (w), 1616 (w), 1475 (m), 1457 (w), 1384 (w), 1184 (s), 1126 (vs), 1096 (vs), 1062 (vs), 1044 (vs), 1017 (s), 886 (w; $[NBu_4]^+$), 875 (w), 799 (w), 766 (m), 738 (w; $[NBu_4]^+$), 714 (w), 705 (w), 641 $cm^{-1}$ (w); MS (MALDI−): *m/z*: 540 $[Pt(CF_3)_5]^-$; elemental analysis calcd (%) for $C_{26}H_{41}F_{15}N_2Pt$: C 36.2, H 4.8, N 3.25; found: C 36.0, H 4.6, N 3.15.

*Method B*: Pyridine (60 mm$^3$, 0.75 mmol) was added to a solution of **4** (0.2 g, 0.25 mmol) in $Me_2CO$ (15 mL) at room temperature. After 24 h of stirring, the solution was concentrated to dryness. Treatment of the resulting residue with *i*PrOH (3 mL) at 0 °C rendered a white solid, which was filtered, washed with *n*-hexane (3×3 mL), dried in vacuo, and identified as **7** (0.15 g, 0.17 mmol, 68 % yield).

Crystals suitable for X-ray diffraction analysis were obtained by slow evaporation of a solution of **7** (5 mg) in $CHCl_3$ (2 mL) at room temperature.

**Synthesis of $[NBu_4][Pt(CF_3)_5(tht)]$ (8)**: Tetrahydrothiophene (tht; 54 mm$^3$, 0.61 mmol) was added to a solution of **5** (0.25 g, 0.30 mmol) in $Me_2CO$ (15 mL) at room temperature. After 24 h of stirring, the solution was concentrated to dryness. Treatment of the resulting residue with $Et_2O$ (5 mL) at 0 °C rendered a white solid, which was filtered, dried in vacuo, and identified as **8** (0.24 g, 0.27 mmol, 90 % yield). $^1$H NMR ([D$_2$]dichloromethane): $\delta = 3.09$ (m, 4H; α-$CH_2$), 1.92 ppm (m, 4H; β-$CH_2$); $^{13}$C{$^1$H} NMR ([D$_2$]dichloromethane): $\delta = 38.1$ (s; α-$CH_2$), 29.2 ppm (s; β-$CH_2$); IR (KBr): $\tilde{\nu} = 2968$ (m), 2880 (w), 1474 (m), 1384 (w), 1262 (w), 1178 (s), 1112 (vs), 1092 (vs), 1066 (vs), 1051 (vs), 964 (w), 895 (w), 882 (w; $[NBu_4]^+$), 804 (w), 740 (w; $[NBu_4]^+$), 729 (w), 712 (w), 662 (w), 330 cm$^{-1}$ (w); MS (MALDI−): *m*/*z*: 540 $[Pt(CF_3)_5]^-$, 490 $[Pt(CF_3)_4F]^-$, 440 $[Pt(CF_3)_3F_2]^-$, 402 $[Pt(CF_3)_3]^-$, 352 $[Pt(CF_3)_2F]^-$; elemental analysis calcd (%) for $C_{25}H_{44}F_{15}NPtS$: C 34.5, H 5.1, N 1.6, S 3.7; found: C 34.2, H 5.3, N 1.85, S 3.5.

**Synthesis of $[NBu_4]_2[Pt(CF_3)_5Cl]$ (9)**: $[NBu_4]Cl$ (0.43 g, 1.56 mmol) was added to a solution of **4** (0.25 g, 0.31 mmol) in $Me_2CO$ (15 mL) at room temperature. After 10 days of stirring, the solution was concentrated to dryness. Treatment of the resulting residue with *i*PrOH (3 mL) at 0 °C rendered a white solid, which was filtered, washed with *n*-hexane (3× 3 mL), dried in vacuo, and identified as **9** (0.26 g, 0.24 mmol, 77 % yield). IR (KBr): $\tilde{\nu} = 2963$ (s), 2877 (m), 1484 (m), 1474 (m), 1382 (w), 1179 (m), 1163 (w), 1096 (vs), 1081 (vs), 1034 (s), 882 (w; $[NBu_4]^+$), 802 (w), 741 (w; $[NBu_4]^+$), 344 (w; ν(Pt−Cl)), 330 cm$^{-1}$ (w); MS (MALDI−): *m*/*z*: 540 $[Pt(CF_3)_5]^-$, 506 $[Pt(CF_3)_4Cl]^-$, 490 $[Pt(CF_3)_4F]^-$; elemental analysis calcd (%) for $C_{37}H_{72}ClF_{15}N_2Pt$: C 41.9, H 6.8, N 2.6; found: C 42.4, H 7.2, N 2.6.

**Synthesis of $[NBu_4]_2[Pt(CF_3)_5Br]$ (10)**: $[NBu_4]Br$ (0.20 g, 0.62 mmol) was added to a solution of **4** (0.25 g, 0.31 mmol) in $Me_2CO$ (15 mL) at room temperature, and the resulting mixture was warmed for 48 h in an oil bath at 60 °C. The solution was then concentrated to dryness. Treatment of the resulting residue with *i*PrOH (3 cm$^3$) at 0 °C rendered a white solid, which was filtered, washed with *n*-hexane (3×3 mL), dried in vacuo, and identified as **10** (0.30 g, 0.27 mmol, 87 % yield). IR (KBr): $\tilde{\nu} =$ 2964 (m), 2877 (w), 1616 (w), 1485 (m), 1475 (m), 1382 (w), 1175 (s), 1094 (vs), 1050 (vs), 1032 (vs), 882 (w; $[NBu_4]^+$), 800 (w), 741 (w; $[NBu_4]^+$), 710 (w), 338 (w), 328 cm$^{-1}$ (w); MS (MALDI−): *m*/*z*: 550 $[Pt(CF_3)_4Br]^-$, 540 $[Pt(CF_3)_5]^-$, 490 $[Pt(CF_3)_4F]^-$, 402 $[Pt(CF_3)_3]^-$; elemental analysis calcd (%) for $C_{37}H_{72}BrF_{15}N_2Pt$: C 40.2, H 6.6, N 2.5; found: C 40.25, H 6.55, N 2.6.

Table 3. Crystal data and structure refinement for **2**·$CH_2Cl_2$, **5**, **6′**, and **7**.

| | **2**·$CH_2Cl_2$ | **5** | **6′** | **7** |
|---|---|---|---|---|
| formula | $C_{37}H_{72}F_{15}IN_2Pt{\cdot}CH_2Cl_2$ | $C_{23}H_{39}F_{15}N_2Pt$ | $C_{30}H_{20}F_{15}OPPt$ | $C_{26}H_{41}F_{15}N_2Pt$ |
| $M_r$ | 1236.88 | 823.65 | 907.52 | 861.70 |
| $T$ [K] | 100(2) | 100(2) | 100(2) | 123(2) |
| crystal system | monoclinic | triclinic | orthorhombic | orthorhombic |
| space group | *C*2/*c* | $P\bar{1}$ | *Pbcm* | *Pbca* |
| *a* [pm] | 1980.96(4) | 1059.52(2) | 750.514(7) | 1628.65(1) |
| *b* [pm] | 1554.28(2) | 1228.60(2) | 1774.046(15) | 1939.17(1) |
| *c* [pm] | 1888.98(4) | 1256.72(2) | 2273.92(2) | 2051.64(2) |
| α [°] | 90 | 69.364(2) | 90 | 90 |
| β [°] | 120.787(3) | 89.393(2) | 90 | 90 |
| γ [°] | 90 | 88.457(2) | 90 | 90 |
| $V$ [nm$^3$] | 4996.47(16) | 1530.39(5) | 3027.60(5) | 6479.55(8) |
| $Z$ | 4 | 2 | 4 | 8 |
| $\rho_{calcd}$ [g cm$^{-3}$] | 1.644 | 1.787 | 1.991 | 1.767 |
| $\mu$ [mm$^{-1}$] | 3.617 | 4.692 | 4.805 | 4.437 |
| $F$(000) | 2464 | 808 | 1744 | 3392 |
| 2θ range [°] | 7.6–57.9 | 8.4–57.8 | 8.5–57.8 | 8.4–57.8 |
| index range | $-25 \le h \le 26$ | $-13 \le h \le 13$ | $-10 \le h \le 10$ | $-22 \le h \le 21$ |
| | $-21 \le k \le 19$ | $-16 \le k \le 16$ | $-24 \le k \le 23$ | $-25 \le k \le 26$ |
| | $-25 \le l \le 25$ | $-16 \le l \le 16$ | $-30 \le l \le 30$ | $-27 \le l \le 27$ |
| reflns collected | 27658 | 26743 | 62303 | 133552 |
| unique reflns | 6053 | 7252 | 3906 | 8207 |
| $R$(int) | 0.0230 | 0.0415 | 0.0365 | 0.0403 |
| completeness [%] to $\theta = 25.00°$ | 99.6 | 99.5 | 99.5 | 99.5 |
| transmission max/min | 0.2929/0.2650 | 0.8345/0.3533 | 0.6200/0.2017 | 0.4559/0.2151 |
| data/restraints/params | 6053/0/293 | 7252/0/371 | 3906/0/234 | 8207/102/460 |
| final $R$ indices ($I > 2\sigma(I)$)[a] | $R_1 = 0.0199$ | $R_1 = 0.0264$ | $R_1 = 0.0209$ | $R_1 = 0.0246$ |
| | $wR_2 = 0.0482$ | $wR_2 = 0.0499$ | $wR_2 = 0.0480$ | $wR_2 = 0.0589$ |
| $R$ indices (all data) | $R_1 = 0.0215$ | $R_1 = 0.0383$ | $R_1 = 0.0271$ | $R_1 = 0.0383$ |
| | $wR_2 = 0.0486$ | $wR_2 = 0.0629$ | $wR_2 = 0.0489$ | $wR_2 = 0.0611$ |
| GOF[b] on $F^2$ | 1.037 | 1.001 | 1.057 | 1.089 |

[a] $R_1 = \Sigma(|F_o| - |F_c|)/\Sigma|F_o|$; $wR_2 = [\Sigma w(F_o^2 - F_c^2)^2/\Sigma w(F_c^2)^2]^{1/2}$; $w = [\sigma^2(F_o^2) + (g_1P)^2 + g_2P]^{-1}$; $P = (1/3)[\max\{F_o^2, 0\} + 2F_c^2]$. [b] Goodness-of-fit $= [\Sigma w(F_o^2 - F_c^2)^2/(n_{obsd} - n_{param})]^{1/2}$.

**X-ray structure determinations**: Crystal data and other details of the structure analyses are presented in Table 3. Suitable crystals for X-ray diffraction studies, obtained as indicated in the corresponding entry in the Experimental Section, were mounted at the end of a quartz fiber. The radiation used in all cases was graphite monochromated $Mo_{K\alpha}$ ($\lambda = 71.073$ pm). X-ray intensity data were collected using an Oxford Diffraction Xcalibur diffractometer. The diffraction frames were integrated and corrected for absorption by using the CrysAlis RED program.[66]

The structures were solved by Patterson and Fourier methods and refined by full-matrix least-squares on $F^2$ with SHELXL-97.[67] All non-hydrogen atoms were assigned anisotropic displacement parameters and refined without positional constraints, except as noted below. All hydrogen atoms were constrained to idealized geometries and assigned isotropic displacement parameters equal to 1.2 times the $U_{iso}$ values of their attached parent atoms (1.5 times for the $CH_3$ atoms). In the structure of **2**·$CH_2Cl_2$, the position of the I atoms was found to be disordered and, given the symmetry imposed by the space group on the anion, overlapped with two $CF_3$ groups. The two I atoms found were refined with partial occupancy 0.45/0.05. In the structure of **6′**, one fluorine atom, F(9), is disordered over two positions and refined with partial occupancy 0.5. For **7**, two of the $CF_3$ ligands were disordered over two sets of positions and refined with partial occupancy 0.5. Some restraints were applied in the geometry and thermal parameters of these groups. Full-matrix least-squares refinement of these models against $F^2$ converged to final residual indices given in Table 3.

CCDC-814128 (**2**·$CH_2Cl_2$), 814129 (**5**), 814130 (**6′**), and 814131 (**7**) contain the supplementary crystallographic data for this paper. These data can be obtained free of charge from The Cambridge Crystallographic Data Centre via www.ccdc.cam.ac.uk/data_request/cif.

## Acknowledgements

This work was supported by the Spanish MICINN (DGPTC)/FEDER (project CTQ2008-06669-C02-01/BQU) and the Gobier-

  

no de Aragón (Grupo Consolidado E21: Química Inorgánica y de los Compuestos Organometálicos).

[1] R. P. Hughes, *J. Fluorine Chem.* **2010**, *131*, 1059; F. G. A. Stone, *J. Fluorine Chem.* **1999**, *100*, 227; R. P. Hughes, *Adv. Organomet. Chem.* **1990**, *31*, 183; J. C. Tatlow, *J. Fluorine Chem.* **1984**, *25*, 99; R. Nyholm, *Q. Revs. Chem. Soc.* **1970**, *24*, 1; F. G. A. Stone, *Endeavour* **1966**, *25*, 33; R. D. Chambers, T. Chivers, *Organomet. Chem. Rev.* **1966**, *1*, 279; P. M. Treichel, F. G. A. Stone, *Adv. Organomet. Chem.* **1964**, *1*, 143; R. E. Banks, R. N. Haszeldine, *Adv. Inorg. Chem. Radiochem.* **1961**, *3*, 337; J. J. Lagowski, *Q. Revs. Chem. Soc.* **1959**, *13*, 233.

[2] E. R. Sigurdson, G. Wilkinson, *J. Chem. Soc. Dalton Trans.* **1977**, 812.

[3] A. L. Galyer, G. Wilkinson, *J. Chem. Soc. Dalton Trans.* **1976**, 2235; L. Galyer, K. Mertis, G. Wilkinson, *J. Organomet. Chem.* **1975**, *85*, C37.

[4] V. Pfennig, N. Robertson, K. Seppelt, *Angew. Chem.* **1997**, *109*, 1410; *Angew. Chem. Int. Ed. Engl.* **1997**, *36*, 1350; J. F. Gibson, G. M. Lack, K. Mertis, G. Wilkinson, *J. Chem. Soc. Dalton Trans.* **1976**, 1492; K. Mertis, G. Wilkinson, *J. Chem. Soc. Dalton Trans.* **1976**, 1488.

[5] R. D. Dresdner, T. J. Mao, J. A. Young, *J. Am. Chem. Soc.* **1958**, *80*, 3007; R. D. Dresdner, *J. Am. Chem. Soc.* **1956**, *78*, 876; R. Dresdner, *J. Am. Chem. Soc.* **1955**, *77*, 6633.

[6] R. J. Lagow, J. A. Morrison, *Adv. Inorg. Chem. Radiochem.* **1980**, *23*, 177.

[7] R. J. Lagow, J. L. Margrave, *Prog. Inorg. Chem.* **1979**, *26*, 161; E. K. Liu, R. J. Lagow, *J. Chem. Soc. Chem. Commun.* **1977**, 450; N. J. Maraschin, B. D. Catsikis, L. H. Davis, G. Jarvinen, R. J. Lagow, *J. Am. Chem. Soc.* **1975**, *97*, 513; N. J. Maraschin, R. J. Lagow, *Inorg. Chem.* **1973**, *12*, 1458.

[8] T. J. Juhlke, J. I. Glanz, R. J. Lagow, *Inorg. Chem.* **1989**, *28*, 980; R. A. Jacob, L. L. Gerchman, T. J. Juhlke, R. J. Lagow, *J. Chem. Soc. Chem. Commun.* **1979**, 128; R. J. Lagow, L. L. Gerchman, R. A. Jacob, J. A. Morrison, *J. Am. Chem. Soc.* **1975**, *97*, 518.

[9] D. Naumann, H. Butler, J. Fisher, J. Hanke, J. Mogias, B. Wilkes, *Z. anorg. allg. Chem.* **1992**, *608*, 69; L. J. Krause, J. A. Morrison, *J. Am. Chem. Soc.* **1981**, *103*, 2995; R. J. Lagow, R. Eujen, L. L. Gerchman, J. A. Morrison, *J. Am. Chem. Soc.* **1978**, *100*, 1722.

[10] E. Bernhardt, G. Henkel, H. Willner, G. Pawelke, H. Bürger, *Chem. Eur. J.* **2001**, *7*, 4696.

[11] D. Naumann, N. V. Kirij, N. Maggiarosa, W. Tyrra, Y. L. Yagupolskii, M. S. Wickleder, *Z. anorg. allg. Chem.* **2004**, *630*, 746.

[12] B. Menjón, S. Martínez-Salvador, M. A. Gómez-Saso, J. Forniés, L. R. Falvello, A. Martín, A. Tsipis, *Chem. Eur. J.* **2009**, *15*, 6371.

[13] N. Maggiarosa, W. Tyrra, D. Naumann, N. V. Kirij, Y. L. Yagupolskii, *Angew. Chem.* **1999**, *111*, 2392; *Angew. Chem. Int. Ed.* **1999**, *38*, 2252.

[14] D. Naumann, W. Tyrra, *J. Organomet. Chem.* **1989**, *368*, 131.

[15] D. Naumann, T. Roy, K.-F. Tebbe, W. Crump, *Angew. Chem.* **1993**, *105*, 1555; *Angew. Chem. Int. Ed. Engl.* **1993**, *32*, 1482.

[16] W. Dukat, D. Naumann, *Rev. Chim. Miner.* **1986**, *23*, 589.

[17] E. Bernhardt, M. Finze, H. Willner, *J. Fluorine Chem.* **2004**, *125*, 967; J. A. Schlueter, J. M. Williams, U. Geiser, J. D. Dudek, S. A. Sirchio, M. E. Kelly, J. S. Gregar, W. H. Kwok, J. A. Fendrich, J. E. Schirber, W. R. Bayless, D. Naumann, T. Roy, *J. Chem. Soc. Chem. Commun.* **1995**, 1311.

[18] U. Preiss, I. Krossing, *Z. anorg. allg. Chem.* **2007**, *633*, 1639; J. A. Schlueter, U. Geiser, A. M. Kini, H. H. Wang, J. M. Williams, D. Naumann, T. Roy, B. Hoge, R. Eujen, *Coord. Chem. Rev.* **1999**, *190–192*, 781.

[19] S. Balters, E. Bernhardt, H. Willner, T. Berends, *Z. Anorg. Allg. Chem.* **2004**, *630*, 257; S. Balters, DPhil Thesis, University of Wuppertal (Germany), **2005** [urn:nbn:de:hbz:468–20050702].

[20] R. J. Lagow, L. L. Gerchman, R. A. Jacob (Massachusetts Institute of Technology, Cambridge, MA), US-A 3992424, **1976**, p. 7; [ R. J. Lagow, L. L. Gerchman, R. A. Jacob, *Chem. Abstr.* **1977**, *86*, 72887]; R. J. Lagow, L. L. Gerchman, R. A. Jacob (Massachusetts Institute of Technology, Cambridge, MA), US-A 3954585, **1976**, p. 8; [R. J. Lagow, L. L. Gerchman, R. A. Jacob, *Chem. Abstr.* **1976**, *85*, 160324].

[21] J. A. Morrison, *Adv. Inorg. Chem. Radiochem.* **1983**, *27*, 293.

[22] Coupling with 12 neighbor F atoms should result in a 13-multiplicity signal with 1:12:66:220:495:792:924:792:495:220:66:12:1 relative intensity distribution, the outer, less-intense features of which are not observed to emerge from baseline noise.

[23] Attempts to hinder the dissociation of the iodo ligand in **3** by lowering the temperature failed, as the oxidative addition process itself was revealed to be extremely temperature-sensitive. Thus, after 5 days at 3 °C, unreacted **1**, and $nC_4F_9I$ were the only products observed in the reaction medium ($^{19}F$ NMR spectroscopy).

[24] a) R. P. Hughes, R. B. Laritchev, L. N. Zakharov, A. L. Rheingold, *Organometallics* **2005**, *24*, 4845; b) R. P. Hughes, S. M. Maddock, I. A. Guzei, L. M. Liable-Sands, A. L. Rheingold, *J. Am. Chem. Soc.* **2001**, *123*, 3279; c) R. P. Hughes, J. T. Sweetser, M. D. Tawa, A. Williamson, C. D. Incarvito, B. Rhatigan, A. L. Rheingold, G. Rossi, *Organometallics* **2001**, *20*, 3800; d) R. P. Hughes, T. le Husebo, A. L. Rheingold, L. M. Liable-Sands, G. P. A. Yap, *Organometallics* **1997**, *16*, 5; see also: J. Banus, H. J. Emeléus, R. N. Haszeldine, *J. Chem. Soc.* **1951**, 60.

[25] R. Minkwitz, R. Bröchler, M. Berkei, *Z. anorg. allg. Chem.* **1996**, *622*, 1749.

[26] N. V. Kirij, Y. L. Yagupolskii, N. Maggiarosa, W. Tyrra, D. Naumann, *J. Fluorine Chem.* **2001**, *112*, 213.

[27] In the electrochemical reduction of $CF_3I$, both the radical $CF_3^{\bullet}$ and the anion $(CF_3)^-$ are formed: C. P. Andrieux, L. Gelis, M. Medebielle, J. Pinson, J. M. Saveant, *J. Am. Chem. Soc.* **1990**, *112*, 3509.

[28] R. A. Rossi, A. B. Pierini, A. B. Peñéñory, *Chem. Rev.* **2003**, *103*, 71.

[29] W. B. Farnham, *Chem. Rev.* **1996**, *96*, 1633. For recent evidence of the intermediacy of fluorinated carbanions in the chemistry of transition-metal compounds, see: B. D. Panthi, S. L. Gipson, A. Franken, *Organometallics* **2010**, *29*, 5890; J. G. Cordaro, R. G. Bergman, *J. Am. Chem. Soc.* **2004**, *126*, 16912; see also Ref. [24b].

[30] Permanent dipole moments, $\mu$, and relative permitivity values, $\varepsilon_r$ (usually known as dielectric constants), for the referred solvents at 25 °C are quoted from: C. Reichardt, *Solvents and Solvent Effects in Organic Chemistry*, 3rd ed., Wiley-VCH, Weinheim, **2003**, Table A-1, pp. 472–475.

[31] J. D. Atwood, *Inorganic and Organometallic Reaction Mechanisms*, 2nd ed., Wiley, New York, **1997**, Chapter 3, pp. 71–94.

[32] J. A. Davies, F. R. Hartley, *Chem. Rev.* **1981**, *81*, 79.

[33] S. F. Rach, F. E. Kühn, *Chem. Rev.* **2009**, *109*, 2061; B. N. Storhoff, H. C. Lewis, Jr., *Coord. Chem. Rev.* **1977**, *23*, 1.

[34] The small differences in chemical shifts as well as in coupling constants observed in Ref. [19] and in the current work might well be due to the different cation used in each case: $K^+$ versus $[NBu_4]^+$.

[35] T. Yagyu, Y. Suzaki, K. Osakada, *Organometallics* **2002**, *21*, 2088.

[36] J. D. Scollard, M. Day, J. A. Labinger, J. E. Bercaw, *Helv. Chim. Acta* **2001**, *84*, 3247.

[37] T. G. Appleton, H. C. Clark, L. E. Manzer, *Coord. Chem. Rev.* **1973**, *10*, 335.

[38] L. Johansson, O. B. Ryan, C. Rømming, M. Tilset, *Organometallics* **1998**, *17*, 3957.

[39] P. Schützenberger, *C. R. Hebd. Sceances Acad. Sci.* **1870**, *70*, 1134; P. Schützenberger, *Bull. Soc. Chim. Fr.* **1868**, *10*, 188; P. Schützenberger, *Ann. Chim. Phys.* **1868**, *15*, 100.

[40] D. B. dell'Amico, F. Calderazzo, G. dell'Amico, *Gazz. Chim. Ital.* **1977**, *107*, 101.

[41] B. von Ahsen, R. Wartchow, H. Willner, V. Jonas, F. Aubke, *Inorg. Chem.* **2000**, *39*, 4424.

[42] C. Crocker, P. L. Goggin, R. J. Goodfellow, *J. Chem. Soc. Chem. Commun.* **1978**, 1056.

[43] D. B. dell'Amico, F. Calderazzo, F. Marchetti, S. Merlino, *J. Chem. Soc. Dalton Trans.* **1982**, 2257.

[44] J. Forniés, M. A. Gómez-Saso, A. Martín, F. Martínez, B. Menjón, J. Navarrete, *Organometallics* **1997**, *16*, 6024.

  

[45] N. Mina-Camilde, C. E. Manzanares, J. F. Caballero, *J. Chem. Educ.* **1996**, *73*, 804.

[46] S. Martínez-Salvador, B. Menjón, J. Forniés, A. Martín, I. Usón, *Angew. Chem.* **2010**, *122*, 4382; *Angew. Chem. Int. Ed.* **2010**, *49*, 4286.

[47] J. E. Huheey, E. A. Keiter, R. L. Keiter, *Inorganic Chemistry*, 4th ed., Harper Collins, New York, **1993**, pp. 182–199; see also: S. G. Bratsch, *J. Chem. Educ.* **1985**, *62*, 101; A. L. Allred, *J. Inorg. Nucl. Chem.* **1961**, *17*, 215.

[48] J. Goodman, V. V. Grushin, R. B. Larichev, S. A. Macgregor, W. J. Marshall, D. C. Roe, *J. Am. Chem. Soc.* **2010**, *132*, 12013.

[49] Plain facts, such as the substantial acidity increase upon going from $CH_3CO_2H$ ($pK_a = 4.76$) to $CF_3CO_2H$ ($pK_a = -0.25$) as well as upon going from $CH_3SO_3H$ ($pK_a = -2.6$) to $CF_3SO_3H$ ($pK_a = -14$) can hardly be explained assuming that $CF_3$ is an even better σ-donor group than $CH_3$; $pK_a$ values quoted from: D. H. Ripin, D. A. Evans, http://www2.lsdiv.harvard.edu/labs/evans/pdf/evans_pKa_table.pdf. As early as 1972, H. C. Clark provided an explanation for the observed high *trans* influence of the $CF_3$ group in transition-metal chemistry, which appears far more sensible to us: "The trifluoromethyl group is almost as high in this series [referring to the *trans* influence order] as the methyl group (i.e., has almost the same effect on Pt hybridization) which would not be expected on the basis of a comparison between the electronegativities of the two groups. Despite the smaller degree of charge transfer to Pt, the trifluoromethyl group must form very strong covalent bonds with platinum, with much s character" (see Ref. [50]). This model was later confirmed by Puddephatt and his co-workers on the basis of UV-photoelectron spectroscopic data and SCF-MS-Xα calculations on carefully selected trifluoromethyl–platinum(II) compounds: see Ref. [51].

[50] T. G. Appleton, M. H. Chisholm, H. C. Clark, L. E. Manzer, *Inorg. Chem.* **1972**, *11*, 1786.

[51] D. S. Yang, G. M. Bancroft, R. J. Puddephatt, J. S. Tse, *Inorg. Chem.* **1990**, *29*, 2496.

[52] Data (713) were retrieved from the Cambridge Structural Database (see Ref. [53]) that correspond to terminal Pt–CO derivatives regardless of the metal oxidation state, having rejected those structures with $\measuredangle$Pt-C-O $\leq 170°$ as a valid criterion for linearity. Upper value of Pt–CO distance (199.4(3) pm): E. E. Korshin, G. Leitus, L. J. W. Shimon, L. Konstantinovski, D. Milstein, *Inorg. Chem.* **2008**, *47*, 7177. Lower value of Pt–CO distance (162(4) pm): A. Albinati, P. Leoni, L. Marchetti, S. Rizzato, *Angew. Chem.* **2003**, *115*, 6172; *Angew. Chem. Int. Ed.* **2003**, *42*, 5990. Upper value of C≡O distance (128.5 pm): J. C. Calabrese, L. F. Dahl, P. Chini, G. Longoni, S. Martinengo, *J. Am. Chem. Soc.* **1974**, *96*, 2614. Lower value of C≡O distance (102(1) pm): Z. Béni, R. Ros, A. Tassan, R. Scopelliti, R. Roulet, *Dalton Trans.* **2005**, 315.

[53] I. J. Bruno, J. C. Cole, P. R. Edgington, M. Kessler, C. F. Macrae, P. McCabe, J. Pearson, R. Taylor, *Acta Crystallogr. Sect. B* **2002**, *58*, 389.

[54] H. Willner, M. Bodenbinder, R. Bröchler, G. Hwang, S. J. Rettig, J. Trotter, B. von Ahsen, U. Westphal, V. Jonas, W. Thiel, F. Aubke, *J. Am. Chem. Soc.* **2001**, *123*, 588.

[55] H. Willner, F. Aubke, *Chem. Eur. J.* **2003**, *9*, 1668; H. Willner, F. Aubke, *Organometallics* **2003**, *22*, 3612; H. Willner, F. Aubke, in *Inorganic Chemistry Highlights* (Eds.: G. Meyer, L. Wesemann, D. Naumann), Wiley-VCH, Weinheim, **2002**, Chapter 11, pp. 195–212; H. Willner, F. Aubke, *Angew. Chem.* **1997**, *109*, 2506; *Angew. Chem. Int. Ed. Engl.* **1997**, *36*, 2402.

[56] A. Bondi, *J. Phys. Chem.* **1964**, *68*, 441.

[57] V. Y. Kukushkin, V. K. Bel'skii, E. A. Aleksandrova, E. Y. Pan'kova, V. E. Konovalov, V. N. Yakovlev, A. I. Moiseev, *Zh. Obshch. Khim.* **1991**, *61*, 318; V. Y. Kukushkin, V. K. Bel'skii, E. A. Aleksandrova, E. Y. Pan'kova, V. E. Konovalov, V. N. Yakovlev, A. I. Moiseev, *Russ. J. Gen. Chem.* **1991**, *61*, 284.

[58] E. Pitcher, A. D. Buckingham, F. G. A. Stone, *J. Chem. Phys.* **1962**, *36*, 124.

[59] W. E. Tyrra, *J. Fluorine Chem.* **2001**, *112*, 149.

[60] J. Browning, P. L. Goggin, R. J. Goodfellow, M. G. Norton, A. J. M. Rattray, B. F. Taylor, J. Mink, *J. Chem. Soc. Dalton Trans.* **1977**, 2061.

[61] B. P. Andreini, D. B. dell'Amico, F. Calderazzo, M. G. Venturi, G. Pelizzi, A. Serge, *J. Organomet. Chem.* **1988**, *354*, 357.

[62] D. R. Russell, P. A. Tucker, S. Wilson, *J. Organomet. Chem.* **1976**, *104*, 387.

[63] M. Berkei, J. F. Bickley, B. T. Heaton, *Z. Naturforsch. Teil B* **2002**, *57*, 610.

[64] W. C. Wolsey, *J. Chem. Educ.* **1973**, *50*, A335.

[65] The signal corresponding to the C≡N group was not observed.

[66] CrysAlis RED: Program for X-ray CCD Camera Data Reduction, Version 1.171.32.19, Oxford Diffraction Ltd., Oxford, **2008**.

[67] G. M. Sheldrick, SHELXL-97: Program for the Refinement of Crystal Structures from Diffraction Data, University of Göttingen, Göttingen, **1997**.

Received: February 25, 2011
Published online: June 3, 2011

  

Dalton Transactions

Dynamic Article Links

Cite this: *Dalton Trans.*, 2011, **40**, 10440

www.rsc.org/dalton

**PAPER**

# Efficient and stereoselective syntheses of isomeric trifluoromethyl-platinum(IV) chlorides†

**Sonia Martínez-Salvador,[a] Pablo J. Alonso,[b] Juan Forniés,*[a] Antonio Martín[a] and Babil Menjón[a]**

***Received 1st April 2011, Accepted 25th May 2011***
**DOI: 10.1039/c1dt10557d**

The homoleptic, square-planar trifluoromethylplatinate(II) compound $[NBu_4]_2[Pt(CF_3)_4]$ (**1**) reacts with $SOCl_2$ undergoing oxidative addition of a S–Cl bond to give the octahedral species $[NBu_4]_2$[*trans*-$Pt(CF_3)_4Cl(SOCl)]$ (**4**), that contains the unusual chlorosulfinyl ligand. Compound **4** readily evolves into the dichloro-derivative $[NBu_4]_2$[*cis*-$Pt(CF_3)_4Cl_2]$ (**2**), whereby the "$Pt(CF_3)_4$" unit undergoes a stereochemical rearrangement from an initial square-planar (equatorial) geometry to a final sawhorse disposition within the global Pt octahedral environment. Compound **2** is more reactive than the corresponding $[NBu_4]_2$[*trans*-$Pt(CF_3)_4Cl_2]$ (**3**) stereoisomer and thus affords the trichloro-derivative $[NBu_4]_2$[*fac*-$Pt(CF_3)_3Cl_3]$ (**5**) by treatment with the stoichiometrically required amount of HCl(aq). Stereoisomer $[NBu_4]_2$[*mer*-$Pt(CF_3)_3Cl_3]$ (**6**) has been obtained by oxidative addition of $Cl_2$ to the organoplatinum(II) precursor $[NBu_4]_2[Pt(CF_3)_3Cl]$. All the synthetic procedures described here proceed in high yields and in a stereoselective manner. The optical properties of the *cis*-/*trans*-$[Pt(CF_3)_4Cl_2]^{2-}$ and *fac*-/*mer*-$[Pt(CF_3)_3Cl_3]^{2-}$ diastereomeric couples (diffuse reflectance) as well as the solid-state geometries of the latter couple (single-crystal X-ray diffraction methods) are conveniently compared.

## Introduction

Stereoisomerism has played a key role in the development of coordination chemistry.[1] A driving force leading to Alfred Werner's hypothesis on the polyhedral nature of metal environments in coordination compounds,[2] was precisely the known existence of pairs of halo-ammine compounds of $Co^{III}$ and $Pt^{II}$ with the same stoichiometry, but displaying sharply different colours. Similar phenomena were also known in $Pt^{IV}$ chemistry, as two different compounds with formula $PtCl_4{\cdot}2NH_3$ had been prepared by C. Gerhardt (1850) and P. T. Cleve (1870).[3] Those compounds were only recognised much later as the *trans* and *cis* isomers of $[PtCl_4(NH_3)_2]$, respectively. A definite degree of mastery has been achieved ever since in obtaining – or at least detecting and identifying – mixed octahedral $Pt^{IV}$ complexes in their different stereoisomeric forms.[4,5] Such compounds are usually difficult to separate when obtained admixed, hence it is highly desirable to have stereospecific methods at one's disposal to prepare them.

In contrast to the stereochemical variety commonly found in $Pt^{IV}$ coordination compounds, the situation in organoplatinum(IV) chemistry is rather different as in this case mainly one stereochemical arrangement seems to be favoured.[6] This feature had already been noted by Tobias[7] and can be related to the high *trans* influence assigned to σ-organyl groups that results in considerable destabilisation of the M–L bond in *trans* position.[8,9] The fact that "*two soft ligands in mutual trans position will have a destabilizing effect on each other when attached to class b metal atoms*" was termed "antisymbiotic effect" by Pearson.[10] This may well be the reason that explains why all structurally-characterised octahedral organoplatinum(IV) compounds containing $PtMe_4$ or $PtMe_3$ units invariably show *cis*‡ or *fac*§ geometries, respectively. Similar stereochemical preferences would be expected for trifluoromethyl-platinum(IV) derivatives, in view of the high *trans* influence assigned to the $CF_3$ group – almost as high as that assigned to the $CH_3$ group.[12] However, there seem to be just two octahedral trifluoromethyl-platinum(IV) compounds for which the molecular structure has been established, *viz*. the mononuclear derivative $[NBu_4]_2$[*trans*-$Pt(CF_3)_4Cl_2]$[13] and the dinuclear species $K_2[\{Pt(CF_3)_2F_2\}_2(\mu\text{-}OH)_2]{\cdot}2H_2O$.[14]

[a]*Instituto de Síntesis Química y Catálisis Homogénea (ISQCH), Facultad de Ciencias, Universidad de Zaragoza–C.S.I.C., C/Pedro Cerbuna 12, E-50009, Zaragoza, Spain. E-mail: juan.fornies@unizar.es*

[b]*Instituto de Ciencia de Materiales de Aragón (ICMA), Universidad de Zaragoza–C.S.I.C., C/Pedro Cerbuna 12, E-50009, Zaragoza, Spain*

† CCDC reference numbers 819387 (**4′′**), 819388 (**5′**·$1.25Me_2CO$) and 819389 (**6**·$0.42CH_2Cl_2$). For crystallographic data in CIF or other electronic format see DOI: 10.1039/c1dt10557d

‡ Data (8) were retrieved from the Cambridge Structural Database (see ref. 11) corresponding to six-coordinate platinum derivatives containing the $PtMe_4$ unit. In all cases the sum of all Me–Pt–Me′ angles within the unit (ranging between 595 and 625°) approached 630°, which is the expected value for a sawhorse arrangement (or, equivalently, a *cis* arrangement of the heteroligands). A 720° value would, in turn, be expected for an equatorial arrangement.

§ Data (177) were retrieved from the Cambridge Structural Database (see ref. 11) corresponding to six-coordinate platinum derivatives containing the $PtMe_3$ unit with no higher methyl content. In all cases did the sum of all Me–Pt–Me′ angles within the unit approach 270°, which is the value expected for a *facial* arrangement (observed values are comprised between 249 and 283°). A 360° value would, in turn, be expected for a *meridional* arrangement.

Here we report on efficient synthetic procedures to stereoselectively obtain salts of any of the following trifluoromethylplatinum(IV) isomeric couples: *cis*-/*trans*-$[Pt(CF_3)_4Cl_2]^{2-}$ and *fac*-/*mer*-$[Pt(CF_3)_3Cl_3]^{2-}$. All these compounds can be isolated in high yields and have been characterised by a combination of analytic, spectroscopic and X-ray diffraction methods. The *cis* and *fac* isomers had been previously detected to form in 7 : 3 ratio by reaction of $[NBu_4]_2[Pt(CN)_4]$ with ClF in $CH_2Cl_2$ solution,[14] but they were not isolated in pure form.

### The *cis*-/*trans*-$[Pt(CF_3)_4Cl_2]^{2-}$ diastereomeric couple

The homoleptic, organoplatinum(II) derivative $[NBu_4]_2[Pt(CF_3)_4]$ (**1**) reacts with $SOCl_2$ in acetone solution at room temperature (Scheme 1) giving rise to $[NBu_4]_2$[*cis*-$Pt(CF_3)_4Cl_2$] (**2**). The reaction takes place in a quantitative and stereoselective manner in just 15 min ($^{19}F$ NMR). After the appropriate workup, compound **2** can be isolated as a pale solid in 71% yield. The stereochemistry of **2** can be secured through the analysis of its spectroscopic properties.¶ Thus, the $^{19}F$ NMR spectrum of **2** consists of two septets located at $\delta_F = -24.4$ and $-31.7$ ppm in 1 : 1 integrated ratio (Fig. 1) that we assign to the $CF_3$ groups *trans* to Cl and *trans* to $CF_3$, respectively, in line with both their chemical shifts and the sharply different values of their $^{195}Pt$-satellites: $^2J(^{195}Pt,^{19}F)$ = 465 and 284 Hz. The multiplicity of these signals is due to mutual coupling between the chemically inequivalent nuclei with $^4J(^{19}F,^{19}F) = 5.7$ Hz.

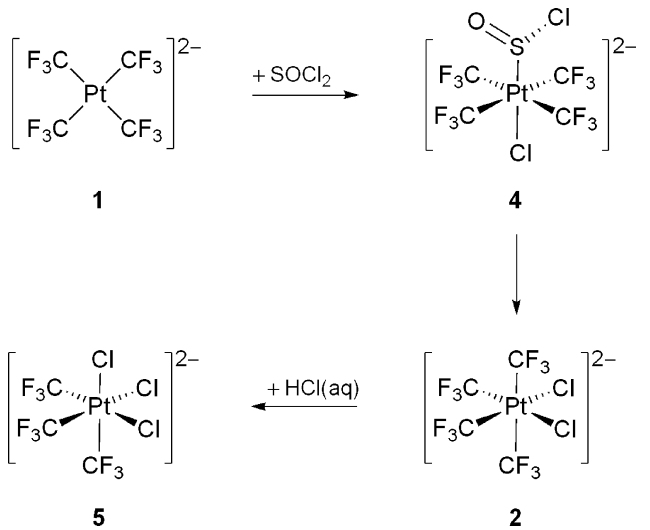


**Scheme 1** The *cis* → *fac* path *via* oxidative addition of $SOCl_2$ to **1** ($[NBu_4]^+$ is the counterion in all cases).

Theoretical calculations at the B3P86/LANL2DZ level predicted the [*cis*-$Pt(CF_3)_4Cl_2]^{2-}$ stereoisomer (with local $C_{2v}$ symmetry) to be slightly more stable than the corresponding [*trans*-$Pt(CF_3)_4Cl_2]^{2-}$ one (with local $D_{4h}$ symmetry).[13] The *cis* stereoisomer was found to be the main product obtained by reaction of $[NBu_4]_2[Pt(CN)_4]$ with ClF in $CH_2Cl_2$.[14] However, only the *trans* stereoisomer was obtained in high yield by oxidative addition of

¶ The spectroscopic properties of compound **2** in solution are in reasonable agreement with those previously assigned to the [*cis*-$Pt(CF_3)_4Cl_2]^{2-}$ anion (see ref. 14).

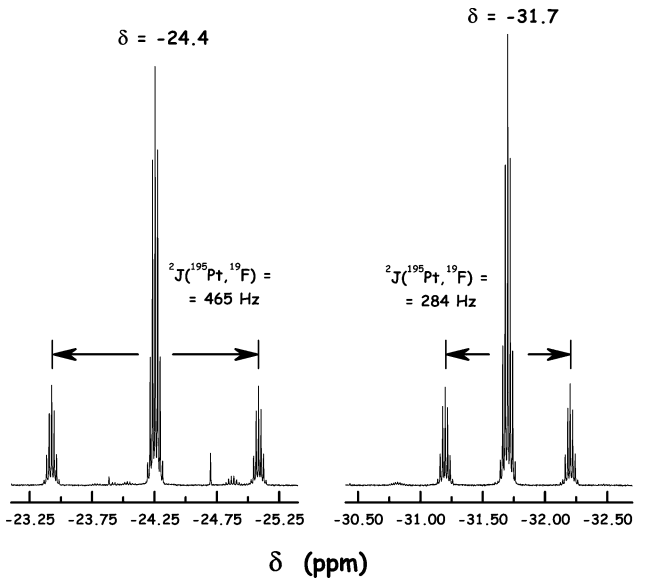


**Fig. 1** Room-temperature $^{19}F$ NMR spectrum of compound **2** in [$^2$H]acetone solution with spectral parameters indicated. Both signals belong to the same spin system, as they show a mutual coupling of $^4J(^{19}F,^{19}F) = 5.7$ Hz.

$Cl_2$ to **1** at low temperature (Scheme 2a). The $^{19}F$ NMR spectrum of $[NBu_4]_2$[*trans*-$Pt(CF_3)_4Cl_2$] (**3**) consists of a singlet at $\delta_F$ = −34.0 flanked by $^{195}Pt$-satellites with a value of $^2J(^{195}Pt,^{19}F)$ = 268 Hz.[13] Attempts to promote isomerisation to the presumably more stable *cis* species by thermal treatment failed.[13] In fact, we had not previously observed a rearrangement of this kind. It is, therefore, quite remarkable that the room-temperature reaction of **1** with $SOCl_2$ (Scheme 1) proceeds with a stereochemical rearrangement of the "$Pt(CF_3)_4$" unit from an initial square-planar geometry in **1** to a final sawhorse disposition within the global Pt octahedral environment in **2**. In order to gain a deeper insight into the process, we carried out the same reaction at low temperature, hoping to detect some intermediate species.

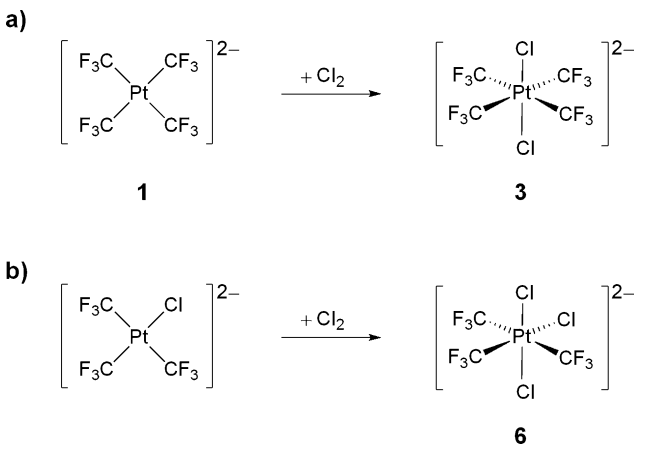


**Scheme 2** Synthetic procedures to obtain: (a) the *trans* (**3**) and (b) the *mer* (**6**) stereoisomers ($[NBu_4]^+$ is the counterion in all cases).

When compound **1** is reacted with $SOCl_2$ in acetone solution at −78 °C, the initially pale yellow solution turns green. The low-temperature $^{19}F$ NMR spectrum of the reaction medium shows

that the singlet at $\delta_F = -23.6$ ppm and $^2J(^{195}Pt,^{19}F) = 548$ Hz, corresponding to the starting material **1**, has quantitatively evolved into another singlet at $\delta_F = -32.1$ ppm and $^2J(^{195}Pt,^{19}F) = 262$ Hz, which does not correspond to the *trans* stereoisomer **3**. The significant reduction in the $^2J(^{195}Pt,^{19}F)$ value suggests that oxidation of the metal centre has already occurred, but the lack of multiplicity in the signal indicates that the aforementioned geometric rearrangement in the "$Pt(CF_3)_4$" unit has still not taken place. The observed spectroscopic features suggest that a highly symmetric organoplatinum(IV) species has been quantitatively formed.

From the reaction medium, a green solid can be isolated at low temperature, whose elemental analysis (including S) together with the commented spectroscopic properties suggest its formulation as $[NBu_4]_2$[*trans*-$Pt(CF_3)_4Cl(SOCl)$] (**4**). In order to confirm this formulation we sought to establish the molecular structure by X-ray diffraction methods. Although this was not possible directly on compound **4** due to the lack of suitable crystals, we succeeded in obtaining single-crystals of the salt $[N(PPh_3)_2]_2$[*trans*-$Pt(CF_3)_4Cl(SOCl)$] (**4″**), that were found to be suitable for X-ray diffraction purposes. The structure of the [*trans*-$Pt(CF_3)_4Cl(SOCl)]^{2-}$ anion is depicted in Fig. 2. The Pt centre is located in an octahedral environment with all four $CF_3$ groups in the equatorial plane. The average Pt–C distance (210.6(5) pm) is similar to that found in compound **3** (209.2(5) pm), also displaying a similar geometric arrangement.[13] The axial Cl–Pt–S(O)Cl unit is comparable to the Cl–Ir–S(O)Cl one found in the only precedent of a metal complex containing the chlorosulfinyl ligand for which the molecular structure has been established, *viz*. $[IrCl_2(SOCl)(PEt_3)_2(CO)]$.[15] The latter compound and **4** both derive from the oxidative addition of a S–Cl bond in the $SOCl_2$ molecule to the corresponding parent species: *trans*-$[IrCl(PEt_3)_2(CO)]$ or **1**.

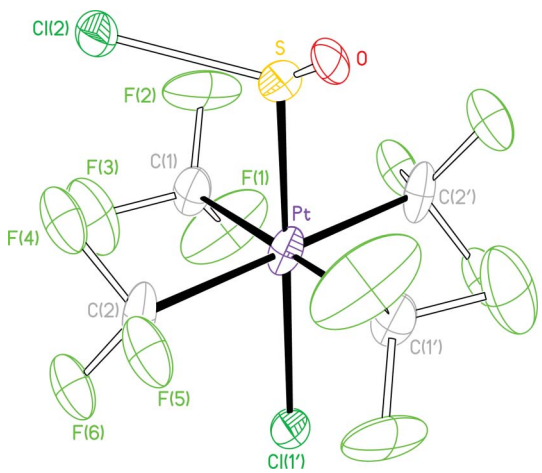


**Fig. 2** Thermal ellipsoid diagram (50% probability) of the anion of $[N(PPh_3)_2]$[*trans*-$Pt(CF_3)_4Cl(SOCl)$] (**4″**), with only the higher-occupancy positions represented. Selected bond lengths (pm) and angles (°) with estimated standard deviations: Pt–Cl(1) 257.4(9), Pt–S 222.0(10), average Pt–C 210.6(5), S–O 128(2), S–Cl(2) 217(2); average *cis* C–Pt–C′ 90.00(17), *trans* C–Pt–C′ 180.0 (crystallographically imposed), Cl(1)–Pt–S 179.5(10), average Cl(1)–Pt–C 90.0(4), Pt–S–Cl(2) 105.0(8), Pt–S–O 119.5(10).

Acetone solutions of **4** at room temperature spontaneously evolve into **2** in 15 min (Scheme 1). Although the fate of the SO fragment could not be unambiguously established, it can be concluded that compound **4** is, in fact, an intermediate species in the synthesis of **2**.

### The *fac*-/*mer*-$[Pt(CF_3)_3Cl_3]^{2-}$ diastereomeric couple

Compound **2** reacts in acetone solution at room temperature with an equimolar amount of HCl(aq) affording $[NBu_4]_2$[*fac*-$Pt(CF_3)_3Cl_3$] (**5**). The reaction (Scheme 1) takes place in a quantitative manner ($^{19}F$ NMR) and involves the stereoselective loss of one of the $CF_3$ *trans* to $CF_3$ groups in the starting material **2**. The $^{19}F$ NMR spectrum of the reaction medium consists of a singlet at $\delta_F = -26.0$ ppm with $^2J(^{195}Pt,^{19}F) = 457$ Hz, in reasonable agreement with the spectroscopic properties previously assigned to the stereoisomer [*fac*-$Pt(CF_3)_3Cl_3]^{2-}$ in solution.[14] From the reaction medium, compound **5** was isolated as a pale solid in 73% yield.

We were able to establish the geometry of the [*fac*-$Pt(CF_3)_3Cl_3]^{2-}$ anion (local $C_{3v}$ symmetry; Fig. 3) by X-ray diffraction methods on single-crystals of $[PPh_4]_2$[*fac*-$Pt(CF_3)_3Cl_3]\cdot 1.25Me_2CO$ (**5′**$\cdot 1.25Me_2CO$), a salt that was obtained following the same procedure as that described to prepare **5**. The *facial* arrangement of the "$Pt(CF_3)_3$" unit in **5′** seems to be particularly favoured in trialkyl-derivatives of $Pt^{IV}$, since it has been invariably found in the plethora of structurally-characterised organoplatinum(IV) compounds containing the non-fluorinated "$Pt(CH_3)_3$" fragment.§ Although the molecular structure of the non-fluorinated homologous species $[AsPh_4]_2[PtMe_3X_3]$ (X = Cl, Br) has not been unambiguously established, a *facial* geometry has also been assigned on the basis of their spectroscopic properties.[16] The average Pt–C distance in **5′** (205.7(7) pm) is indistinguishable from that observed in the tetranuclear species $[\{PtMe_3\}_4(\mu_3\text{-}I)_4]$ (Pt–C 206(1) pm),[17] $[\{PtMe_3\}_4(\mu_3\text{-}N_3)_4]$ (Pt–C 205(6) pm)[18] or $[\{PtMe_3\}_4(\mu_3\text{-}SMe)_4]$ (Pt–C 207(2) pm),[17] all of them showing a cubane-like structure. Shorter Pt–C bond lengths are usually found in perfluoroalkylmetal derivatives compared to their non-fluorinated counterparts, a feature that has been commonly assigned to the *C*-donor

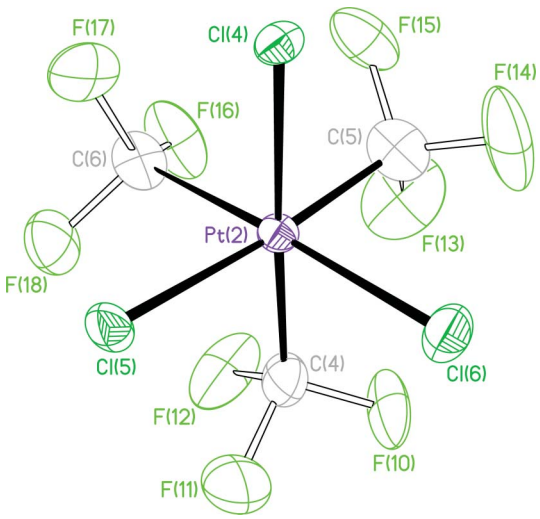


**Fig. 3** Thermal ellipsoid diagram (50% probability) of one of the crystallographically independent [*fac*-$Pt(CF_3)_3Cl_3]^{2-}$ anions found in single crystals of **5′**$\cdot 1.25Me_2CO$. Selected bond lengths (pm) and angles (°) with estimated standard deviations: average Pt–C 205.7(7), average Pt–Cl 241.9(2); average C–Pt–C′ 91.8(3), average Cl–Pt–Cl′ 87.91(5), average *cis* Cl–Pt–C 90.1(3), average *trans* Cl–Pt–C 175.7(2).

atom having a higher s character in the former case than in the latter.[12,19] The comparable Pt–C distances observed in **5′** and in the aforementioned [{$PtMe_3$}$_4$($\mu_3$-X)$_4$] compounds (X = I, $N_3$, SMe) can be assigned to the different global charge on these complex species. In this context, it is interesting to note that shorter Pt–C bond lengths (201(1) and 202(1) pm) have been found in the mononuclear cationic compound [*fac*-$PtMe_3(OCMe_2)_3$][$BF_4$].[20] Similar values have also been reported for the tetranuclear derivative [{$PtMe_3$}$_4$($\mu_3$-$O_3SCF_3$)$_4$] (average Pt–C 200(3) pm).[21] Although the latter species is neutral, the presence of poorly-coordinating trifluoromethylsulfato ligands acting in a triply-bridging fashion seems to result in incomplete compensation of the formal positive charge associated with the $PtMe_3$ unit.‖

Considering the lack of structurally characterised trimethylplatinum(IV) derivatives with *mer* geometry we sought to prepare the *mer* stereoisomer of the $[Pt(CF_3)_3Cl_3]^{2-}$ stoichiometry. For this purpose we reacted the organoplatinum(II) precursor $[NBu_4]_2[Pt(CF_3)_3Cl]$[23] in $CH_2Cl_2$ solution at −78 °C with the stoichiometrically required amount of $Cl_2$ (in $CCl_4$ solution). As a result, the desired species $[NBu_4]_2$[*mer*-$Pt(CF_3)_3Cl_3$] (**6**) was quantitatively and stereoselectively formed (Scheme 2b). The $^{19}F$ NMR spectrum of the reaction medium shows a similar pattern to that observed for the starting material, but with sharply different associated spectroscopic parameters. The spectrum consists of a septet at $\delta_F$ = −23.5 ppm with $^2J(^{195}Pt,^{19}F)$ = 426 Hz and a quartet at $\delta_F$ = −33.4 ppm with $^2J(^{195}Pt,^{19}F)$ = 269 Hz in 1 : 2 integrated ratio (Fig. 4). The latter signal is assignable to the mutually *trans* standing $CF_3$ groups and the former one to the remaining $CF_3$ group located *trans* to Cl. Both signals belong to the same spin system as evidenced by the mutual coupling between the two chemically inequivalent $CF_3$ groups with $^4J(^{19}F,^{19}F)$ = 4.8 Hz.

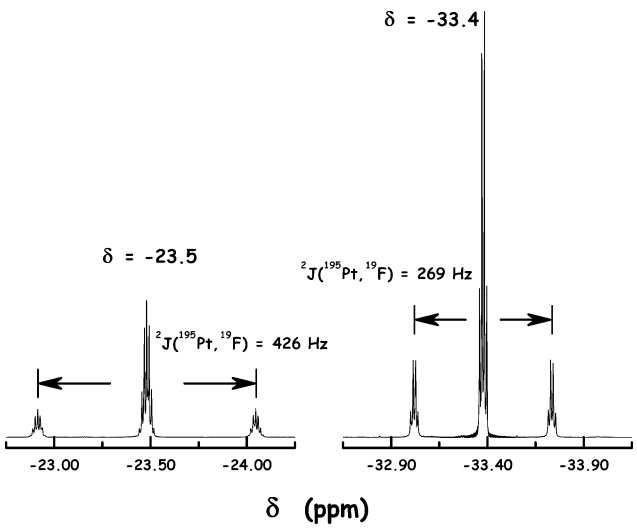


**Fig. 4** Room-temperature $^{19}F$ NMR spectrum of compound **6** in [$^2$H]acetone solution with spectral parameters indicated. Both signals belong to the same spin system, as they show a mutual coupling of $^4J(^{19}F,^{19}F)$ = 4.8 Hz.

‖ It has been established that the $PtMe_3$ unit in the tetranuclear compound [{$PtMe_3$}$_4$($\mu_3$-$O_3SCF_3$)$_4$] still shows a significant Lewis acidity, which has been quantified as 27% of the acidity of $BBr_3$ using Child's crotonaldehyde method (see ref. 22).

From the reaction medium compound **6** was isolated as a pale yellow solid in 88% yield.

The crystal and molecular structures of compound **6** have been established by X-ray diffraction on single-crystals of the solvate **6**·0.42$CH_2Cl_2$. A structural drawing of the [*mer*-$Pt(CF_3)_3Cl_3]^{2-}$ anion (local $C_{2v}$ symmetry) is given in Fig. 5. The Pt–C distances involving the mutually *trans* standing $CF_3$ groups are virtually identical (209.9(6) and 210.9(6) pm) and indistinguishable from those observed in stereoisomer **3** (average Pt–C 209.2(5) pm)[13] and in compound **4″** (average Pt–C 210.6(5) pm), where all four $CF_3$ groups are located *trans* to other $CF_3$ groups in the equatorial positions. The remaining Pt–C distance, involving the $CF_3$ group *trans* to Cl, is significantly shorter (202.7(6) pm) and this fact can be assigned to the lower *trans* influence of Cl in comparison with that of the $CF_3$ group.[9,12] Similar structural features are observed in the $PtCl_3$ unit. Thus, the Pt–Cl distances along the Cl–Pt–Cl axis are identical to each other (232.2(2) and 232.6(2) pm) and indistinguishable from those observed in stereoisomer **3** (average Pt–Cl 232.9(1) pm),[13] where the Cl ligands are located in *trans* positions. Finally, a significantly longer Pt–Cl distance is found (241.0(2) pm) for the Cl ligand *trans* to $CF_3$ according to the high *trans* influence associated with alkyl and perfluoroalkyl groups.[9,12] In fact, the latter Pt–Cl distance is significantly longer than the average value observed for terminal Cl ligands in six-coordinate Pt derivatives (232.6 pm).[24]

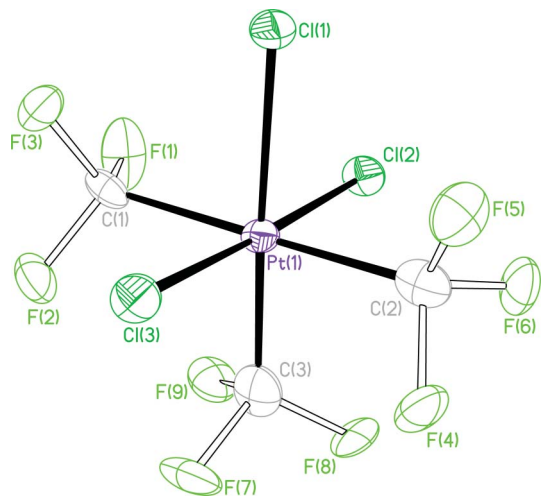


**Fig. 5** Thermal ellipsoid diagram (50% probability) of one of the crystallographically independent [*mer*-$Pt(CF_3)_3Cl_3]^{2-}$ anions found in single crystals of **6**·0.42$CH_2Cl_2$. Selected bond lengths (pm) and angles (°) with estimated standard deviations: Pt(1)–C(1) 210.9(6), Pt(1)–C(2) 209.9(6), Pt(1)–C(3) 202.7(6), Pt(1)–Cl(1) 241.0(2), Pt(1)–Cl(2) 232.6(2), Pt(1)–Cl(3) 232.2(2); C(1)–Pt(1)–C(2) 176.2(2), C(1)–Pt(1)–C(3) 92.1(2), C(1)–Pt(1)–Cl(1) 88.2(2), C(1)–Pt(1)–Cl(2) 92.78(15), C(1)–Pt(1)–Cl(3) 86.67(15), C(2)–Pt(1)–C(3) 90.5(2), C(2)–Pt(1)–Cl(1) 89.49(15), C(2)–Pt(1)–Cl(2) 90.16(14), C(2)–Pt(1)–Cl(3) 90.29(14), C(3)–Pt(1)–Cl(1) 175.76(16), C(3)–Pt(1)–Cl(2) 87.65(15), C(3)–Pt(1)–Cl(3) 94.85(15), Cl(1)–Pt(1)–Cl(2) 88.11(7), Cl(1)–Pt(1)–Cl(3) 89.39(7), Cl(2)–Pt(1)–Cl(3) 177.46(7).

## Optical properties

The optical properties of the *cis*-/*trans*-$[Pt(CF_3)_4Cl_2]^{2-}$ and *fac*-/*mer*-$[Pt(CF_3)_3Cl_3]^{2-}$ stereoisomeric couples have also been

studied. No evidence of luminescent behaviour has been observed for any of them at room temperature. Their electronic spectra have been determined on powder samples by diffuse reflectance (Fig. 6). Although an in-depth analysis of the obtained spectra is beyond the scope of the present work, we will try to rationalise them by comparison with previous studies on electronic spectra of octahedral $Pt^{IV}$ derivatives[25–27] paying particular attention to the symmetry properties of the different species.

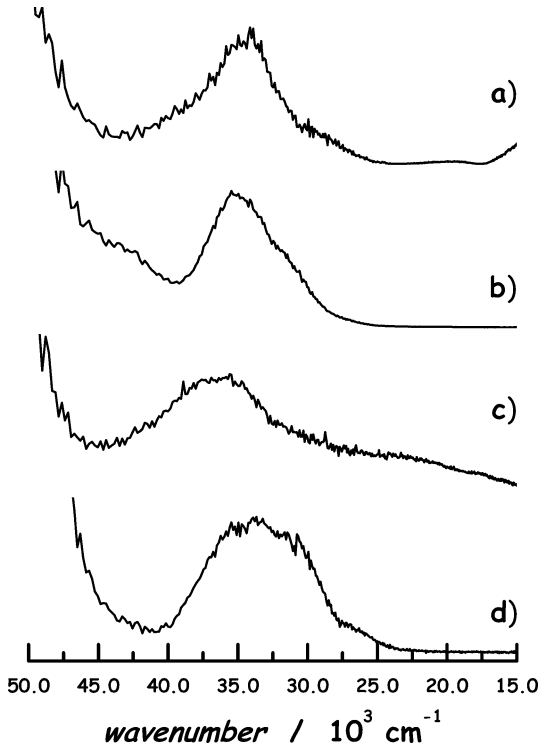


**Fig. 6** Optical spectra of compounds: (a) **2**, (b) **3**, (c) **5** and (d) **6** obtained by diffuse reflectance on the corresponding powder samples.

The electronic ground state of purely octahedral $Pt^{IV}$ complexes, $[PtX_6]^q$ ($q$ = –2 or +4, depending on the anionic or neutral character of the X ligand), is the spin and orbital singlet $^1A_1$ corresponding to the $t_{2g}^6$ configuration. The absorptions appearing at high energy (≥30000 $cm^{-1}$) are usually assigned to the spin-allowed d–d transitions to the excited states $^1T_1$ and $^1T_2$, and sometimes also to the spin-forbidden $^1A_1 \rightarrow {}^3T_1$ transition. These transitions are naturally shifted depending on the field strength of the X ligand.[28]

In the heteroleptic species [*trans*-$Pt(CF_3)_4Cl_2]^{2-}$, the decrease in local symmetry to $D_{4h}$ should entail a splitting in the $T_1$ and $T_2$ orbital triplets. The transitions to each of these "triplets" would be expected to lie between those corresponding to the homoleptic species $[Pt(CF_3)_6]^{2-}$ and $[PtCl_6]^{2-}$. The spectrum of the latter species shows a band at *ca.* 28000 $cm^{-1}$, which has been assigned to the $^1A_1 \rightarrow {}^1T_1$ transition.[26,27] Although the electronic spectrum of $[Pt(CF_3)_6]^{2-}$ is not known, the corresponding $^1A_1 \rightarrow {}^1T_1$ transition would be expected to be shifted to higher energies considering that σ-alkyl groups are stronger ligands than halogens.[28] It is therefore reasonable to assign the band at *ca.* 35500 $cm^{-1}$ with a shoulder at 31500 $cm^{-1}$ observed in the spectrum of **3** (Fig. 6b) to electronic transitions to the split $^1T_1$ level. A similar explanation can be given for the dominant features in the spectrum of the [*cis*-$Pt(CF_3)_4Cl_2]^{2-}$ stereoisomer (**2**) consisting of a band at 34300 $cm^{-1}$ with a shoulder at *ca.* 29000 $cm^{-1}$ (Fig. 6a). An additional weaker band at *ca.* 19550 $cm^{-1}$ (Fig. 6a) can be assigned to the spin-forbidden $^1A_1 \rightarrow {}^3T_1$ transition that would become partially allowed in the $C_{2v}$ local symmetry of the [*cis*-$Pt(CF_3)_4Cl_2]^{2-}$ species. The electronic spectrum of [*mer*-$Pt(CF_3)_3Cl_3]^{2-}$ (Fig. 6d), a species also with $C_{2v}$ local symmetry, can be qualitatively explained in a similar way. The presence of just three strong-field $CF_3$ groups in **6** would justify the bathochromic shift of the main absorption to *ca.* 33600 $cm^{-1}$.

The electronic spectrum of the [*fac*-$Pt(CF_3)_3Cl_3]^{2-}$ stereoisomer (Fig. 6c), although roughly similar to those just discussed, shows some subtle differences with the pattern observed for the remaining species. The main features consist of a high-energy band at *ca.* 35600 $cm^{-1}$ with a shoulder at *ca.* 37600 $cm^{-1}$. These absorptions can be assigned to transitions to the levels derived from the splitting of the excited state $^1T_1$ under a $C_{3v}$ local symmetry. The hypsochromic shift observed in this case can be related to the shortening in the average Pt–C distance observed in the solid-state structure of **5′** (Fig. 5), which should involve an increase in the ligand-field contribution of the $CF_3$ groups. Two further absorptions are observed in the spectrum of **5** in the low-energy region (Fig. 6c). The position of one of them (*ca.* 17200 $cm^{-1}$) is close to that calculated for the spin-forbidden $^1A_1 \rightarrow {}^3T_1$ transition in the homoleptic complex $[PtCl_6]^{2-}$.[27] The release of the selection rules associated with the symmetry lowering to the trigonal $C_{3v}$ local environment in **5′** could well be responsible for the intensity increase in the referred transition. Similarly, the broad absorption at *ca.* 28000 $cm^{-1}$ could be associated to the $^1A_1 \rightarrow {}^3T_2$ transition.

### Concluding remarks

In this paper, we describe efficient synthetic methods to stereoselectively obtain salts of any of the following trifluoromethylplatinum(IV) isomeric couples: *cis*-/*trans*-[$Pt(CF_3)_4Cl_2]^{2-}$ and *fac*-/*mer*-[$Pt(CF_3)_3Cl_3]^{2-}$. All these isomeric species (with $d^6$ electron configuration) are stereochemically stable, thus enabling their isolation and characterisation as pure substances. Characterisation of these compounds relies mainly on their spectroscopic properties. Additionally, salts of the *fac*-/*mer*-[$Pt(CF_3)_3Cl_3]^{2-}$ stereoisomeric couple have also been structurally characterised by single-crystal X-ray diffraction methods, thus enabling a direct comparison of their corresponding geometries. Finally, the thermally unstable derivative $[NBu_4]_2$[*trans*-$Pt(CF_3)_4Cl(SOCl)$] containing the unusual chlorosulfinyl ligand has been detected, isolated and thoroughly characterised. This intermediate species has been found to be instrumental in opening the *cis* → *fac* path.

As organotransition-metal chemistry involving the trifluoromethyl group, $CF_3$, continues to grow, it becomes evident that, in certain aspects, it takes the lead over the results obtained with the non-fluorinated methyl group, $CH_3$. Thus, the stereochemical variety presented here has no parallel in methyl-platinum chemistry, which is by far better developed.

## Experimental

### General procedures and materials

Unless otherwise stated, the reactions and manipulations were carried out under purified argon using Schlenk techniques.

Solvents were dried using an MBraun SPS-800 System. Compounds $[NBu_4]_2[Pt(CF_3)_4]$,[13] $[NBu_4]_2[Pt(CF_3)_3Cl]$,[23] and $[N(PPh_3)_2]Cl$[29] were obtained as described elsewhere. Solutions of chlorine were prepared by bubbling a stream of dry $Cl_2$(g) through $CCl_4$ and were titrated by standard redox methods before use. Elemental analyses were carried out using a Perkin Elmer 2400 CHNS/O Series II microanalyzer. IR spectra of KBr discs were recorded on the following Perkin–Elmer spectrophotometers: 883 (4000–200 $cm^{-1}$) or Spectrum One (4000–350 $cm^{-1}$). Optical spectra were registered on a Thermo Electron Corporation Evolution 600 UV-Vis spectrophotometer equipped with a Praying Mantis integrating sphere accessory. Mass spectra were recorded by MALDI-TOF techniques on Bruker MicroFlex or AutoFlex spectrometers. NMR spectra were recorded on any of the following spectrometers: Varian Gemini-300, Bruker ARX 300 or Bruker ARX 400. Unless otherwise stated, the spectroscopic measurements were carried out at room temperature. Chemical shifts of the measured nuclei (δ in ppm) are given with respect to the standard references in use: $CFCl_3$ ($^{19}F$) and 2 M aqueous $Na_2[PtCl_6]$ solution ($^{195}Pt$). NMR parameters associated with the cations are unexceptional and are therefore omitted.

### Synthesis of $[PPh_4]_2[Pt(CF_3)_4]$ (1′) and $[N(PPh_3)_2]_2[Pt(CF_3)_4]$ (1″)

The addition of $[PPh_4]Br$ (0.22 g, 0.52 mmol) dissolved in $^i$PrOH (3 $cm^3$) or $[N(PPh_3)_2]Cl$ (0.30 g, 0.52 mmol) dissolved in $^i$PrOH (3 $cm^3$) to $Me_2CO$ (5 $cm^3$) solutions of **1** (0.25 g, 0.26 mmol) at room temperature caused the immediate precipitation of white solids, which were filtered out, washed with *n*-hexane (3 × 3 $cm^3$), vacuum dried and identified as **1′** (0.28 g, 0.24 mmol, 92% yield) or **1″** (0.37 g, 0.24 mmol, 92% yield), respectively. Anal. Found for **1′**: C 54.1, H 3.7; $C_{52}H_{40}F_{12}P_2Pt$ requires: C 54.3, H 3.5%. IR of **1′** (KBr): $\tilde{\nu}_{max}/cm^{-1}$ = 1585 (s), 1484 (s), 1440 (vs), 1337 (w), 1316 (w), 1192 (w), 1165 (w), 1109 (vs), 1063 (vs), 967 (br), 930 (s), 852 (w), 806 (w), 761 (s), 722 (vs), 689 (vs), 615 (w), 531 (vs), 524 (vs), 469 (w), 320 (m). Anal. Found for **1″**: C 58.7, H 3.8, N 1.95; $C_{76}H_{60}F_{12}N_2P_4Pt$ requires: C 59.0, H 3.9, N 1.8%. IR of **1″** (KBr): $\tilde{\nu}_{max}/cm^{-1}$ = 1587 (w), 1482 (m), 1438 (s), 1295 (sh), 1277 (m), 1251 (s), 1185 (w), 1114 (vs), 1064 (vs), 970 (vs), 961 (vs), 801 (w), 751 (m), 723 (vs), 691 (s), 552 (vs), 532 (vs), 502 (s), 443 (w), 396 (w), 319 (w).

### Synthesis of $[NBu_4]_2$[*cis*-$Pt(CF_3)_4Cl_2$] (2)

To a $Me_2CO$ (15 $cm^3$) solution of **1** (0.20 g, 0.21 mmol) at room temperature was added $SOCl_2$ (15 $mm^3$, 0.21 mmol). After 5 min of stirring, the by then dark orange solution was concentrated to dryness. Treatment of the resulting residue with $^i$PrOH (3 $cm^3$) at 0 °C gave rise to a cream solid that was filtered, washed with *n*-hexane (3 $cm^3$), vacuum dried and identified as **2** (0.16 g, 0.15 mmol, 71% yield). Anal. Found: C 42.2, H 6.9, N 2.7; $C_{36}H_{72}Cl_2F_{12}N_2Pt$ requires: C 42.1, H 7.1, N 2.7%. IR (KBr): $\tilde{\nu}_{max}/cm^{-1}$ = 2963 (s), 2876 (m), 1483 (m), 1474 (m), 1382 (w), 1163 (vs), 1096 (vs), 1074 (vs), 1039 (sh), 883 (m; $NBu_4^+$), 802 (w), 741 (m; $NBu_4^+$), 338 (m; Pt–Cl), 331 (w; Pt–Cl). $^{19}F$ NMR ([$^2$H]acetone): δ (ppm) = −24.4 [septet, $^4J(^{19}F,^{19}F)$ = 5.7 Hz, $^2J(^{195}Pt,^{19}F)$ = 465 Hz], −31.7 [septet, $^2J(^{195}Pt,^{19}F)$ = 284 Hz]. $^{195}Pt$ NMR ([$^2$H]acetone): δ (ppm) = −1785 [septet of septets, $^2J(^{19}F,^{195}Pt)$ = 465 Hz (assignable to the $CF_3$ groups *trans* to Cl), $^2J(^{19}F,^{195}Pt)$ = 284 Hz (assignable to the mutually *trans*-standing $CF_3$ groups)]. MS (MALDI–): *m*/*z* =506 $[Pt(CF_3)_4Cl]^-$.

### Synthesis of $[PPh_4]_2$[*cis*-$Pt(CF_3)_4Cl_2$] (2′)

The addition of $[PPh_4]Br$ (82 mg, 0.20 mmol) dissolved in $^i$PrOH (3 $cm^3$) to a $Me_2CO$ (5 $cm^3$) solution of **2** (0.10 g, 0.10 mmol) at room temperature caused the immediate precipitation of a pale blue solid, which was filtered out, washed with *n*-hexane (3 × 3 $cm^3$), vacuum dried and identified as **2′** (0.11 g, 0.09 mmol, 90% yield). Anal. Found: C 51.2, H 3.2; $C_{52}H_{40}Cl_2F_{12}P_2Pt$ requires: C 51.2, H 3.3%. IR (KBr): $\tilde{\nu}_{max}/cm^{-1}$ = 1584 (w), 1482 (w), 1442 (m), 1161 (m), 1094 (vs), 1069 (s), 996 (w), 762 (w), 723 (m), 690 (m), 528 (s), 338 (w; Pt–Cl), 329 (w; Pt–Cl). NMR data associated with the [*cis*-$Pt(CF_3)_4Cl_2]^{2-}$ anion in solution are in keeping with those found for the $[NBu_4]^+$ salt (**2**).

### Synthesis of $[NBu_4]_2$[*trans*-$Pt(CF_3)_4Cl(SOCl)$] (4)

To a $Me_2CO$ (15 $cm^3$) solution of **1** (0.20 g, 0.21 mmol) at −78 °C was added $SOCl_2$ (15 $mm^3$, 0.21 mmol) and the mixture was stirred for 30 min at the same temperature. The, by then, dark green solution was concentrated to dryness. Treatment of the resulting residue with $^i$PrOH (3 $cm^3$) at 0 °C gave rise to a green solid that was filtered, washed with *n*-hexane (3 $cm^3$), vacuum dried and identified as **4** (0.15 g, 0.14 mmol, 67% yield). Anal. Found: C 40.5, H 6.6, N 2.8, S 2.9; $C_{36}H_{72}Cl_2F_{12}N_2OPtS$ requires: C 40.2, H 6.75, N 2.6, S 3.0%. IR (KBr): $\tilde{\nu}_{max}/cm^{-1}$ = 2963 (s), 2876 (s), 1483 (m), 1473 (m), 1381 (w), 1260 (w), 1211 (w), 1161 (m), 1126 (vs), 1096 (vs), 1058 (vs), 1041 (sh), 882 (m; $NBu_4^+$), 802 (m), 740 (m; $NBu_4^+$), 425 (w), 399 (w; Pt–Cl), 333 (w), 316 (w). $^{19}F$ NMR ([$^2$H]acetone): δ (ppm) = −32.1 [s, $^2J(^{195}Pt,^{19}F)$ = 262 Hz]. $^{195}Pt$ NMR ([$^2$H]acetone, −30 °C): δ (ppm) = −1735 [m, $^2J(^{19}F,^{195}Pt)$ = 262 Hz]. MS (MALDI–): *m*/*z* = 506 $[Pt(CF_3)_4Cl]^-$, 402 $[Pt(CF_3)_3]^-$.

### Synthesis of $[N(PPh_3)_2]_2$[*trans*-$Pt(CF_3)_4Cl(SOCl)$] (4″)

Compound **4″** was prepared from **1″** (0.20 g, 0.13 mmol) and $SOCl_2$ (9 $mm^3$, 0.13 mmol) by using a similar procedure to that described for the synthesis of **4**. Compound **4″** was obtained as a light green solid (0.15 g, 0.09 mmol, 70% yield). Anal. Found: C 54.6, H 3.5, N 1.6, S 2.0; $C_{76}H_{60}Cl_2F_{12}N_2OP_4PtS$ requires: C 54.75, H 3.6, N 1.7, S 1.9%. IR (KBr): $\tilde{\nu}_{max}/cm^{-1}$ = 1588 (w), 1483 (w), 1439 (m), 1268 (m), 1184 (w), 1158 (w), 1116 (vs), 1094 (vs), 1055 (vs), 997 (s), 789 (w), 748 (w), 723 (s), 692 (s), 548 (s), 533 (s), 501 (m), 420 (w), 395 (w; Pt–Cl). NMR data associated with the [*trans*-$Pt(CF_3)_4Cl(SOCl)]^{2-}$ anion in solution are in keeping with those found for the $[NBu_4]^+$ salt (**4**).

Crystals suitable for X-ray diffraction analysis were obtained by slow diffusion of a layer of $Et_2O$ (15 $cm^3$) into a solution of 5 mg of **4″** in 5 $cm^3$ of $CH_2Cl_2$ at −30 °C.

### Synthesis of $[NBu_4]_2$[*fac*-$Pt(CF_3)_3Cl_3$] (5)

To a $Me_2CO$ (15 $cm^3$) solution of **2** (0.20 g, 0.19 mmol) at room temperature was added HCl(aq) (16 $mm^3$, 0.19 mmol). After 2 days of stirring, the reaction mixture was concentrated to dryness. Treatment of the resulting residue with $^i$PrOH (3 $cm^3$) at 0 °C gave rise to a white solid that was filtered, washed with *n*-hexane

(3 $cm^3$), vacuum dried and identified as **5** (0.14 g, 0.14 mmol, 73% yield). Anal. Found: C 41.9, H 7.5, N 2.7; $C_{35}H_{72}Cl_3F_9N_2Pt$ requires: C 42.3, H 7.3, N 2.8%. IR (KBr): $\tilde{\nu}_{max}/cm^{-1}$ = 2962 (s), 2875 (m), 1483 (m), 1382 (w), 1148 (vs), 1106 (vs), 1096 (sh), 1093 (vs), 1068 (vs), 882 (w; $NBu_4^+$), 802 (w), 741 (w; $NBu_4^+$), 726 (w), 334 (w; Pt–Cl), 319 (w; Pt–Cl), 294 (w). $^{19}F$ NMR ([$^2H$]acetone): $\delta$ (ppm) = −26.0 [s, $^2J(^{195}Pt,^{19}F)$ = 457 Hz]. $^{195}Pt$ NMR ([$^2H$]acetone): $\delta$ (ppm) = −1470 [m, $^2J(^{19}F,^{195}Pt)$ = 457 Hz]. MS (MALDI−): $m/z$ = 506 $[Pt(CF_3)_4Cl]^-$, 472 $[Pt(CF_3)_3Cl_2]^-$.

### Synthesis of $[PPh_4]_2[fac\text{-}Pt(CF_3)_3Cl_3]$ (5′)

Compound **5′** was prepared from **2′** (0.20 g, 0.16 mmol) and HCl(aq) (14 $mm^3$, 0.16 mmol) by using a similar procedure to that just described for the synthesis of **5**. Compound **5′** was obtained as a purple solid (0.16 g, 0.13 mmol, 81% yield). Anal. Found: C 52.0, H 3.3; $C_{51}H_{40}Cl_3F_9P_2Pt$ requires: C 51.6, H 3.4%. IR (KBr): $\tilde{\nu}_{max}/cm^{-1}$ = 3061 (w), 2963 (w), 1585 (w), 1484 (w), 1441 (m), 1261 (w), 1146 (s), 1107 (vs), 1095 (vs), 1093 (vs), 1065 (vs), 996 (w), 802 (w), 755 (w), 723 (s), 689 (s), 528 (vs), 333 (w; Pt–Cl), 318 (w; Pt–Cl), 294 (w). NMR data associated with the $[fac\text{-}Pt(CF_3)_3Cl_3]^{2-}$ anion in solution are in keeping with those found for the $[NBu_4]^+$ salt (**5**).

Crystals suitable for X-ray diffraction analysis with formula $[PPh_4]_2[fac\text{-}Pt(CF_3)_3Cl_3]\cdot 1.25Me_2CO$ were obtained by slow diffusion of a *n*-hexane layer (15 $cm^3$) into a solution of 5 mg of **5′** in 5 $cm^3$ of $Me_2CO$ at 4 °C.

### Synthesis of $[NBu_4]_2[mer\text{-}Pt(CF_3)_3Cl_3]$ (6)

To a $CH_2Cl_2$ (15 $cm^3$) solution of $[NBu_4]_2[Pt(CF_3)_3Cl]$ (0.20 g, 0.22 mmol) at −78 °C was added $Cl_2$ dissolved in $CCl_4$ (1.9 $cm^3$, 0.65 mmol). The mixture was stirred while the medium was allowed to reach room temperature. The by then light yellow solution was concentrated to dryness. Treatment of the resulting residue with $^i$PrOH (3 $cm^3$) at 0 °C gave rise to a light yellow solid that was filtered off, washed with *n*-hexane (3 $cm^3$), vacuum dried and identified as **6** (0.19 g, 0.19 mmol, 88% yield). Anal. Found: C 42.2, H 7.1, N 2.8; $C_{35}H_{72}Cl_3F_9N_2Pt$ requires: C 42.3, H 7.3, N 2.8%. IR (KBr): $\tilde{\nu}_{max}/cm^{-1}$ = 2962 (s), 2876 (m), 1483 (m), 1382 (w), 1261 (w), 1135 (s), 1095 (vs), 1064 (vs), 1026 (s), 882 (m; $NBu_4^+$), 802 (w), 740 (m; $NBu_4^+$), 359 (m; Pt–Cl), 323 (w; Pt–Cl). $^{19}F$ NMR ([$^2H$]dichloromethane): $\delta$ (ppm) = −23.5 [septet, $^4J(^{19}F,^{19}F)$ = 4.8 Hz, $^2J(^{195}Pt,^{19}F)$ = 426 Hz], −33.4 [quartet, $^2J(^{195}Pt,^{19}F)$ = 269 Hz]. $^{195}Pt$ NMR ([$^2H$]acetone): $\delta$ (ppm) = −1405 [quartet of septets, $^2J(^{19}F,^{195}Pt)$ = 426 Hz (assignable to the $CF_3$ group *trans* to Cl), $^2J(^{19}F,^{195}Pt)$ = 269 Hz (assignable to the mutually *trans*-standing $CF_3$ groups)]. MS (MALDI−): $m/z$ = 472 $[Pt(CF_3)_3Cl_2]^-$.

Crystals suitable for X-ray diffraction analysis with formula $[NBu_4]_2[mer\text{-}Pt(CF_3)_3Cl_3]\cdot 0.42CH_2Cl_2$ were obtained by slow diffusion of a $Et_2O$ layer (15 $cm^3$) into a solution of 5 mg of **6** in 5 $cm^3$ of $CH_2Cl_2$ at 4 °C.

### X-Ray structure determinations†

Crystal data and other details of the structure analyses are presented in Table 1. Suitable single crystals were mounted on a quartz fibre in a random orientation and held in place with fluorinated oil. Data collections were performed at 100 K temperature on an Oxford Diffraction Xcalibur CCD diffractometer using graphite-monochromated Mo-K$\alpha$ radiation ($\lambda$ = 71.073 pm) with a nominal crystal to detector distance of 5.0 cm. Unit cell dimensions were determined from the positions of 12095 reflections from the main dataset for **4″**, 34983 reflections for **5′**·1.25$Me_2CO$, and 29355 reflections for **6**·0.42$CH_2Cl_2$. The diffraction frames were integrated and corrected for absorption using the CrysAlis RED package.[30] Lorentz and polarisation corrections were applied.

The structures were solved by direct methods. All non-hydrogen atoms were assigned anisotropic displacement parameters. The hydrogen atoms were constrained to idealised geometries and

**Table 1** Crystal data and structure refinement for compounds **4″**, **5′**·1.25$Me_2CO$ and **6**·0.42$CH_2Cl_2$

| | **4″** | **5′**·1.25$Me_2CO$ | **6**·0.42$CH_2Cl_2$ |
|---|---|---|---|
| Formula | $C_{76}H_{60}Cl_2F_{12}N_2OP_4PtS$ | $C_{51}H_{40}Cl_3F_9P_2Pt\cdot 1.25Me_2CO$ | $C_{35}H_{72}Cl_3F_9N_2Pt\cdot 0.42CH_2Cl_2$ |
| $M_r$ | 1667.19 | 1259.81 | 1028.77 |
| Crystal system | Monoclinic | Monoclinic | Triclinic |
| Space group | $P2_1/n$ | $P2_1/c$ | $P\bar{1}$ |
| $a$/pm | 1094.37(5) | 1973.96(2) | 1647.22(3) |
| $b$/pm | 1356.15(7) | 1300.13(2) | 1995.00(3) |
| $c$/pm | 2374.95(8) | 4000.65(6) | 2432.05(5) |
| $\alpha$/° | 90 | 90 | 113.165(2) |
| $\beta$/° | 100.253(4) | 91.152(1) | 109.539(2) |
| $\gamma$/° | 90 | 90 | 90.920(1) |
| $V$/$nm^3$ | 3.4684(3) | 10.2652(2) | 6.8235(2) |
| $Z$ | 2 | 8 | 6 |
| $D_c$/g $cm^{-3}$ | 1.596 | 1.630 | 1.502 |
| $T$/K | 100(2) | 100(2) | 100(2) |
| $\mu$/$mm^{-1}$ | 2.302 | 3.025 | 3.373 |
| $F$(000) | 1668 | 5008 | 3141 |
| 2$\theta$ range/° | 8.3–57.8 | 8.3–57.8 | 8.3–52.0 |
| Collected reflections | 31175 | 116092 | 109252 |
| Unique reflections | 8259 | 24566 | 26713 |
| $R_{int}$ | 0.0459 | 0.0686 | 0.0804 |
| $R_1$, $wR_2$[a] ($I > 2\sigma(I)$) | 0.0479, 0.1160 | 0.0554, 0.1127 | 0.0444, 0.0881 |
| $R_1$, $wR_2$[a] (all data) | 0.0764, 0.1234 | 0.0951, 0.1209 | 0.0832, 0.0932 |
| GOF ($F^2$)[b] | 1.018 | 1.018 | 1.000 |

[a] $R_1 = \sum(|F_o| - |F_c|)/\sum|F_o|$; $wR_2 = [\sum w(F_o^2 - F_c^2)^2/\sum w(F_o^2)^2]^{1/2}$; $w = [\sigma^2(F_o^2) + (g_1P)^2 + g_2P]^{-1}$; $P = (1/3)[\max\{F_o^2,0\} + 2F_c^2]$. [b] Goodness-of-fit = $[\sum w(F_o^2 - F_c^2)^2/(n_{obs} - n_{param})]^{1/2}$.

 

assigned isotropic displacement parameters equal to 1.2 times (1.5 times for the methyl hydrogen atoms) the $U_{iso}$ values of their respective parent carbon atoms.

For **4″**, the presence of a crystallographic inversion centre at the position occupied by the Pt atoms results in several problems that preclude a satisfactory resolution of the structure. The existence of this inversion centre and the validity of the spatial group chosen ($P2_1/n$) have been confirmed by lowering the symmetry (to $P2_1$ or $Pn$) with unsatisfactory results, and by analyses performed with the PLATON crystallographic software.[31] Since the anion itself does not have an inversion centre, the presence of the crystallographic one on the Pt causes the positions of the mutually *trans* SOCl and Cl fragments to be disordered over two sets of positions with half occupancy. The existence of two relatively heavy atoms of a similar weight, such as S and Cl in very close positions, results in some degree of uncertainty in their exact location. This is probably due to the fact that the electron density maps cannot precisely locate two defined maxima in this high electron density region. For this reason, the geometrical parameters involving S and Cl are of limited reliability and can only be taken as an indication. Moreover, the O atom appears disordered over two positions which have been refined with partial occupancy 0.3 and 0.2; the S–O distances had to be restrained to acceptable values. Finally, one of the $CF_3$ ligands is severely disordered, and the F atoms have been modelled in three different conformations with partial occupancy 0.4/0.4/0.2. For this $CF_3$ group geometrical constrains had to be used.

For **5′**·1.25$Me_2CO$, the $Z'$ value is 2 and one anion (Pt(1)) and one solvent molecule show some degree of disorder. In the anion, this disorder involves two Cl and two $CF_3$ ligands. All the disorder was dealt with using restraints in the geometry and thermal displacement parameters of the atoms involved, until reasonable geometries and values were achieved. No hydrogens were added to the disordered solvent atoms.

For **6**·0.42$CH_2Cl_2$, due to the mediocre quality of the crystals obtained, which is reflected in its relatively low density, the packing of the constituent chemical moieties is not very compact. With a $Z'$ value of 3, all but one anion, one cation and one solvent molecule show some degree of disorder. This disorder is especially severe for two of the anions and one $[NBu_4]^+$ cation. All the disorder was dealt with using restraints in the geometry and thermal displacement parameters of the atoms involved, until reasonable geometries and values were achieved. No hydrogens were added to some of the disordered C atoms.

Full-matrix least-squares refinement of these models against $F^2$ converged to final residual indices given in Table 1. All the structures were refined using the SHELXL-97 program.[32]

## Acknowledgements

This work was supported by the Spanish MICINN (DGPTC)/FEDER (Project CTQ2008-06669-C02-01/BQU) and the Gobierno de Aragón (Grupo Consolidado E21: *Química Inorgánica y de los Compuestos Organometálicos*).

## References

1 L. H. Gade, *Chem. unserer Zeit*, 2002, **36**, 168; G. B. Kauffman, in *Coordination Chemistry – A Century of Progress*, ed. G. B. Kauffman, ACS Symposium Series 565, American Chemical Society, Washington, DC 1994, ch. 1, pp. 2–33; G. B. Kauffman, *Inorganic Coordination Compounds*, Heyden & Son Ltd, London, UK 1981, ch. 6, pp. 86–136; G. B. Kauffman, *Coord. Chem. Rev.*, 1975, **15**, 1.
2 A. Werner, in *Nobel Lectures Chemistry 1901–1921*, Elsevier, Amsterdam, 1966, pp. 256–269; A. Werner, *Z. Anorg. Allg. Chem.*, 1893, **3**, 267.
3 *Gmelins Handbuch der Anorganischen Chemie Platin Teil D*, Verlag Chemie GmbH, Weinheim, Germany, 8th edn, 1957, pp. 554–557.
4 W. Preetz, G. Peters and D. Bublitz, *Chem. Rev.*, 1996, **96**, 977.
5 P. Murray and K. R. Koch, *J. Coord. Chem.*, 2010, **63**, 2561; W. J. Gerber, P. Murray and K. R. Koch, *Dalton Trans.*, 2008, 4113; J. Kramer and K. R. Koch, *Inorg. Chem.*, 2007, **46**, 7466; K. R. Koch, M. R. Burger, J. Kramer and A. N. Westra, *Dalton Trans.*, 2006, 3277; B. Shelimov, J.-F. Lambert, M. Che and B. Didillon, *J. Am. Chem. Soc.*, 1999, **121**, 545; C. Carr, P. L. Goggin and R. J. Goodfellow, *Inorg. Chim. Acta*, 1984, **81**, L25.
6 V. K. Jain, G. S. Rao and L. Jain, *Adv. Organomet. Chem.*, 1987, **27**, 113.
7 R. S. Tobias, *Inorg. Chem.*, 1970, **9**, 1296.
8 A. Pidcock, R. E. Richards and L. M. Venanzi, *J. Chem. Soc. A*, 1966, 1707.
9 T. G. Appleton, H. C. Clark and L. E. Manzer, *Coord. Chem. Rev.*, 1973, **10**, 335.
10 R. G. Pearson, *Inorg. Chem.*, 1973, **12**, 712.
11 I. J. Bruno, J. C. Cole, P. R. Edgington, M. Kessler, C. F. Macrae, P. McCabe, J. Pearson and R. Taylor, *Acta Crystallogr., Sect. B: Struct. Sci.*, 2002, **58**, 389.
12 T. G. Appleton, M. H. Chisholm, H. C. Clark and L. E. Manzer, *Inorg. Chem.*, 1972, **11**, 1786.
13 B. Menjón, S. Martínez-Salvador, M. A. Gómez-Saso, J. Forniés, L. R. Falvello, A. Martín and A. Tsipis, *Chem.–Eur. J.*, 2009, **15**, 6371.
14 S. Balters, E. Bernhardt, H. Willner and T. Berends, *Z. Anorg. Allg. Chem.*, 2004, **630**, 257; S. Balters, Ph.D. Thesis, University of Wuppertal, 2005 [urn:nbn:de:hbz:468-20050702].
15 A. J. Blake, R. W. Cockman and E. A. V. Ebsworth, *Acta Crystallogr., Sect. C: Cryst. Struct. Commun.*, 1992, **48**, 1658.
16 G. C. Stocco, F. Stocco-Gattuso, N. Bertazzi and L. Pellerito, *J. Coord. Chem.*, 1976, **5**, 55.
17 K. H. Ebert, W. Massa, H. Donath, J. Lorberth, B.-S. Seo and E. Herdtweck, *J. Organomet. Chem.*, 1998, **559**, 203.
18 M. Atam and U. Müller, *J. Organomet. Chem.*, 1974, **71**, 435.
19 D. S. Yang, G. M. Bancroft, R. J. Puddephatt and J. S. Tse, *Inorg. Chem.*, 1990, **29**, 2496.
20 H. Junicke, C. Bruhn, D. Ströhl, R. Kluge and D. Steinborn, *Inorg. Chem.*, 1998, **37**, 4603.
21 S. Schlecht, J. Magull, D. Fenske and K. Dehnicke, *Angew. Chem., Int. Ed. Engl.*, 1997, **36**, 1994.
22 V. Hsieh, A. G. de Crisci, A. J. Lough and U. Fekl, *Organometallics*, 2007, **26**, 938; R. F. Childs, D. L. Mulholland and A. Nixon, *Can. J. Chem.*, 1982, **60**, 801.
23 S. Martínez-Salvador, B. Menjón, J. Forniés, A. Martín and I. Usón, *Angew. Chem., Int. Ed.*, 2010, **49**, 4286.
24 A. G. Orpen, L. Brammer, F. H. Allen, O. Kennard, D. G. Watson and R. Taylor, *J. Chem. Soc., Dalton Trans.*, 1989, S1.
25 V. F. Plyusnin, E. M. Glebov, V. P. Grivin, Y. V. Ivanov, A. B. Venediktov and H. Lemmetyinen, *J. Photochem. Photobiol., A*, 2001, **141**, 159; W. D. Blanchard and W. R. Mason, *Inorg. Chim. Acta*, 1978, **28**, 159; H. H. Patterson, W. J. DeBerry, J. E. Byrne, M. T. Hsu and J. A. LoMenzo, *Inorg. Chem.*, 1977, **16**, 1698; L. E. Cox and D. G. Peters, *Inorg. Chem.*, 1970, **9**, 1927; G. N. Henning, P. A. Dobosh, A. J. McCaffery and P. N. Schatz, *J. Am. Chem. Soc.*, 1970, **92**, 5377.
26 G. Eyring, T. Schönherr and H.-H. Schmidtke, *Theor. Chim. Acta*, 1983, **64**, 83; D. L. Swihart and W. R. Mason, *Inorg. Chem.*, 1970, **9**, 1749.
27 R. K. Yoo and T. A. Keiderling, *J. Phys. Chem.*, 1990, **94**, 8048.
28 J. Chatt and R. G. Hayter, *J. Chem. Soc.*, 1961, 772.
29 J. K. Ruff and W. J. Schlientz, *Inorg. Synth.*, 1974, **15**, 84.
30 *CrysAlis REDProgram for X-ray CCD camera data reduction*, Version 1.171.32.19, Oxford Diffraction Ltd, Oxford, UK, 2008.
31 A. L. Spek, *Acta Crystallogr., Sect. A*, 1990, **46**, c34.
32 G. M. Sheldrick, *SHELXL-97 Program for the refinement of crystal structures from diffraction data*, University of Göttingen, Göttingen, Germany, 1997.

## 9. Apéndice

Factores de impacto (**I.F.**) y áreas científicas de las diferentes revistas científicas en las que han sido publicados los trabajos presentados:

- Chem. Eur. J. (Chemistry Multidisciplinary)
  **I.F. =** 5.48 (18 de 147)
- Angew. Chem. Int. Ed. (Chemistry Multidisciplinary)
  **I.F. =** 12.73 (5 de 147)
- Dalton Trans. (Chemistry Inorganic & Nuclear)
  **I.F. =** 3.65 (7 de 43)